Integrated Design by Optimization of Electrical Energy Systems

# Integrated Design by Optimization of Electrical Energy Systems

Edited by
Xavier Roboam

iSTE

WILEY

First published 2012 in Great Britain and the United States by ISTE Ltd and John Wiley & Sons, Inc.

Apart from any fair dealing for the purposes of research or private study, or criticism or review, as permitted under the Copyright, Designs and Patents Act 1988, this publication may only be reproduced, stored or transmitted, in any form or by any means, with the prior permission in writing of the publishers, or in the case of reprographic reproduction in accordance with the terms and licenses issued by the CLA. Enquiries concerning reproduction outside these terms should be sent to the publishers at the undermentioned address:

ISTE Ltd
27-37 St George's Road
London SW19 4EU
UK

www.iste.co.uk

John Wiley & Sons, Inc.
111 River Street
Hoboken, NJ 07030
USA

www.wiley.com

© ISTE Ltd 2012

The rights of Xavier Roboam to be identified as the author of this work have been asserted by him in accordance with the Copyright, Designs and Patents Act 1988.

British Library Cataloguing-in-Publication Data
A CIP record for this book is available from the British Library
ISBN: 978-1-84821-389-0

Printed and bound in Great Britain by CPI Group (UK) Ltd., Croydon, Surrey CR0 4YY

FSC
www.fsc.org
MIX
Paper from responsible sources
FSC® C013604

# Table of Contents

**Preface** . . . . . xi

**Chapter 1. Mission and Environmental Data Processing** . . . . . 1
Amine JAAFAR, Bruno SARENI and Xavier ROBOAM

1.1. Introduction . . . . . 1
1.2. Considerations of the mission and environmental variables . . . . . 3
1.2.1. Mission representation through a nominal operating point . . . . . 4
1.2.2. Extraction of a "sizing" temporal chronogram . . . . . 4
1.2.3. Representation of an environmental variable or mission resulting from statistical analysis . . . . . 5
1.3. New approach for the characterization of a "representative mission" . . . . . 6
1.3.1. Characterization indicators of the mission and environmental variables . . . . . 7
1.3.2. Mission and environmental variables at the heart of the system: an eminently systemic bidirectional coupling . . . . . 13
1.4. Classification of missions and environmental variables . . . . . 16
1.4.1. Classification without *a priori* assumption on the number of classes . . . . . 17
1.4.2. Mission classification for hybrid railway systems . . . . . 18
1.5. Synthesis of mission and environmental variable profiles . . . . . 21
1.5.1. Mission or environmental variable synthesis process . . . . . 21
1.5.2. Elementary patterns for profile generation . . . . . 23
1.5.3. Application to the compacting of a wind speed profile . . . . . 24
1.6. From classification to simultaneous design by optimization of a hybrid traction chain . . . . . 25
1.6.1. Modeling of the hybrid locomotive . . . . . 27

1.6.2. Optimization model . . . . . 30
1.6.3. Mission classification . . . . . 32
1.6.4. Synthesis of representative missions . . . . . 33
1.6.5. Simultaneous design by optimization . . . . . 37
1.6.6. Design results comparison . . . . . 38
1.7. Conclusion . . . . . 39
1.8. Bibliography . . . . . 41

**Chapter 2. Analytical Sizing Models for Electrical Energy Systems Optimization**. . . . . 45
Christophe ESPANET, Daniel DEPERNET, Anne-Claire SAUTTER and Zhenwai WU

2.1. Introduction. . . . . 45
2.2. The problem of modeling for synthesis . . . . . 46
2.2.1. Modeling for synthesis. . . . . 46
2.2.2. Analytical and numerical modeling . . . . . 48
2.3. System decomposition and model structure. . . . . 55
2.3.1. Advantage of decomposition . . . . . 56
2.3.2. Application to the example of the hybrid series-parallel traction chain for the hybrid electrical heavy vehicle. . . . 58
2.4. General information about the modeling of the various possible components in an electrical energy system . . . . . 60
2.5. Development of an electrical machine analytical model . . . . . 61
2.5.1. The various physical fields of the model and the associated methods for solving them . . . . . 62
2.5.2. Application to the example of a hybrid electrical heavy vehicle: modeling of a magnet surface-mounted synchronous machine . . . . . 64
2.6. Development of an analytical static converter model . . . . . 73
2.6.1. The various physical fields of the model and associated resolution methods. . . . . 73
2.6.2. Application to the example of a hybrid electrical heavy vehicle: modeling of inverters feeding synchronous machines. . . . . 75
2.7. Development of a mechanical transmission analytical model . . . . . 82
2.7.1. The various physical fields of the model and associated resolution methods. . . . . 82
2.7.2. Application to the example of a hybrid electric heavy vehicle: modeling of the Ravigneaux gear set. . . . . 83
2.8. Development of an analytical energy storage device model . . . . . 91
2.9. Use of models for the optimum sizing of a system. . . . . 91
2.9.1. Introduction . . . . . 91

2.9.2. Consideration of operating cycles . . . . . 94
2.9.3. Independent component optimization . . . . . 97
2.9.4. Simultaneous component optimization . . . . . 100
2.10. Conclusions . . . . . 102
2.11. Bibliography . . . . . 103

**Chapter 3. Simultaneous Design by Means of Evolutionary Computation** . . . . . 107
Bruno SARENI and Xavier ROBOAM

3.1. Simultaneous design of energy systems . . . . . 107
3.1.1. Introduction to simultaneous design . . . . . 107
3.1.2. Simultaneous design by means of optimization . . . . . 109
3.1.3. Problems relating to simultaneous design using optimization . . . . 110
3.2. Evolutionary algorithms and artificial evolution . . . . . 113
3.2.2. Evolutionary algorithms principle . . . . . 114
3.2.3. Key points of evolutionary algorithms . . . . . 115
3.3. Consideration of multiple objectives . . . . . 119
3.3.1. Pareto optimality . . . . . 119
3.3.2. Multi-objective optimization methods. . . . . 120
3.3.3. Multi-objective evolutionary algorithms . . . . . 121
3.4. Consideration of design constraints. . . . . 123
3.4.1. Single objective problem . . . . . 123
3.4.2. Multi-objective problem . . . . . 125
3.5. Integration of robustness into the simultaneous design process . . . . . 126
3.5.1. Robust design . . . . . 126
3.5.2. Vicinity and uncertainty . . . . . 127
3.5.3. Characterization of robustness . . . . . 128
3.6. Example applications . . . . . 130
3.6.1. Design of a passive wind turbine system . . . . . 130
3.6.2. Simultaneous design of an autonomous hybrid locomotive . . . . . 143
3.7. Conclusions. . . . . 150
3.8. Bibliography . . . . . 151

**Chapter 4. Multi-Level Design Approaches for Electro-Mechanical Systems Optimization** . . . . . 155
Stéphane BRISSET, Frédéric GILLON and Pascal BROCHET

4.1. Introduction. . . . . 155
4.2. Multi-level approaches . . . . . 156
4.3. Optimization using models with different granularities . . . . . 160
4.3.1. Principle of SM . . . . . 162
4.3.2. Mathematical example . . . . . 164

4.3.3. SM variants . . . . . 166
4.3.4. Safety transformer application . . . . . 172
4.4. Hierarchical decomposition of an optimization problem . . . . . 178
4.4.1. Target cascading for optimal design . . . . . 178
4.4.2. Formulation of the TC method . . . . . 180
4.4.3. Mathematical example . . . . . 183
4.4.4. Railway traction engine example . . . . . 186
4.5. Conclusion . . . . . 187
4.6. Bibliography . . . . . 188

**Chapter 5. Multi-criteria Design and Optimization Tools** . . . . . 193
Benoit DELINCHANT, Laurence ESTRABAUD, Laurent GERBAUD and Frédéric WURTZ

5.1. The CADES framework: example of a new tools approach . . . . . 194
5.2. The system approach: a break from standard tools . . . . . 195
5.2.1. Some component definitions . . . . . 196
5.2.2. From integrated environments to collaborative tool frameworks . . . . . 197
5.2.3. A centered model canvas: from generation to utilization . . . . . 198
5.2.4. Some "business" application frameworks . . . . . 201
5.3. Components ensuring interoperability around a framework . . . . . 203
5.3.1. Model types: white box, black box . . . . . 203
5.3.2. Black boxes: positive collaboration and re-use . . . . . 205
5.3.3. Object, component, and service paradigms . . . . . 206
5.3.4. ICAr software components: model normalization for sizing . . . . 209
5.4. Some calculation modeling formalisms for optimization . . . . . 210
5.4.1. Analytical formalisms: algebraic and algorithmic . . . . . 210
5.4.2. Physical models within various formalisms . . . . . 213
5.4.3. The generation chain . . . . . 218
5.5. The principles of automatic Jacobian generation . . . . . 218
5.5.1. The Jacobian: complementary data for the model . . . . . 218
5.5.2. Derivation of mathematical expressions . . . . . 219
5.5.3. Algorithm derivation . . . . . 221
5.5.4. Derivation of specific formulations . . . . . 222
5.6. Services using models and their Jacobian . . . . . 223
5.6.1. Sensitivity study . . . . . 223
5.6.2. Composition of models . . . . . 224
5.6.3. Optimal design . . . . . 226
5.7. Applications of CADES in system optimization . . . . . 227
5.7.1. Overall optimization of a structure . . . . . 227
5.7.2. Evaluation of the potential of a structure . . . . . 229
5.7.3. Comparison between structures . . . . . 230

5.8. Perspectives . . . . . 231
5.8.1. Towards optimization using dynamic modeling . . . . . 231
5.8.2. Towards robust design . . . . . 233
5.8.3. Robust optimization under reliability constraints . . . . . 234
5.8.4. Towards the Internet . . . . . 235
5.9. Conclusions . . . . . 238
5.10. Bibliography . . . . . 239

**Chapter 6. Technico-economic Optimization of Energy Networks** . . . . . 247
Guillaume SANDOU, Philippe DESSANTE, Marc PETIT
and Henri BORSENBERGER

6.1. Introduction . . . . . 247
6.2. Energy network modeling . . . . . 249
6.2.1. Context . . . . . 249
6.2.2. Notations . . . . . 249
6.2.3. Objective function . . . . . 250
6.2.4. Constraints . . . . . 251
6.2.5. Expression of the problem and eventual linear reformulation . . . . 253
6.2.6. Position of the problem processed relative to the problem
of energy network management . . . . . 254
6.3. Resolution of the energy network optimization problem
for a deterministic case . . . . . 255
6.3.1. State of the art . . . . . 255
6.3.2. Resolution by dynamic programming
and Lagrangian relaxation . . . . . 257
6.3.3. Resolution by genetic algorithm . . . . . 262
6.4. Introduction to uncertainty consideration . . . . . 266
6.4.1. Consideration of uncertainties . . . . . 266
6.4.2. Recourse notion . . . . . 267
6.5. Consideration of uncertainties on consumer demand . . . . . 269
6.5.1. Safety margin . . . . . 269
6.5.2. Scenario tree uncertainty modeling . . . . . 269
6.5.3. Resolution by dynamic programming and
Lagrangian relaxation . . . . . 270
6.5.4. Conclusion . . . . . 272
6.6. Consideration of uncertainties over production costs . . . . . 273
6.6.1. Introduction . . . . . 273
6.6.2. Mathematical formulation . . . . . 274
6.6.3. Resolution . . . . . 275
6.6.4. Example . . . . . 277
6.7. From optimization to control . . . . . 279
6.7.1. The predictive approach principle . . . . . 279

6.7.2. Example . . . . . 279
6.8. Conclusions. . . . . 280
6.9. Bibliography . . . . . 281

**List of Authors** . . . . . 287

**Index** . . . . . 291

# Preface

The increasingly competitive field of system design is driving designers to produce ever more efficient systems, minimizing investment, and ownership costs. The analysis, synthesis, and management methods presented in the book *Systemic Design Methodologies for Electrical Energy Systems* by the same editor and published by ISTE, and John Wiley and Sons, clearly contribute to the optimization of energy systems. However, the techniques, algorithms, and optimization tools explained in this book enable us to elucidate performance, as the number of inter-element and inter-domain couplings and interactions between the system and its mission and environment complicate the designer's task. The process of *design by optimization*, which consists of coupling a model to an optimization algorithm using software, is thus most useful. Multiple criteria, traditionally optimized for energy systems, involve geometry (mass or volume), energy efficiency (loss, consumption, pollution), and dynamic performance. These criteria are optimized under different constraints related to quality (harmonic content, electromagnetic compatibility (EMC)), stability, and technological consistency (thermal, magnetic, etc.). The inherent costs obviously need to be considered and enable coupling of various highly heterogeneous points of view: optimization thus becomes *technico-economic*.

Even while intensive research and development in this area continues, we see now how systems analysis through system simulation has matured, with the development of some particularly effective tools and solvers, such as Matlab/Simulink©, Saber©, Simplorer©, Modelica/Dymola© and VHDL-AMS. The use of virtual prototyping has thus become commonplace in industry to accelerate design cycles and minimize costs. The aeronautics industry is a particularly typical example of this, with the European MOET

project dedicated to more electrical networks in aircraft. In this project, Airbus, as leader and systems provider, imposed the delivery of multiple levels of analysis modeling ("functional, behavioral") on its 61 academic and industrial partners, in parallel with the equipment developed, in order to enable systems characteristic "electrical network" studies. Thus, while the last decade was notable for an "increase in power" of systems analysis by simulation, we can be sure that the current decade should see the advent of design by optimization; hence providing justification for this book to which it is entirely dedicated.

Chapter 1 deals with the coupling between the system, its environment, and the mission to be accomplished. It firstly proposes innovative approaches, enabling the representation of mission profiles or environmental variables (habitat, boundary conditions). The authors then propose classification and synthesis methods for profile processing. These approaches are of interest further along the design process and make use of optimization algorithms. Profile, notably mission classification, helps designers to segment the range of products designed. It may be based on "clustering" techniques. For the synthesis process, the idea is to present pertinent profiles with regards to the design criteria and constraints. Similarly, environmental and system mission profile information needs to be compacted where possible to facilitate processing within the context of optimization, which imposes a high number of iterations on the device models and environmental variables. These different approaches are illustrated using some typical examples, such as the design of an electric-diesel hybrid locomotive, including an electrochemical storage.

Chapter 2 deals with the *sizing model*, which is an essential aspect of design and optimization. According to Edgar Morin, one of the pioneers of the systemic approach introduced in *Systemic Design Methodologies for Electrical Energy Systems*, "the intelligibility of the complex occurs through modeling." However, while the word "model" can be used in many different ways, a design model, and more specifically referring to design by optimization, presents a number of specificities that the authors provide by more specifically insisting on analytical models that are well suited to the systemic context. Some examples of design models dedicated to electrical engineering, i.e. machines, electronic power converters, and related areas (such as mechanical transmission) are detailed. The different physical concepts that need to be jointly represented in order to be compatible with the design objectives are presented. The example of the optimization of a thermo-electric hybrid heavy vehicle is proposed by way of illustration.

The three main "pillars" of system design, namely, *architecture*, *sizing* and *management* are intimately linked. Thus, the sizing of an energy system cannot be carried out without thorough knowledge of the way in which the power flows between sources, storage and loads combined within an architecture. Chapter 3, therefore, presents the "simultaneous design approach", which is an eminently complex process, as different stages of the design process are coupled (integrated), stages that are often sequential for purposes of simplification. The use of optimization techniques is an effective way to enable such integration. This chapter explains how an optimization problem is raised; these problems are often multi-criteria and are nearly always under constraints. Amongst the various optimization methods, evolutionary algorithms are very well suited to solving highly heterogeneous problems with mixed variables (continuous and discrete). The hybrid locomotive example from Chapter 1 is used again in order to illustrate how the design problem is posed and resolved.

How do we handle the complexity of the system design process, particularly through optimization, given its multi-physical and multi-tasking context? Chapter 4 provides part of the answer to this question, with the aim of defining an effective approach to *design by optimization*. Two points are dealt with more precisely: complexity linked to *multiple levels of model granularity* (description detail), with techniques such as "space mapping" enabling us to pass from an accurate level of modeling to one that, although more "basic", is more "efficient" in terms of computation time. Secondly, complexity arising from different viewpoints and optimization levels: it would be unwise to optimize everything within one and the same loop, in order to enable simultaneous understanding of basic physical component behaviors, up to more "complicated" (in terms of size) and "complex" (in terms of interactions) systems. The design by optimization approach is therefore "multi-loop" and methods such as "target cascading" bring about tangible elements in order to move between levels.

Chapter 5 provides a vision of *future tools* for design by analysis and optimization, by illustrating the concrete case of the CADES framework. These tools, which use an architecture based on software components and cooperative modules, are armed to respond to model capitalization, reutilization, and interoperability problems in a vision system. Some automatic generation methods, which transform high-level or "professional formalisms" (such as electric circuits and three-dimensional representation) into executable programming code are associated with this. In this context, the authors have defined a software component standard called ICAr, which

is used for sizing by optimization. Having the Jacobian of the model available is a considerable asset in sensitivity analysis and in the implementation of gradient optimization algorithms. We thus show how it is possible to formally produce this Jacobian precisely and systematically. These components are also destined to be put together to form a more general system. Some sample applications of the CADES framework are provided, such as the optimization of an electromagnetic structure (transformer).

Chapter 6, "Technico-economic optimization of electrical energy networks", completes this book and concerns the optimum management of electrical networks. This optimization is found within the opening of energy markets, leading to a strong level of competition, which is forcing producers to optimize the management of production plants. The emergence of new technologies, combined with the growth in computation power has enabled the management of production installations to be improved. This chapter presents the modeling approach for this type of system, which must integrate the uncertainties linked to the unfamiliarity or simplification of the model with a view to its optimization, or the uncertainties stemming from the provisional nature and planning of the system operation (such as real consumer demand and economic fluctuations). Optimization of network management can be carried out using a deterministic linear programming model, or by using genetic algorithms. It can also be conducted on models that take uncertainties into account in order to propose more robust solutions. Problems corresponding to the approach are those relating to the assignment of units: several simple examples enable us to understand the various approaches and to judge their relevance.

**Recap of the key points discussed in *Systemic Design Methodologies of Electrical Energy Systems: Analysis, Synthesis, and Management* also published by ISTE**

Chapter 1 "Introduction to the systemic approach to design": this introductory chapter presents the history and basis of the systemic approach. A lexicon defines the main terms and concepts inherent in this vision.

Chapter 2 "Bond graph formalism, for an energetic and dynamic approach to the analysis and synthesis of multi-physical systems": the essential concepts of the bond graph are summarized, with attention paid to

its capacity for modeling of multi-physical systems and their energy exchanges. The inter-domain transformations between electricity and related domains (magnetic, mechanical, chemical, hydraulic, photonic, etc.) are represented. From the concepts of bond graph causality and bi-causality, an introduction to systems analysis (such as structural analysis and model reduction), synthesis and sizing is finally proposed.

Chapter 3 "Graphical formalisms for multi-physical energy systems: from COG to EMR": two other graphical formalisms, which complement the formalism above, are presented; they are specifically oriented towards the synthesis of control structures for energy systems. Causal ordering graphs (COG) consist of a functional description of elementary systems, taking into account the physical causality of sub-systems, which enable the control structure to be deduced through inversion of the model. Energetic macroscopic representation (EMR) is used for the functional description of more complex systems, graphically emphasizing the energy properties of sub-systems and their interactions.

Chapter 4 "Robustness: a new approach for integrating energy systems": robustness is inherent in the capacity of devices that need to function under rated conditions, including within an uncertain environment. An original approach, based on robustness using μ-analysis, is proposed in order to analyze and design integrated energy systems with a particular focus on control performance and system stability. The analysis strategy is illustrated by a case study linked to the sizing of an "HVDC" power channel for an electrical network for aircraft; this analysis is carried out with reference to dynamic criteria.

Chapter 5 "Quality and stability of direct current networks": a review of quality and stability methods is proposed in this chapter. After a summary of the standard principles in place for DC networks, a quality analysis method based on the causal analysis of interactions is described, before we develop a number of analysis techniques for asymptotic and general stability: analysis criteria such as impedance specification (Middlebrook) and the Routh Hurwitz criterion are presented. The development of analytical models in order to characterize impedance of the main power structures (power converters and motor drives) is also proposed. These approaches, which are specifically dedicated to DC networks, are applicable across many domains, such as aeronautics and space, shipping networks, and ground transport systems.

Chapter 6 “Energy management strategies for multisource systems, including storage”: this chapter begins with innovative energy management strategies for multisource systems hybridized by storage devices. Then, the authors focus on frequency based management strategies, which ensure power sharing between sources and storage devices. This power sharing is, itself, based on the attribution of a specific frequency range to each constituent, this frequency range being based on the energy and power density (Ragone diagram) of each constituent. These strategies are illustrated using typical case studies, particularly for autonomous systems for the decentralized electricity generation, ground transportation and embedded aeronautical networks.

Chapter 7 “Stochastic approach applied to the sizing of energy systems and networks”: whereas systems must be increasingly optimized in terms of performance, traditional electrical network sizing techniques are usually not suited to variations in the power of loads during operation. The authors therefore propose a method for forecasting power flow, based on probabilistic load models. A Monte Carlo algorithm thus allows designers to estimate density and probability functions on the power networks and their duration of occurrence. Some illustrations for an electrical network for aircraft enable the applicability of this approach to be analyzed.

Chapter 8 “Stochastic approach applied to safety in energy systems and networks”: the proposed methodology aims to estimate security indices for energy systems, particularly for distributed electrical grids. This method is based on a stochastic simulation using the Monte Carlo algorithm. It contains a methodology that is effective for simulating certain phases of the lifecycle of a network containing constituent defects.

Chapter 1

# Mission and Environmental Data Processing

## 1.1. Introduction

Energy systems design, particularly electrical, is nowadays increasingly influenced by social issues linked to energy economy policies and reducing the impact on the environment. To this end, numerous technical demands are added, such as volume and mass, lifetime, reliability (see Chapter 8, [ROB 12]), quality (susceptibility, harmonic pollution), stability (see Chapter 5 [ROB 12]), and recyclability. Being strongly linked to cost criteria, these demands require design to be tackled according to a "technico-economic" approach. Thus, the end of the 20$^{th}$ Century was marked by a notable evolution towards a more complete evaluation of costs over the whole of the lifecycle of the system (production, maintenance, and usage costs, even dismantling/recycling costs). Faced with these new considerations, designers are called upon to consider the environment in which their systems will evolve in more detail. Fundamentally, it is imperative to evolve toward a "systems design" approach from the outset; thus enabling an understanding of the coupling between system constituents and facilitation and the integration of the utility of the device and environmental variables.

---

Chapter written by Amine JAAFAR, Bruno SARENI and Xavier ROBOAM.

*Integrated Design by Optimization of Electrical Energy Systems* Edited by Xavier Roboam
© 2012 ISTE Ltd. Published 2012 by ISTE Ltd.

This heterogeneous and complex set of requirements is pushing designers towards a "simultaneous design" approach, which truly integrates systems design, as indicated in this introductory chapter (see also Chapter 1 of [ROB 12]). Simultaneous design is an approach that considers the system as a whole, where the fundamental questions of system architecture, sizing and management are integrated (see Figure 1.2). As we will see in Chapter 3 of this book, simultaneous design can be handled using optimization techniques, which is where multiple levels of difficulty are jointly associated with the design problem.

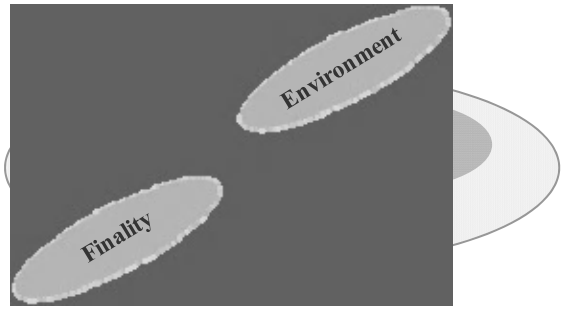


**Figure 1.1.** *Simultaneous systems design approach*

The integration of the "mission" (or finality) and environmental variables into the design process is particularly difficult, as the mission profile duration, and environmental variables (such as temperature, wind, and sunshine) are generally longer than the dominant time constants of the system, leading to significant processing times (simulation, optimization), which limit research into optimum solutions. This difficulty becomes all the more critical from the moment the system under design needs to satisfy not only a unique profile (mission and/or environmental variable), but a family or class of profiles with occasionally different characteristics. Indeed, in a profile database, there is generally no single "dominant" profile with regards to the set of design criteria and constraints (indicators); frequently, only a single part of a profile is "relevant" with regards to a first indicator, whereas another profile part is particularly constraining with regards to a second indicator, etc. The selection of a representative "sizing" profile is not therefore straightforward and constitutes an essential stage; it is an "integral part" of the systems design process.

Therefore, this current chapter presents a methodological approach aimed at mission and, more generally, environmental variable (mission, storage, boundary conditions) "profile processing". This approach constitutes the essential upstream phase of a systems design process. The first incontrovertible phase of the design process, the "classification" and "synthesis" of profiles relative to the environmental variables of the system, guarantees the quality of the device under design, and this is conditional on pertinent design criteria and constraints.

We place particular emphasis in this chapter on the contribution of our approach in the context of design by optimization, dealt with in Chapter 3, which, as it requires a large number of iterations (design solution evaluation), forces the use of "compact profiles" at a data level (such as time, frequency and statistical).

In this chapter, we provide a brief overview of how the mission and environmental variables are taken into account in the design process. We highlight the basic concepts of our new approach to processing these variables. We describe two applications, which will serve to illustrate our proposal; these examples concern the processing of railway missions for the design of a hybrid locomotive and the processing of wind energy resources. For each example, we formulate the set of pertinent indicators with regards to design criteria and constraints. These two deliberately very distinct examples enable the generic nature of the proposed methodological approach to be illustrated. Then, we discuss the classification of missions and environmental variables according to the design indicators, and describe the representative reduced duration mission synthesis process for which the characterization indicators correspond to the real data reference characteristics. Finally, we apply this approach to the "simultaneous design" by optimization of an economic hybrid locomotive in terms of energy and environmental respect.

## 1.2. Considerations of the mission and environmental variables

In this section, we propose innovations regarding integration and consideration of missions and environmental variables in systems design, particularly in electrical engineering and, more generally, for multiphysical energy devices.

### 1.2.1. *Mission representation through a nominal operating point*

The design of certain artifacts, such as electric motors, is often tackled by considering sizing at a nominal operating point [MES 98]. This point is easily identifiable for industrial applications, where the charge is considered to be constant and where the "traction" speed is set. This relatively simple approach is immediately challenged for electrical traction applications under variable conditions, where the operating points follow torque-speed trajectories. In principle, it is not easy to reduce the unit from a trajectory to a single nominal operating point, nor is it very pertinent. For the nominal sizing point, a possible simplification consists of considering a point relative to the maximum torque and speed of the trajectories, i.e. a point that energetically controls the trajectory points. This approach enables a response to the problem of energetic sizing, but mostly results in an undersizing of the system relative to the total requirement. In addition, the energy efficiency of the system is optimized in an operating zone close to the nominal point, which does not necessarily correspond to points of the highest occurrence points. It is therefore possible, within a second approach, to consider as a sizing point some particular operating points (such as the point of highest occurrence), but this solution may conversely result in "oversizing", which does not enable the whole of the trajectory to be satisfied. Finally, the recent experience of the LAPLACE/GENESYS research group [DEA 12] has shown that certain points that were not energetically relevant could turn out to be critical, with regards to certain design criteria or constraints; one example is the case of normative quality constraints of wave forms at the input of an actuation system, which are violated during low speed, yet "power hungry" operation.

### 1.2.2. *Extraction of a "sizing" temporal chronogram*

Here, this type of approach is illustrated using the design of an electrical aeronautical emergency network as an example [LAN 06]. This involved the sizing of a basic hybrid emergency network for a ram air turbine (RAT) acting as a source of energy, ensuring a power level close to the average power associated with a storage element acting as a power source in order to feed the fluctuating part of the mission. In this scenario, the power required is defined through the use of "essential" network charges in the case of total motor loss. An emergency mission sample is then established indicating the different flight phases in the case of complete motor loss. As this sample is specified over a long time interval (around 30 minutes), it may be useless,

and tiresome, to apply this to the whole mission, as that would lead to rather prohibitive simulation times. Therefore, the aim is to analyze the dynamic behavior of the system with adequate modeling levels. For this emergency mission, only the most critical energy need has been extracted by expertly localizing a phase considered to be "relevant" and of reasonable duration with regards to the objectives of systems analysis; this phase, which corresponds to a low altitude and low speed turbulent environment configuration, constitutes a critical part for the emergency source. Indeed, this refers to a phase during which the principal charges fed in emergency mode and the flight controls are the subject of high-powered maneuvers, whereas the relative wind at the RAT is of low intensity.

This simple and pragmatic approach has been well used in systems design. However, its main disadvantage is with regards to the representativeness of the extracted profile, which is not formally assured as far as all of the design indicators (criteria/constraints) are concerned.

### 1.2.3. *Representation of an environmental variable or mission resulting from statistical analysis*

#### 1.2.3.1. *Use of statistical distributions of environmental variables*

The taking into account of relative statistical occurrences at operating points of a system is fundamental if we want this to be best optimized across the whole operational cycle. As a first approximation, we can consider the mission to be a succession of static conditions balanced by their occurrences. The disadvantage of this method is the absence of consideration of dynamic aspects linked to the transitions between the different operating points. However, if these behaviors are not preponderant in general reporting, it may turn out to be pertinent and offer a particular interest with regards to the minimizing of computation times. Additionally, we note that it is quite possible to synthesize temporal samples from statistical occurrences if we want to retrospectively include dynamic aspects. This approach was notably used for wind signal generation for the wind energy industry. It consists of generating a reduced duration temporal signal by using a random number generator with a probability density of the real wind statistical distribution [ABD 07].

1.2.3.2. *Use of classification methods*

Within an increasingly significant ecological context, Europe has recently become involved in the standardization of requirements, notably in the area of transportation. For example, in the automobile sector, although standard cycles enable a comparison to be established between the consumption and pollution of vehicles within the same European sphere, the latter hardly describe the actual usage conditions of the vehicle. In order to remedy this insufficiency, IFSTTAR (*Institut Français des Sciences et Technologies des Transports, de l'Aménagement et des Réseaux* – French Institute of Transport Science and Technology, Organization and Networks), along with other partners, is committed to determining representative cycles of vehicle usage and operating conditions. The idea is to extract representative speed profiles from significant database analysis, or, more precisely, to classify actual recorded traffic sequences, on the one hand according to the traffic conditions (such as speed, acceleration, temperature, and traffic location), which give rise to typical classifications, and on the other to usage conditions (such as routes, distance, and starting conditions), which enable route classification (urban, road, and motorway) to be defined [JOU 99; AND 04]. The cycles selected are typically determined according to a chain or sequencing of representative profiles of the classes obtained.

A second example concerns wind energy resource analysis, where temporal wind speed sequences, characterized by similar static distributions, are grouped into classifications. This similarity can be described using the first statistical moments (mean, standard deviation) [CAL 04], or more precisely using all of the characteristics of the statistical distribution, by considering all of the statistical moments [CAL 11]. The distribution obtained suggests, for a given number of classes, the standard distribution defining each class, as well as the associated probability that a sequence belongs to a class. The representative temporal chronogram for each class is then obtained from the statistical characteristics of its standard distribution.

## 1.3. New approach for the characterization of a "representative mission"

The innovation presented in the last section has drawn attention to the significance of the notion of "mission sizing" within the context of systems design. However, the methods set out, even if they appear to satisfy under certain circumstances, still present some limitations. For example, for the case of the extraction of a relevant temporal chronogram with reduced

duration, the designer ignores the information content of the initial mission, which contributes, however greatly, to the system performance specification. Furthermore, it is not always easy to recognize the most constraining (in terms of scalability) "part" of the mission, with regards to a heterogeneous set of criteria and constraints, particularly when a family or full set of missions is available. Frequently, this portion of the mission is scalable (a power ridge, for instance) according to certain criteria, whereas another might be in relation to some other constraint (energy or thermicity, for example), and so on.

In order to remedy some of these limitations, one solution consists of simulating all missions or environmental variables from the list of specifications, in order to evaluate system design performance, criteria and constraints. However, this solution is rarely acceptable, as it greatly increases computation times, which often turn out to be prohibitive, particularly in designing optimization features for which the mission profile is "replayed" many times during convergence of the process. The analysis and simplification (compacting) of missions and/or environmental variables therefore appears to be an essential stage in the improvement of design effectiveness. They enable the best possible and most effective (regarding heterogeneous criteria, such as energy efficiency, lifetime and cost) sizing solutions to be established. In the design process it is, in fact, more judicious to consider a single pertinent mission, which is of low duration and representative of all missions (reference database)[1]. This final essential point is the subject of this chapter.

### 1.3.1. *Characterization indicators of the mission and environmental variables*

The representative profile synthesis approach that we are proposing in this chapter is particularly based on the definition of pertinent characterization indicators with regards to systems design. More specifically, this concerns determining the essential characteristics of the system being designed: temporal (such as maximum and mean power, harmonic distortion, and energy), frequency (such as cyclability and quality) and statistical (such

1 In the interests of clarity, we use the term "profile" to describe the mission (finality) of a system, or more generally one of its environmental variables. By "real profile" ($P_{real}$) we refer to the mission or environmental variable actually measured and available in "database" form, and by "fictive profile" ($P_{fictive}$), the mission or environmental variable processed (synthesized profile of shorter duration).

as occurrences and probability density) characteristics. This system expertise thus enables us to obtain a definition or mathematical formulation of the indicators used. The reference indicator values are derived directly from one or more of the real profiles (see Figure 1.2). The information content of the compact fictive profile generates values for these same design indicators: the synthesis process converges from the moment that the profile indicators generated correspond to the reference indicators.

Generally, two families of indicators are identified: sizing and performance indicators. The first of these is relative to the design constraints, which impact directly on the architecture, sizing (such as the size of the system's various energy blocks and the mass/volume constraint), and energy management of the system. The second family is relative to the performance criteria (notably energy efficiency, cycling, and lifetime).

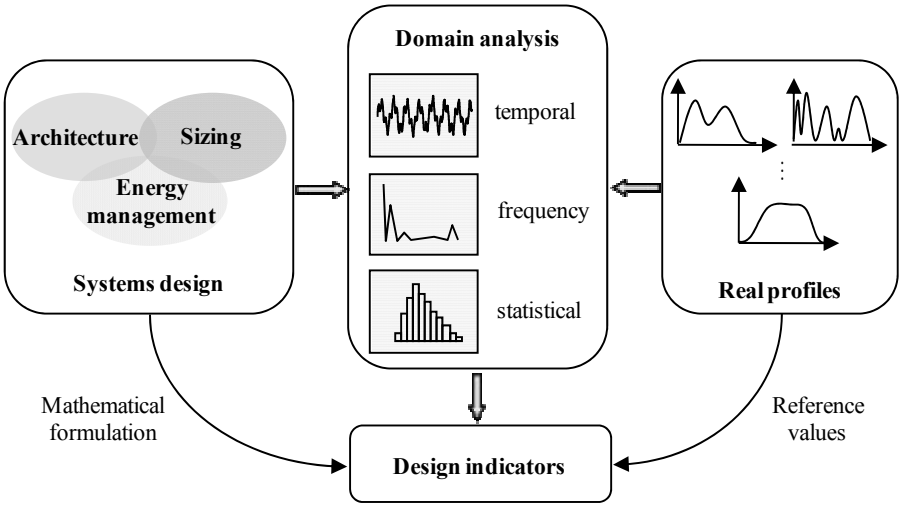


**Figure 1.2.** *Extraction of characterization indicators for the mission and environmental variables*

We now proceed to the extraction of design indicators, based on two illustrated examples.

1.3.1.1. *System design of a hybrid locomotive*

This first example exists within the context of the PLATHEE (*PLAte-forme pour Trains Hybrides Économes en Énergie et Respectueux de*

*l'Environnement* – Platform for energy and environmentally efficient hybrid trains) project, undertaken by ADEME and directed by the French railway operator SNCF [THI 08]. Within the context of this project, SNCF and GENESYS (*Groupe de recherche en Énergie Électrique et Systémique* – Electrical and systemic energy research group) from the LAPLACE laboratory (*Laboratoire Plasma et Conversion d'Énergie* – Plasma and energy conversion laboratory) were focused on the design, sizing, and energy management of an autonomous hybrid locomotive, which was ecologically clean and which needed to fulfill the same missions as a diesel-only locomotive. Diesel-electric hybridization consists of replacing the initial diesel engine by another, much smaller engine, and complementing the lack of power using a storage device; in practice, within this project, a double hybridization using Ni-Cd (nickel-cadmium) accumulator batteries and ultracapacitors was considered, but here we are simplifying the structure by only considering a single storage device (simple hybridization using batteries), conforming to the following synoptic chart. The energy management strategy ensures that the diesel engine provides the average power for the mission and that the batteries ensure the fluctuating power (see Figure 1.3).

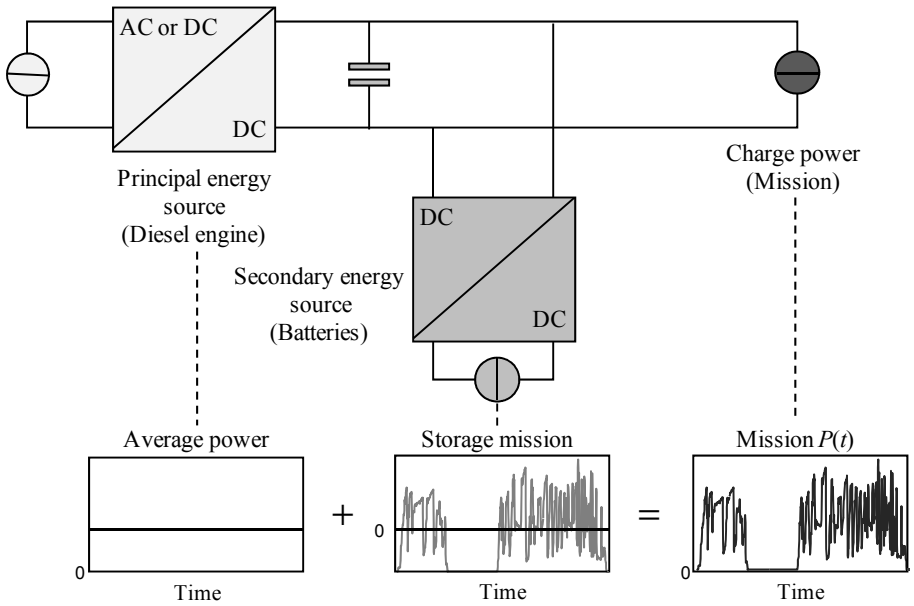


**Figure 1.3.** *Architecture and energy management of the hybrid locomotive*

Two families of indicators are defined in this example: three sizing indicators enabling the specification of the energy/power characteristics if the energy sources and two performance and lifetime indicators.

The sizing indicators are:

– The maximum power to be provided: $P_{max}$

In order to satisfy the mission(s) from the specification list, the system being designed must be capable of providing the increased peak power for all of the reference data.

$$P_{\max} = \max_{t \in [0, \Delta t_{miss}]} P(t) \qquad [1.1]$$

where $P(t)$ is the instantaneous power of the reference mission of duration $\Delta t_{miss}$.

– The average power to be provided: $P_{avg}$

According to the energy management strategy previously set out, the average power of the mission is a fundamental indicator with regards to sizing the principal energy source. In other words, the nominal power of the diesel engine ($P_{NDE}$) must correspond approximately to the average value of the mission signal.

– The useful energy of the storage system: $E_u$

The useful storage energy represents the amount of energy necessary in order to satisfy the storage mission by taking into account the charge and discharge phases. $E_s(t)$ is used to represent the instantaneous evolution of energy in the storage device[2]:

$$E_s(t) = -\int_0^t (P(\tau) - P_{avg})\, d\tau \text{ where } t \in [0, \Delta t_{miss}] \qquad [1.2]$$

The useful energy is thus defined by:

$$E_u = \max_t (E_s(t)) - \min_t (E_s(t)) \qquad [1.3]$$

2 The minus sign in equation [1.2] respects the following sign convention: with regards to the storage element, charge powers are positive, whereas discharge powers are negative.

The performance and lifetime indicators are:

– The statistical distribution of the mission: $I_{stat}$

The statistical indicator represents the average energy efficiency of the system through occurrences of power levels during the mission. It is expressed by the statistical distribution (frequency histogram) of the mission, or equally by its distribution function (cumulative frequency statistics).

– The number of cycles imposed at the storage system: $Nb_{cyc}$

We consider the number of cycles used per battery pack as a typical indicator of lifetime. The count of the number of cycles is based on the "Rainflow" method [DRO 97; BAE 08]. The number of equivalent cycles ($Nb_{cyc}$) is then obtained by the weighted sum of cycles based on their depth of discharge. The weighting coefficients result from the construction curve, which gives the number of complete cycles that the storage element is capable of providing, based on its depth of discharge (a characteristic known as "cycle to failure").

This example is resumed in Chapter 3, which covers simultaneous design by optimization.

1.3.1.2. *Processing wind speed for the design of a wind turbine*

This second example aims to illustrate the processing of environmental variables. This belongs to the context of the optimum design of a wind turbine system. It therefore deals with processing wind speed (the primary energy vector) with a view to integrating it into a simultaneous design by optimization process, in order to reduce the processing cost. Note that, in this application, we are limiting ourselves to the processing of wind speed in order to synthesize a shorter representative profile that respects a set of design indicators pertinent for wind turbine systems.

The temporal and statistical wind speed analysis phase has enabled the exposure of two families of indicators, established with regards to typical wind energy design criteria.

The sizing indicators are:

– The maximum speed: $V_{max}$

This indicator reflects the effect of gusts of wind during sizing of the wind turbine.

$$V_{\max} = \max_{t \in [0, \Delta t_{profile}]} V(t) \qquad [1.4]$$

where $V(t)$ represents the instantaneous wind speed on a temporal horizon $\Delta t_{profile}$.

– The average cubic speed: $<V^3>$

This refers to an energetically highly pertinent indicator, since is reflects the useful average power captured by the wind. Indeed the useful instantaneous power of the wind turbine is directly proportional to the cubic speed of the wind.

The performance indicators are:

– The statistical distribution of the wind speed: *pdf*

It is important to consider the statistical distribution of the wind speed (probability density function (pdf)) in wind turbine design. The fictive profile that we are proposing to generate must therefore follow the same real wind speed statistical distribution, measured over a very wide horizon. Amongst the probability distributions, which may characterize the wind speed statistical distribution, we note the log-normal, bivariate Gaussian and Weibull distributions. The Weibull distribution is traditionally considered as being the most adequate, with statistical properties of real wind [KEL 92].

– Wind turbulence: $I_{turb}$

Wind turbulence is a crucial phenomenon in estimating the lifetime of wind turbines, notably in evaluating its mechanical fatigue. It is therefore important to integrate a turbulence characterization indicator into the representative temporal signal. Often the rapid dynamic of wind speed is modeled, over each sampling period $T_e$ (typically 10 minutes), using a Gaussian distribution with a null mean and standard deviation $\sigma$ [STR 90]. We thus characterize wind turbulence, over each interval $i$ of time $T_e$, by the standard deviation $\sigma_i$ of the corresponding Gaussian distribution. We thereafter define the turbulence indicator $I_{turb}$ over the whole wind profile by the mean value of the standard deviations $\sigma_i$.

$$I_{turb} = <\sigma_i> \text{ where } i = [1, \text{integer part}(\Delta t_{profile} / T_e)] \qquad [1.5]$$

### 1.3.2. *Mission and environmental variables at the heart of the system: an eminently systemic bidirectional coupling*

Most of the time, the effect of environmental variables (such as temperature and ambient pressure, sunshine and wind speed) on the system, as well as the success of the mission, are represented unidirectionally, marking the boundary conditions of the device. In other words, the environmental variables have an influence on the system and affect its evolution, but we consider that the evolution of the system caused by variations in environmental variables has no impact on the environment itself.

It should be noted, on a global level, that this unidirectional vision of the environment is nowadays increasingly being challenged, notably by the environmental footprint concept. In such a case, the environment (here, the Earth's atmosphere) becomes an integral part of the Earth system and interacts bidirectionally. In general, if we go a little further into this reflection, we can show that a bidirectional coupling between system and environment may also exist at an artifact level. The designed system, according to a set of criteria and constraints, may, in some way, influence its mission and environmental variables, or rather the "representation that we ourselves make of these environmental variables" (see Figure 1.4); more specifically, the way in which the system is designed, where its operational characteristics (indicators) may influence the representation of the mission itself or of certain environmental variables.

This is, for example, typical of electrical vehicle design, for which the driving method is clearly different from that of a traditional thermally driven vehicle; we can thus refer to "eco-driving" from the moment that the driver of the electrical vehicle takes note of its energy gage (the state of battery charge), or changes his braking habits in order to favor electrical recovery; in this typical case, the "eco-driving mission" is modified by the characteristics of the designed system. The example of the PLATHEE hybrid locomotive is also typical insofar as SNCF established speed profiles by taking account of the hybrid characteristic of propulsion and its sizing; we could even consider going as far as optimizing the mission profile in order to fully profit from storage, in order to consume/pollute everything by ensuring a minimum of comfort and performance (hourly).

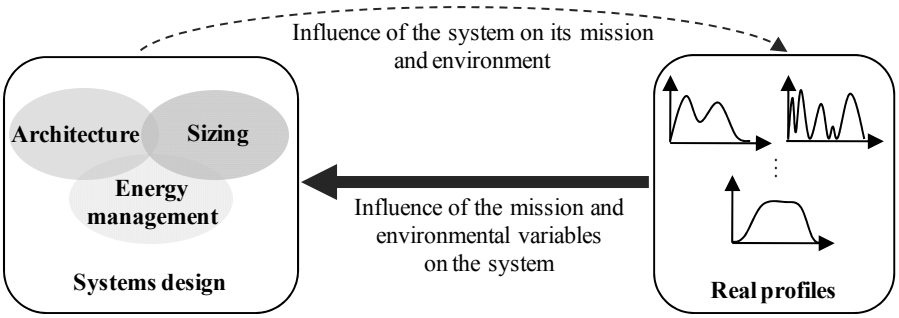


**Figure 1.4.** *Bidirectional coupling between the system and its environment*

Here we are faced with a system coupling between the environment (mission) and the system under design, which is certainly exciting, but rather complex, as "everything depends on everything and its opposite…" This fundamental question is described more generally and virtually metaphysically in the introductory Chapter 1 of [ROB 12], which evokes the concepts of finality and "teleology", which have been introduced as essential elements by the pioneers of systems design. The designer must, therefore, face up to this new coupling, the method of classification and synthesis proposed here, which aids design at this level.

More specifically, according to our representative fictive profile synthesis approach ($P_{fictive}$), the way in which we propose to process the reference real profile ($P_{real}$) intimately depends on the design of the system through definition of the design indicators. The result is therefore that the system design characteristics have a strong influence on the fictive profile being generated, which will be considered to be a "relevant profile". At this level, we therefore also introduce a bidirectional coupling between system and environment (see Figure 1.5). For example, for a wind chain, the peak value of the representative fictive profile ($P_{fictive}$), must imperatively correspond to the maximum real wind speed value, which constitutes a typical sizing indicator of the wind system.

However, this raises an additional and complex coupling problem. Indeed, in certain system classes, it is occasionally necessary to define some *a priori* assumptions in order to specify the full set of reference design indicators. These assumptions concern system design characteristics, relative to architecture and/or sizing and/or energy management. The example of the hybrid system in Figure 1.6, comprising a principal energy source (diesel

engine) and a storage device, is a good illustration. Indeed, these two energy sources are connected through an energy node in order to satisfy one or more charge profiles. Yet, in order to correctly size the storage element, taking account of criteria and constraints that are pertinent to the system (such as consumption and lifetime), we are obliged to make an *a priori* assumption on the principal energy source sizing approach, and this occurs even before initiating the fictive profile synthesis process. We thus assume, in principle, that the principal source will ensure the mean value of power consumed. This assumption, which here touches on energy management and sizing, is necessary in order to specify the reference indicators, which are energy characteristic indicators. However, we are therefore faced with a supplementary coupling between "fictive profile" and "systems design", such as that illustrated in Figure 1.5.

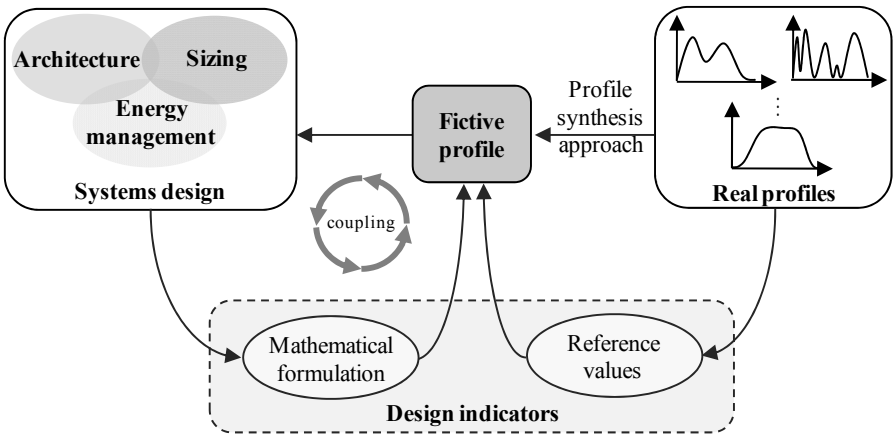


**Figure 1.5.** *Bidirectional coupling between the system and its sizing fictive profile*

The previous analysis, linked to the processing of the mission and environmental variables within the context of a systemic approach, has enabled us to raise a set of couplings between the profile synthesis approach, choice of characterization indicators, and characteristics of systems design (Figure 1.7). These couplings perfectly illustrate the foundation of the systems approach, whereas its pioneers, such as *Bertalanffy* [BER 73], evoke notions of "integrating the finality (mission) to the design" or of "purpose-built models". In short, "the mission, or rather the representation that we make of it, is situated right at the heart of systems design".

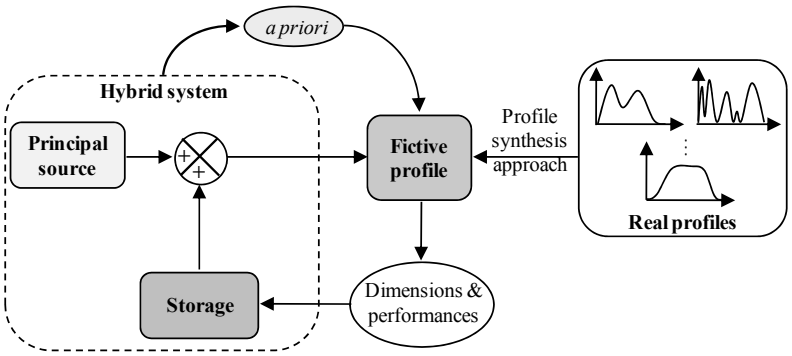


**Figure 1.6.** *Architecture of a hybrid system with storage*

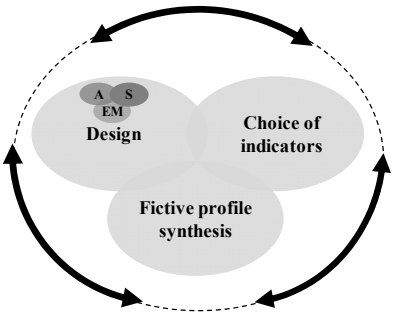


**Figure 1.7.** *The fictive profile synthesis approach at the heart of systems design*

## 1.4. Classification of missions and environmental variables

From the systems point of view, the classification of mission profiles, or, more generally, of environmental variables according to pertinent indicators with regards to design criteria and constraints, is part of a set of decision-making tools and constitutes a ridge phase, which is essential to the design process. Indeed, it must enable the designer to evaluate the interest in a device, which is specifically optimized for a given class, relative to the mission and/or environmental variable profiles, and this is compared with a device capable of simultaneously satisfying a set of classes. In other words, taking the well known example of the car, "what do we gain by classifying and segmenting a vehicle range (urban, road, off-road, etc.) from the point of view of the cost/performance ratio, and this with regards to usage and its occurrences?"

Classifying or segmenting may thus enable a notable improvement in certain criteria, such as the energy efficiency of the system. This is the case, for example, when, regarding a classification according to energy indicators, the segments or classes obtained are different from the commercial segmentation or usage of the system.

### 1.4.1. *Classification without* a priori *assumption on the number of classes*

The most widespread unsupervised classification techniques (where no information on the class of the element is provided) are: the aggregation method around cluster centers, also called the K–means method [FOR 65; MAC 67], the hierarchical classification and the mixed classification [LEB 00]. Nevertheless, the disadvantage of these methods is the requirement to know the number of classes. In principle, this parameter is fixed for the aggregation method around cluster centers and mixed classification, and in the case of hierarchical classification, is determined by expertise in partitioning trees.

The problem of choosing the number of classes has been solved following the appearance of partitioning criteria, indicating a compromise between maximization of inter-class and minimization of intra-class distances. Numerous partitioning criteria can be used [SHE 05]. The most widely used are the Davies-Bouldin (DB) [DAV 79], Calinski and Harabasz (CH) [CAL 74], and silhouette (SIL) [KAU 90] indices. The method of classification without *a priori* assumption on the number of classes consists of optimizing one or more of the partitioning criteria by integrating the number of classes into an optimization parameter [JAA 10a]. This allows the optimum number of classes of dataset to be determined, and, at the same time, individuals to be assigned to appropriate classes. In general, even if the number of classes has already been fixed, classification problems are highly multimodal. This multimodality is all the more acute when the number of classes becomes variable. Faced with this type of typically multimodal problem, the niching genetic algorithms (GA) generally offer interesting performances by reducing the risk of premature convergence towards a local optimum, as we will see in Chapter 3 of this book [SAR 98].

In [JAA 10a], we developed a genetic algorithm for the classification of data with a number of variable classes. We chose the silhouette index as the partitioning criterion. This algorithm is based on the use of restricted tournament selection (RTS) [HAR 95], as well as a self-adaptive

recombination technique [NGU 08], with the objective of maximizing the silhouette index. In the following section, we present an application of this algorithm to benchmark railway mission classifications.

### 1.4.2. *Mission classification for hybrid railway systems*

In this section, we study a mission classification example, which is useful in the sizing of integrated hybrid energy sources in multi-segment railway traction chains; the requirement (mission) specified in the study is the provision of power $P(t)$. The architecture of these hybrid energy sources is based on a coupling between a principal energy sources (for example, a diesel engine or overhead line) and a secondary source, which is often represented by a storage organ (such as batteries and ultracapacitors), as explained in the last section (see Figure 1.3).

This example constitutes a "benchmark" of 105 railway missions and enables the interest in classification to be illustrated in a multi-segment hybrid power systems design context. It comprises three subsets of missions from three different railway systems: the BB63000 and BB460000 locomotives and the TGV POS (*Paris – Eastern France – Southern Germany*) auxiliaries. As far as the first two systems are concerned, this refers to two diesel locomotives with nominal power of 610 kW and 1 MW, respectively. The third railway system is different from the first two. Here the power source of the TGV auxiliaries is hybridized relative to passenger comfort (such as heat, climate, lighting, and catering). The hybridization of these auxiliaries thus consists of embedding storage bricks that are exploited in the absence or presence of the catenary.

All of the missions are characterized according to the triplet of sizing indicators $\{P_{max}, P_{avg}, E_u\}$ introduced in section 1.3.1.1. The numbers of missions per initial class assigned, as well as the positions of the corresponding barycenters, are summarized in Table 1.1.

| | Number of missions | Barycenter coordinates ($P_{max}$ (kW), $P_{avg}$ (kW), $E_u$ (kWh)) |
|---|---|---|
| TGV auxiliaries | 63 | (189, 80, 13) |
| BB 63000 | 15 | (455, 91, 24) |
| BB 460000 | 27 | (711, 35, 50) |

**Table 1.1.** *Characteristics of 105 initial missions from the three railway systems*

The representation of the subsets of initial missions according to the triplet $\{P_{max}, P_{avg}, E_u\}$ is given in Figure 1.8a. Their barycenters are also represented by the plain motifs. The classification result is given by Figure 1.8b. The class characteristics found are also given in Table 1.2.

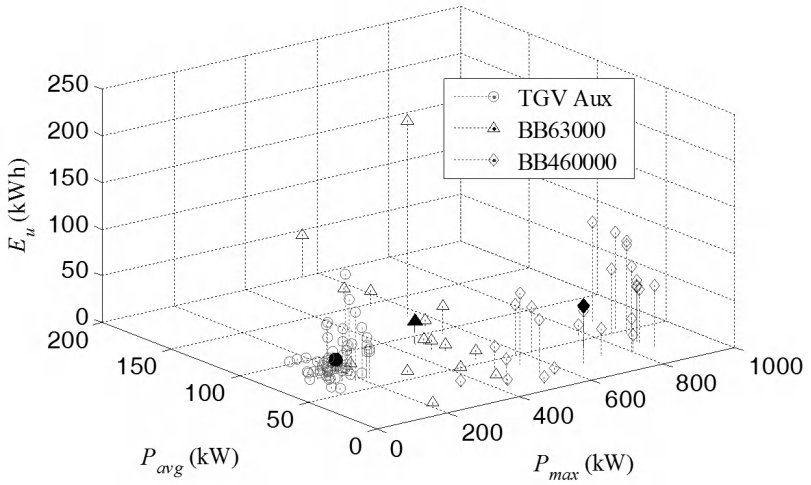


(*a*) *Initial distribution of missions*

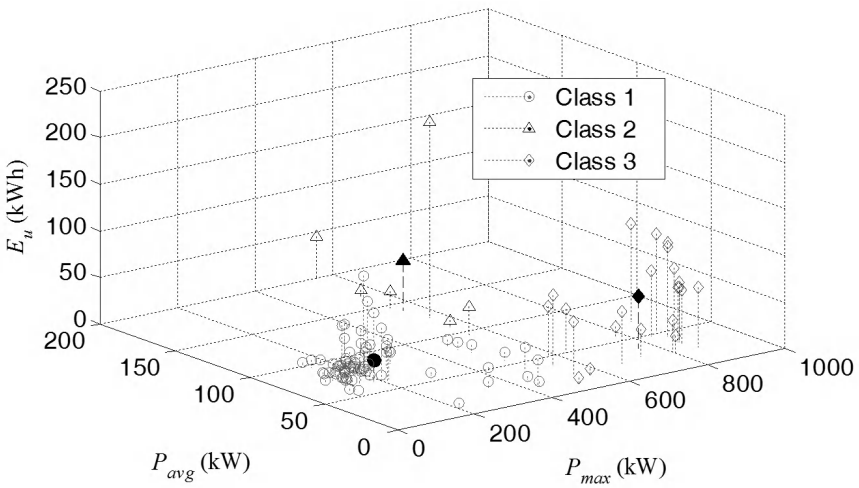


(*b*) *Classification result*

**Figure 1.8.** *Mission classification examples of three railway systems*

We observe that we can practically obtain the initial classification by identifying three different classes. The difference between the initial classification and that resulting from the genetic algorithm is only 12% (13 missions are not assigned to their original classes). This difference is not due to bad convergence of the algorithm. Indeed, although three different power systems are available, nothing prevents their missions from presenting similar energy/power indicators $\{P_{max}, P_{avg}, E_u\}$. Figure 1.8b shows that all missions are generally correctly classified, apart from those belonging to the recovery zone of the initial subsets. Within this low power and low energy area, missions can be achieved by the three power systems.

| | Number of missions | Barycenter coordinates ($P_{max}$ (kW), $P_{avg}$ (kW), $E_u$ (kWh)) |
|---|---|---|
| Class 1 | 76 | (225, 75, 13) |
| Class 2 | 6 | (553, 141, 53) |
| Class 3 | 23 | (762, 37, 56) |

**Table 1.2.** *Characteristics of classes obtained after classification*

From this example, we have not only validated the effectiveness of the classification method, but also shown the usefulness of such an approach in an environmental variables analysis process (here, mission profiles) in advance of system design. Classification may thus form part of a decision-making tool in the absence of *a priori* assumptions on the environmental variable profiles brought into play. For example, let us assume that we have no information on the initial classes assigned (BB63000, BB460000 and TGV auxiliary) from the 105 railway missions thus processed; it is as a result of the classification that we will obtain three different segments. In such a configuration, the designer will raise the question of the cost-effectiveness of designing a "catch all" hybrid power system, which satisfies all missions, or, conversely, a system per mission class. In section 1.6, we will discuss an example of system design that makes use of classification and segmentation.

The fact that three families of missions are obtained owing to classification, corresponding strongly to the initial classes, proves the pertinence of the mission characterization indicator triplet $\{P_{max}, P_{avg}, E_u\}$. In section 1.6, we will see how these indicators will serve as the basis for the synthesis of a representative mission of a class or family of missions.

## 1.5. Synthesis of mission and environmental variable profiles

Following on from the classification methodology of the mission and environmental variable profiles presented in the last section, the question that comes to mind is knowing how to best integrate the set of profiles from one class into a system design approach. In other words, we are looking to represent the information of the set of profiles using a single shorter representative fictive profile, in order to minimize simulation costs within a system design process, particularly in the context of simultaneous design by optimization. We are developing a temporal profile synthesis method to enable a signal to be constructed, whereby the design indicators correspond to the reference indicators determined from a set of real profiles.

### 1.5.1. *Mission or environmental variable synthesis process*

The shorter representative profile synthesis process is based on the reconstruction of a mission or environmental variable profile by concatenation or aggregation of elementary patterns. Through an appropriate parametering of these patterns, the problem will be solved using optimization [JAA 10b]. Indeed, it is a matter of finding a good range of pattern parameters, such that the system obtained satisfies a given set of design indicators for the environmental variable in question. Three types of simple patterns are implemented: the sine, cardinal sine, and the segment. In the following section, we will return to the details of these patterns.

The fact that a complex signal with strong variability is generated requires an increase in the number of patterns, which notably increases the complexity of the optimization problem. Furthermore, as a consequence of the particularly oscillatory form of the patterns processed above (specifically for the sine and cardinal sine), the opposite resultant problem is often multimodal. Genetic algorithms are particularly well suited to solving this type of problem. In this sense we propose the use of a genetic algorithm, with the "Clearing" method being used as the niching operator [PET 96] associated with a self-adaptive recombination procedure [NGU 08].

The profile synthesis by optimization process is shown in Figure 1.9. The first stage consists of building the environmental variable signal or profile $S(t)$ from the $\mathbf{x}$ chromosome generated using the genetic algorithm, using the concatenation or sum of $N_m$ elementary patterns, characterized by $p$ parameters. The duration $\Delta t_{profile}$ of the obtained signal is considered to be a

problem input. Although we are taking care to ensure that the synthesized profile is as compact as possible, the choice of its duration must check certain constraints relative to the design indicators. In the following stage, we proceed to the computation of the profile indicators thus generated. These are then compared with the reference indicators $I_{jref}$ and hence enable the *error function* $\varepsilon$ (the function to be minimized using the genetic algorithm), expressed by equation [1.6], to be evaluated. This function is defined as the sum of standardized quadratic errors from the following set of indicators:

$$\varepsilon = \sum_j \left( \frac{I_j - I_{jref}}{I_{jref}} \right)^2 \qquad [1.6]$$

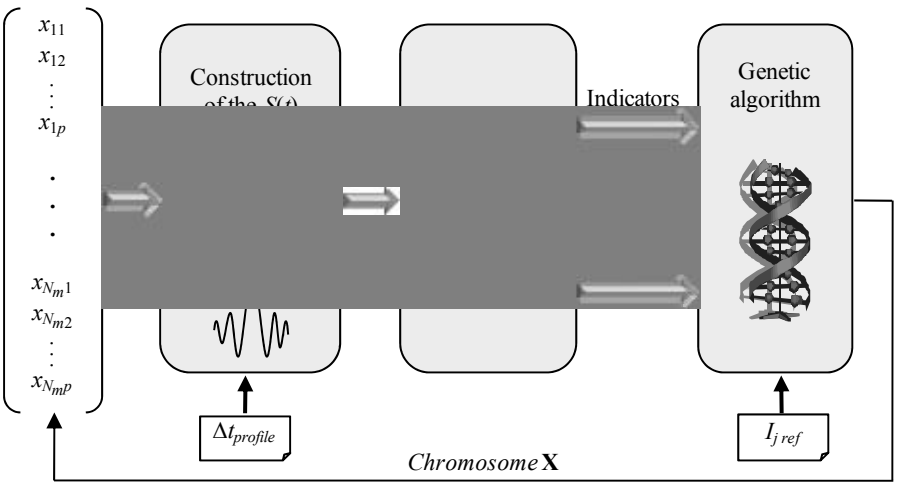


**Figure 1.9.** *Mission or environmental variable profile synthesis process*

Beyond the quadratic distance between indicators and reference values, it may be necessary to impose certain constraints on the signal generated. These constraints (denoted $g_k$) are formulated in terms of inequalities ($g_k$ (**x**) $\leq 0$) and integrated in the error function as a form of penalty:

$$\varepsilon = \sum_j \left( \frac{I_j - I_{jref}}{I_{jref}} \right)^2 + \sum_k \lambda_k \max(0, g_k(x))^2 \qquad [1.7]$$

where $\lambda_k$ is the penalty factor associated with the corresponding constraint. The value for this coefficient must be wisely chosen in order to guarantee a balanced "weight" between the different constraints when they are being violated and a sufficiently significant penalty, compared with the errors for different indicators.

### 1.5.2. *Elementary patterns for profile generation*

We are looking to model the real temporal profile of the mission or environmental variable using elementary patterns with low numbers of parameters. Indeed, for more significant numbers of parameters for a pattern, the complexity of the signal synthesis by optimization problem is higher. Three types of elementary pattern are proposed in order to represent the signal corresponding to the environmental variable.

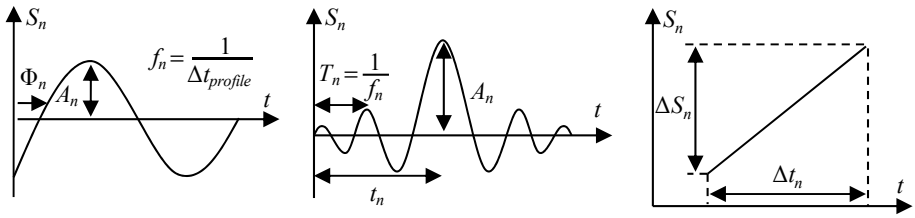


(*a*) *Sine* (*b*) *Cardinal sine* (*c*) *Segment*

**Figure 1.10.** *Elementary patterns*

The first model considers profile $S(t)$ as being the sum of the average value and a certain number of harmonics characterized by their amplitudes, phases and frequencies. An elementary pattern is none other than a harmonic with rank $n$, characterized by three parameters: an amplitude $A_n$, phase $\Phi_n$ and frequency $f_n$, which is a multiple of the inverse of the desired profile duration $\Delta t_{profile}$, as shown in Figure 1.10a.

The second model is based on the use of the cardinal sine. The principle of generating a profile or signal is identical to that of the sine method, i.e. the

adding together of $N_m$ cardinal sines, each characterized by three parameters: an amplitude $A_n$ ($0 \leq A_n \leq S_{max}$), frequency coefficient $f_n$ ($f_{min} \leq f_n \leq f_{max}$), and a temporal localization coefficient $t_n$ ($0 \leq t_n \leq \Delta t_{profile}$), as illustrated in Figure 1.10b. Finally, the segment model consists of representing an environmental variable profile by a concatenation or aggregation of $N_m$ segments. For the synthesis process in Figure 1.9, an elementary pattern is a segment characterized by its amplitude $\Delta S_n$ and duration $\Delta t_n$, as shown in Figure 1.10c.

### 1.5.3. *Application to the compacting of a wind speed profile*

This example, which was introduced earlier, concerns the system design of a wind chain for which the environmental variable is wind speed. In order to optimize the processing cost during phases of design by optimization, it is thus wise to consider a wind speed profile of minimum duration, but which remains pertinent with regards to design criteria and constraints. We apply the representative profile synthesis process previously described for the compacting of 2 months of wind speed measurements at the "Petit-Canal" site in Guadeloupe [CAL 11], with a sampling step of 1 second.

Let us recall that the design indicators relative to wind characterization are: the maximum speed $V_{max}$, average cubic speed $<V^3>$, statistical distribution *pdf*, and the turbulence indicator $I_{turb}$. In addition to these design indicators, we impose a constraint relative to the dynamics of wind speed: the maximum wind speed gradient (acceleration of air mass). For the data from the wind speed site at "Petit-Canal" in Guadeloupe, the maximum gradient is 12 m/s$^2$. In the representative profile synthesis by optimization process, this constraint is expressed as follows:

$$g = \frac{dv}{dt} - 12 \leq 0 \qquad [1.8]$$

Many tests have been carried out using the three elementary patterns (sine, cardinal sine, and segment). The best results are obtained using the segment pattern. Figure 1.11 gives a result for a 3 hour representative profile synthesis obtained by the concatenation of 217 patterns.

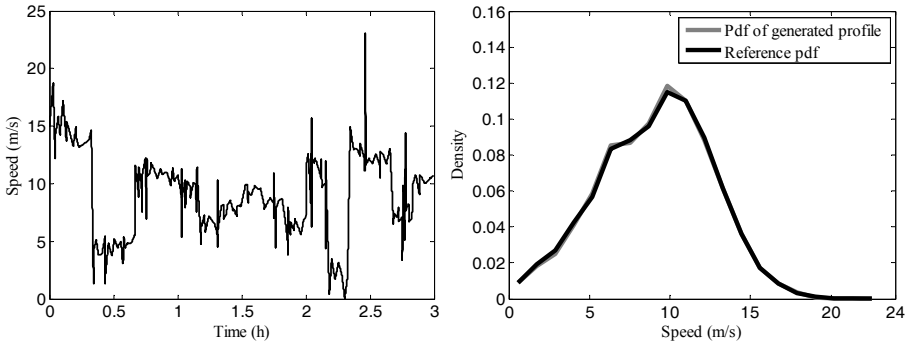


(*a*) *Generated profile* (*b*) *Statistical distribution*

**Figure 1.11.** *Result of a 3 hour representative profile synthesis process*

| | Reference indicators | Indicators from generated profile | Error (%) |
|---|---|---|---|
| $V_{max}$ (m/s) | 23.1 | 23.1 | 0.0 |
| $<V^3>$ ($m^3/s^3$) | 1076 | 1076 | 0.0 |
| $I_{turb}$ | 0.72 | 0.74 | 2.7 |

**Table 1.3.** *Representative profile design indicators*

Let us note that here we obtain "almost ideal" results, in the sense of design indicators, whereas the database of 2 months of measurements (1500 hours) is compacted in a ratio of 500:1 (~1500/3).

## 1.6. From classification to simultaneous design by optimization of a hybrid traction chain

In this section, we illustrate the general system approach via a set of railway missions, starting with the classification of environmental variable profiles and ending with simultaneous design by optimization, by using the representative and compact profile synthesis processes. The idea is to design a hybrid locomotive that is optimized for each mission class, and to compare the cost of annual ownership of the systems obtained, compared with the design of a single locomotive capable of satisfying all mission classes at once.

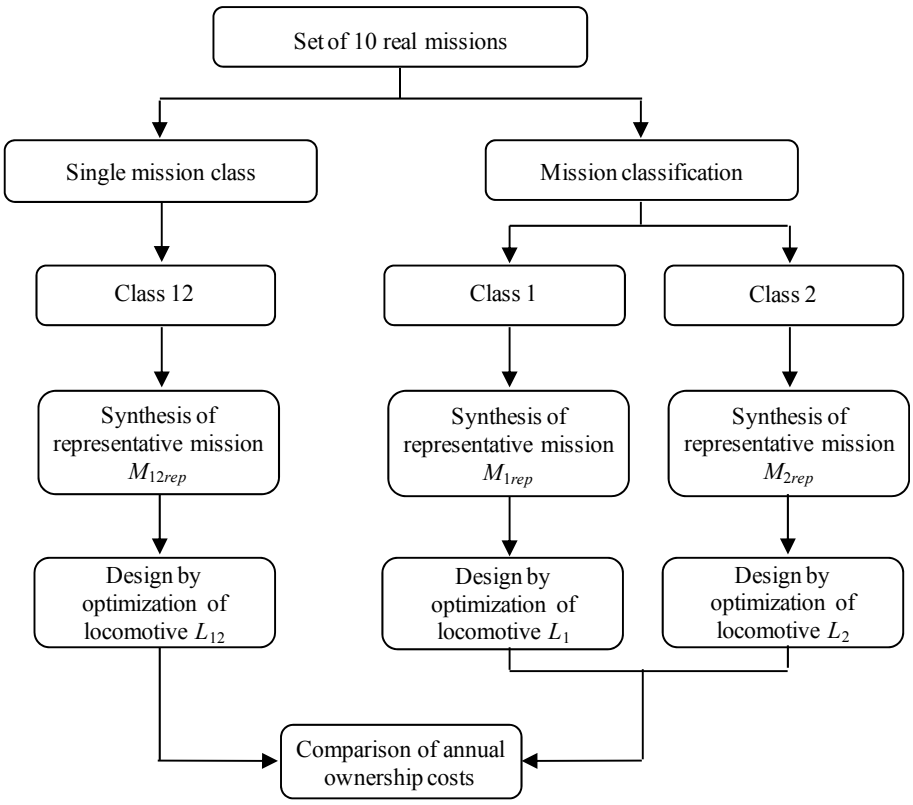


**Figure 1.12.** *General system approach, from classification to optimum design*

This general approach to system design is founded on a reference database corresponding to an example using 10 railway missions with iso-times (4 hours per mission) relative to diesel locomotives. We make the hypothesis that the storage state of charge, Ni-Cd batteries, is set to 100% after each 4 hour mission sequence. In Figure 1.12 we show the various stages of the proposed comparative study. Let us note that the classification of the set of missions leads to two different classes. In the sections that follow we return to the details of this approach.

## 1.6.1. *Modeling of the hybrid locomotive*

### 1.6.1.1. *Power flow model*

The power flow model for the diesel engine is shown in Figure 1.13. It enables us to determine the power provided by $P_{DE}$, the quantity of fuel consumed $Q_{fuel}$, and quantity of $CO_2$ emitted ($Q_{CO2}$(kg) = 2.66 × $Q_{fuel}$(L)), from the reference power of the diesel engine $P_{DEref}$ and its stop/start instruction ($MA_{DE}$ = 0 or 1) [GRA 06]. The quantity of fuel burnt is obtained from the cartography of consumption for the diesel engine $C_s(P_{DE\text{-}r})$. The set of these models is detailed in [AKL 08].

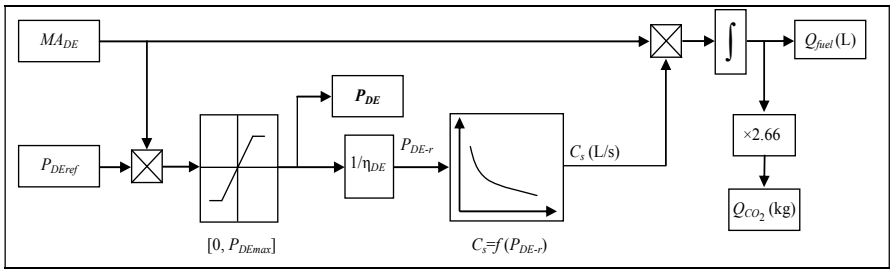


**Figure 1.13.** *Power flow model for the diesel engine*

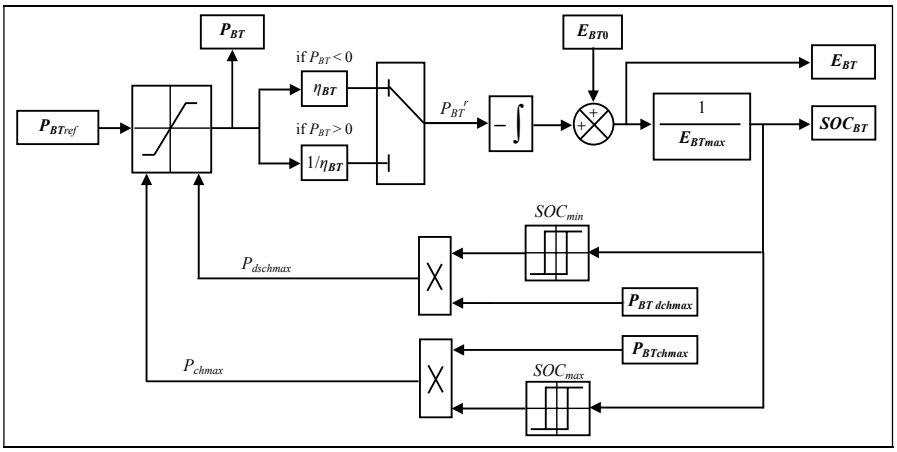


**Figure 1.14.** *Battery power flow model*

The battery power flow model (see Figure 1.14) has the following parameters: the reference mission of the batteries ($P_{BTref} = P_{mission} - P_{NDE}$, where $P_{NDE}$ defines the nominal power of the Diesel engine); the maximum discharge $P_{BTdchmax}$ and charge $P_{BTchmax}$ power of the battery pack; and the efficiency $\eta_{BT}$ and the quantity of initial energy $E_{BT0}$. By setting the thresholds of minimum battery $SOC_{min}$, and maximum $SOC_{max}$ state of charge, we determine the maximum discharge $P_{dchmax}$, and charge $P_{chmax}$, which is allowed per pack of batteries, by instantaneously taking account of its state of charge. For example, when the battery state of charge reaches the threshold $SOC_{min}$, the maximum discharge power possible $P_{dchmax}$ changes from $P_{BTdchmax}$ to 0. To close, this power flow model enables us to determine the battery power $P_{BT}$, energy $E_{BT}$, and state of charge $SOC_{BT}$.

### 1.6.1.2. *Static electrical model*

The static electrical model enables the dimensions resulting from the power flow model (power, energy) to be translated into electrical dimensions (current, voltage). In order not to complicate the design problem, the diesel engine electrical model is not taken into account. Figure 1.15 gives the static electrical model of accumulator batteries, which is a simplified $R$ and $E$ model. The current $i_{BT}$ and voltage $v_{BT}$ are obtained from the power drawn from a single cell $p_{BT}$ ($p_{BT} = P_{BT}/(NP_{BT} \times NS_{BT})$) where $NP_{BT}$ and $NS_{BT}$ are the number of parallel and series battery cells. The battery cell state of charge is obtained from the ratio of the charge quantity $q_{BT}$ of the cell to its nominal capacity $C$ ($C = 135$ Ah). The charge quantity $q_{BT}$ is defined as the sum of the integral of the current $i_{BT}$ and the initial charge quantity of the cell ($q_0$). We report that according to the sign convention, the battery discharge current is considered to be positive.

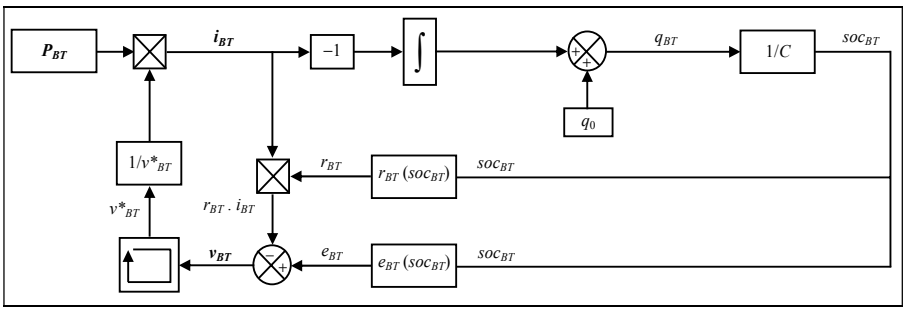


**Figure 1.15.** *Battery static electrical model*

1.6.1.3. *Geometric model*

From data provided by manufacturers, the volume in cubic meters of the diesel engine may be expressed in terms of its nominal power $P_{NDE}$ in watts using the following relation:

$$\Omega_{DE} = 3\times10^{-5} P_{NDE} + 0.09 \qquad [1.1]$$

The volume of the batteries, taking account of cooling systems and associated electronic modules (such as charge state balancing and thermal control), is given by the following:

$$\Omega_{BT} = \lambda_{BT} \times NP_{BT} \times NS_{BT} \times \Omega_{BT0} \qquad [1.2]$$

where $\Omega_{BT0} = 4.33\times10^{-3}$ m$^3$ and $\lambda_{BT} = 1.8$ represents the assembly coefficient, which takes into consideration intercellular spaces, electronic modules and cooling systems.

The volume of battery converters ($\Omega_{CBT}$) is approached using the volume of filter inductors. For further details on how this volume is determined, we refer the reader to [AKL 09].

1.6.1.4. *Battery lifetime model*

The lifetime of the battery $DV_{BT}$ is directly related to the number of battery cycles consumed during the mission. It is expressed by the product of the number of cycles consumed by the cell $Nb_{cyc}$ and the number of batteries in series "*S*" and in parallel "*P*" ($NP_{BT} \times NS_{BT}$).

1.6.1.5. *Cost model*

The estimate of the cost of the diesel engine, based on its nominal power, is given by the following:

$$C_{DE}[\text{k€}] = 0.28\times P_{NDE} + 14.5 \qquad [1.3]$$

According to the SNCF, by considering the maintenance and upkeep, a diesel engine costs three times its purchase price at the end of 10 years. The relationship thus enables the annual cost to be expressed by:

$$C_{DE}[\text{k€}/yr] = \frac{3}{10}(0.28\times P_{NDE} + 14.5) = 0.084P_{NDE} + 4.35 \qquad [1.4]$$

For batteries, taking into account converter installation and maintenance costs, the cost of a Ni-Cd battery cycle is estimated to be €0.122 [AKL 09]. By using the lifetime indicator ($DV_{BT}$) evaluated for a typical mission of length $\Delta t_{miss}$ and which is repeated $\Delta t_{yr}/\Delta t_{miss}$ times (where $\Delta t_{yr}$ represents a year of use, typically at 8 hours per day), the annual cost of the batteries is expressed by the following:

$$C_{BT}[\text{k€}/yr] = 0.122 \times 10^{-3} \times DV_{BT} \times \frac{\Delta t_{yr}}{\Delta t_{miss}} \qquad [1.5]$$

Let $C_{fuel0}$ be the unit price of a liter of fuel in k€. The annual cost of fuel is thus written:

$$C_{fuel}[\text{k€}/yr] = C_{fuel0} \times Q_{fuel} \times \frac{\Delta t_{yr}}{\Delta t_{miss}} \qquad [1.6]$$

### 1.6.2. *Optimization model*

#### 1.6.2.1. *Optimization parameters*

In this case study, the nominal power of the diesel engine is not considered to be an optimization parameter. It is set prior to the mission characteristics. The necessary optimization parameters for sizing of the hybrid locomotive are therefore:

– $NS_{BT}$: the number of battery cells in series. Taking into account the maximum voltage bus, this number is limited to 456 cells;

– $NP_{BT}$: the number of battery blocks in parallel. Taking into account the volume constraint, this number is limited to 32 blocks;

– $V_{bus}$: the continuous bus voltage varies between 50 and 650 V; and

– $F_{bd}$: the breakdown frequency varies between 1 and 10 kHz.

#### 1.6.2.2. *Optimization constraints*

In order to reduce the computation time of the simultaneous design by optimization process, the constraints are split into two categories:

– pre-simulation constraint. Without the need to simulate the system, these constraints are directly evaluated from the parameters of a given configuration;

- $g_1$: constraints linked to the energy source volume.

This constraint takes no account of converter volume. In the knowledge that the volume available for energy sources is limited to $\Omega_{SEmax}$, $g_1$ is thus written:

$$g_1 = \Omega_{BT} + \Omega_{DE} - \Omega_{SEmax} \leq 0 \qquad [1.7]$$

- $g_2$: constraints linked to the minimum number of batteries.

For a given nominal power of diesel engine, this constraint reflects the fact that the number of batteries must be sufficient in order to fulfill the mission. Its expression is as follows:

$$g_2 = N_{BTmin} - NP_{BT} \times NS_{BT} \leq 0 \qquad [1.8]$$

The minimum number of battery cells ($N_{BT\,min}$) is determined from a battery sizing procedure based on a power flow model [AKL 08],

- $g_3$: constraints linked to battery voltage.

Taking into account the elevated structure of choppers (the batteries towards the bus) and of the maximum cyclic ratio $\alpha_{max}$, the maximum voltage of a battery block $V_{BTmax}$ must then be less than $\alpha_{max} \times V_{bus}$. If the maximum voltage of a battery element is known, the constraint $g_3$ is written:

$$g_3 = NS_{BT} V_{BTmax} - \alpha_{max} \times V_{bus} \leq 0 \qquad [1.9]$$

– post-simulation constraints:

- $g_4$: constraints linked to energy system volume

This constraint takes account of energy source and associated battery block converter volumes, the whole constraint becoming contained within 32 $m^3$.

$$g_4 = \Omega_{BT} + \Omega_{DE} + \Omega_{CBT} - 32 \leq 0 \qquad [1.10]$$

1.6.2.3. *Optimization criteria*

The objective of the hybridization approach consists of minimizing the investment and usage costs, as well as the environmental cost (in $CO_2$ tonnes), relative to a diesel-only locomotive of the same power. Since we know that the quantity of $CO_2$ released is proportional to the quantity of fuel

consumed (1 liter of fuel produces to 2.66 kg of $CO_2$), the environmental cost optimization can, therefore, be reflected in the optimization of the quantity of fuel consumed, which enables us to reduce the optimization problem to a single criteria defined by the annual cost of ownership ($C_f$). It is thus a question of minimizing the annual cost of ownership, while, at the same time, integrating the costs of investment and usage (maintenance, lifetime, and fuel consumption).

$$C_f = C_{DE} + C_{BT} + C_{fuel} \qquad [1.11]$$

### 1.6.3. *Mission classification*

In this first general systems approach phase, we move to the classification of all 10 railway missions according to the sizing indicators $\{P_{max}, P_{avg}, E_u\}$. The result obtained by applying the genetic classification algorithm is given in Figure 1.16. The characteristics of the classes found are also given in Table 1.4.

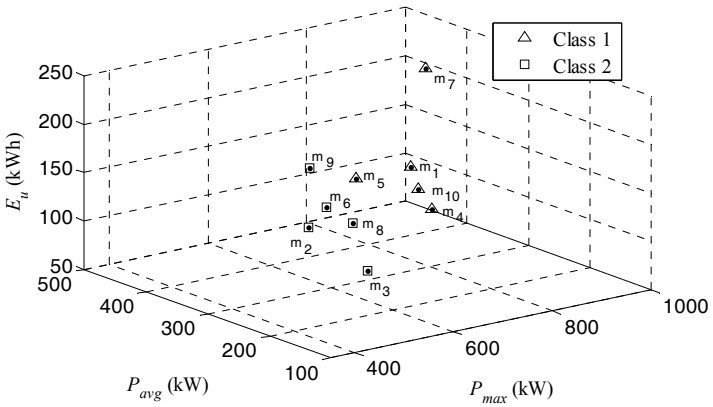


**Figure 1.16.** *Classification of missions according to sizing indicators*

| | Number of missions | Missions | Barycenter coordinates ($P_{max}$ (kW), $P_{avg}$ (kW), $E_u$ (kWh)) |
|---|---|---|---|
| Class 1 ($C_1$) | 5 | $\{m_1, m_4, m_5, m_7, m_{10}\}$ | (881.1, 400, 125.7) |
| Class 2 ($C_2$) | 5 | $\{m_2, m_3, m_6, m_8, m_9\}$ | (479.3, 200.1, 156.4) |

**Table 1.4.** *Characteristics of classes obtained following classification*

### 1.6.4. *Synthesis of representative missions*

In this second study phase, we apply the representative and compact mission synthesis process for each mission class: $C_1$, $C_2$ (each comprising 5 missions) and $C_{12}$, which is formed from the total mission population. The reference indicators enabling the characterization of the representative mission are chosen in the following way:

– the sizing indicators, apart from the average power $P_{avg\ ref}$, are set at the more constraining values for all missions within a class. This enables us to guarantee that the system under design will satisfy all missions of the studied class. A specific study of railway missions has proven the benefit of setting the average reference power $P_{avg\ ref}$ at the average concatenation value for all missions. We recall that this power value corresponds to the sizing of the diesel engine, a device for which consumption and "pollution" are optimum when the latter operates at its nominal power;

– the performance and lifetime indicators are considered to be average. The choice of useful reference energy $E_{u\ ref}$ enables the storage size to be determined and, as a consequence, we are able to estimate the number of cycles consumed for each mission. The number of reference cycles $N_{cyc\ ref}$ is thus determined by the average value of the numbers of cycles per hour across all missions. For the statistical reference indicator $I_{stat\ ref}$, we consider the distribution function of the total mission at the end of the concatenation of all missions from the class in question.

Contrary to the wind speed compaction example discussed in the last section, the nature of the design indicators in the case of railway missions imposes substantial minimum times. This refers most particularly to the useful energy indicator or the number of cycles, which are closely coupled with the mission duration.

#### 1.6.4.1. *Class $C_1$ representative mission: $M_{1rep}$*

We set the duration of the representative mission for class $C_1$ at 4 hours, which corresponds to a saving of 5 over the total duration of concatenated missions (20 hours).

The result of the synthesis is given in Figure 1.17. This is a representative mission $M_{1rep}$, which is obtained through the concatenation of 125 segments and which perfectly respects the reference indicators (see Table 1.5 and Figure 1.18).

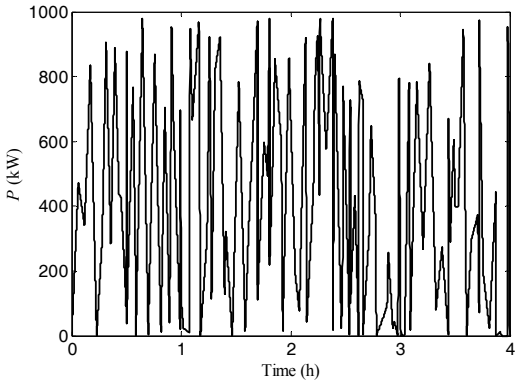


**Figure 1.17.** *Representative mission $M_{1rep}$*

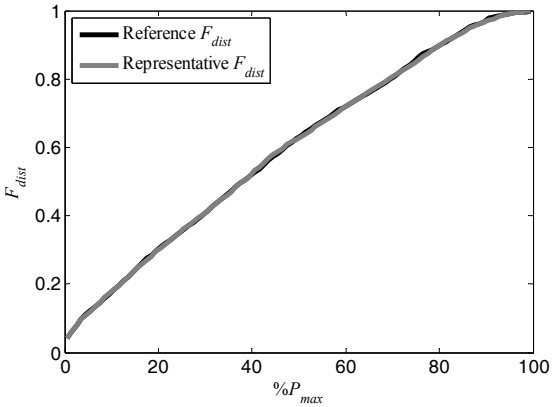


**Figure 1.18.** *Distribution functions*

| | Reference indicators | Representative mission indicators | Error (%) |
|---|---|---|---|
| $P_{max}$ (kW) | 980 | 980 | 0.0 |
| $P_{avg}$ (kW) | 400 | 400 | 0.0 |
| $E_u$ (kWh) | 169.5 | 169.5 | 0.0 |
| $Nb_{cyc}$ (/h) | 0.155 | 0.155 | 0.0 |
| $I_{stat}$ | – | – | 0.4 |

**Table 1.5.** *Characterization indicators of the representative mission $M_{1rep}$*

1.6.4.2. *Class $C_2$ representative mission: $M_{2rep}$*

The duration of the representative mission for class $C_2$ is set at 6 hours, which corresponds to a saving of 3.3 over the total duration of concatenated missions (20 hours). The result of synthesis is given in Figure 1.19. This is a representative mission $M_{2rep}$, which is obtained through the concatenation of 126 segments and which perfectly respects the reference indicators (see Table 1.6 and Figure 1.20).

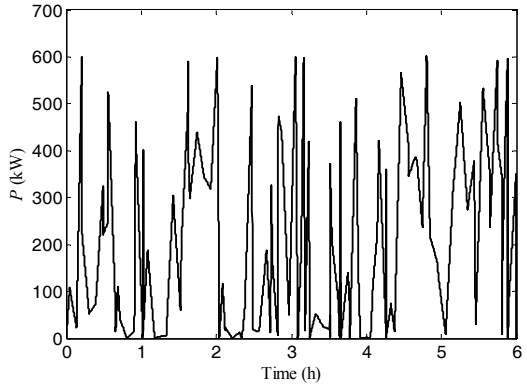


**Figure 1.19.** *Representative mission $M_{2rep}$*

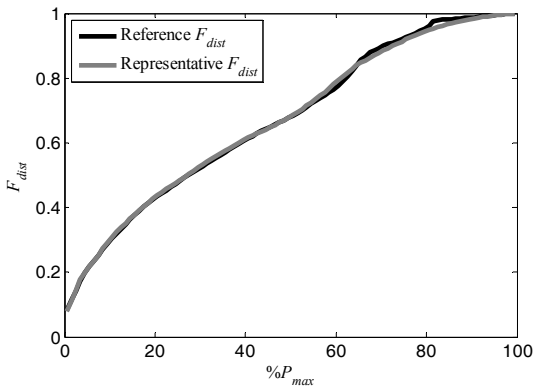


**Figure 1.20.** *Distribution functions*

| | Reference indicators | Representative mission indicators | Error (%) |
|---|---|---|---|
| $P_{max}$ (kW) | 601 | 601 | 0.0 |
| $P_{avg}$ (kW) | 200 | 201 | 0.5 |
| $E_u$ (kWh) | 194.5 | 194.5 | 0.0 |
| $Nb_{cyc}$ (/h) | 0.11 | 0.11 | 0.0 |
| $I_{\text{stat}}$ | – | – | 0.8 |

**Table 1.6.** *Characterization indicators of the representative mission $M_{2rep}$*

### 1.6.4.3. *Class $C_{12}$ representative mission: $M_{12rep}$*

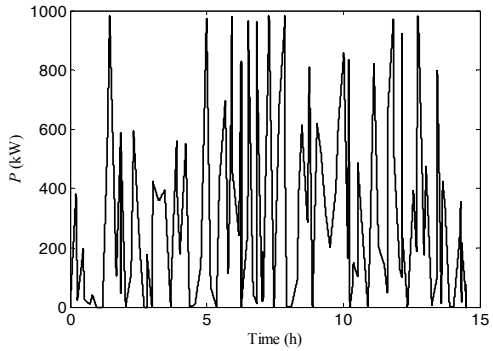


**Figure 1.21.** *Representation mission $M_{12rep}$*

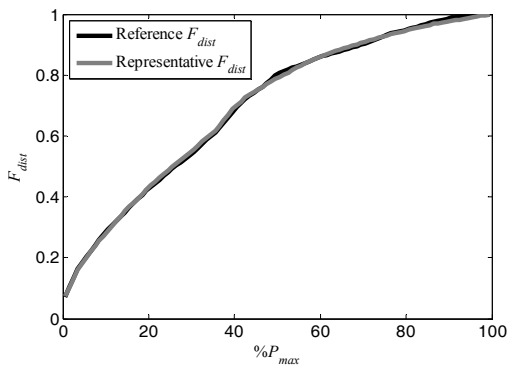


**Figure 1.22.** *Distribution functions*

The class $C_{12}$ representative mission $M_{12rep}$, which simultaneously integrates classes $C_1$ and $C_2$ is given by Figure 1.21.

This is a fictive mission of 14.5 hours' duration, which thus enables a saving of 2.8 compared with the total mission duration (40 hours). The latter is obtained by the concatenation of 148 segments and perfectly respects the reference indicators (see Table 1.7 and Figure 1.22).

| | Reference indicators | Representative mission indicators | Error (%) |
|---|---|---|---|
| $P_{max}$ (kW) | 980.5 | 980.5 | 0.0 |
| $P_{avg}$ (kW) | 300 | 300 | 0.0 |
| $E_u$ (kWh) | 569.3 | 569.3 | 0.0 |
| $Nb_{cyc}$ (/h) | 0.04 | 0.04 | 0.0 |
| $I_{stat}$ | – | – | 0.8 |

**Table 1.7.** *Characterization indicators of the representative mission $M_{12rep}$*

### 1.6.5. *Simultaneous design by optimization*

Having determined the representative missions, we proceed in this section to the simultaneous design of three hybrid locomotives, optimized per mission class. Let $L_1$, $L_2$ and $L_{12}$ denote the hybrid locomotives, sized for classes $C_1$, $C_2$ and $C_{12}$, respectively, from representative missions $M_{1rep}$, $M_{2rep}$ and $M_{12rep}$. In order to validate the consistency of the design results and to emphasize the efficiency, in terms of computation time, of the representative mission synthesis process, we also size three hybrid locomotives, optimized per real mission class. In other words, it is a matter of designing a hybrid locomotive for each mission class, by considering the concatenation of all missions of the studied class to be a "sizing" mission, under the hypothesis that the battery state of charge will be reduced to its initial value after each 4 hour mission. Thus, we denote the hybrid locomotives sized for each class $C_1$, $C_2$, and $C_{12}$ from real "sizing" missions $M_{1tot}$, $M_{2tot}$, and $M_{12tot}$, by $L_{1tot}$, $L_{2tot}$, and $L_{12tot}$. Under the hypothesis that all initial missions are realized with same occurrence over a year as over the base of 8 hours of use per day for each locomotive, the design results are given in Table 1.8. The optimization algorithm used at the heart of the simultaneous design process is based on a genetic algorithm (see Chapter 3) and is coupled to the different hybrid locomotive models presented at the start of this section.

The design results obtained for each mission class prove the effectiveness of the representative mission synthesis process in the system design approach. Indeed, we obtain practically the same sizing from the hybrid locomotive by considering the fictive representative mission together with

concatenation of real missions in the envisaged class[3]. For the three mission classes studied in this way, we note a significant saving in terms of calculation time ($T_c$) between the two approaches. Indeed, the previous optimization results were obtained after 1,000 generations with a population of 100 individuals. Under these conditions, design with representative missions being synthesized enables a saving over the optimization time, which is increased to 4.5 days for class $C_1$, 4 days for class $C_2$, and 6.6 for class $C_{12}$.

| | | Class $C_1$ | | | Class $C_2$ | | | Class $C_{12}$ | |
|---|---|---|---|---|---|---|---|---|---|
| Variables | | $L_{1tot}$ | $L_1$ | | $L_{2tot}$ | $L_2$ | | $L_{12tot}$ | $L_{12}$ |
| $P_{DE}$ (kW) | | 400 | 400 | | 200 | 200 | | 300 | 300 |
| $NP_{BT}$ | | 10 | 10 | | 12 | 12 | | 11 | 11 |
| $NS_{BT}$ | | 437 | 421 | | 444 | 440 | | 429 | 421 |
| $N_{BT}$ | | 4,370 | 4210 | | 5,328 | 5,280 | | 4,719 | 4,631 |
| $V_{bus}$ (V) | | 640 | 624 | | 636 | 630 | | 614 | 602 |
| $F_{dec}$ (kHz) | | 7.3 | 8.1 | | 5.4 | 5.1 | | 4.9 | 5.7 |
| $C_f$ (k€/yr) | | 397.2 | 421.8 | | 202.8 | 191 | | 318.5 | 350.4 |
| $T_c$ (s) | | 4.9 | 1 | | 4.9 | 1.4 | | 9 | 3.3 |

**Table 1.8.** *Results of design by optimization in hybrid locomotives*

### 1.6.6. *Design results comparison*

Based on 8 hours per day use for each locomotive, the 10 initial class $C_{12}$ missions, with a total length of 40 hours are repeated 73 times over the course of one year, whereas the five missions in class $C_1$ of the same length are each repeated 146 times each year. In order to evaluate the interest in the classification (or segmentation) we compare the average annual costs of the two locomotives $L_1$ and $L_2$ with that of locomotive $L_{12}$:

– average annual cost of $L_1$ and $L_2$ = 0.5 × (Cost ($C_1$)/$L_1$ + Cost ($C_2$)/$L_2$) = 306 k€/year;

– annual cost of $L_{12}$ = 350 k€/year.

3 The difference in annual ownership costs obtained between design with fictive representative samples and with real missions is principally due to errors in estimating the annual costs of fuel. Indeed, the stop/start nature of the diesel engine is dependent on the battery state of charge, which itself is dependent on the form of the mission, even if all of the characterization indicators are perfectly respected.

We observe that, for this 10 mission example, the design of two locomotives optimized per mission class enables a saving of €44,000/year (~13%/year) compares with a single locomotive capable of satisfying all missions on the list of specifications. Conversely, although it is less profitable financially, the solution for the single equivalent locomotive is slightly better ecologically. Indeed, the annual use of this locomotive generates around 502 tonnes of $CO_2$, against 518 tonnes of $CO_2$ (approx. +3%) emitted during an average annual exploitation of locomotives $L_1$ and $L_2$. The choice of whether to design a single $L_{12}$ locomotive, or two different locomotives $L_1$ and $L_2$, is governed by a compromise between financial and ecology aspects; beyond the result of this particular application, the interest in the complete approach (classification – mission synthesis – simultaneous design) that we have proposed is to facilitate the choice of the design user, here SNCF, in terms of segmentation of the product range and then sizing. These choices can be put into perspective with regards to the essential design criteria (here ownership and climate costs).

## 1.7. Conclusion

The optimum design of energy systems is increasingly complex, requiring a shift towards an increasingly integrated approach, including many design perspectives (architecture, sizing, management), which address a large number of heterogeneous criteria and constraints and which are associated with various disciplines. These systems must satisfy a design finality (mission) and become immersed in the environment with which they are interacting. These diverse, often close, pairings are at the source of the complexity of the systems approach, requiring a methodological approach to facilitate the design process. This chapter contributes scientifically by positioning itself upstream of this process by specifically highlighting the integration of the mission and environmental variables into a system design approach.

In the first phase of the study, and having highlighted the innovation of considering the mission and environmental variables in the design of energy systems, we have addressed the basic concepts of our new approach to processing mission and environmental variables. This approach is initially based on an analysis phase, which requires a high level of expertise in the system within its environment, in order to define the pertinent characterization indicators with regards to design criteria and constraints.

The "classification" of mission or environmental variable profiles according to the pertinent indicators, with regards to design criteria and constraints, makes use of a set of decision-making tools. With this in mind, we have developed a classification algorithm based on the optimization of a partitioning criterion (the silhouette index) and associated with a genetic algorithm with niching. This algorithm has then been validated on a sample of railway mission profile dedicated to three distinct power systems. The results obtained show the capacity of the approach to uncover quite distinct classes, but also reveals the possibility of challenging certain "accepted ideas" on the segmentation of products and markets.

"Representative and compact profile synthesis" consists of generating a fictive profile that is "relevant" and of minimum duration from a family of real profiles of differing characteristics, which conform to a certain set of reference design indicators. Profile synthesis is based on the aggregation or concatenation of elementary patterns (triangle, sine, or cardinal sine) for which the number of parameters is determined by optimization using a genetic algorithm. By referring to the two examples of real railway missions and wind resource profiles, we have shown the capacity for the synthesis process to generate a representative profile of reduced duration and which responds perfectly to the reference design indicators. For these two examples, the best results are obtained with an elementary segment pattern. As far as the reduction or compaction rate of the initial horizon of real profiles is concerned, this is clearly higher for wind speed compaction than for railway missions. This shows that the compaction rate is strongly linked to the nature of design indicators, which may require substantial minimum times.

Finally, we have presented an application of the complete approach proposed in this chapter, from classification to mission synthesis; this example concerned the optimum design of an energy-efficient and environmentally friendly hybrid locomotive. Through this hybridization example we have shown the significance of the railway mission classification approach in order to help designers evaluate the relevance of a specific locomotive, which has been dedicated and optimized by mission class, compared with a single locomotive capable of satisfying all classes. Our approach, therefore, forms an "aid to market segmentation associated with an aid to systems design", for designer-users such as, in this case, SNCF. We have highlighted the effectiveness of the compact duration representative synthesis profile within the design by optimization process. This approach has led to notable savings in computation times, which can

last several days compared with design by optimization, which considers the concatenation of the set of missions from the specification list as a typical mission.

## 1.8. Bibliography

[ABD 07] ABDELLI A., Optimisation multicritère d'une chaîne éolienne "passive", PhD thesis, INP Toulouse, 2007.

[AKL 08] AKLI C.R., Conception systémique d'une locomotive hybride autonome, PhD thesis, INP Toulouse, 2008.

[AKL 09] AKLI C.R., ROBOAM X., SARENI B., JEUNESSE A., "Integrated optimal design of a hybrid locomotive with multiobjective genetic algorithms", *International Journal of Applied Electromagnetics and Mechanics*, vol. 4, pp. 151-162, 2009.

[AND 04] ANDRE M., "ARTEMIS European driving cycles for measuring car pollutant emissions", *Science of the Total Environment*, vol. 334-335, pp. 73-84, 2004.

[BAE 08] BAEK S.H., CHO S.S., JOO W.S., "Fatigue life prediction based on the Rainflow cycle counting method for the end beam of a freight car bogie", *International Journal of Automotive Technology*, vol. 9, pp. 95-101, 2008.

[BER 73] BERTALANFFY L.V., *Théorie générale des systèmes*, translated by Jean Benoîst Chabrol, Dunod, Paris, 1973.

[CAL 04] CALIF R., BLONBOU R., DESHAIES B., "Wind velocity measurements analysis for time scales smaller than 1 hour: application to wind energy forecasting", *Proceedings of the 24th AIAA/ASME Wind Energy Symposium*, 2004.

[CAL 11] CALIF R., EMILION R., SOUBDHAN T., "Classification of wind speed distributions using a mixture of Dirichlet distributions", *Renewable Energy*, vol. 36, no. 11, pp. 3091-3097, 2011.

[CAL 74] CALINSKI R.B., HARABAZ J., "A dendrite method for cluster analysis", *Commun. Statistics*, vol. 3, pp. 1-27, 1974.

[DAV 79] DAVIES D.L., BOULDIN D.W., "A cluster separation measure", *IEEE Trans. Pattern Anal. Machine Intell.*, vol. PAMI-1, pp. 224-227, 1979.

[DEA 12] DE ANDRADE A., Optimisation conception intégrée par optimisation multicritère d'un système d'actionnement électrique pour l'aéronautique, PhD thesis, INP Toulouse, 2012.

[DRO 97] DROUILHET S., JOHNSON B.L., "A battery life prediction method for the hybrid power applications", *35th AIAA Aerospace Sciences Meeting and Exhibit*, Reno, United States, January 1997.

[FOR 65] FORGY E.W., "Cluster analysis of multivariate data: efficiency versus interpretability of classifications", *Biometric Society Meetings*, Riverside, California, 1965.

[GRA 06] GRAHAM L.A., "Greenhouse gas emissions from light duty vehicles under a variety of driving conditions", in *Proc. IEEE EIC Climate Change Technol.*, pp. 1-8, 2006.

[HAR 95] HARIK G., "Finding multimodal solutions using restricted tournament selection", *Proceedings of the Sixth International Conference on Genetic Algorithms*, Morgan Kaufmann, San Francisco, CA, USA, 1995.

[JAA 10a] JAAFAR A., SARENI B., ROBOAM X., "Clustering analysis of railway driving missions with niching", *International Journal for Computation and Mathematcs in Electrical and Electronic Engineering*, vol. 31, no. 3, pp. 920-931, 2010.

[JAA 10b] JAAFAR A., SARENI B., ROBOAM X., "Signal synthesis by means of evolutionary algorithms", *Inverse Problems in Science and Engineering*, vol. 20, no. 12, pp. 93-104, 2010.

[JOU 99] JOUMARD R., ANDRE M., VIDON R., TASSEL P., PRUVOST C., Influence du cycle de conduite sur les émissions unitaires de polluants des voitures particulières, INRETS report, no. LTE 9902, December 1999.

[KAU 90] KAUFMAN L., ROUSSEEUW P.J., *Finding Groups in Data: an Introduction to Cluster Analysis*, Wiley, New York, 1990.

[KEL 92] KELLER J.K., "Simulation of wind with 'K' parameter", *Wind Engineering*, vol. 16, pp. 307-312, 1992.

[LAN 06] LANGLOIS O., Conception d'un réseau de secours électrique pour l'aéronautique, PhD thesis, INP Toulouse, 2006.

[LEB 00] LEBART L., MORINEAU A., TABARD N., *Statistique exploratoire multidimensionnelle*, Dunod, Paris, 2000.

[MAC 67] MACQUEEN J., "Some methods for classification and analysis of multivariate observations", *in Proc. 5th Berkeley Symposium on Mathematical Statistics and Probability*, Berkeley, California, 1967.

[MES 98] MESSINE F., NOGAREDE B., LAGOUANELLE J.L, "Optimal design of electromechanical actuators: a new method based on global optimization", *IEEE Transactions on Magnetics*, vol 34, pp. 299-308, 1998.

[NGU 08] NGUYEN-HUU H., SARENI B., WURTZ F., RETIÈRE N., ROBOAM X., "Comparison of self-adaptive evolutionary algorithms for multimodal optimization", *10th International Workshop on Optimization and Inverse Problems in Electromagnetism* (OIPE'2008), Ilmenau, Germany, September 2008.

[PET 96] PETROWSKI A., "A clearing procedure as a niching method for genetic algorithms", *Proceedings of the IEEE International Conference on Evolutionary Computation*, Nagoya, Japan, pp. 798-803, May 1996.

[ROB 12] ROBOAM X., *Systemic Design Methodologies for Electrical Energy Systems*, ISTE Ltd., London and John Wiley and Sons, New York, forthcoming, 2012.

[SAR 98] SARENI B., KRÄHENBÜHL L., "Fitness sharing and niching methods revisited", *IEEE Trans. on Evolutionary Computation*, vol 3, pp. 97-106, 1998.

[SHE 05] SHENG W., SWIFT S., ZHANG L., LIU X., "A weighted sum validity function for clustering with a hybrid niching genetic algorithm", *IEEE Transactions on Systems, Man, and Cybernetics-Part B*: *Cybernetics*, vol 35, pp. 1156-1167, 2005.

[STR 90] STRARRON D.A., STENGELZ R.F., "Stochastic prediction techniques for wind shear hazard assessment", *Journal of Guidance, Control, and Dynamics*, vol 15, pp. 1224-1229, 1990.

[THI 08] THIOUNN M., "PLATHEE – a platform for energy efficiency and environmentally friendly hybrid trains", *8th World Congress on Railway Research*, COEX, Seoul, Korea, May, 2008.

Chapter 2

# Analytical Sizing Models for Electrical Energy Systems Optimization

## 2.1. Introduction

This chapter proposes a methodology and component models for the development of a general electrical energy system model with a view to its optimal sizing.

In the first section, the authors set out the problem of modeling within a design process, by specifically showing the value of analytical modeling in this context.

In the next section, the authors present some general details of the methodology, enabling the modeling of an electrical energy system to be structured. They illustrate their words by applying the methodology to the example of a hybrid electrical heavy vehicle.

In the next sections, the authors review analytical models of the main components of an electrical energy system, such as: electrical machines, static converters, mechanical transmissions, and energy storage systems. To clarify and illustrate the modeling approach, the authors present analytical models of components of the hybrid electrical heavy vehicle discussed in this chapter.

---

Chapter written by Christophe ESPANET, Daniel DEPERNET, Anne-Claire SAUTTER and Zhenwai WU.

*Integrated Design by Optimization of Electrical Energy Systems* Edited by Xavier Roboam
© 2012 ISTE Ltd. Published 2012 by ISTE Ltd.

Finally, in an attempt to show the use of the analytical models proposed within the context of system sizing by optimization, the authors conclude the chapter by comparing two results of optimization: the first concerns the individual optimal design of each component of the hybrid electrical heavy vehicle and the second concerns the simultaneous sizing of all components of the system.

## 2.2. The problem of modeling for synthesis

In this first section, we describe the importance of modeling in a design process. In particular, we justify the value of analytical simulation models in a sizing by optimization method.

### 2.2.1. *Modeling for synthesis*

We begin this section with some general details about modeling. We first set out what we understand by the term "model"; then we distinguish simulation from sizing models.

#### 2.2.1.1. *Model concept*

In this chapter, the model concept should be understood in mathematical terms. In very general terms, a model is an abstract or existent construction that enables the physical behavior of a device to be predicted. Within various technical domains, reduced scale prototypes have long been used to enable the behavior of a much larger model to be predicted either by analogy or by homothety. With the progress in computers, models (and even prototypes) have become increasingly "virtual". Thus we understand a model to be a mathematical construction linking parameters to each other. In this context, a model can thus be used to either analyze a device or to design it.

#### 2.2.1.2. *Simulation and sizing models*

In order to better understand the distinction between simulation and sizing models, we can illustrate the problem using Figure 2.1. The traditional problem for physicists is to represent the physical behavior of a device using mathematical equations. In this case we refer to either analysis or simulation. However, the problem for designers is to determine the construction and control parameters of a system within its environment, understand the level of performance that can be attained, and the constraints to be taken into consideration, which are detailed in the specifications. In this case, we refer

to either synthesis or sizing. The models used thus correspond to inverse analysis models. In this sense, we can refer to simulation models as being "direct models" and sizing models to be "inverse models". Furthermore, as explained in Chapter 3 of this book, optimization is a useful tool for producing the inverse of an analysis model, with a view to transforming it into a synthesis model; therefore, we seek input parameters of the analysis model, which satisfy equations for the constraints model from the specifications and which, furthermore, optimize one or more criteria [KON 93; WUR 96]. In this context, simulation models remain the required basis for development of a model, or, more generally, a design tool, insofar as these models enable the criteria to be optimized and the pertinent constraints to be evaluated.

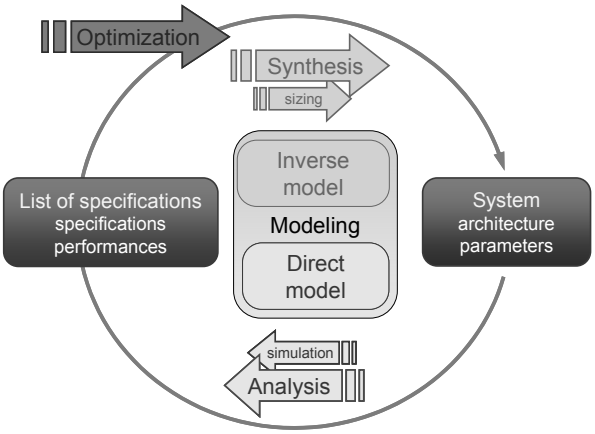


**Figure 2.1.** *Analysis and synthesis within a design process*

### 2.2.1.3. *Knowledge and behavior models*

Within a design process, analysis models should, wherever possible, precede the creation of any real prototype, as they form the basis of the process that enables the manufacture of the real device. In this context, these models are preferably knowledge rather than behavior models, which are, indeed, interpolated (black box) models and mathematically reflect the experimental behavior of a real system. The testing required in order to determine the parameters of the behavior model thus require the pre-existence of the device. The validity of the parameters will not always be ensured during variations in the descriptive parameters of the device, which is not, for example, compatible with the use of optimization. In any event, a

little qualification is needed. Indeed, device complexity, the lack of knowledge of certain physical phenomena, and the difficulty in solving mathematical equations lead, in some cases, to the use of empirical or interpolated and/or extrapolated models, which do not rely directly on the laws of physics, but rather on the *experience* of designers. We can quote, for example, the $B-H$ laws of magnetic materials, or even the empirical correlations enabling the calculation of convection heat transfer coefficients. However, behavior models are more delicate as, in essence, their validity limits are harder to define precisely, and during optimal sizing, it will be preferable to avoid them where possible.

### 2.2.2. *Analytical and numerical modeling*

#### 2.2.2.1. *Development of a mathematical model*

The development of a mathematical knowledge model relies on the resolution of some general laws that govern device behavior in a given physical environment. Figure 2.2 presents the two development stages of such a model, by taking the example of the development of an electromagnetic model. The first stage consists of expressing a device in equation form, by drawing on general physical equations, constitutive material laws, and boundary conditions. In electromagnetism, these equations generally lead to a spatiotemporal differential problem. The second stage consists of solving these equations. Here, two main approaches can be considered. The first consists of finding, when possible, analytical solutions to the equations, whereas the second consists of discretizing the variables and numerically solving the equations.

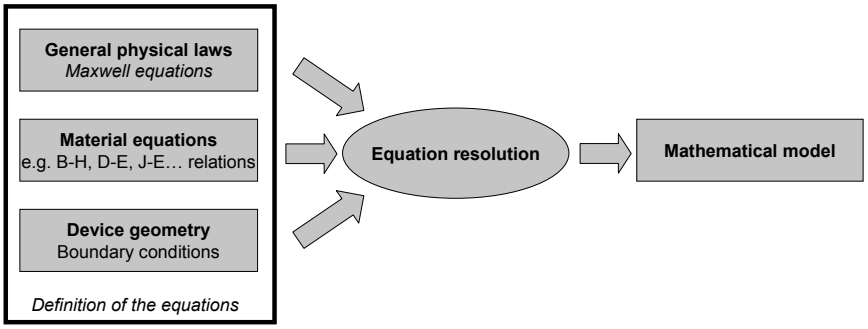


**Figure 2.2.** *Development of a mathematical physical device model (example of an electromagnetic model)*

2.2.2.2. *Distinction between analytical and numerical models*

There are numerous points of view within the electrical engineering design community regarding the distinction made between numerical and analytical models. Although this is rather a theoretical debate, here we are proposing some strict definitions that enable the limitation between the two types of modeling to be addressed, and most importantly, to then deduce the advantages and relative disadvantages of each type of model and, consequently, their relative roles with a design process.

The limitation between a numerical and analytical model rests on the use of a numerical algorithm. Thus a model will be said to be analytical if its resolution does not require the use of numerical method for approximate resolution of a differential equation or a large algebraic system, or even simply a nonlinear equation.

In order to illustrate this let us take the example of the response of an inductive circuit to a level of voltage (see Figure 2.3); the circuit initially being at rest.

Firstly, let us consider that the inductance is constant. In this case, the temporal response from the circuit is as follows:

$$i(t) = \frac{U}{R}\left(1 - e^{-\frac{t}{L/R}}\right) \qquad [2.1]$$

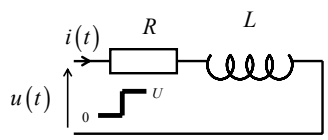


**Figure 2.3.** *Response of an inductive circuit to a period of voltage*

Conversely, if the inductance is not constant, but is dependent on the current flowing through it, the differential equation:

$$R\,i + \frac{d\left(L(i)\,i\right)}{dt} = u \Rightarrow R\,i + L(i)\frac{di}{dt} + \frac{dL}{di}\frac{di}{dt}i = u \qquad [2.2]$$

which governs the temporal evolution of the current cannot generally be resolved analytically, and it is necessary to use a numerical integration method, which consists of temporarily discretizing the current. The first case is therefore known as an *analytical model*, whereas the second case is known as a *numerical model*.

Limitation is sometimes discussed in certain cases. For example, the use of reluctance networks in order to calculate the magnetic field in a device is a well-used method in the design of electrical actuators [JUF 95]. In this case, the Kirchoff network equations may be explicitly analytical. Conversely, if the system is very large and nonlinear (which is the most common case in practice), solving the network implies the use of a numerical resolution algorithm for a nonlinear system of $n$ equations with $n$ unknowns. Nodal networks in thermal modeling are a similar example. In this case, insofar as the equations to be solved are analytically explained, we refer nowadays to *semi-analytical* models, but in the sense of the definitions above, this is clearly a numerical model.

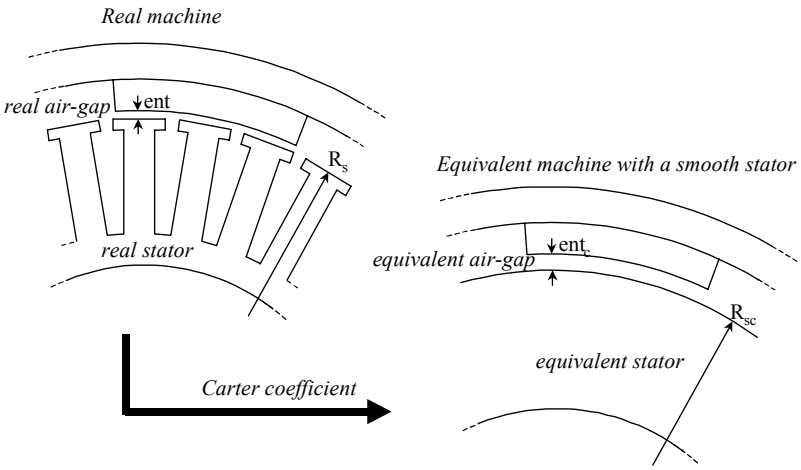


**Figure 2.4.** *Simplified geometry of a surface-mounted, synchronous, permanent magnet device with an external rotor: simplification of geometry with a view to solving Maxwell equations using the variable separation method*

Another example of magnetic models currently in use corresponds to those that rely on the solution to Maxwell equations using the variable separation method, which thus leads to solutions expressed in Fourier series form. We occasionally refer to *meshless* methods. For simple geometries,

solutions may be analytically expressed. Indeed, if the number of areas considered is limited, the number of integration coefficients to be determined in order to solve Maxwell equations is similarly limited, and we can thus analytically solve the Cramer system, which is verified by the integration coefficients. For example, for a surface-mounted magnet device with an external rotor, for which slotting effects (stator homogenization and correction of the gap through application of the Carter coefficient; see Figure 2.4) are neglected, the flux density $B$ into the air gap, for no load operation, is expressed within a cylindrical base as follows [ZHU 93]:

$$B(r,\theta) = \sum_{n\neq 0} \left( \alpha_{\mathrm{n}}\, r^{pn} + \beta_{\mathrm{n}}\, r^{-pn} \right) cos\left(n\,p\theta\right) \qquad [2.3]$$

where $p$ is the number of pole pairs, $\alpha_{\mathrm{n}}$ and $\beta_{\mathrm{n}}$ are constants dependent on the geometry of the machine and the magnetic properties of the magnets and $n$ is the harmonic rank.

Even if this equation appears to define an analytical model, implementation is clearly numerical. Indeed, even if the series is convergent, its limits cannot be explicitly determined. Thus, the choice of the number of harmonics in the Fourier series always defines modeling as numerical, in the sense of the definitions given at the start of this section.

Furthermore, when we are looking to solve the Maxwell equations in slots [DUB 09], we thus obtain a large number of areas and the number of integration coefficients to be determined is higher, which requires block matrix inversion. The model is thus doubly numerical; the large Cramer system must be solved and the number of harmonics in the Fourier series must be very carefully chosen.

2.2.2.3. *Role of analytical models in a design process*

Analytical, semi-analytical and numerical models all have their advantages and each has a role to play in the design process. We will discuss the advantages of each type of model and show how analytical and semi-analytical models can be used at each stage of sizing by optimization.

2.2.2.3.1. Advantages of analytical and semi-analytical models

The properties described in this section apply to analytical, but also semi-analytical models for which the formulation of equations to be solved is analytical:

– The first clear advantage is the *calculation time for the model*. This point is certainly modulated by the constant increase in computer processing power and by the ability for parallel calculations to take place across multiple processors; however, the fact that systems containing a significant number of components can be modeled (from a few units to several dozen), using increasingly multi-physical models, taking into account transitory responses and evaluations on a significant number of operating points, or on long and complex missions, has probably forced the focus onto model calculation times. Additionally, in an industrial context, calculation time is a significant factor in the competitiveness of the design activity. Finally, the use of a model in an optimal design context implies a significant number of evaluations of the simulation model, in order to satisfy constraints and optimize criteria. This is all the more so if a stochastic optimization algorithm is used, for which convergence requires many hundreds to many thousands of iterations.

– In any event, calculation time is not the only advantage of analytical models in a system design context. The other major advantage is the *explicit characteristic*[1] of the information contained in the analytical model, which enables a better physical interpretation of equations than a numerical model, which requires numerous evaluations in order to extract the physical information contained in the model. Let us consider a very simple case in order to illustrate this. Knowing an analytical relationship between two variables $x$ and $y$, for example $y=\sin(x)$, enables an instant understanding of the influence of $x$ on $y$. If a set of numerical simulations were required in order to extract the same information, clearly a large number of calculations would be required. At the very least, the Shannon theorem indicates two evaluations per period, but this assumes that the frequency is already known. In summary, the explicit characteristic of equations of an analytical or semi-analytical model enables rapid understanding of the relationships existing between the various parameters of the model and favors design choices, notably during the pre-sizing phases.

– The third factor is the greater ease offered by analytical or semi-analytical approaches in the production of multi-physical component models, on one hand, and component model couplings on the other. For example, in an electrical drive model, the electrical, magnetic, mechanical, and thermal modeling of an actuator, its power source, and the mechanical transmission

1 We refer here to an explicit characteristic, but this should not be confused with mathematical implicit or explicit modeling concepts, which rely on the existence or otherwise of algebraic loops in the model.

is a highly complex objective to accomplish numerically (for numerical and also eventually data processing reasons, if various tools are used that do not necessarily communicate together) and this will probably lead to excessive calculation times.

– Finally, the fourth factor applies to the flexibility of analytical models. Recent developments in formal calculation and in the automated processing of mathematical equations (such as substitution, derivation, and model parameter analysis automation) enable the development of extremely high-speed tools for the automated processing of models, even for the development of models. For example, in Chapter 5, the authors show how it is possible to automatically obtain equations for a reluctance network from a graphical model (itself expressed automatically in equation form) or also how it is possible to process analytical or semi-analytical models using formal or even code derivation, in order to obtain the model gradient and thus to program a sensitive calculation and optimization tool. Additionally, analytical models may, in certain cases, enable optima to be analytically calculated and thus to create local optimizations. For example, optimization of a complete permanent magnet electrical drive may contain local optimization of currents from the $d$ and $q$ axes within a more complex optimization loop [AUB 11], for which the optimization is entirely analytically expressed.

2.2.2.3.2. Limitations of analytical and semi-analytical models and advantages of numerical models

We are now developing the advantages of numerical modeling in a design process. These advantages most often correspond to the limitations of analytical or semi-analytical models, which show the complementary nature of the two approaches well:

– The first limitation of analytical models corresponds to their development time, which is generally long and which often requires complex calculations, and to the difference in generic numerical tools, which enables the model to be solved to be rapidly defined. Thus, during the development of an analytical model, automatic equation tools may be useful for facilitating this stage by avoiding calculation errors and automatically generating equations that are sometimes very long and difficult to describe.

– Secondly, solving physical equations often requires strong hypotheses regarding the physical properties of modeled components (linearity of the $B-H$ characteristic of laminations, or the absence of loss in an electronic power component, for example), or the considered geometry

(homogenization of a slotted area in an electrical machine, or further simplification of complex forms). Of course, these hypotheses limit the validity of the model and it is essential that this is well defined in order to impose constraints during the research of an optimum, if the need arises. Sensitivity analyses may also become necessary in order to study the influence of certain hypotheses on the result of an optimization and its robustness.

– Finally, based on hypotheses enabling physical equations to be solved explicitly, analytical models enable a low degree of genericity compared with numerical tools. Each new model thus requires a large number of equations to be redone, particularly if we change the development hypotheses of the model.

In order to produce a synthesis on what has just been explained, we propose two figures. First, Figure 2.5 compares the different model types and shows the compromise that exists between the execution time for the model and the level of modeling precision. Then, based on the respective advantages of numerical and analytical models, we can propose the five-stage decomposition described in Figure 2.6 for the unraveling of a typical design process. The figure describes the type of model preferentially used at each stage. It is advisable, however, to qualify the proposed vision. Indeed, as the authors explain in Chapter 4 of this book, it is possible to combine different levels of modeling in device design. Thus, the *space-mapping* or *target cascading* approaches enable the optimization of a device or system by changing the level of modeling during optimization in order to accelerate the convergence time, at the same time as the precision of the solution.

Finally, even if there appears to be great complementarity between analytical and numerical approaches during a design process, the optimization stage is preferentially achieved by use of an analytical model. In Chapters 3 and 5, the authors focus on the formulation and resolution of the problem of optimization. In a complementary way, in this chapter we consider the problem of developing the model by limiting ourselves, as we have just explained, to analytical or semi-analytical modeling. Chapter 5 presents tools enabling the automation of the construction of this type of model. In this chapter, by concentrating on an existent example, we emphasize a method of structuring an analytical model, and we detail some simple methods to enable the establishment of different parts of the model.

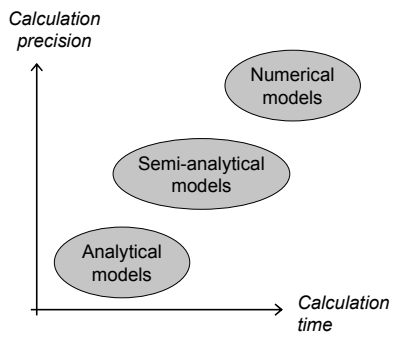


**Figure 2.5.** *Role of different model types in a precision versus resolution time context*

## 2.3. System decomposition and model structure

In this section, we explain how breaking the system down into components enables better structuring of the system model. By way of illustration, the proposed method is then applied to an example of a hybrid electrical heavy vehicle.

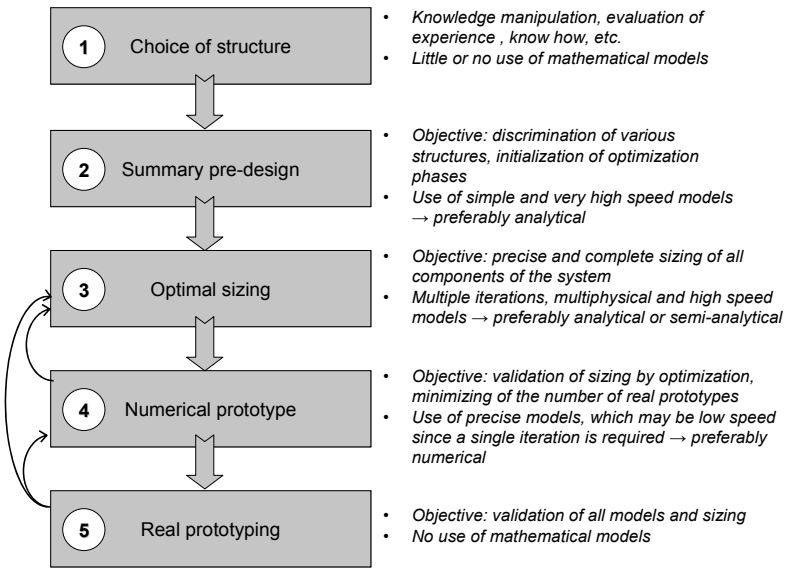


**Figure 2.6.** *Proposal for an organigram for the execution of a typical design process and the type of model used at each stage*

### 2.3.1. *Advantage of decomposition*

In general, a system is a fairly complex assembly of components that are elementary in terms of their interactions. Certainly, it is difficult to clearly define the boundary between a component and a system; for example, an actuator may be seen as being an elementary component of energy conversion, but also as a system comprised of components, such as the magnetic circuit, coil winding(s), or rolling bearings. In the context of this chapter on electrical energy, in order to attempt to adopt a more precise definition, we will assume that a *component* is a system element with an elementary function and which produces a conversion, a storage, or an energy transformation function. Thus, a combined machine and converter comprises of two *components* for which the function and type of energy conversion produced can be defined; in terms of the motor operation, the function of the static converter is to provide processed electrical energy to the electrical machine, whose function is to produce a movement in order to drive a mechanical load. Regarding energy, the role of the converter is to ensure electrical energy transformation and the role of the electrical machine is to ensure an electromechanical energy conversion.

The first stage in the development of a system model is thus its decomposition into eventual sub-systems, then ultimately, into elementary components. The role of this decomposition is to set out the operational and energy links of the system and to list the components to be modeled. This enables the modeling work to be structured. In the area of electrical energy, the following different components are generally, but not exclusively, found: electromechanical (reversible) converters, static electrical converters, energy storage devices, mechanical converters from electrochemical generators, and photovoltaic generators. Assembling these components enables the main energy chains currently encountered in electrical engineering, and more specifically in the domain of energy, to be obtained: such as production, transmission, and energy storage grids, onboard or embedded grids, and electromechanical conversion chains. Beyond clarifying the operation of the system, decomposition into components then enables us to fall back on fairly generic component modeling and on the use of the high abundance of literature on component modeling, particularly analytical modeling.

Of course, system modeling also requires us to take into account, not only the structural aspect of components, but also the functional aspects. This means that structural models (i.e. those expressing component performance in terms of its geometric and physical parameters (so as to be able to size the

device)) and functional models (which enable us to describe how components are controlled in order to ensure a given operation of the system) are required. For example, in the simple case of a machine converter assembly, we need models that link, for instance, the coupling, efficiency, and heating of the electrical machine to the geometric and physical parameters defining the laminations and coil windings, but also models expressing, based on the control function of the machine and converter, the maximum voltage, maximum current, heating, and so on, of the electronic power components. This double modeling (in varying degrees according to the practical cases considered) is thus absolutely necessary in the context of system design. Previous design approaches only took account of either the structural or functional aspects or then both sequentially, i.e. machine design was *initially* undertaken in order to obtain a particular torque and a particular speed, *then* converter sizing was undertaken in order to be able to correctly power the motor when looking to obtain the operating points from the list of specifications, and *finally* the choice of converter control (such as pulse-width or plain wave modulation) and machine control (such as vector control of an asynchronous machine, or scalar or open loop power control). Design over operating cycles and/or taking into account component lifetimes, and/or general variables such as the energy cost over the lifecycle, all require the general modeling associated with structure and control models.

The final stage in the decomposition of the system is to identify the variables of models that are positioned at interfaces and which enable the coupling of models to each other. This stage enables the double compatibility between models, mathematical and physical, to be verified; thus the coupling of an inverter model with an alternating three-phase machine model, assuming common variables between the two in order for them to be used in a modeling and/or system sizing process. If the machine is modeled using a Park model, then the converter model will need to express the three voltages as input for the machine model. Conversely, if the machine is represented by a single-phase electrical schematic, the converter will preferably be represented by voltage drops or additional internal resistances in the model. Finally, a representation of the machine using an electromechanical response surface and receiving electrical power at the input will require another response surface to deliver this electrical power. Therefore, with this simple example, the importance of having compatible physical and mathematical modeling approaches is evident; these should be ensured upstream of the moment of decomposition of the system and from the definition of modeling approaches for each component.

### 2.3.2. *Application to the example of the hybrid series-parallel traction chain for the hybrid electrical heavy vehicle*

In this chapter we consider a specific example to illustrate the explanation. This concerns the design of a hybrid series-parallel traction chain (see Figure 2.7), using an epicyclic gear set in order to ensure the coupling of the mechanical power provided by the various electrical and internal combustion engine (ICE). This hybrid traction chain is designed around the epicyclic gear set, which enables two reversible electrical machines to be mechanically coupled (operating sequentially as engine or alternator), a ICE and the addition of a differential attached to the wheels. This enables a power node to be produced. Electrically, the two machines are linked, using reversible voltage inverters, to a DC bus upon which is placed an energy pack, which may be comprised of batteries and ultra-capacitors interfaced via reversible current choppers. This structure has been implemented for the Toyota Prius car (apart from the use of ultra-capacitors) and we are voluntarily moving into a different context, consisting of applying this structure to a heavy vehicle, which may, for example, be a private waste collection or a light-armored military vehicle. The objective is to design the complete system on the basis of the specifications that describe the functionality and performance of the vehicle, i.e. from the complete traction chain, which is thus a representative system design example.

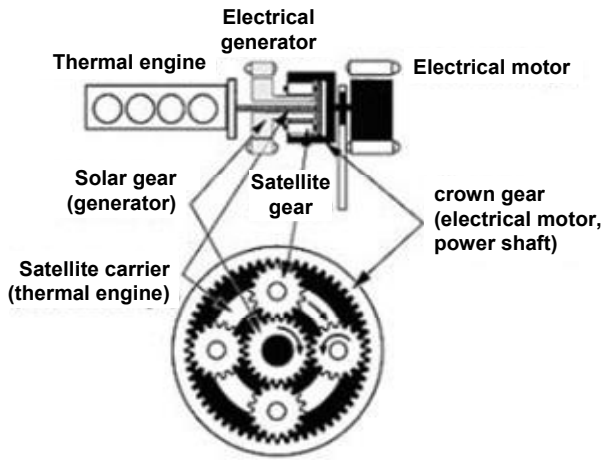


**Figure 2.7.** *Hybrid series/parallel architecture with epicyclic gear set (source: INRETS)*

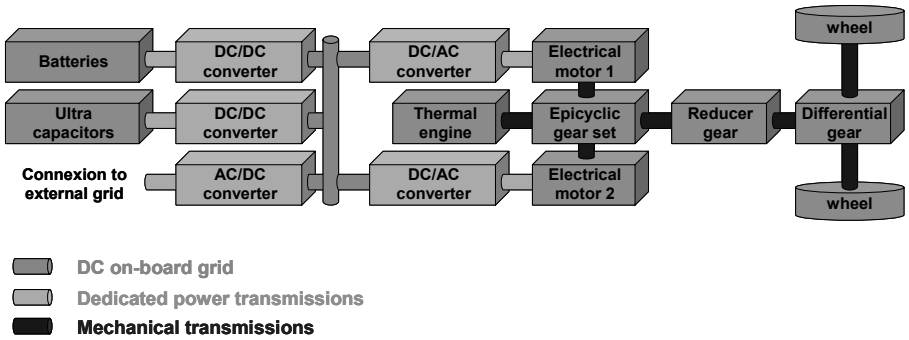


**Figure 2.8.** *Illustration of the hybrid traction structure*

If we apply the principle of decomposition to the system to be designed for this hybrid driving system, we arrive at the following elementary components:

– the ICE: this will be excluded from the scope of our investigation and will be assumed to pre-exist in the study described shortly, as the sizing of a thermal engine is a complex operation that deviates from the electrical engineering context of this chapter;

– the two reversible electrical machines;

– the two reversible voltage inverters;

– the mechanical transmission and specifically the epicyclic gear set: given the coupling and power constraints encountered here, the gear set will be double and of the Ravigneaux type;

– the energy pack, including storage devices, and reversible choppers: the sizing of these components, although pertinent in the context of this book, is not handled here, essentially so as not to make this chapter excessively long; this being the case, the system considered here remains sufficiently complex and wide ranging for the proposal to remain pertinent and of general interest.

Finally, Figure 2.8 presents a decomposition of the complete system into components. A supplementary stage not presented here would be to specify component interface (or coupling) parameters, i.e. the parameters that should be determined simultaneously during general sizing. This work will be partially achieved in the following sections.

## 2.4. General information about the modeling of the various possible components in an electrical energy system

In this section, we describe the features common to all sizing component models included in an electrical energy system. In the following sections, we address the peculiarities linked to the considered components: electrical actuators, static converters, storage devices, electrical energy storage devices, and finally, mechanical transmissions.

Insofar as this book falls within the context of systems sizing by optimization, there are effectively groups of equations common to the modeling of different components.

The first group of equations models the geometrical aspects of components. During sizing, mass and volume (overall dimensions) are key parameters. Thus, each component model should include volume and mass calculations. Two approaches are then possible:

– the first conforms to a complete design vision for the component, which is generally the case for actuators. It is then necessary to use simple geometric relations that enable the volume of each component part to be expressed;

– the second approach conforms to a choice of catalog components, which is often the case, for example, with storage components (such as capacitors and coil windings) or electronic switches. In this case, for each element, data for volume and mass need to be collected from a list of possible choices.

A second set of equations common to all components refers to cost. Once more, this is a common and essential aspect of approaches to sizing, whatever the component considered, especially within an industrial context. Note that the cost should not be reduced to a simple raw material cost, but it should be, as far as possible, representative of the complete lifecycle of the device. For energy devices, it should therefore equally integrate, for instance, the energy cost over the lifetime defined in the list of specifications and the cost of maintenance, including that of eventual replacements (for batteries, for example). This part is often indefinable and requires strong hypotheses on the predictions for the changes in certain costs (the cost of materials, for example), or even on manufacturing costs.

A third aspect focuses on the environmental impacts. In every case, system sizing should take into account all interactions with the external environment, in the largest possible sense. This refers to interactions that may be thermal, vibratory, acoustic or electromagnetic (ECM), but also linked to the deterioration of the environment (depletion of energy resources, raw materials and water, for example). The analytical modeling of physical dimensions in relation to these interactions is also indefinable here, either due to a lack of understanding of useful information (such as environmental impacts), or due to modeling difficulties (due to acoustic noise or ECM waves emitted, for example).

Finally, another significant aspect, which notably has an impact on component sizing, concerns ageing. Indeed, in system sizing approaches it is not unknown for components to be replaced over the operating duration of the device. That may, for instance, be the case with batteries or ultra-capacitors [AUB 11], which as a consequence require the integration of ageing models in order to evaluate the lifespan of the component. The key factor in this case is temperature, and Arrhenius' law, with its basis in chemical kinetics, is often used [GUI 10]. The lifetime of a component $\tau_v$ at temperature $T$ is linked to the life of a component $\tau_{v_{ref}}$ at a reference temperature $T_{ref}$ by an exponential law of the following type:

$$\tau_v = \tau_{v_{ref}} \cdot e^{\frac{T-T_{ref}}{k}} \qquad [2.4]$$

where $k$ is a characteristic parameter of the component. This formula is, for example, used for the thermal ageing of electronic components, but also electrical insulators or occasionally again, by extension, energy storage devices.

## 2.5. Development of an electrical machine analytical model

Whether in an electrical drive or in energy generation, electrical machines are very widely used to produce mechanical energy (a movement) or, reversibly, to produce electrical energy. There is an extremely rich source of literature on the subject of analytical modeling, and it is not possible here to

be exhaustive with regards to the description of all possible modeling approaches; also we only focus here on the most traditional.

### 2.5.1. *The various physical fields of the model and the associated methods for solving them*

#### 2.5.1.1. *Magnetic modeling*

The first, most regularly studied physical property is electromagnetism and, particularly, the calculation of magnetic fields in machines. The base equations are Maxwell equations and equations for magnetic materials. They can be dealt with on two levels. The first, local, consists of calculating the magnetic field and flux density at any point by solving Maxwell equations.

In an analytical approach it is only possible to solve them under certain geometric symmetry and linearity conditions. The method traditionally used is the separation of variables when mathematically possible, and the solutions obtained are then expressed as a Fourier series. The advantage of this approach is that it is local and, therefore, enables geometric effects, such as slotting, to be considered, but is limited in terms of the nonlinearity of the $B-H$ characteristics of magnetic materials. A second approach consists of considering less local dimensions, such as the magnetic flux in the various areas of the device and magnetomotive forces, which require decomposition of the device into flux tubes, which result in a *magnetic network*, where the flux sources are magnetomotive forces created using permanent magnets or coil windings. The limitation of the approach is the requirement to have preliminary knowledge of the magnetic fluxes paths, but its advantage is the possibility for nonlinear reluctances to be taken into account. A final approach consists of returning directly to the integral forms of the Maxwell equations: the magnetic flux conservation law and Ampere's theorem, which can be applied on a specific flux line in order to enable the flux density in the air gap to be determined. This in fact comes down to the use of a reluctance grid, but on a very limited mesh number (one, in the limit case). In this case, it is necessary to assume a form of flux density in the air gap, the solution enabling its amplitude to be determined, for example.

#### 2.5.1.2. *Electromechanical modeling*

The second physical property concerns the electromechanical behavior of machines. This is generally handled using electrical schemes including voltage sources (corresponding to voltages induced through flux variation),

resistances describing losses (through a Joule effect or in the magnetic circuit), and inductances and mutuals describing the storage of magnetic energy. This is possible as a result of the magnetic model for expressing induced voltages and inductances based on geometric parameters. Resistances used to model copper losses are a direct result of Ohm's law, which enables them to be expressed based on geometric parameters. Resistances used to model magnetic losses firstly require magnetic models for the calculation of losses in iron. Mostly, this calculation relies on a decomposition of the losses into a first component linked to the circulation of Foucault currents, created through magnetic field variations, a second component link to the phenomenon of hysteresis and the displacement of Weiss domains in materials, and finally, a third supplementary losses component. Then, with the magnetic losses known, resistances are introduced in order to model the dissipative phenomenon.

2.5.1.3. *Thermal modeling*

The third physical property is heat. Again, multiple approaches are possible. The first consists of establishing a thermal network, which models heat exchanges in the machine in network form. This approach is complicated, as the network can be relatively important if all exchanges are to be considered, and as there is much uncertainty regarding certain thermophysical parameters, such as convection coefficients.

Clearly a much simpler approach consists of restricting the current density in the copper and the lineic current density at the outer periphery of the stator, which, as it were, enables the sizing of the machine to be adjusted based on the type of coolant considered. The underlying idea is that the sizing of the coolant is uncoupled from the sizing of the machine; we size the machine for an effective current density (eventually calculated on operating cycle) and then size the cooling circuit, so as to be able to release the heat generated by the losses and to maintain copper and permanent magnets temperatures over an acceptable interval.

2.5.1.4. *Mechanical modeling*

Finally, the last physical property is mechanics. Beyond the equations for the mechanics of the solid, which enable the equation for the rotation of the turning parts to be determined hourly, it is also a question of determining local movements, resulting from vibrations or internal constraints based on fatigue, for example. This part is relatively specialized and will not be addressed in this chapter.

### 2.5.2. *Application to the example of a hybrid electrical heavy vehicle: modeling of a magnet surface-mounted synchronous machine*

We present here in summary form the example of a magnet surface-mounted synchronous machine with an internal rotor [SLE 92]. This type of machine is used for the motor and generator of the series-parallel hybrid driving system, described in section 2.2.3. As explained before, the model of the machine is organized according to the nature of the equations.

2.5.2.1. *Geometric and physical equations*

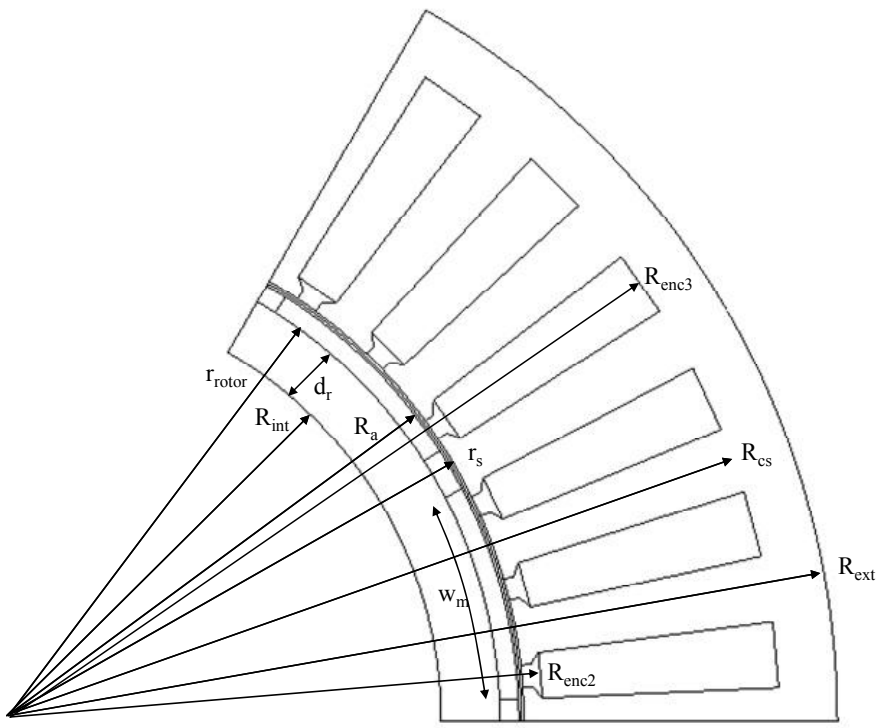


*General view of the machine*

**Figure 2.9.** *Geometry of a magnetic surface-mounted magnet synchronous machine*

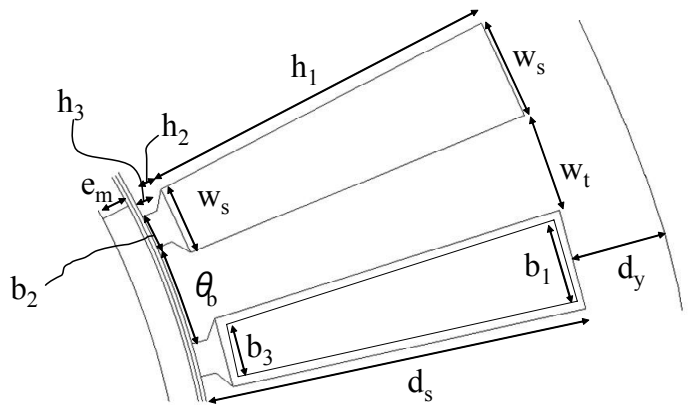


*Slot detail*

**Figure 2.9.** *(Continued) Geometry of a magnetic surface-mounted magnet synchronous machine*

Deduced from geometric structures, it is possible to express the various relations existing between the geometric parameters, but also between the volumes and masses of machines. To illustrate this, we provide the following examples:

$$r_{\text{rotor}} = R_{\text{int}} + d_{\text{r}} \qquad [2.5]$$

$$m_{\text{rotor}} = mv_{\text{rot}} \cdot \pi \left( r_{\text{rotor}}{}^{2} - R_{\text{int}}{}^{2} \right) l_{\text{r}} \qquad [2.6]$$

where $d_{\text{r}}$, $m_{\text{rotor}}$, $mv_{\text{rot}}$ and $l_{\text{r}}$ are the height and mass of the rotor cylinder head and density of steel used in its manufacture and the length of the machine active parts, which is assumed to be equal at the stator and the rotor, respectively; the other parameters are described in Figure 2.9.

The winding is overlapped with a diametric coil span; it has $N_{\text{epp}}$ slot(s) per pole, phase and it is also three-phase. We are assuming that there is only one coil winding channel per phase.

The physical equations, themselves, consist of describing the physical properties of the materials used in the manufacture of electrical machines.

For example, we quote the example of the $B-H$ relationship, which describes hard or soft (saturable) ferromagnetic materials. In this case, the $B-H$ equation is useful in order to establish the state of material saturation and thus a realistic value for the flux density in the air gap. Here we give, for example, the $B-H$ relationship for a rigid magnet in its useful zone (such as rare earth based magnets):

$$B_{\text{aim}} = B_{\text{ra}} - \mu_0 \mu_{\text{ra}} H_{\text{aim}} \qquad [2.7]$$

where $B_{\text{ra}}$ and $\mu_{\text{ra}}$ are the remnant flux density and the relative magnetic permeability of the permanent magnet.

The particularity of the geometric and physical equations is that they are not dependent on function. They are therefore defined once for all, whatever the machine operation.

2.5.2.2. *Magnetic model of the machine*

The aim of the magnetic machine model is to establish the magnetic flux density over all points of the electrical machine. For this we use a one-dimensional model here (flux conservation and Ampere's theorem). Within the context of this example, we will not develop the consideration of magnetic saturation [ESP 99] and we will assume linear operation. During the optimization stage, this will imply that flux density needs to be constrained in the different part of the magnetic circuit.

Firstly, the slotted stator is transformed into a smooth stator by applying a Carter coefficient. This transformation enables us to take into account, *on average*, the fact that the field lines, which are developed in the face of a slot, have a longer path in the air gap. In surface-mounted permanent magnet machines, based on the fact that the permeability of the magnets is close to that of air, the Carter coefficient does not apply to the real air gap $g$, but to the effective air gap $g_{\text{eff}}$, including the thickness of the magnets, $h_{\text{a}}$, and modulated using the relative permeability of the magnets:

$$g_{\text{eff}} = g + h_{\text{a}} / \mu_{\text{ra}} \qquad [2.8]$$

The Carter coefficient $K_c$ is expressed by:

$$K_c = \frac{w_e}{w_e - \frac{4g_{eff}}{\pi}\left[\frac{b_2}{2g_{eff}} arctan\left(\frac{b_2}{2g_{eff}}\right) - ln\left(\sqrt{1+\left(\frac{b_2}{2g_{eff}}\right)^2}\right)\right]} \quad [2.9]$$

where $w_e$ is the tooth space and $b_2$ the slot pitch. The corrected air gap $g_c$ is therefore expressed by:

$$g_c = K_c\, g_{eff} - h_a / \mu_{ra} \quad [2.10]$$

By assuming a rectangular form of no load flux density in the air gap (constant flux density under a magnet, positive or negative according to the polarity of the magnets, and null otherwise) and assuming that the permeability of iron is very high compared to that of air, the application of Ampere's theorem on a line of average field enables the maximum amplitude of flux density to be calculated:

$$B_{ev} = B_{ra} / \left(1 + \mu_{ra}\, g_c\, h_a\right) \quad [2.11]$$

By decomposing flux density using a Fourier series, it is finally possible to obtain the first harmonic of the flux density in the air gap:

$$B_{ev1} = 4/\pi\, B_e\, sin\left(\alpha_a\right) \quad [2.12]$$

where $\alpha_a$ is the ratio of the semi-permanent magnet pitch to the pole pitch. The flux in the air gap under a pole $\Phi_{ev}$ can then be computed by integration of the flux density under the pole, and we obtain:

$$\Phi_{ev} = r_s\, \tau_p\, l_r\, B_{ev} / \pi \quad [2.13]$$

Some flux conservation laws later enable flux and flux density to be calculated in all zones of the magnetic circuit: rotor yoke, stator yoke and teeth. For example, the no load flux amplitudes $\Phi_{dv}$ and flux density $B_{dv}$ in the teeth are:

$$\Phi_{\mathrm{dv}} = \phi_{\mathrm{ev}} / 2 \qquad [2.14]$$

$$B_{\mathrm{dv}} = \phi_{\mathrm{dv}} \Big/ \left( h_{\mathrm{cs}}\, d_{\mathrm{y}} \right) \qquad [2.15]$$

We will return to this later when we discuss the load operation.

2.5.2.3. *Electrical model*

The electrical model consists of a traditional equivalent single-phase scheme established under permanent and balanced sinusoidal three-phase conditions (see Figure 2.10).

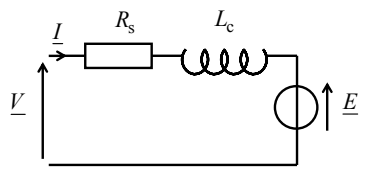


**Figure 2.10.** *Equivalent single phase electrical schematic of a smooth pole synchronous machine*

We assume that magnetic losses do not appreciably affect the electrical behavior of the machine (EMF and stator current). Consequently, the effect of iron losses is not shown in this equivalent scheme.

In this electrical scheme, $R_{\mathrm{s}}$ is the resistance of a phase, $L_{\mathrm{c}}$ is the cyclical inductance, and $\underline{E}$ is the complex representation of the EMF, induced in open circuit within a phase and assumed to be sinusoidal. Additionally, $\underline{V}$ and $\underline{I}$ are the complex representations of simple voltage and phase current, which are also assumed to be sinusoidal.

The cyclic inductance of a phase $L_{\mathrm{c}}$ is expressed based on the magnetizing inductance $L_{\mathrm{m}}$, the leakage inductance $L_{\mathrm{f}}$, and the mutual inductance $M_{\mathrm{s}}$:

$$L_{\mathrm{c}} = L_{\mathrm{m}} - M_{\mathrm{s}} + L_{\mathrm{f}} \qquad [2.16]$$

These three inductances can then be expressed based on the geometric parameters of the machine, defined in Figure 2.9, and on the number of

conductors per slot $N_{ce}$, by assuming that all of the turns of the machine are in series and that the distribution of the stator flux in the air gap is sinusoidal. The stator coil coefficient is denoted by $K_b$.

$$L_m = N_{ce}^2 \frac{4\mu_0 l_r r_s}{\pi\left(K_c g + \frac{e_m}{\mu_r}\right)} K_b^2 N_{epp} \qquad [2.17]$$

$$L_f = 2\mu_0 l_r p N_{epp} N_{ce}^2 \left(\frac{2h_1}{3(b_1+b_3)} + \frac{2h_2}{b_2+b_3} + \frac{h_3}{b_2}\right) \qquad [2.18]$$

$$M_s = \frac{L_m}{2} \qquad [2.19]$$

In the same way, the stator resistance of a phase $R_s$ is deduced from the copper conductivity $\sigma_{cu}$ and the geometric parameters of the stator coil winding.

$$R_s = 2p N_{ce}^2 \frac{l_r + l_{tb}}{\sigma_{cu} S_{enc} K_r} \qquad [2.20]$$

where $S_{enc}$, $K_r$ and $l_{tb}$ are the cross-section of a slot, the copper fill factor in the slot and the length of end winding, respectively.

The RMS induced voltage $E$ in a phase is, itself, expressed from the RMS value for the open-circuit flux of a phase for one turn per slot:

$$\Phi_s = \sqrt{2} K_b N_{epp} N_{ce} B_{ev1} r_s l_r \qquad [2.21]$$

$$E = \omega \phi_s \qquad [2.22]$$

where $\omega$ is the electric pulsation of stator quantities (such as voltage and current) which is expressed as a function of the angular rotation speed $\Omega$ by:

$$\omega = p\Omega \qquad [2.23]$$

If we break down the complex representations for the current and the voltage into two components according to the EMF axis (the $q$ axis) and a delay axis of $\pi/2$ (the $d$ axis), the following relationships can then be written:

$$\underline{V} = V_{\mathrm{d}} + j\,V_{\mathrm{q}} \qquad [2.24]$$

$$\underline{I} = I_{\mathrm{d}} + j\,I_{\mathrm{q}} \qquad [2.25]$$

$$\underline{E} = j\,\omega\Phi_{\mathrm{s}} \qquad [2.26]$$

$$V_{\mathrm{d}} = R_{\mathrm{s}}\,I_{\mathrm{d}} - L_{\mathrm{c}}\,\omega I_{\mathrm{q}} \qquad [2.27]$$

$$V_{\mathrm{q}} = R_{\mathrm{s}}\,I_{\mathrm{q}} - L_{\mathrm{c}}\,\omega I_{\mathrm{d}} + E \qquad [2.28]$$

Note that the parameters above do not coincide with $d$ and $q$ ones, provided by the Park transformation.

Insofar as the motor is powered by a three-phase voltage inverter, the RMS value for the maximum voltage that can be applied to a phase, using MLI operation without over-modulation, is expressed based on the continuous bus voltage $V_{\mathrm{bus}}$:

$$V = \sqrt{V_{\mathrm{d}}^{\,2} + V_{\mathrm{q}}^{\,2}} = V_{\mathrm{bus}} \Big/ \left(2\sqrt{2}\right) \qquad [2.29]$$

2.5.2.4. *Power balance*

Insofar as energy criteria are central to the optimal design of systems, it is necessary to express the various powers and losses involved in electrical machines.

By considering engine operation, the input power is the electrical power $P$, which is expressed based on complex representations for voltage and current:

$$P = 3\,\mathrm{Re}\{\underline{V}^{*}\,\underline{I}^{*}\} = 3\left(V_{\mathrm{d}}\,I_{\mathrm{d}} + V_{\mathrm{q}}\,I_{\mathrm{q}}\right) \qquad [2.30]$$

Electromagnetic power $P_{em}$ enables the electromagnetic torque $C_{em}$ to be expressed from the effort produced by the motor:

$$P_{em} = C_{em}\,\Omega = 3E\,I_q \qquad [2.31]$$

$$C_{em} = 3p\,\Phi_s\,I_q \qquad [2.32]$$

There are three different types of losses existing in electric machines:

– copper (Joule) losses in the copper from stator coil windings;

– magnetic (or iron) losses in the magnetic circuit;

– mechanical losses due to friction between the rotating parts and either the fixed parts or air.

Stator copper losses are simply expressed (by ignoring skin and proximity effects in the conductors):

$$P_J = 3R_s\,I^2 = 3R_s\left(I_d{}^2 + I_q{}^2\right) \qquad [2.33]$$

Iron losses in the rotor are ignored, even if permanent magnets or rotor solid yokes may be the location for intensive Foucault currents as a result of harmonic rotating fields, which are asynchronous of rotation speed. Also, as far as magnetic losses are concerned, to calculate the magnetic losses in the stator, we assume that the iron losses have only two components: the losses due to Foucault currents and those linked to the hysteresis phenomenon. For a sinusoidal variation in flux density, of amplitude $B$ and pulse $\omega$, the Foucault losses are expressed by:

$$P_{Fouc} = \frac{\sigma_{stat}\,e_{stat}{}^2}{24mv_{stat}}\omega^2 B^2 = k_{Fouc}\omega^2 B^2 \qquad [2.34]$$

where $\sigma_{stat}$, $e_{stat}$ and $mv_{stat}$ are the conductivity, thickness and density of the laminations, respectively.

The hysteresis losses are of the form:

$$P_h = k_h\omega B^2 \qquad [2.35]$$

where $k_h$ is a characteristic coefficient of the plates.

The pulse $\omega$ is directly linked to the rotation speed and the flux density in each part of the machine is linked to the field created by the magnets, but also to the armature reaction field. In order to calculate the load flux density, it is necessary to consider the resulting flux in a phase:

$$\underline{\Phi}_{\text{res}} = \underline{\Phi}_{\text{s}} + L_{\text{c}}\, I_{\text{d}} + j\, L_{\text{c}}\, I_{\text{q}} \qquad [2.36]$$

The flux density variations in the different parts of the machine follow the magnetic flux variations in a phase. For example, we can express the load flux density charging in a tooth $B_{\text{dc}}$ based on the no load flux density $B_{\text{dv}}$:

$$B_{\text{dc}} = B_{\text{dv}} \frac{\Phi_{\text{res}}}{\Phi_{\text{s}}} \qquad [2.37]$$

Then, the load iron losses in a tooth $P_{\text{ferdc}}$ are expressed by:

$$P_{\text{ferdc}} = k_{\text{h}} \omega B_{\text{dc}}{}^{2} + k_{\text{Fouc}} \omega^{2} B_{\text{dc}}{}^{2} \qquad [2.38]$$

This approach enables the flux variation in the machine which is linked to the armature reaction field to be taken into consideration, particularly during flux weakening operations, where the reduction of flux along the rotor pole axes enables the phase voltage of the machine to be reduced, but also the losses in iron.

In the example considered here, the mechanical losses in the electric machines are also ignored.

2.5.2.5. *Thermal stress*

In this example, with regards to the thermal aspects, we are simply limiting ourselves to limit the current density in the slots, without evaluating temperatures in the various parts of the machine. The value of the RMS current density in the stator conductors is then:

$$J_{\text{s}} = \frac{N_{\text{ce}}\, I}{K_{\text{r}}\, S_{\text{enc}}} \qquad [2.39]$$

## 2.6. Development of an analytical static converter model

Power electronics or "static" converters are used in order to process electrical energy with a view to its subsequent use (for example, in order to power electrical machines with variable speed and torque) or to be stored. In a sizing context, mainly two physical properties are modeled. The first concerns electrical aspects: the examination of commutation sequences enables relationships between the electrical variables and their characteristics to be obtained (mostly by use of ideal components) as well as the effective or average values on each side of the converter. This enables current and voltage rating of switching components to be sized, but also those of the passive components, which are eventually used in filters (capacitors or inductors). The second physical property concerns the thermal level. Firstly, the study of switching properties or the use of charts enables the losses in the component to be determined. Then cooling conditions enable the calculation of temperatures of the components, which enables the sizing of thermal cooling and, as explained above, the determination of lifespan.

### 2.6.1. *The various physical fields of the model and associated resolution methods*

Some electrical variables internal to switching static converters present strong dicontinuities. However, a model to precisely determine internal converter phenomena would require calculation of electrical variables with a temporal accuracy, which is often incompatible with the calculation speed required. The need to preserve the simplicity of calculations incorporated into an optimization algorithm requires expression of the model equations of static converters based on average values of electrical variables. Thus, the model is based on the formulation of variables to be optimized from average values of electrical variables, i.e. without solving the differential equations enabling the precise temporal determination of these variables, and this while taking into account transitory parameters, such as the switching frequency, for example.

The general principle of static converter modeling can be split into various stages:

– determination of electrical operational equations: the expressions of average electrical value equations will be used to define the electrical parameters required for sizing;

– determination of equations characterizing semi-conductors and eventual passive elements: electrical, inductive, capacitive, magnetic dielectrical and thermal behaviors;

– determination of measurements enabling quantification of the criteria to be minimized: mass, volume, and losses in passive elements;

– definition of constraints across all of the calculated parameters, whatever their nature: size limitations, levels of admissible loss, and temperatures, which are limited on internal electrical measurements, input and outlook.

The characteristics of static converters are always closely linked to the nature of the loads with which they are associated. For example, it is practically impossible to disassociate the sizing of electrical machines from that of the converters powering them, not even to enable electric actuators to reach predicted operating conditions (speed and torque), or even to make the electrical power source compatible with the actuators. In this case, the separate optimization of the converter, assuming the electrical variables are known, is not truly relevant. Conversely, the problem of optimally designing the electrical actuator could not be resolved without the prior acceptance of a sizing of the static converter that powers it, in particular, in order to define the stresses on electrical measurements. This is so, for example, with inverters powering alternative machines, which have no passive components for which sizing is critical, but for which the level of losses is closely linked to the electrical variables imposed by the continuous source and the alternative load. Thus, modeling of static converters should highlight the potential impact of electrical variables (imposed by actuators and sources) on the influence that converters have on the criteria.

When architecture, technology and the integration characteristics of a static converter are imposed, modeling may occasionally be limited to the calculation of losses. Conversely, when the static converter contains elements for which sizing is critical, the model must include calculation of the relevant dimensions (this is the case, for example, for the boost converter, which contains a smoothing inductance, for which the mass, volume, and cost may be preponderant factors).

The following section presents the example of voltage source inverter modeling, which may enable the powering of hybrid propulsion electrical machines, which have already been considered in the sections above.

### 2.6.2. *Application to the example of a hybrid electrical heavy vehicle: modeling of inverters feeding synchronous machines*

The modeling example presented in this section applies to inverters powering permanent magnet synchronous electrical machines. This type of static converter (DC/AC converters) is integrated with the hybrid traction of a heavy vehicle for which the outline schematic is shown in Figure 2.8. The model must enable the sizing of two distinct inverters, since the electrical machines are not necessarily identical.

The electrical engines are powered by a DC voltage onboard grid. The converters associated with electrical machines must ensure a continuous/alternative conversion and allow for control into the four quadrants of electrical machines. The structure selected is therefore the voltage inverter represented in Figure 2.11, which therefore enables these requirements to be satisfied.

The approach for the sizing of converters consists of traditional two-level voltage source inverter structures, controlled by pulse width modulation, so as to power electrical machines without any appreciable harmonic defects. Thus the modulation strategy selected is an asynchronous sinusoidal modulation and the carrier frequency chosen is sufficiently high (of the order of 10 kHz), which enables the control of the electrical machines considered to be close to sinusoidal conditions. The dead times *Ts*, which enable risk-free short-circuit commutation of the bridge, will be ignored during modeling, given their low impact on losses and sizing.

The optimization of the inverter topology and the reduction of losses in semi-conductors through commutation frequency reduction are not dealt with here, but could be envisaged. It should then include some corrective measures for the degradation of current wave forms in electrical machines and therefore of torque ripple and supplementary losses that they produce. The consideration of harmonic phenomena linked to pulse width modulation should become necessary in this case and should be integrated into electrical machine modeling.

In this example, the cooling system is influenced by the structure of the vehicle. It comprises a water-glycol mix, which is retrospectively measured in order to ensure the thermal performance of the components. The heat transfer structure does not form part of the sizing of the converter.

The aim is to model the losses in the converters, having previously selected simple structures to be configured and to be controlled. The choices are applied to the design of independent converters. The study of the mechatronic integration of power electronics in electrical machines is not discussed for reasons of simplicity, but could be relevant in order to enable volume minimization. It would then be necessary to pay particular attention to the resolution of thermal and electromagnetic problems linked to any phenomenon characterizing the physical interaction between the inverter and the electrical machine. It would then no longer be possible for the modeling of inverters and electrical machines to be separately tackled.

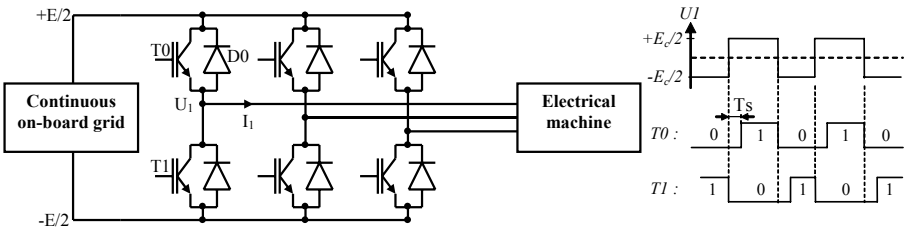


**Figure 2.11.** *Power converter associated with electrical machines*

Here, the model is reduced to the calculation of losses in power converters, which are distributed as follows:

– conduction losses in insulated gate bipolar transistors (IGBT);

– conduction losses in diodes;

– commutation losses in IGBTs;

– commutations losses in diodes.

The losses in the inverter are analytically expressed based on the electrical variables, by assuming the operating condition to be as for a sinusoidal current. This hypothesis may be justified by the inductive behavior of electrical machines and by the choice of a sufficiently high commutation frequency to limit the current harmonics. Thus, the dissipative behavior of the converter becomes entirely predictable for the dynamic internal converter parameters. When the amplitudes and phase currents emitted from the inverter are unknown, analytical modeling of electromechanical behavior of the electrical machine enables them to be determined from the control laws chosen (torque, power, speed, DC

voltage). Determining semi-conductors is rather linked to technological or integration choices that are dependent on market rates and on location environment. Thus, the types of component are imposed within consistent ranges. IGBT and manufacturer's inverter diode parameters, DC voltage and machine currents constitute the input data for loss modeling. As an example, Table 2.1 lists these characteristics for Semikron IGBT SKM600GB066D modules.

| **Parameter** | **Symbol** | **Value** |
|---|---|---|
| Manufacturer voltage for measurement of $E_{on}$, $E_{off}$ | $V_{Eon_off}$ | 300 V |
| Manufacturer current for measurement of $E_{on}$, $E_{off}$ | $I_{Eon_off}$ | 600 A |
| Energy dissipated by IGBT turn-on | $E_{on}$ | $7.5\times10^{-3}$ $J$ |
| Energy dissipated by IGBT turn-off | $E_{off}$ | $29.5\times10^{-3}$ $J$ |
| Drop-in direct IGBT voltage | $V_{CEsat}$ | 1.9 V |
| Commutation frequency | $F_{com}$ | 10,000 Hz |
| Drop-in direct diode voltage | $V_{F0}$ | 1 V |
| Energy dissipated by diode turn-off | $E_{rr}$ | $25\times10^{-3}$ $J$ |
| Continuous input voltage | $V_{bus}$ | 540 V |

**Table 2.1.** *Semi-conductor characteristics given by the manufacturer*

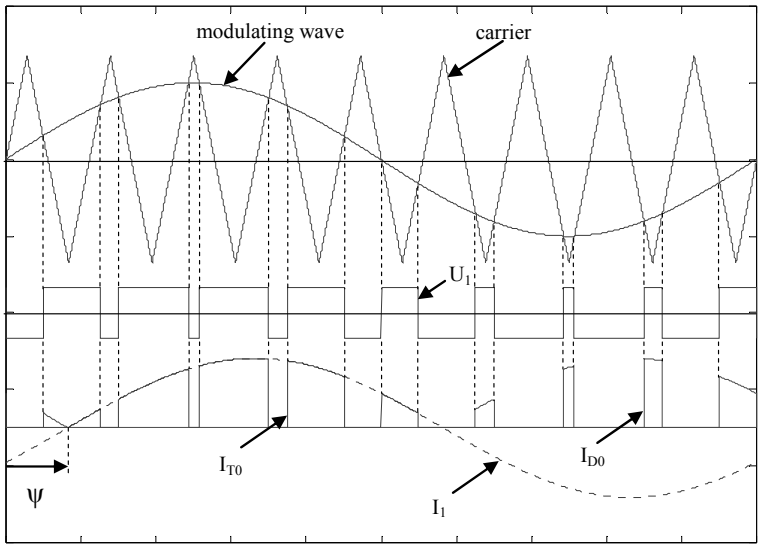


**Figure 2.12.** *Current construction in semi-conductors*

Figure 2.12 illustrates the method for determining currents in the upper IGBT, *T0*, and its inverse diode *D0* in the case of bipolar sinusoidal modulation control of the inverter. The currents in the semi-conductors are only equal to the currents circulating in the machine during the conduction delay imposed by modulation. The sign of the current defines which component, the IGBT or the diode, is in conduction. Since all controls can be reproduced through symmetry and as the machine is balanced, the conduction, dissipation, other IGBT, and other diode conditions are identical.

2.6.2.1. *Conduction losses in IGBTs and diodes*

Conduction losses in semi-conductors are obtained by firstly determining their dissipation characteristic under static conditions, which is generally given by the manufacturer. Figure 2.13 illustrates the curves giving the drop-in voltage at the IGBT and diode terminals, based on the current and the junction temperature conditions. Various levels of modeling precision are then possible according to whether or not a high level of precision in loss evaluation is required, and whether temperature conditions are determinant in the understanding of losses. We can then consider models with varying degrees of complexity:

– a fixed voltage drop approximating the general state of the component for simpler models;

– a null current voltage drop and a dynamic resistance based on temperature. The dotted curves illustrate models defined from a constant dynamic resistance for a junction temperature of 150°C for IGBTs and diodes;

– a voltage drop identical to that given by the manufacturer, stored in table form or reconstructed by polynomial approximation [DEP 95].

The conduction losses in each IGBT are expressed by integration over an electrical period $T$ of the instantaneous power at the component terminals, which are obtained from the product of the current circulating in the component and the corresponding voltage drop. The calculation is applied here to the case of a simplified model that combines the voltage drop to that obtained under nominal component conditions, increasing losses in the semi-conductors, which safeguards against the likelihood of under-sizing when the actual operating mode of the converter is not known precisely. The simplicity of the model also enables the corresponding calculation load to be

limited. The equation expressing the power dissipated by IGBT conduction is given by:

$$P_{\text{condT}} = \frac{1}{T} \cdot \int_0^T V_{\text{CEsat}} \cdot I_{\text{T}}(t) \cdot dt \qquad [2.40]$$

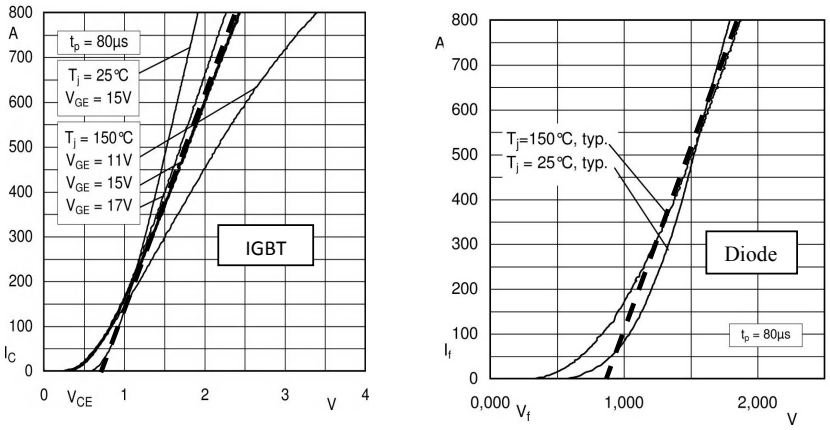


**Figure 2.13.** *Static voltage drop characteristics in IGBTs and diodes*

The assumption of a bipolar sinusoidal modulation sets the duty cycle based on the initial phase, the modulation rate, and the phase shift between voltage and current of the electrical machine:

$$\alpha(t) = \frac{1}{2} + m \cdot \sin(\omega t + \psi) \qquad [2.41]$$

where $m$ represents the modulation rate and $\psi$ the phase shift between the modulator (reflecting the machine voltage $V$) and the current $I$ from the same machine phase, which is taken as a reference value. From this we can then deduce the current in the IGBTs based on the phase current (combined with a sinusoidal current) and ultimately the conduction losses per IGBT. They are given by the expression below, where $I_{\max}$ and $V_{\max}$ represent the phase current and voltage amplitudes respectively:

$$P_{\text{condT}} = \frac{V_{\text{CEsat}} \cdot I_{\max}}{2} \cdot \left[ \frac{1}{\pi} + \frac{V_{\max}}{2 \cdot V_{\text{bus}}} \cdot \cos(\psi) \right] \qquad [2.42]$$

The conduction losses in the diodes are obtained by applying the same calculation methods and by taking into consideration conduction that is complementary to that of IGBTs over each carrier period interval.

$$P_{\text{condD}} = \frac{V_{\text{FO}} \cdot I_{\max}}{2} \cdot \left[ \frac{1}{\pi} - \frac{V_{1\max}}{2 \cdot V_{\text{bus}}} \cdot \cos(\psi) \right] \qquad [2.43]$$

2.6.2.2. *Commutation losses in IGBTs and diodes*

The commutation losses in IGBTs are obtained by extrapolating the dissipated energy values given by the manufacturer based on the voltages and currents observed during commutation, using linear approximation. The curve in Figure 2.14, which has been provided by the manufacturer, shows the virtually linear dependence of commutation losses in IGBTs ($E_{\text{on}}$ and $E_{\text{off}}$), based on cut-off or initiation currents and reverse recovery losses in diodes ($E_{\text{rr}}$) based on the diode current.

Thus the power dissipated per transistor for each initiation is defined as the sum of dissipated energies for 1 second at initiation, by adjusting the value of losses $E_{on}$ given by the manufacturer for a current $I_{Eon_off}$ and a voltage $V_{Eon_off}$, to values for current $I$ and voltage $V_{\text{bus}}$, which are applied to the component, as expressed by the following equation:

$$P_{\text{onT}} = \sum_{i=1}^{N(1s)} E_{\text{on}} \frac{I(i)}{I_{\text{Eon_off}}} \cdot \frac{V_{\text{bus}}}{V_{\text{Eon_off}}} \qquad [2.44]$$

By approximating the distribution of commutations as being uniform over the positive alternance (which is all the more justified when the commutation frequency is high), the average value of the current over the considered alternance may replace the current during commutation. The IGBT losses at initiation are then expressed by the following equation:

$$P_{\text{onT}} = \frac{E_{\text{on}} \cdot I_{\max} \cdot V_{\text{bus}}}{\pi \cdot I_{\text{Eon_off}} \cdot V_{\text{Eon_off}}} \cdot F_{\text{com}} \qquad [2.45]$$

Proceeding in the same way for losses at IGBT extinction, the following equation is obtained:

$$P_{\text{offT}} = \frac{E_{\text{off}} \cdot I_{\max} \cdot V_{\text{bus}}}{\pi \cdot I_{\text{Eon_off}} \cdot V_{\text{Eon_off}}} \cdot F_{\text{com}} \qquad [2.46]$$

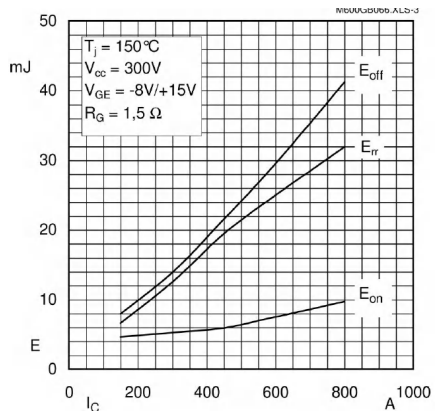


**Figure 2.14.** *Evolution of IGBT and diode losses, based on current*

Commutation losses in diodes are the result of reverse recovery and are not dependent, at a given current, on voltage. Each diode extinction is accompanied by an energy dissipation $E_{\text{rr}}$, matched to the value of the current in the diode at the moment of its extinction.

$$P_{\text{comD}} = \frac{E_{\text{rr}} \cdot I_{\max}}{\pi \cdot I_{\text{Eon_off}}} \cdot F_{\text{com}} \qquad [2.47]$$

2.6.2.3. *Total converter losses*

The total IGBT losses are then simply expressed using the equation below:

$$P_{\text{T}} = P_{\text{condT}} + P_{\text{onT}} + P_{\text{offT}} \qquad [2.48]$$

Similarly, the total diode losses are expressed using the following equation:

$$P_{\text{D}} = P_{\text{condD}} + P_{\text{comD}} \qquad [2.49]$$

Finally, from this the total inverter semi-conductor losses are deduced:

$$P_{\text{ond}} = 6 \cdot (P_{\text{D}} + P_{\text{T}}) \qquad [2.50]$$

## 2.7. Development of a mechanical transmission analytical model

The mechanical transmissions used in electrical systems are devices that enable certain characteristics of one or more movements to be changed. The first step is to choose the type of gearing device from the functional constraints, such as: reduction or multiplication, transformation from rotational to transfer movement (endless screw), change of direction of the axis of rotation (spherical gear set) and power addition (epicyclic gear set). Then, the gearings are essentially comprised of mechanical sections using gears. The shape and material used to produce geared sections are then defined from considerations linked to factors such as the resistance of the materials, the noise emitted, transmission efficiency, and performance tolerance. The sizing of these devices may consist of using existing devices whose performances are closest to the objectives, but it may also be necessary to custom-size the gearings, which requires geometric parameters to be determined, such as radii, lengths, and gearing geometries. It is precisely these parameters that can be modeled and optimized based on the mechanical constraints of the transmission: the torque to be transmitted and the rotation speed of each gearing section. The equations implemented are from solid mechanics, but it is also necessary to take account of other constraints linked to normalized pinion sizes and to good gearing conditions, which aim to limit noise and wear and tear and fatigue on the teeth. These constraints are defined in other reference works and can easily be translated in the form of constraints in a problem of optimum sizing.

### 2.7.1. *The various physical fields of the model and associated resolution methods*

Mechanical transmissions are comprised of multiple gearings, which should be sized in order to enable the mass, bulk and efficiency to be optimized, while still conforming to size constraints and material resistance. Modeling these should take the following studies into consideration:

– geometric: definition and relationships between the size parameters of the gear wheels and other mechanical sections;

– kinematic: relationships between the geared wheels, the torques to which they are subjected and their radii. This study also enables the power transmitted by each geared wheel to be determined;

– material resistance: this corresponds to equations emanating from standards expressing the contact pressure and resistance to bending of the gears. These measurements are then required in order to restrict the diameters, widths, and modules that define gear wheel geometry;

– power losses: equations defining gearing losses and enabling the efficiency of the complete system to be determined. The mixing/ventilation and gearing losses are most commonly encountered.

### 2.7.2. *Application to the example of a hybrid electric heavy vehicle: modeling of the Ravigneaux gear set*

The Ravigneaux gear set, which was designed in two stages, enables the distribution of mechanical power between the vehicle wheels, the thermal engine, and both electrical machines. It comprises a crown, a satellite holder, two satellites, and two solar gearings, numerically referenced in order to ease the equating of variables associated with each of these elements. The thermal motor is linked to solar gearing #4, the electric machine #1 to crown #5, the electric machine #2 to solar gearing #1 and the output (connected to the wheels via the mechanical transmission) to satellite carrier #6, as illustrated in Figure 2.15. This is a simplified theoretical representation as the real structure contains three satellites #2 and three satellites #3, symmetrically distributed over the circumference of the set in order to spread the effort. However, its mechanical structure is technically more complex.

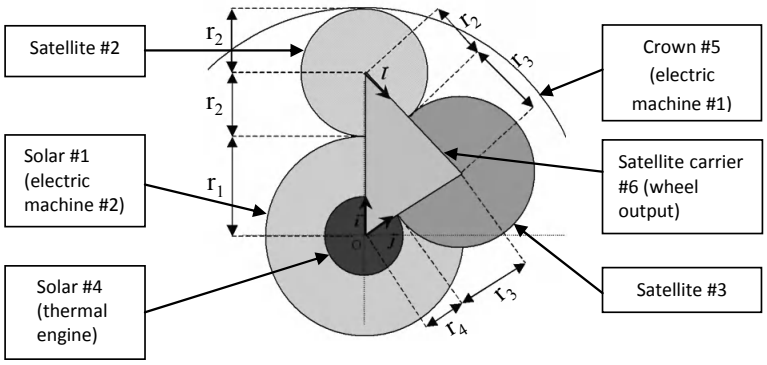


**Figure 2.15.** *Theoretical schematic of the epicyclic gear set*

### 2.7.2.1. *Geometric dimensions of the Ravigneaux gear set*

The epicyclic gear set uniquely comprises parallel, straight toothed gears, which can be dimensionally characterized, as shown in Figure 2.16. The module *m* is defined as being the ratio, common to the pinions and the crown, between the primitive diameter *d* and the number of teeth *Z*. In this case, it is therefore the same for all gears in our epicyclic gear set. It is a normalized constant for which the possible values come from the ISO 54 standard. The relative equations for the dimensions of the gearing are summarized in Table 2.2. When the radii are used in the expressions, they will carry the notation *r* and the same index as the diameter to which it corresponds.

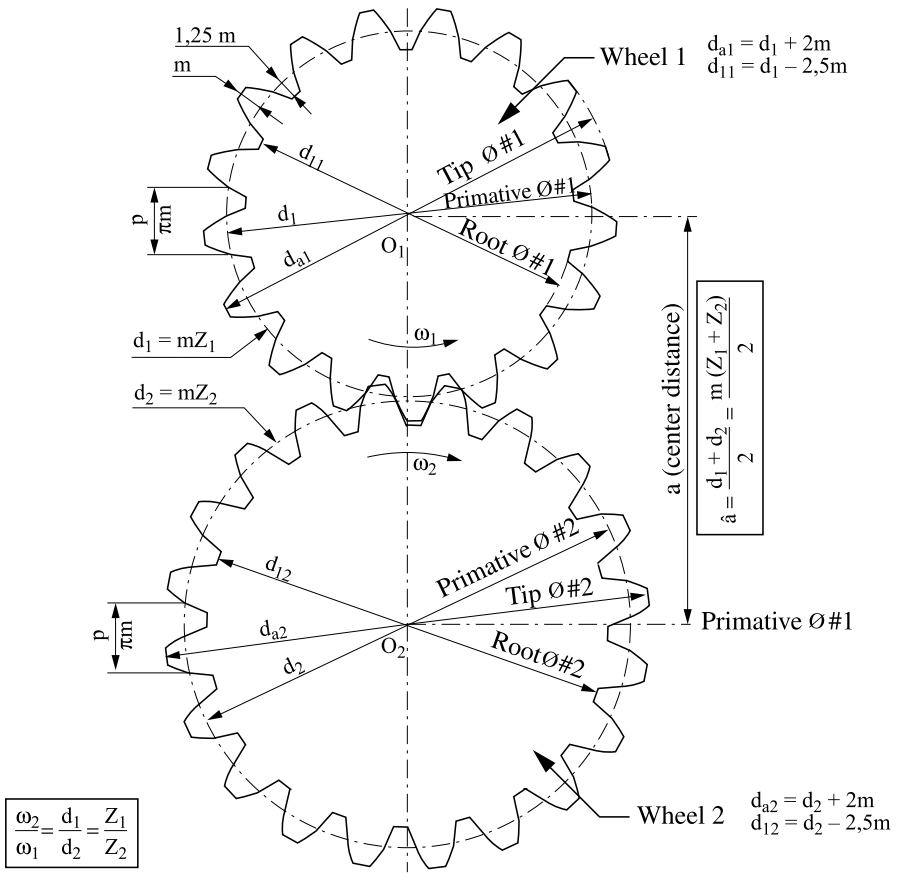


**Figure 2.16.** *Principal characteristic dimensions of straight toothed gearings (source: [FAN 01])*

| Title | Symbol | Formula |
|---|---|---|
| Module | $m$ | Normal values |
| Number of teeth | $Z$ | |
| Primitive step | $p$ | $p=\pi m$ |
| Primitive diameter | $d$ | $d=mZ$ |
| Tip diameter | $d_a$ | $d_a=d+2m$ |
| Root diameter | $d_f$ | $d_f=d-2.5m$ |
| Base diameter | $d_b$ | $d_b=d\cos\alpha$ |
| Projection | $h_a$ | $h_a=m$ |
| Cavity | $h_f$ | $h_f=1.25m$ |
| Tooth height | $h$ | $h=2.25m$ |
| Tooth thickness | $s$ | $s_1=e_1=s_2=e_2=\pi m/2$ |
| Interval | $e$ | $s_1+e_1=s_2+e_2=p$ |
| Gearing width | $b$ | $b=km\ (5 \leq k \leq 16)$ |
| Center distance | $a$ | $a=(d_1+d_2)/2$ |
| Pressure angle | $\alpha$ | $\alpha=20°$ |

**Table 2.2.** *Characteristic dimensions of a straight toothed gearing*

### 2.7.2.2. *Kinematic relationships from the Ravigneaux gear set*

Kinematics enables relationships between torques and rotational speeds of the components of the Ravigneaux gear set to be expressed. The equations can be obtained either from analytical kinematics or using the Willis method.

Relationships between rotational speeds and gearing radii:

$$n_1 = \frac{n_6(r_1+r_4)-n_4r_4}{r_1} \qquad [2.51]$$

$$n_2 = \frac{n_6(r_1+r_2)-n_1r_1}{r_2} \qquad [2.52]$$

$$n_3 = \frac{n_6(r_3+r_4)-n_4r_4}{r_3} \qquad [2.53]$$

$$n_5 = \frac{2n_6(r_1 + r_2) - n_1 r_1}{r_1 + 2r_2} \qquad [2.54]$$

Relationships giving output torques:

$$C_1 = \left(\frac{r_1}{2(r_1 + r_2)}\right)\left(\frac{r_1 - r_4 + 2r_2}{r_4} C_4 - C_6\right) \qquad [2.55]$$

$$C_5 = r_5\left(\frac{-r_1 - r_4}{2(r_1 + r_2) r_4} C_4 - \frac{1}{2(r_1 + r_2)} C_6\right) \qquad [2.56]$$

2.7.2. 3. *Material resistance*

The study of material resistance is based on the ISO 6336 standard "Calculation of load capacity of spur and helical gears", which defines the influencing factors characterizing the reciprocal reaction efforts between gearings [AFN 06]. This standard enables the contact pressure and tooth root bend to be determined, which will, in turn, enable us to define a stress based on the choice of primitive diameters, widths and gearing module, in order to avoid any risk of gear set rupture. The corresponding calculations are determined from the expression of several dozen available factors for the standard. This part of the model is certainly one of the most resource-hungry in terms of calculation time.

2.7.2.4. *Power losses*

There are many reasons for power losses in gear transmissions, such as surface state or the type of lubricant, for example, and can be determined through calculation or by testing. Many reasons for energy dissipation can be distinguished, friction between teeth and the lubrication process being the main causes. They have a direct bearing on efficiency since they generate power losses. Currently there are numerous studies being undertaken in this area and various patterns are emerging. Here we are using the theory developed by G. Henriot [HEN 99], who defines power loss $P_V$ as the sum of the power losses, which are independent $P_N$ and dependent $P_L$ on the load:

$$P_V = P_N + P_L \qquad [2.57]$$

The efficiency of the gear set is therefore defined from the input power $P_A$ as follows:

$$\eta = \frac{P_A - (P_L + P_N)}{P_A} \qquad [2.58]$$

The lost power $P_L$ is combined with the gearing losses and $P_N$ to the mixing and ventilation losses in the gearings. This model is described as follows.

*Gearing losses*

The gearing losses between two pinions are expressed from the two combined profiles corresponding to the approach and recess periods. The corresponding approach and recess lengths are expressed from the geometric properties of the two pinions ($r_a$: tip radius, $r_b$: base radius, $r$: primitive radius, and $\alpha$: pressure angle):

– approach length $g_f$:

$$g_f = \sqrt{\left(r_{a2}^2 - r_{b2}^2\right)} - r_2 \sin\alpha \qquad [2.59]$$

– recess length $g_a$:

$$g_a = \sqrt{\left(r_{a1}^2 - r_{b1}^2\right)} - r_1 \sin\alpha \qquad [2.60]$$

The tangential component $Q$ of the contact force is dependent on the friction coefficient $f$ and the normal effort due to the contact reaction $F_n$:

$$Q = F_n \cdot f \qquad [2.61]$$

The friction coefficient $f$ is not uniform and is dependent on many factors. It increases when the load increases, reduces when the slip speed increases and reduces when the oil viscosity increases (increase of the thickness of the oil film). Its value is between 0.02 and 0.07. In our case, we are using an average value $f_m = 0.04$ .

The work lost through friction from the start to the end of gearing is expressed as a function of Q and of the total slip from the combined profiles $G_a$:

$$t_\mu = Q \cdot G_a = F_n \cdot f_m \cdot \left( \frac{1}{r_1} + \frac{1}{r_2} \right) \frac{g_f^2 + g_a^2}{2\cos\alpha} \qquad [2.62]$$

The work lost through friction for a complete wheel turn is therefore given by:

$$\zeta_\mu = F_n \cdot f_m \left( \frac{1}{r_1} + \frac{1}{r_2} \right) \frac{g_f^2 + g_a^2}{2\cos\alpha} \cdot \frac{2\pi}{(g_f + g_a)/r_2 \cos\alpha} \qquad [2.63]$$

Let:

$$\xi_\mu = \pi \cdot r_2 \cdot F_n \cdot f_m \cdot \left( \frac{1}{r_1} + \frac{1}{r_2} \right) \frac{g_f^2 + g_a^2}{g_f + g_a} \qquad [2.64]$$

However, the work provided by the motive pinion to the wheel is:

$$\zeta_m = F_t \cdot 2\pi \cdot r_2 = F_n \cdot \cos\alpha \cdot 2\pi \cdot r_2 \qquad [2.65]$$

Efficiency is therefore given by the following equation:

$$\eta = \frac{\zeta_m - \zeta_\mu}{\zeta_m} = 1 - f_m \left( \frac{1}{r_1} + \frac{1}{r_2} \right) \frac{g_f^2 + g_a^2}{2(g_f + g_a)\cos\alpha} \qquad [2.66]$$

The power losses can therefore be expressed based on the efficiency $\eta$ of the input torque $T_1$ and the input rotation speed $n_1$:

$$P_M = T_1 \cdot n_1 \cdot (1 - \eta) \qquad [2.67]$$

These formulae are applied to the pinion interfaces quoted above in order to give the total power losses $P_L$ in the gearing:

– solar gearing #1 and satellite #2;

– solar gearing #3 and satellite #4;

– satellite #2 and crown #5;

– satellite #2 and satellite #3.

*Mixing and ventilation losses*

Gears rotate virtually submerged in a reservoir of oil for the purposes of lubrication. When the oil is mixed it creates warming resulting in mechanical losses. Power losses from ventilation represent the power lost as a result of the aerodynamic drag of the teeth in the air-oil mixture in a gearbox. These mixing and ventilation losses $P_{WG}$ are estimated separately for each wheel or pinion according to the following formula [HEN 99]:

$$P_{WG} = \frac{d_W^2 n^2 b_W \cos^3 \beta_W m_n 1,42\times10^{-11}}{A} \qquad [2.68]$$

where:

$d_W$: primitive operating diameter of the wheel;

$n$: rotation speed in rpm of the wheel;

$b_W$: width of the tooting;

$\beta_W$: primitive incline (in our case, $\beta_W = 0$);

$m_n$: real module;

$A$: absolute viscosity function $\xi$ of the lubricant at 95°C, where:

$$A \cong \frac{22440}{\xi} = 1.9\times10^6 \, s\cdot m / kg \qquad [2.69]$$

where $\xi$ is dependent on the kinematic viscosity and the density of the fluid, as described in [DAL 99].

The sum of the mixing and ventilation losses gives the total mixing and ventilation loss $P_N$.

2.7.2.5. *Mass of the Ravigneaux gear set*

The masses of each of the pinions, the gear set crown, and the transmission shafts are calculated from their geometric parameters and from

the density of the steel. The calculation is uniquely presented for solar gearing #1, for example, with other calculations being carried out according to the same principle. The solar gearing #1 linked to electric machine #2 comprises a spurred wheel with a hole in the center for the shaft. The volume occupied by the pinion is determined first of all, without considering the teeth:

$$V_{\text{cylinder1}} = \pi \cdot \left( r_{\text{f1}}^2 - r_{\text{shaft1}}^2 \right) \cdot b_{12} \qquad [2.70]$$

The volume occupied by the teeth separately is calculated as follows:

$$V_{\text{teeth1}} = \left[ \left( \frac{\left( s_{\text{a1}} + s_{\text{b1}} \right)\left( r_{\text{a1}} - r_{\text{b1}} \right)}{2} \right) \cdot b_{12} + s_{\text{b1}} \cdot \left( r_{\text{b1}} - r_{\text{f1}} \right) \cdot b_{12} \right] \cdot z_1 \qquad [2.71]$$

where:

$$\begin{cases} s_{\text{a1}} = r_{\text{a1}} \left[ \dfrac{s}{r_1} + 2\left( \left( \tan\alpha - \alpha \right) - \left( \tan\alpha_{\text{a1}} - \alpha_{\text{a1}} \right) \right) \right] \\ \alpha_{\text{a1}} = \arccos\left( \dfrac{r_1}{r_{\text{a1}}} \cos\alpha \right) \\ s_{\text{b1}} = r_{\text{b1}} \left[ \dfrac{s}{r_1} + 2\left( \tan\alpha - \alpha \right) \right] \end{cases} \qquad [2.72]$$

The mass of solar gearing #1 is then determined from the two volume expressions:

$$m_{\text{solar gearing1}} = V_{\text{cylinder_1}} \cdot \rho_{\text{steel}} + V_{\text{teeth_1}} \cdot \rho_{\text{steel}} \qquad [2.73]$$

The calculation of the total mass of the gear set is obtained from the sum of the masses of each component of the gearing set. We then obtain:

$$m_{\text{gearset}} = m_{\text{solar gearing1}} + 3 \cdot m_{\text{satellite2}} + 3 \cdot m_{\text{satellite3}} + m_{\text{solar gearing4}} + m_{\text{crown5}} + m_{\text{satellite carrier6}} + m_{\text{shafts}} \qquad [2.74]$$

2.7.2.6. *Bulk of the Ravigneaux gear set*

The total bulk of the gearing set is defined from that of crown #5, since this surrounds the whole system. It is therefore given by the expression:

$$V_{\text{total}} = \pi \cdot r_{\text{tot}}^2 \cdot b_5 \qquad [2.75]$$

where:

$r_{\text{tot}}$: Outer radius of crown #5;

$b_5$: Total width of crown #5.

## 2.8. Development of an analytical energy storage device model

Energy storage devices are widely used in all embedded applications, but also increasingly to compensate for electrical power fluctuations produced by generators using renewable energy sources. The sizing of these storage elements essentially occurs through research into the adequacy of the device's energy capacities (energy and power) for the researched objective. It is clear that in virtually all cases, sizing consists of choosing one or more components that are best suited and determining the number required from this. Under these conditions, the factors determining the sizing, which need to be defined for an operating cycle are: the maximum energy to be stored, the maximum operating voltage, the maximum load and/or unload power, and the maximum load and/or unload current. The models to be implemented are therefore electrical models, which enable these electrical factors to be determined over an operating cycle.

## 2.9. Use of models for the optimum sizing of a system

### 2.9.1. *Introduction*

General optimization strategy is based on the simultaneous design of all of the components of the vehicle traction chain. Figure 2.17 illustrates the different variables of these components, i.e.:

– imposed components: these are fixed components, which are not included in sizing, such as the thermal engine, which is chosen from commercially available engines, and vehicle wheels associated with the transmission, which cannot be modified. The torques and rotational speeds

of the shafts of these components, ($C_4$, $n_4$) and ($C_6$, $n_6$), respectively, are the link variables imposed by the elements themselves;

– components to be optimized: these are components that are not pre-defined, such as batteries, ultra-capacitors, both electrical machines, their associated converters, and the Ravigneaux gear set. The link variables between these components need to be defined at the same time as the sizing of components and can therefore also be optimized. This is the case for torques and rotational speeds of the shafts of both electrical machines ($C_5$, $n_5$, $C_1$, and $n_1$), their feeding voltages and currents ($V_{m1}$, $I_{m1}$, $V_{m2}$, and $I_{m2}$), the continuous grid voltage $V_{bus}$, voltages at battery terminals $V_{bat}$, and ultra-capacitors $V_c$.

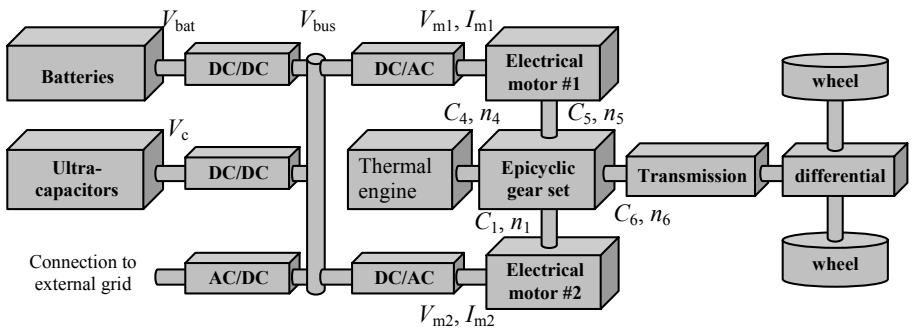


**Figure 2.17.** *Link variables between components*

The optimum sizing of components that are not pre-defined occurs by expressing the modeling equations for each, which express an objective function $J_i$ defined from the variables to be optimized. This objective function may concern bulk, mass, losses or efficiency, according to the choice of the designer. Finally, the design constraints are expressed.

When optimization occurs individually, knowledge of the link variable values defining the inputs and outputs of the components being optimized is essential. This enables us to ensure compatibility between the system components. The order in which the components are sized may be significant if sizing of the first components enables the input or output variables to be used for subsequent components. When optimization is general, only constraints on the link variables are necessary. Components are simultaneously optimized by minimizing a cost function $J_{total}$, defined as being the sum of the cost functions for each component:

$$J_{\text{total}} = \sum J_{\text{i}} \qquad [2.76]$$

The application example discussed here corresponds to the optimization of more than 50 parameters comprised of input measurements of component models and described non-exhaustively in the equations in this chapter. The constraints are applied at the same time to the input parameters and certain output parameters, depending on the situation. The cost functions, described in the following sections, must integrate the provisional usage profile of the component being considered. Indeed, the evaluation of losses in a cost function, for example, requires the choice of one or more operating points (mission profile) at which they will be calculated. It is thus necessary to determine the most representative operating points for the usage of the component. When the usage profiles are quite complex, multiple operating points affected by factors weighting their occurrence rate are defined from a statistical pre-study of theoretical usage profiles for the component. The operating points and their weighting then correspond to their weighted barycentric values [DAG 11]. This approach, which is described in the next section, is applied to the consideration of a simplified theoretical hybrid vehicle mission profile. Other approaches have been specifically presented on this subject in the preceding chapter.

Once the component models have been described, the optimization of a component consists of formulating the criterion to be optimized, then defining the constraints that set the valid ranges of the variable parameters, and finally, initializing all of the input parameters to sufficiently consistent values to enable easy convergence of the algorithm. When the criteria used present local minima, it may be interesting, or even indispensable in certain situations, to multiply the optimization processes by modifying the initialization of the parameters so as to sample their range of validity. This method increases the chances of convergence towards the general minimum, obtained by comparing solutions, but is more costly to optimize and costly in calculation time when the number of parameters and the sample results are high.

Some algorithms, such as those presented in Chapter 3, explore the whole of the parametric space in order to define the general and/or local minima. A sensitivity study of criteria minimized with variations in certain parameters may occasionally become necessary. This occurs when the parameters are subject to variation or imprecision around their theoretical value, during manufacture of the component [DEP 96]. This study may lead to a general

minimum being discriminated against in favor of a more stable local minimum for which performance is further ensured.

Criteria optimization is achieved using the CADES software described in Chapter 5, which uses an algorithm applying the Jacobean partial derivative matrix. It is necessary to define a final satisfactory value for the criteria, as well as the solution for which convergence can be considered to be achieved. The state of variables at the end of convergence then defines one or more of the optimum components. When only discrete values for the variables are accepted as solutions, an initial optimization is first achieved by allowing them to be entirely free and constantly variable. Optimization is then resumed having fixed the discrete variables at the closest authorized value. This is the case, for example, for the number of pairs of magnetic poles from permanent magnet electrical engines or even the pinion module from the epicyclic gear set.

In the rest of this section, we present an example of separate sizing of components for the Ravigneaux gear set, both electrical machines and both power inverters. The gear set is first sized in order to define the torque and speed values to which the electrical machines will be subjected in turn, in order to enable their sizing. The inverters will be simultaneously sized with the machines, their respective operations being inseparable.

Finally, we present the simultaneous sizing of these same components by maintaining the same input data imposed by the wheels and the control mechanism, and the same stress level. The results will enable the quantitative advantages obtained to be evaluated, the link variables between sized components having been optimized.

### 2.9.2. *Consideration of operating cycles*

In order to optimize the system components, vehicle mission profiles should be introduced. These enable the variables dependent on the general cycle of the system to be minimized, such as, for example, the energy consumed. Therefore an optimum traction level for the anticipated usage can be set. This may be implemented during optimization by favoring the effective utilization zones of the components compared to those that only appear occasionally. In this case, we introduce theoretical mission profiles for a military vehicle, provided by the company Nexter Systems. Figure 2.18 describes the change over time of the speed of the vehicle and the power

transmitted to the wheels. The operating characteristics for each traction component can be deduced from these mission profiles by taking into account the control strategy, which specifies which power paths are active at any instant. Thus, it is possible to define the control profiles of the main traction components: both electrical machine/inverter sets, the battery/chopper set, the ultra-capacitor/chopper set, the thermal engine, the Ravigneaux gear set, and the various mechanical reduction controls. These mission profiles will enable the characteristic operating points for each component to be determined, as well as the occurrence ratios for these points, converted into weighting factors.

The form of the theoretical mission profile enables the four main operating modes for vehicle operation to be identified. These modes are reduced to operating points denoted *P1*, *P2*, *P3*, and *P4*. The transitory conditions, which appear very briefly, involve a quantity of energy that may be ignored in the general energy assessment of the mission. Conversely, they are taken into account during optimization, in the form of sizing constraints (maximum speed and torque of electrical machines, for example). This phase of reducing the mission profile to several characteristic points can be performed using multiple levels of precision. However, reducing the number of operating points used enables the calculation time of the minimization algorithm to be lessened.

At this stage, the occurrence ratios for each operating point are calculated. Each time proportion attributed to the same operating point defines the weighting coefficient of criteria linked to the operating point considered. These weighting coefficients $k_1$, $k_2$, $k_3$ and $k_4$ are constants and are applied to all cost functions dependent on the considered mission profile. They describe the relationship between the duration of each operating point and the general cycle time, being the occurrence percentage for each mode, defined by the control distribution. The sum of these four coefficients is, therefore, equal to 1. Their values, obtained for the considered profile, are:

$$\begin{cases} k_1 = 0.3757 \\ k_2 = 0.2652 \\ k_3 = 0.0939 \\ k_4 = 0.2652 \end{cases} \qquad [2.77]$$

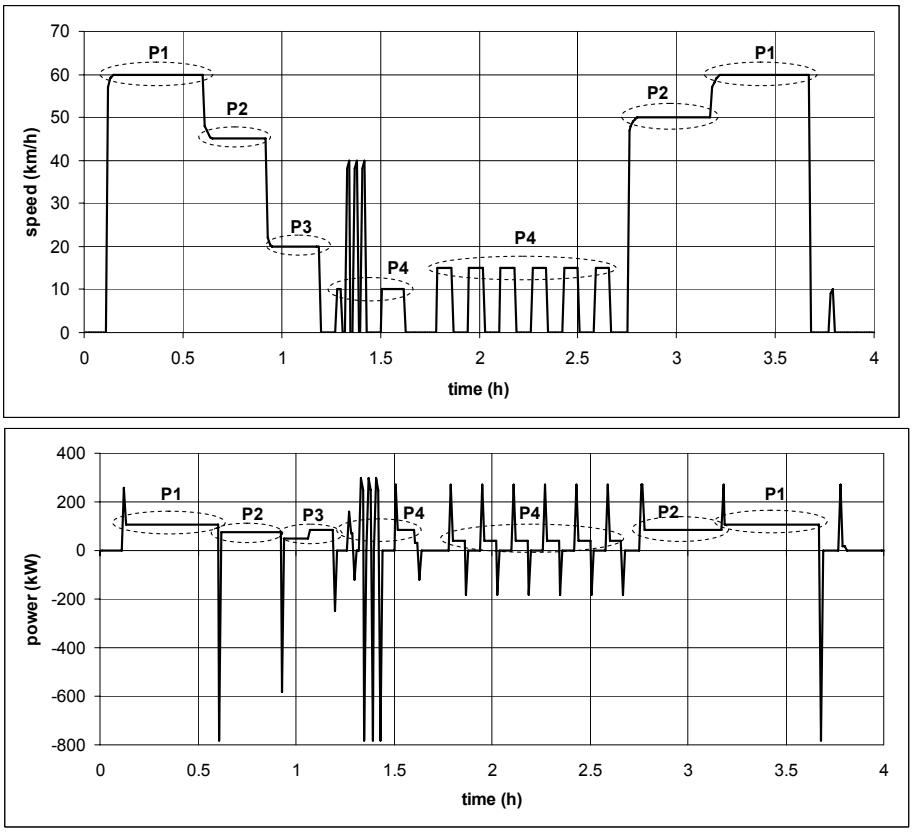


**Figure 2.18.** *Mission profile of a Nexter Systems vehicle. Wheel speed and power based on time*

The characteristics of the mechanical transmission, which includes reducers and a hydraulic coupler, enable the torque and the speed of the shaft of satellite carrier #6 of the Ravigneaux gear set to be inferred from the mission profile. Table 2.3 summarizes these variables, which will be used as input data for the cost function calculations linked to the mission profile, ignoring transmission losses.

The vehicle steering modes for the four simplified profile operating points enable the energy flows to be determined and, therefore, the operating points corresponding to each of the traction components. These are listed in Table 2.4 for the four operating points used in the simplified mission profile.

When use of the thermal engine is required, its power is kept constant in order to ensure optimum operation based on its efficiency map. The distribution of electrical power between the two electrical machines is not defined and remains free during optimization of the Ravigneaux gear set. The power distribution between the vehicle's wheel, its thermal engine, and the two electrical machines will enable the torques and speeds of these four elements to be expressed using the kinematic model for the Ravigneaux gear set.

| **Operating point** | **Average vehicle speed (km/h)** | **Wheel power (W)** | **Satellite carrier #6 speed (wheels; rad/s)** | **Satellite carrier #6 torque (wheels; N.m)** |
|---|---|---|---|---|
| *P1* | 60 | 106,608 | –71.12 | 1,499 |
| *P2* | 47.5 | 78,737 | –56.30 | 1,398 |
| *P3* | 20 | 63,122 | –52.68 | 1,198 |
| *P4* | 13.2 | 26,605 | –75.10 | 354 |

**Table 2.3.** *Component operating points*

| **Operating point (mode)** | **Satellite carrier #6 power (wheels; W)** | **Thermal engine power (W)** | **Power of electrical machines (W)** |
|---|---|---|---|
| *P1* (hybrid) | 106,608 | 90,000 | 16,608 |
| *P2* (thermal + load) | 78,737 | 90,000 | –11,264 |
| *P3* (thermal + load) | 63,122 | 90,000 | –26,878 |
| *P4* (all electrical) | 26,605 | 0 | 26,605 |

**Table 2.4.** *Steering modes and power distribution*

### 2.9.3. *Independent component optimization*

Optimization is limited in this study to the Ravigneaux gear set, the two electrical machines, and the two power inverters.

#### 2.9.3.1. *Criteria synthesis*

To minimize component mass and losses, the latter being linked to the mission profile, the criteria dependent on the component operating point

considered are calculated at various simplified mission profile operating points by applying the corresponding weighting coefficients. Other criteria, which are independent of the mission profiles, are not affected by these coefficients. Then, the cost functions for each component are constructed by adding together the various criteria being minimized, influenced by the normalization coefficients of the various unit measurements.

The criteria defining losses in the Ravigneaux gear set and both of the electric machine-inverter sets are therefore expressed based on their respective expressions for power losses defined during modeling, taken at operating points $P_i$ and weighted by coefficients $k_i$, which characterize the mission profile:

$$\begin{cases} P_{\text{gear set}} = \sum_{i=1}^{4} k_i \cdot P_V(P_i) \\ P_{\text{mot-inv1}} = \sum_{i=1}^{4} k_i \cdot (P_{\text{inv1}}(P_i) + P_{\text{mot1}}(P_i) \\ P_{\text{mot-inv2}} = \sum_{i=1}^{4} k_i \cdot (P_{\text{inv2}}(P_i) + P_{\text{mot2}}(P_i) \end{cases} \quad [2.78]$$

We can thus express the associated cost functions for each of the considered elements, taking into account their mass and power losses:

$$\begin{cases} J_{\text{gear set}} = F_1 \cdot M_{\text{gear set}} + F_2 \cdot P_{\text{gear set}} \\ J_{\text{mot-inv1}} = F_1 \cdot M_{\text{mot1}} + F_2 \cdot P_{\text{mot-inv1}} \\ J_{\text{mot-inv2}} = F_1 \cdot M_{\text{mot2}} + F_2 \cdot P_{\text{mot-inv2}} \end{cases} \quad [2.79]$$

The use of weighting coefficients $F_1$ and $F_2$ enables these functions with different unit values to be normalized, so that their contribution is balanced for the overall cost function. This *a priori* normalization of criteria is discussed in the next chapter, where other multi-criteria methods not requiring normalization (which define Pareto boundaries) are presented. These coefficients are, therefore, determined from an *a priori* evaluation of the different cost functions in order to determine their size order. These values can be refined during an iterative process in order to compensate for eventual evaluation errors, compared with the optimization results, or in

order to favor the minimization of one cost function over another. In particular, it will be possible here for the mass or losses during the matching of the weighting coefficients $F_1$ and $F_2$ to be favored. Note that if the optimization is repeated multiple times with different weighting ratios between criteria, then it is possible to find a set of solutions close to the Pareto boundary, corresponding to the best fit against the objective functions.

2.9.3.2. *Formulation of constraints*

Structural constraints should be formulated for each component. These consist of defining the valid limits for the geometric parameters. They are defined from manufacturing, technological or integration constraints, and may prove tedious when the number of parameters is very high.

Constraints linked to material resistance must be added, always including significant tolerances to ensure system security. They are often linked to component lifetimes. In particular, they are achieved by limiting peripheral electrical machine magnet speeds, torques and speeds for all mechanical shafts, and the contact and flex pressure of pinion teeth. Accepted limits for speed and torque for the input pinions (solar gearing #4; thermal engine and satellite carrier #6; wheels) are as follows:

$$\begin{cases} 0rpm < n_4 < 2200rpm \\ 0N \cdot m < C_4 < 2600N \cdot m \\ -2300rpm < n_6 < 0rpm \\ 0N \cdot m < C_6 < 6000N \cdot m \end{cases} \quad [2.80]$$

These values enable the speed and torque limits characterizing the other gear set pinions to be deduced. Electrical machine speeds are limited to 4,500 rpm, in accordance with the list of specifications.

Finally, functional constraints correspond to limits linked to restrictions on component usage. For example, the rotational speed and torque provided by the thermal engine may vary in an area limited to optimum operation. The result is, therefore, a constraint on variables associated with solar gearing #4 of the gear set for operating points using the thermal engine:

$$\begin{cases} 500N.m \leq C_4 \leq 1000N.m \\ 1000rpm \leq n_4 \leq 2000rpm \end{cases} \quad [2.81]$$

Between them, these constraints also enable the formulation of power distribution rules between certain components. The power transmitted by pinions #1 and #5 are limited to 70 kW, which is the power limit for electrical machines defined in the list of specifications. The power and torque points raised for the mission profile enable the most severe conditions of use for the components to be defined. They must be expressed during the optimization process to certify compliance with the constraints for all the use profile of the component.

2.9.3.3. *Results of optimization*

The Ravigneaux gear set is sized first. The optimum gear set obtained enables the relationships between the torques and speeds of the various pinions to be known. The speed and torque values of the two electrical machines at the four operating points characterizing the mission profile can thus be determined. These values must be determined so that the criteria calculations during optimization of the two electrical machine/inverter sets can take place. The constraints on the maximum speed limits for electrical machines will enable the algorithm to be used to define the ratio of reducers for which they will be coupled to pinions #1 and #5. Table 2.5 summarizes the main characteristics of the independently optimized components.

| | **Gear set** | **Electrical machine/inverter #1** | **Electrical machine/inverter #2** | **Total** |
|---|---|---|---|---|
| Mass (kg) | 18.9 | 158.2 | 60.9 | 238.0 |
| Volume (l) | 4.7 | 37.6 | 14.9 | 57.2 |
| Losses (W) | 397 | 1,633.6 | 573.4 | 2,604.0 |
| Criterion | 1,551 | 9,594.8 | 3,584.3 | 14,730.1 |

**Table 2.5.** *Results of independent component optimization*

### 2.9.4. *Simultaneous component optimization*

In this section, the Ravigneaux gear set and electrical machine/inverter models are associated with a unique optimization process. Thus, contrary to various local optimizations, the electric machine input variables are no

longer imposed, but become linked to the output variables of other components. During the optimization process, the torque and speed of the electrical motor shafts at the four operating points representing the mission profile are not predefined as during the previous independent optimization, but evolve as and when the algorithm converges, since they are dependent on the geometry of the Ravigneaux gear set, which is itself in the process of being optimized. This applies to all components that share variables.

The general optimization function $J_{\text{total}}$ is obtained by simply combining the cost functions of the various elements. It is, therefore, expressed as follows:

$$J_{\text{total}} = J_{\text{gear set}} + J_{\text{mot-inv1}} + J_{\text{mot-inv2}} \qquad [2.82]$$

The constraints on the component parameters remain unchanged. Input parameters are initialized by using the results obtained at the end of independent component optimization. Thus, the algorithm deviates from the reference solution formed from the independent component optimization and adjusts the link variables in order to act favorably on the criteria being optimized.

Table 2.6 groups the results following general optimization. The various results associated with the components taken either individually or collectively are given in order to comparatively analyze the variations inherent in the use of the general optimization strategy.

During independent component optimization, the power distribution between the thermal engine and the two electrical motors, which enables the requirements for the wheels to be satisfied (mission profile), is already defined according to the Ravigneaux gear set design. Therefore, the calculation of the parameters for the Ravigneaux gear set cannot take into account the impact of the choices of power distribution on mass or losses relative to the other components.

Conversely, simultaneous optimization of components enables the parameters of each component and their influence on the generally minimized criteria to be integrated into the calculation. In the example shown here, it enables a decrease in the general criterion integrating the mass and overall component losses. The reduction in mass and power losses are around 2.5% and 4.5% respectively.

| | Gear set | Electrical machine/ inverter #1 | Electrical machine/ inverter #2 | Total |
|---|---|---|---|---|
| Mass (kg) | 19.8 | 184.6 | 27.5 | 231.9 |
| Volume (l) | 5.1 | 43.2 | 7.5 | 55.8 |
| Losses (kW) | 389.5 | 1,589.2 | 509.4 | 2,488.1 |
| Criterion | 1,571.6 | 10,561.5 | 2,120.2 | 14,253.3 |

**Table 2.6.** *Results of simultaneous component optimization*

During independent component optimization, the input data for the electrical machine-inverter sets were perfectly known and calculated from the Ravigneaux gear set model, which enabled consistent, if not generally optimum, sizing. The benefits obtained through simultaneous component optimization are not, therefore, considerable. However, greater improvement in desired performance would be achieved if the different designers, who may not have all the input data at their disposal, were involved in the design. Furthermore, the benefit of a simultaneous design approach, compared with a multi-loop optimization approach, is highly dependent on the level of coupling between sub-systems, whether processed together or separately. Therefore, the choice of either a decoupled or simultaneous approach is a compromise by the designer. His choices will be based on considerations linked to the sensitivity of criteria to the coupling variables between sub-systems and the repercussions on processing time, depending on the complexity of the design problem being tackled. The issue of multi-loop optimization processing, described as "a multi-level approach for the optimum design of electromechanical systems" is the subject of Chapter 4 of this book.

## 2.10. Conclusions

The synthesis of complex systems requires both simulation models and strategies to be developed, enabling the simulation model to be converted into a sizing model. It is now accepted that, for electrical energy systems, optimization is an effective way of enabling this conversion, since it enables solutions to be found that satisfy increasingly restrictive lists of

specifications, and also the best solutions with respect to varied criteria, which might be technical, economic, or even environmental.

In this chapter, we have concentrated on simulation models by focusing on analytical models, which have the advantage of limited calculation times and efficient modeling of the various interactions and couplings that exist between system components. Thus, by drawing on the example of a hybrid heavy vehicle powertrain, we have reviewed the different possible models for electrical machines, static converters and mechanical transmissions; we have specifically concentrated on energy aspects (such as losses and efficiency) by presenting approaches that are simple to implement, such as in an industrial context.

The operational characteristics of models in the context of a sizing by optimization process has then been demonstrated by dealing with the example of the sizing of the hybrid powertrain, including two permanent magnet electrical machines, two inverters to power the machines, and a Ravigneaux planetary gear set. Simultaneous component optimization of the whole device has been compared with the separate optimization of the two electrical sets and the Ravigneaux gear set, at the same time demonstrating the value of some general design approaches.

The logical perspectives of these studies concern the integration of electrical storage systems into the optimization of the hybrid powertrain, which would enable us to move a little closer to the general sizing of whole powertrain, but also to put in place analytical modeling formalisms for such devices. Finally, this would create an opportunity to undertake sizing by optimization for many other electrical energy systems, such as renewable electrical energy production turbines and the cogeneration of multiple energy sources (thermal and electrical, for instance).

## 2.11. Bibliography

[AFN 06] AFNOR 2006, Calcul de la capacité de charge des engrenages cylindriques à dentures droite et hélicoïdale, ISO Standard 6336.

[AUB 11] AUBRY J., Optimisation du dimensionnement d'une chaîne de conversion électrique directe incluant un système de lissage de production par supercondensateurs. Application au houlogénérateur SEAREV, PhD thesis, ENS Cachan, 2011.

[DAG 11] DAGUSÉ B., DESSANTE P., VIDAL P., VANNIER J.-C., THOMAS J.-L., Approche inverse sur la détermination des paramètres électromagnétiques optimaux d'une MSAP appliquée à un véhicule électrique, EF2011, Belfort, December 2011.

[DAL 99] DALLEMAGNE G., "Fluides hydrauliques – facteurs d'influence", *Techniques de l'Ingénieur*, BM6012, January 1999.

[DEP 95] DEPERNET D., GOELDEL D., "Development of a simulation software for losses analysis in three level PWM inverters", *Systems Analysis Modelling Simulation*, vol. 18-19, pp. 787-790, 1995.

[DEP 96] DEPERNET D., DELOIZY M., GOELDEL C., "Optimised PWM waveforms used in a vector control of an induction motor driven by a voltage source inverter", *E.P.E. Chapter Symposium on Electric Drive Design and Applications*, Nancy, 5-7 June, 1996.

[DUB 09] DUBAS F., ESPANET C., "Analytical solution of the magnetic field in permanent-magnet motors taking into account slotting effect: no-load vector potential and flux density calculation", *IEEE Transactions on Magnetics*, vol. 45, pp. 2097-2109, 2009.

[ESP 99] ESPANET C., Modélisation et conception optimale de moteurs sans balais à structure inversee – application au moteur-roue, PhD thesis, University of Franche-Comté, 1999.

[FAN 01] FANCHON J.-L., *Guide des Sciences et Technologies Industrielles*, Paris, Nathan/VUEF, AFNOR, 2001.

[GUI 10] GUILLERMIN C., Vieillissement électrique et thermique d'un composite résine époxyde-silice: étude des charges d'espace et de la conduction, PhD thesis, Joseph Fourier University, 2010.

[HEN 99] HENRIOT G., *Engrenages: Conception, Fabrication, Mise en œuvre*, 7th edition, Dunod, Paris, 1999.

[JUF 95] JUFER M., Électromécanique, in NEIRYNCK J., the *Treaty of Electricity Traité d'électricité de l'École Polytechnique Fédérale de Lausanne*, vol. IX, Presses Polytechniques et Universitaires Romandes, Lausanne, 1993.

[KON 93] KONE A. D., Contribution à la conception des actionneurs électriques par formulation en terme d'optimisation, PhD thesis, National Polytechnic Institute of Toulouse, 1993.

[SLE 92] SLEMON G. R., LIU X., "Modeling and design optimization of permanent magnet motors", *Electric Machines and Power Systems*, vol. 20, pp. 71-92, 1992.

[WUR 96] WURTZ F., Une nouvelle approche pour la conception sous contraintes de machines électriques, PhD thesis, National Polytechnic Institute of Grenoble, 1996.

[ZHU 93] ZHU Z. Q., HOWE D., BOLTE E., ACKERMANN B., "Instantaneous magnetic field distribution in brushless permanent magnet DC motors, part I: open-circuit field", *IEEE Transactions on Magnetics*, vol. 29, pp. 124-142, 1993.

Chapter 3

# Simultaneous Design by Means of Evolutionary Computation

## 3.1. Simultaneous design of energy systems

### 3.1.1. *Introduction to simultaneous design*

Today, the design of electrical energy systems is challenging owing to ever-increasing demands regarding the requirements of the electrical energy matrix. Unlike current devices, which are often oversized in order to fulfill their missions, it is now imperative to design systems as accurately as possible in order to avoid wasted energy. Besides this fundamental objective of energy efficiency, design must nowadays be capable of including other heterogeneous criteria, such as:

– criteria linked to dimensions: bulk, integration, and mass;

– criteria associated with lifetime, reliability, availability and operating safety;

– criteria relating to respecting the environment, for the purpose of reducing all forms of pollution: atmospheric, electromagnetic, sound, or vibratory;

---

Chapter written by Bruno SARENI and Xavier ROBOAM.

*Integrated Design by Optimization of Electrical Energy Systems* Edited by Xavier Roboam
© 2012 ISTE Ltd. Published 2012 by ISTE Ltd.

– economic criteria, such as base cost, depreciation, or ownership cost.

Improvements in performance criteria require a systemic approach to be adopted, where all of the system characteristics are considered in pairs. Generally, the system can be represented by a *functional architecture*, in the form of an arrangement of bodies (or sub-systems) that fulfills one or more of the given functions and which transforms energy and informational flows. There is then a corresponding *physical*, *structural architecture*, comprising a set of elements that enable each function to be fulfilled. The elements are characterized by physical *dimensions* (which are typically geometric or energy-related) and by *structural* parameters linked to constitutive materials. Furthermore, the behavior of energy systems is dependent on the *energy management strategy*, which controls the transfer of energy flows. The optimization of an energy system with regards to the set of criteria previously set out requires its optimum architectural, sizing and energy management characteristics to be determined.

Traditionally, design approaches are sequential, consisting of determination of the system architecture, followed by component sizing, and finally, the establishment of an energy management strategy. However, for multisource systems, the fact that energy management is considered to be a consequence of sizing may result in an oversizing of resources [AKL 08]; sizing then results from a given management method or strategy. In many studies, this reflection has led to sequential design being adopted by reversing the sizing and energy management phases, as shown in Figure 3.1.

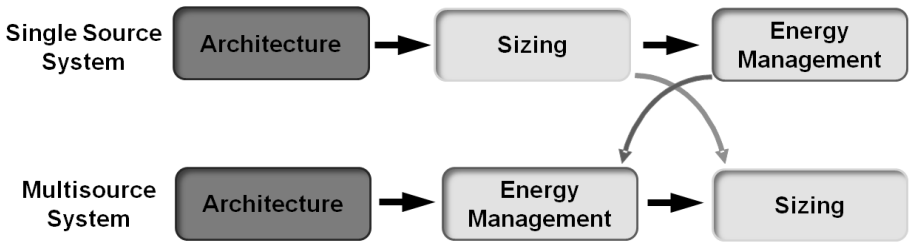


**Figure 3.1.** *Sequential design approaches*

Even if, with the sequential design approach, each stage is subjected to a reflection in terms of local optimization, nothing guarantees optimality of the overall system. Indeed, processing the design phases in sequence does not enable various couplings between parameters relevant to the architecture,

sizing, or management of the system to be taken into account. So as not to break these couplings, it is advisable to adopt a "simultaneous design" approach, which aims to manage the architecture, sizing, and energy management of all of the elements to be determined, as shown in Figure 3.2. This approach has already been introduced in Chapter 1 of this book, by further raising questions relating to system environment and the mission profile.

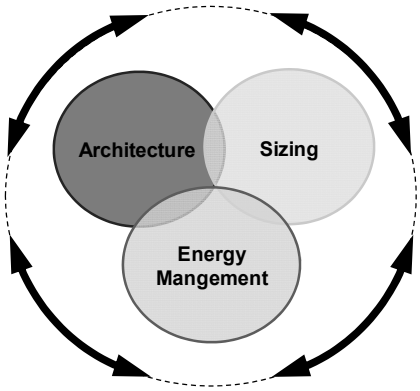


**Figure 3.2.** *Illustration of concurrent design*

### 3.1.2. *Simultaneous design by means of optimization*

One way to understand the complexity inherent in simultaneous design is to reword the design problem as an optimization problem, to be solved using appropriate methods. Complexity is thus reported in terms of the optimization problem, which is generally characterized by:

– a significant number of design variables (decision variables of the optimization problem), which are often combined, discrete, and continuous. Discrete variables relate to the parameters associated with the choice of architecture, structure, and the type of elements or materials, whereas continuous variables are linked to sizing and energy measurement parameters;

– multiple constraints, which are intrinsic to the system as a whole; system elements, which are constitutive or linked to the compatibilities of association between these elements (such as energy, thermal and frequency compatibility). Other constraints generally relate to the finality of the system

(regard for operating and mission cycles) or to aspects relating to quality standards;

– heterogeneous objectives to be optimized, such as the various performance criteria outlined in the introduction to this chapter.

Therefore, simultaneous design of energy systems using optimization usually leads to multi-objective problems with mixed variables, under constraints that can be generally translated into the following mathematical form:

$$\begin{cases} \min_{\mathbf{x}} / \max_{\mathbf{x}} \; f(\mathbf{x}) = \{f_1(\mathbf{x}), f_2(\mathbf{x}), \ldots, f_{n_c}(\mathbf{x})\} \\ \quad g_i(\mathbf{x}) \leq 0 \qquad i = 1, \ldots, n_{ci} \\ \quad h_j(\mathbf{x}) = 0 \qquad j = 1, \ldots, n_{ce} \\ x_{k\,\min} \leq x_k \leq x_{k\,\max} \qquad k = 1, \ldots, n \end{cases} \qquad [3.1]$$

where:

$\mathbf{x} = \{x_1, x_2, \ldots, x_n\}$ is the design variables vector requiring optimization;

$f(\mathbf{x}) = \{f_1(\mathbf{x}), f_2(\mathbf{x}), \ldots, f_{n_c}(\mathbf{x})\}$ : objectives to be optimized;

$g_i(\mathbf{x})$: inequality constraints to be respected;

$h_j(\mathbf{x})$: equality constraints to be respected;

$\mathbf{x}_{\min}$, $\mathbf{x}_{\max}$: domain constraints (boundaries of the design variables);

$n$: number of design variables;

$n_c$: number of criteria to be optimized;

$n_{ci}$: number of inequality constraints;

$n_{ce}$: number of equality constraints.

### 3.1.3. *Problems relating to simultaneous design using optimization*

Solving a simultaneous design problem using optimization is not without its difficulties. We will list these in this section.

3.1.3.1. *Difficulties linked to the modeling of energy systems*

The difficulties encountered by "system" designers with regards to the modeling of energy devices, in the context of concurrent design by means of optimization, are linked to several aspects:

– these systems are strongly heterogeneous and multi-physical. Therefore, it is preferable to represent them using unifying formalisms to more easily overcome physical domain barriers. Additionally, the association of different models at the heart of an optimization processes must be guaranteed, regarding both "physical" validity (consistency and energy transfers) and software interfacing when models are inserted onto various software platforms[1];

– these systems are generally characterized by multiple dynamics scattered in time and space. In the case of temporal simulations, they should nevertheless be represented over horizons that are sufficient to be able to judge their effectiveness in terms of energy criteria (autonomy or consumption, for example) and their capacity for fulfilling the mission for which they were designed; "the movement of a locomotive during its circulation mission is difficult to represent concurrently with the commutation of a power switch at the heart of its static converter". This often leads designers to raise questions regarding the level of representation for each of the system elements and the choice of type of model (analytical, semi-analytical, or numerical using ordinary or partial differential equations, such as for finite element models) based on a compromise regarding precision (granularity) of models versus calculation time. Indeed, modeling must guarantee good representation of the physical and energy phenomena over wide temporal ranges using reasonable calculation times with regards to the optimization process;

– different models must be associated with the validity limits with regards to parameters that vary during optimization. This forces a constant dialog between designers and specialists regarding the various elements of a system in order to best characterize their functional limits, as well as the validity of the associated models. It should be borne in mind that the optimization phase will have a tendency to push the system to its limits in order to guarantee lean sizing!

1 Readers are invited to refer to Chapter 5 for aspects linked to modeling techniques and software interfacing.

We note, finally, that the "price to pay" in modeling a system with a view to its optimization is broadly higher than for an equivalent device being analyzed by simulation. The development cost of modeling is also much higher than the cost of solving the optimization problem in the simultaneous design phase!

3.1.3.2. *Difficulties linked to integration*

The optimization of all performance criteria and constraints in a simultaneous design process implies an appropriate integration of system purpose, notably of its operating cycles. This point was widely discussed in Chapter 1 and we refer readers to this for more detail.

3.1.3.3. *Difficulties linked to optimization problem formulation*

The definition of an optimization specification list is rarely easy. It is not always straightforward to identify appropriate parameters for the level of architecture, sizing, or energy management, which will inform the set of objectives being optimized. Additionally, the total number of design variables should result in a compromise to enable:

– a guaranteed number of degrees of freedom sufficient to apply to all performance criteria;

– a limited number of degrees of freedom so that redundancy between parameters can be avoided and the complexity of the optimization problem can be reduced, so as to facilitate its resolution.

Having set the design variables to be modified during optimization, it is essential to identify all of the constraints that ensure the feasibility of the system and to define the criteria to be optimized. The separation of criteria and constraints is sometimes an intricate process, with one criterion being able to be expressed in terms of a constraint, and vice versa. It should be noted that a constraint is generally associated with a limit value (threshold or tolerance) and, unquestionably, must be satisfied. Conversely, a criterion (or objective) is a measurement that we seek to improve without necessarily having any idea of its "target" value; that is what the optimization process is for! Finally, it is better to limit the number of criteria that require optimization (a maximum of three!). Indeed, multiplying the number of criteria would make research into optimum compromises, as well as the analysis phase of solutions resulting from optimization, difficult.

3.1.3.4. *Difficulties linked to resolution of the optimization problem*

As we have already commented, the complexity of the design problem is shifted towards the optimization problem, which is challenging regarding its characteristics: multi-criteria, mixed variables, objective functions, and highly nonlinear constraints; this dataset cannot necessarily be expressed analytically. In this context, stochastic optimization methods [RAO 09] and, more specifically, evolutionary algorithms are, without doubt, the most suitable for solving such problems.

## 3.2. Evolutionary algorithms and artificial evolution

In this section we pay particular attention to evolutionary algorithms. Our objective is not to develop these methods, which are already the subject of numerous publications, in detail, but we will highlight certain key points.

3.2.1.1. *The theory of natural evolution, a universal theory*

The theory of the natural evolution of species, established by Darwin in 1859 [DAR 59], expresses some general principles that can be transferred beyond natural evolution. Among the fundamental properties relating to the theory of evolution, we focus notably on the notions of *selection*, *adaptation*, *crossovers*, *mutation*, *emergence* and *species*, which are reflected across all evolutionary trees. By way of illustration, Figure 3.3 provides two distinct examples of evolutionary trees showing that the principles of Darwinian theory apply not only to natural species, but also to technical objects [KRA 06].

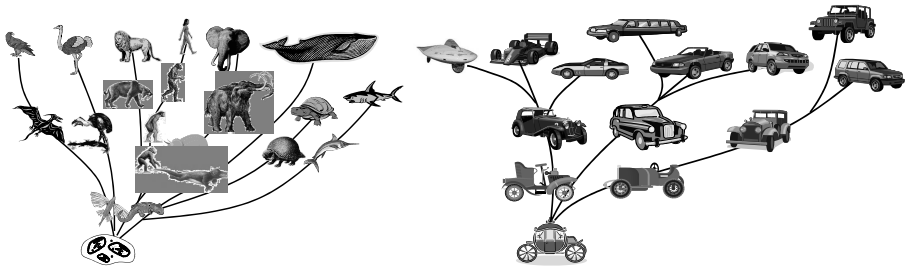

**Figure 3.3.** *Two evolutionary trees illustrating the universality of Darwinian theory*

### 3.2.2. *Evolutionary algorithms principle*

Evolutionary methods rely on an analogy with the theory of natural evolution. In nature, species are capable of adapting to their environments under the pressure of natural selection, and of evolving from their genetic heritage, so as to enhance their adaptation over the generations. This is a metaphor for the Darwinian paradigm, which is used in evolutionary algorithms to solve optimization problems. Table 3.1 shows the mathematical transposition of the Darwinian paradigm.

The evolutionary algorithm consists of a succession of generations that reproduce the principles of natural evolution (see Figure 3.4) applied to a population of individuals using two types of operators:

– Darwinian operators, which transpose mechanisms of natural selection by orienting research towards the most appropriate solutions;

– evolutionary, or variation operators, whose role is to favor the emergence of new solutions. These operators are applied to a representation of solutions (coding or *chromosome*) by imitating genetic mechanisms (crossovers and mutations).

| | |
|---|---|
| Nature | Mathematical optimization |
| Human beings | Solutions requiring optimization |
| Environment | Search space |
| Adaptation | Objective function requiring optimization |
| Species | Set of similar configurations |
| Biological differences | Mathematical distance |

**Table 3.1.** *The Darwinian paradigm: from natural to artificial evolution*

The initial population is obtained by uniform random search (or using *a priori* knowledge) of the search space. The genitor parents are then selected from the population using stochastic or deterministic procedures. Next follows a stage of evolution, where variation operators are applied to the genitors in order to create and explore new solutions (*children*). Finally, a process of replacement is used in order to determine the "survivors" of a generation. The algorithm may be *generational* (with children automatically replacing parents) or *elitist* (one or more parents being deterministically or stochastically preserved). The latter is described as a *steady state*

*evolutionary algorithm*, insofar as only one part of the population is renewed each generation. It should be noted that parent, genitor and child population sizes can be identical or distinct, according to the different algorithms.

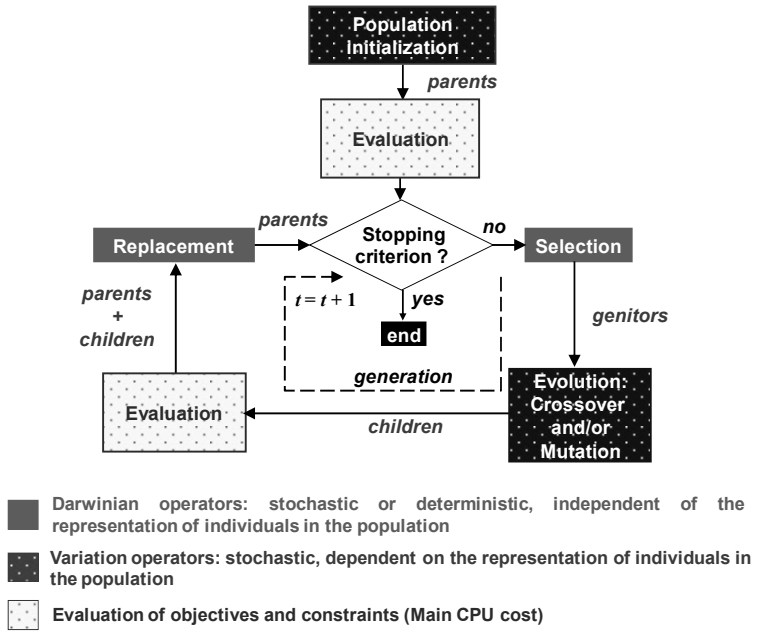


**Figure 3.4.** *General structure of an evolutionary algorithm [KEI 02]*

Among the most popular evolutionary methods, we refer readers to genetic algorithms [HOL 75; GOL 89; MIC 96], evolution strategies [SCH 95; BÄC 96], evolutionary programming [FOG 66; FOG 91], and differential evolution [STO 96].

### 3.2.3. *Key points of evolutionary algorithms*

#### 3.2.3.1. *Genericity as regards classes of optimization problems*

Evolutionary algorithms are relatively robust and efficient methods for processing difficult (multimodal, nonlinear, high number of variables) optimization problems. They may be used in a combinatorial or continuous optimization context and are, therefore, very well suited to solving mixed-variable problems. Only the variation operators (see Figure 3.4) are

dependent on the nature of solutions to be optimized. Other mechanisms used in evolutionary algorithms are generic and can be independently applied to the type of representation of individuals.

In general, solutions to a problem can be represented by a binary string. Binary coding is naturally well suited to the description of discrete variables, but it can also be used for continuous parameters [GOL 89; BÄC 96]. Some techniques can even overcome problems linked to excessive increases in chromosome size (length of the binary string associated with individuals) when precision regarding variable optimization is desired [WHI 91; SCH 92].

However, while this type of coding has largely been used in genetic algorithms, today, it is much less used compared with real coding, which simplifies the implementation of algorithms and can be easily used to represent discrete variables by decoding real variables using an "integer part". For more complex problems, where a different number of parameters exists for each architecture, the coding for each graph used in genetic programming [KOZ 92] may turn out to be necessary. It then becomes imperative that recombination and mutation operators, dedicated to the problem and to specific data structures, are developed (see Figure 3.5), which then complicates implementation via computers for non-specialists. Problems specific to genetic programming, such as congestion, or *bloating*, are then added, which then requires control of crossovers. In order to overcome these difficulties and to avoid using genetic programming, one possible solution is to use a universal chromosome [RAN 03], which codes all of the architectures to be optimized.

This chromosome comprises the concatenation of parameters of all architectures and the addition to this of a gene (described as a structural gene) that defines the type of architecture. Consequently, only the parameters associated with the architecture defined by this gene are used to characterize this individual. Genes relating to other architectures in the chromosome can be said to be "recessive"; the crossover and mutation operators are applied to them, but they are not involved in the decoding. This solution does not require development of specific architectural data structures, or the implementation of particular operators enabling them to cross and mutate. It does have the advantage of greatly facilitating implantation, since standard recombination procedures can be applied to this universal chromosome of recombination (discrete and/or continuous) standards. In addition, the use of recessive genes can be expressed when the

structural gene is mutated, favors the diversity of solutions in the population, and reduces the risk from premature convergence. This approach has been used in Chapter 1 of this book, particularly to solve the problem of environmental data classification by clustering.

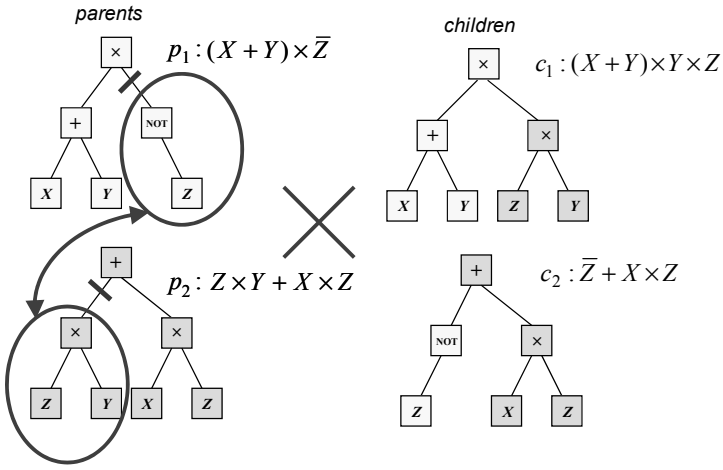


**Figure 3.5.** *Illustration of genetic programming for the optimization of a logical function (crossover mechanism based on sub-branch exchange)*

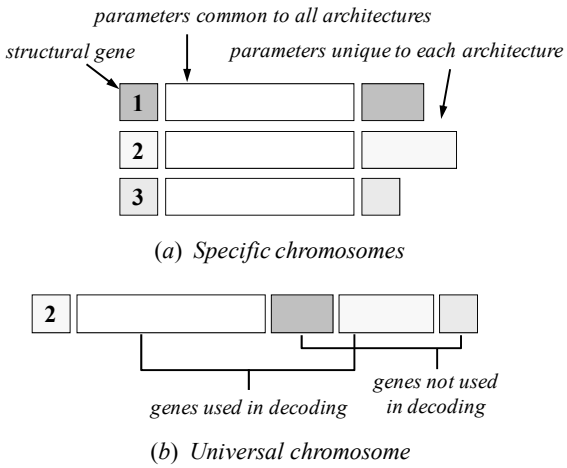


**Figure 3.6.** *Principle of the universal chromosome for the coding of architectures*

3.2.3.2. *The value of niching*

However, traditional evolutionary algorithms (genetic algorithms or standard evolution strategies) have limited efficiency because of the *genetic drift* phenomenon. Indeed, the selection intensity ends by concentrating the population over generations in a unique solution. This concentration then impairs the evolution capacities, as the new recombination mechanisms are, in this case, incapable of producing any new solutions.

In case of premature convergence, the extraction of a local attractor towards a better solution will remain dependent on the mutation operator. To remedy this problem, niching methods were developed in the 1990s [MAF 95]. These enable the preservation of diversity and capacities of evolution by constantly maintaining distinct solutions in the population. They thus enable the investigation of multiple optima in parallel (see Figure 3.7) and offer a higher level of robustness than traditional evolutionary algorithms for multimodal problems. There are two classes of niching methods [SAR 98]:

– *crowding* methods such as RTS (*restricted tournament selection*), which restricts selection between similar individuals;

– fitness readjustment methods, such as *sharing* or *clearing* techniques, which penalize the objective function of localized individuals in high-density regions in space and, conversely, preserve the representative zones for less-densely populated solutions.

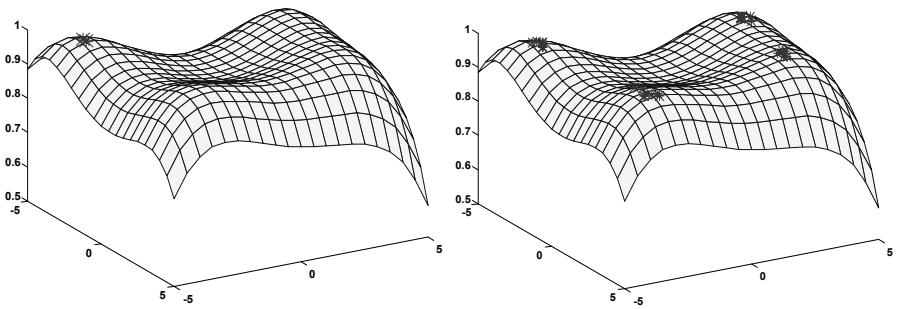


(*a*) *Without niching* (*b*) *With niching*

**Figure 3.7.** *Convergence of an evolutionary algorithm over a multimodal function with four equivalent peaks*

#### 3.2.3.3. *Self-adaptation*

Self-adaptation [EIB 99] in evolutionary algorithms aims to adapt the variation operators to be applied (typically the crossover and mutation procedures) and/or the associated probabilities automatically during research. Therefore, it enables both high desensitization of algorithms, with regards to their control and adjustment parameters, and also an increase in their robustness in the face of problems. The introduction of self-adaptive mechanisms into evolutionary algorithms can be achieved:

– by introducing specific variation operators that present properties of natural self-adaptation. This is the case, for example, for self-adaptive mutations used in evolution strategy or SBX (*simulated binary crossover*), which is used in real coding generic algorithms [MEY 07];

– by adding one or more supplementary genes to the individual chromosome, which encode the type of variation operator to be applied and/or their associated probabilities. This approach benefits from the selection favoring the operators (and/or their associated probability values) producing the best individuals. In order to avoid any premature convergence towards a given operator, the supplementary genes are themselves subjected to recombination and mutation. Their diversity may also be reinforced by the implementation of a specific niching method.

## 3.3. Consideration of multiple objectives

### 3.3.1. *Pareto optimality*

The consideration of multiple performance criteria in the simultaneous design process occurs through the implementation of multi-objective optimization techniques. This then refers to the simultaneous minimization or maximization of a set of $n_c$ objectives of type $f$, related to the design variables $\mathbf{x}$. For this kind of problem, objectives typically conflict with each other. Thus, in most cases, it is impossible to obtain the global minimum at the same point for all objectives. Therefore, the problem has no single optimal solution but a set of efficient solutions representing the best objective trade-offs. These solutions consist of all design variable vectors for which the corresponding objective vectors cannot be improved in any dimension without disimprovement in another. They are known as Pareto-optimal solutions in reference to the famous Italian economist [PAR 96].

Mathematically, Pareto optimality can be expressed in terms of *dominance*. For the simultaneous minimization of objectives, let us consider, for example, two design variable space vectors **x** and **y**; we say that **x** dominates **y** if and only if:

$$\exists m \in 1...n_c \;\Rightarrow\; f_m(\mathbf{x}) < f_m(\mathbf{y}) \quad \text{and} \quad \forall k = 1...n_c \quad f_k(\mathbf{x}) \leq f_k(\mathbf{y}) \qquad [3.2]$$

which signifies that the solution **x** improves at least one of the criteria of **y** without deteriorating the others. A vector that is not dominated by any element from the set of other vectors is said to be *non-dominated* with respect to this set. Vectors that are not dominated over the whole of search space represent Pareto-optimal solutions and constitute the *Pareto-optimal front.* Figure 3.8 illustrates this concept for the minimization of two objectives by showing the dominance in terms of objective of any solution **x** with regards to a given solution **y** and by giving a Pareto front example.

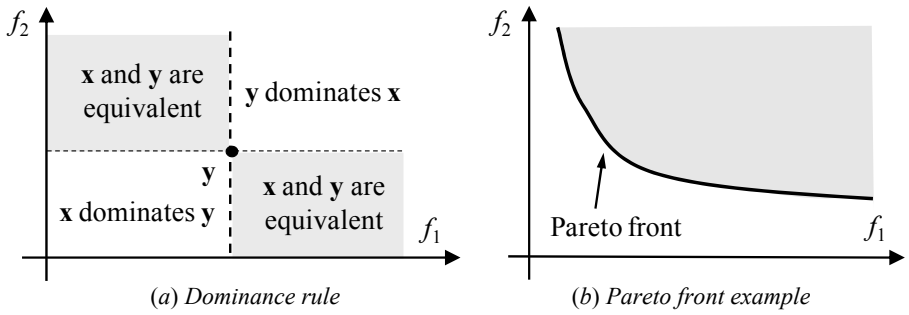


**Figure 3.8.** *Illustration of Pareto optimality – minimization of two objectives*

### 3.3.2. *Multi-objective optimization methods*

Multi-objective optimization methods aim to provide one or more Pareto-optimal solutions. These are divided into three main classes, based on the link between the optimization phase and the decision process, which is necessary in order to reach an optimum compromise [VAN 99; COL 02]:

– *a priori* approaches (decide → research and optimize) group together the set of techniques for which the choice of compromise to be found by the optimization phase is made *a priori* by the designer. These methods notably include the $\varepsilon$-constraint method (also known as the bounded objective

method) and the set of scalar aggregation techniques, such as the criteria weighting, fuzzy or goal-attainment methods. Although they have been widely used in the past, these approaches present a major disadvantage. Indeed, in the traditional situation where criteria do not have the same physical dimensions, they provide a single optimum compromise[2] to designers, for whom sensitivity is generally significant as regards parameters used for the scaling and aggregation of objectives (such as weighting coefficients, normalization factors and target values). It is not always easy to set all of these parameters to ensure good decoupling between the scaling of objectives and the choice of weightings associated with the investigated compromise;

– *progressive* or *sequential* approaches (decide ↔ research and optimize), proceeding through successive optimizations in order to provide a solution to the problem. Designers refine their choice of compromise based on each optimization;

– *a posteriori* approaches (research and optimize → decide) provide a set of optimal compromises to designers from which they can extract the solution to their problems. They essentially group together population-based meta-heuristics capable of investigating multiple optimal compromises in parallel, by exploiting the concept of Pareto dominance. The advantage of these techniques is that they require no objective scaling.

### 3.3.3. *Multi-objective evolutionary algorithms*

Multi-objective evolutionary algorithms are part of the class of *a posteriori* methods described above. They have enjoyed popularity without precedent in the area of multi-objective optimization during the 21st Century; the Coello Coello website [COE 11] contains more than 6,000 references covering various engineering sectors. The best performing multi-objective evolutionary methods use the concept of *elitism*, which aims to preserve non-dominated individuals over generations (see Figure 3.9).

2 It is, however, possible to investigate multiple optimal compromises using *a priori* methods, but this then requires multiple numbers of optimizations (each investigated compromise requires an optimization phase)

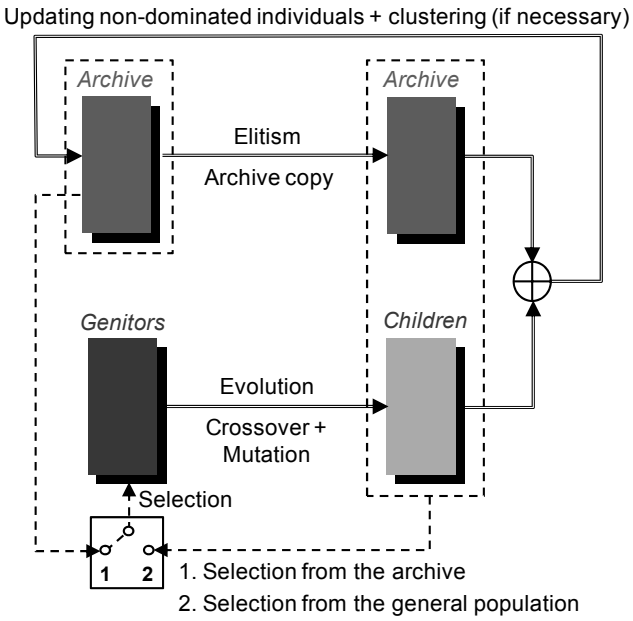


**Figure 3.9.** *Typical structure of a multi-objective evolutionary algorithm*

The non-dominated individuals are stored in an archive associated with the population. This archive is updated for each generation based on new solutions investigated, and is eventually reduced using a *clustering* technique when the number of non-dominated individuals it contains becomes greater than its limit size. Clustering preserves the most representative Pareto-optimal solutions and guarantees an almost uniform distribution of these solutions over the Pareto front. Various algorithms from other publications differ notably in terms of management of the archive, the methods of clustering used, the *fitness assignment*, and the way in which the genitor parents are selected. These may be uniquely chosen in the archive (commutator 1 from Figure 3.9) or in the general population comprising the archive and the children from the previous generation (commutator 2 from Figure 3.9). The most popular algorithms are the SPEA2 [ZIT 01], the PAES [KNO 00], the PESA [COR 00], and the NSGA-II [DEB 00], which is considered to be the incontrovertible reference in multi-objective evolutionary optimization.

### 3.4. Consideration of design constraints

The integration of constraints in the simultaneous design process requires the use of constrained optimization methods. We will distinguish two cases, according to whether the design problem is single objective or multi-objective.

#### 3.4.1. *Single objective problem*

There are numerous constrained optimization methods, but the majority are specified as being either continuous or combinatory problem methods [RAO 09]. Some generic approaches are, however, applicable to mixed-variable problems, including penalty methods, which are the most frequently used. These methods consist of transforming a constrained optimization problem into a non-constrained one, by integrating all of the constraints into an objective function to be optimized. As an example, let us consider the minimization problem given in equation [3.3]:

$$\begin{cases} \min\limits_{\mathbf{x}} f(\mathbf{x}) & \\ g_i(\mathbf{x}) \leq 0 & i = 1,\ldots,n_{ci} \\ h_j(\mathbf{x}) = 0 & j = 1,\ldots,n_{ce} \\ x_{k\,\min} \leq x_k \leq x_{k\,\max} & k = 1,\ldots,n \end{cases} \qquad [3.3]$$

The objective function $f(\mathbf{x})$ can be modified according to [3.4] in order to include inequality constraints:

$$F(\mathbf{x}) = f(\mathbf{x}) + \sum_{i=1}^{n_{ci}} r_i P_i(g_i(\mathbf{x})) \qquad [3.4]$$

where $r_i$ is a constant penalty factor and/or each penalty term $P_i$ is dependent on the associated constraint $g_i$. The penalty term relating to a constraint can be defined by [3.5] for exterior penalty methods:

$$P_i(g_i(\mathbf{x})) = \max(0, g_i(\mathbf{x}))^2 \qquad [3.5]$$

This term is thus 0 when $g_i(\mathbf{x}) \leq 0$ (constraint verified) and is equal to $g_i(\mathbf{x})^2$ when $g_i(\mathbf{x}) > 0$ (constraint violated). Thus, the function $F(\mathbf{x})$ is all the more increased (i.e. penalized) when the constraints are violated. Equality

constraints can be similarly integrated by observing that they can be expressed as two inequality constraints:

$$h_j(\mathbf{x}) = 0 \quad \Leftrightarrow \quad \begin{cases} h_j(x) - \delta \leq 0 \\ -h_j(x) - \delta \leq 0 \end{cases} \qquad [3.6]$$

where $\delta$ is a low-value positive constant. The total number of inequality constraints is thus equal to $m = n_{ci} + 2n_{ce}$ and the index $n_{ci}$ in equation [3.4] can be replaced by $m$ in order to take account of the set of constraints in the function $F(\mathbf{x})$. The penalty factors $r_i$ associated with the penalization terms aim to scale the constraint violation relative to the objective function $f(\mathbf{x})$ so that $F(\mathbf{x})$ is sufficiently increased when the constraint is violated.

To simplify the problem, it is possible to reduce the number of penalty factors to a unique parameter $r$, *if all* constraints are normalized and "equally" scaled. The solution to the constraint problem can thus be investigated sequentially by minimizing the function $F(\mathbf{x})$ and by assigning the penalty factor value $r$ to each iteration [RAO 09].

This mathematical approach does, however, have a disadvantage with regards to the characteristics of the simultaneous design problem. Indeed, it is rarely possible to ensure the continuity of function $F(\mathbf{x})$ between feasible solutions observing the constraints and solutions that are not feasible, since it is not generally possible to evaluate the objective function when certain constraints are violated. As an example, it is difficult to determine the performance of a vehicle if one of the constituent elements is not itself feasible! In this case, it becomes necessary to modify equation [3.4] according to [3.7]:

$$F(\mathbf{x}) = \begin{cases} f(\mathbf{x}) & \text{if } \; g_i(\mathbf{x}) \leq 0, \;\; \forall i = 1, \ldots, m \\ f_{\max} + \sum_{i=1}^{m} r_i P_i(g_i(\mathbf{x})) & \text{otherwise} \end{cases} \qquad [3.7]$$

where the variable $f_{\max}$ should be estimated so that its value is around the maximum size for function $f(\mathbf{x})$ over the search space. More generally, the constraints cannot necessarily be evaluated in parallel; some can only be calculated once others have been verified. Thus for each concurrent design problem, a graph can be established, split into levels, which characterizes the

sequencing between constraints [RAN 03] (see Figure 3.10). Only constraints that are at the same level can be evaluated in parallel. A constraint from a given level can only be calculated if constraints from lower levels are verified. We can also indicate the calculation of the objective function subjected to the same rules on the constraint graph. The higher the number of levels in the graph, the harder the optimization problem becomes. The violated constraints constitute "barriers" to optimization techniques that are blind to constraints at higher levels. This specificity makes the definition of function $F(\mathbf{x})$, and the penalty factors associated with the constraints, particularly difficult.

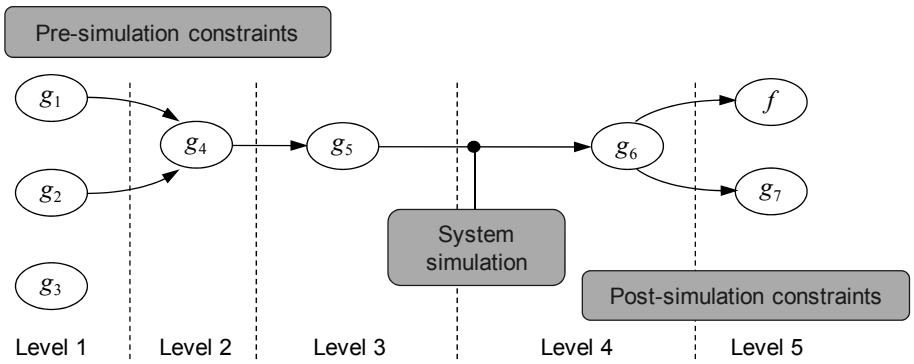


**Figure 3.10.** *Illustration of a constraint graph*

Finally, constraints can be separated into two groups, according to whether they are determined before or after the system simulation (principal cost in central processing unit (CPU) time); we refer to *pre-simulation* constraints as those calculated in advance of simulation, and *post-simulation* as those evaluated after simulation. Pre-simulation constraints are mainly "local" constraints, relating to the system elements and to their association. Post-simulation constraints are mainly "global", relating to the whole system and its operation in the context of its mission and its environment.

### 3.4.2. *Multi-objective problem*

For a multi-objective problem formulated as a scalar problem by aggregating or combining criteria using *a priori* approaches, the use of penalty methods remains possible. For *a posteriori* approaches, the

dominance rule can be extended as follows in order to enable constraints to be taken into account [REG 03]:

– if two solutions **x** and **y** are not feasible, the dominance of **x** over **y** (or that of **y** over **x**) is established in the constraint space;

– if two solutions **x** and **y** are feasible, then dominance of **x** over **y** (or that of **y** over **x**) is established in the objective space;

– if one solution is feasible and the other not, the feasible solution dominates the solution that is not feasible.

These rules enable the concurrent minimization of constraints and the optimization of objectives to be combined, using a Pareto approach in the two spaces.

## 3.5. Integration of robustness into the simultaneous design process

### 3.5.1. *Robust design*

The concepts of robustness and robust design can be easily understood from the illustration in Figure 3.11. This refers to the minimization of a function $f$ in relation to parameter $x$. The function has two minima, at points $A$ and $B$. Point $B$ (the global minimum) is "more efficient" than point $A$ (the local minimum). Conversely, point $A$ is more robust than point $B$ since the degradation of criterion $\Delta f$ over a given vicinity $V(x)$ is more significant in $B$ than in $A$.

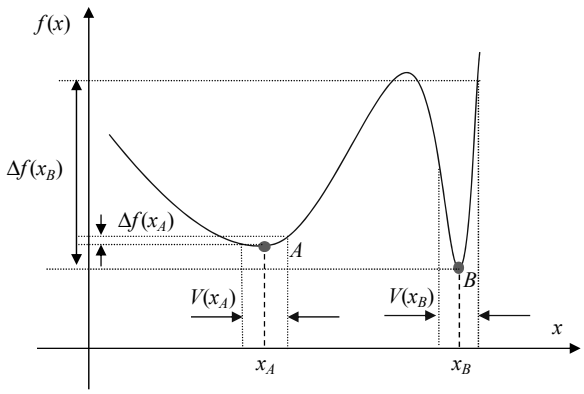


**Figure 3.11.** *Illustration of robustness for a one-dimensional and single objective example*

This single dimension and single objective example is generalized for a vector case with multiple objectives.

In Figure 3.12 we show a similar example to that shown in Figure 3.11 for a bi-objective optimization (minimization of functions $f_1$ and $f_2$) with two parameters $\mathbf{x} = \{x_1, x_2\}$. For a similar vicinity $V(\mathbf{x})$, solution $A$ appears to be more robust than solution $B$ although situated on the Pareto front.

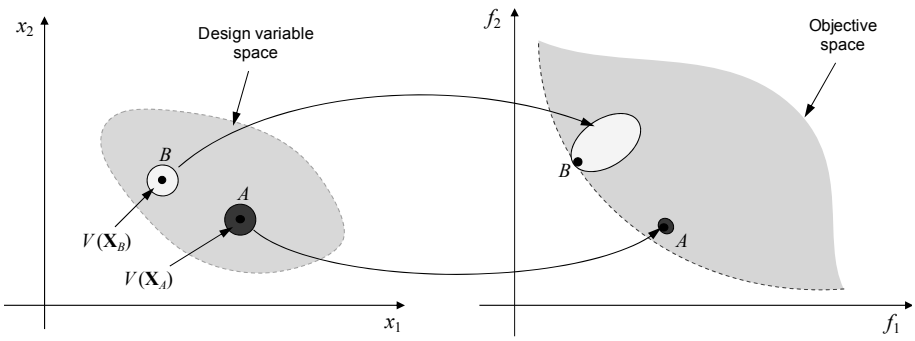


**Figure 3.12.** *Generalization of robustness for a multi-dimensional and multi-objective case*

### 3.5.2. *Vicinity and uncertainty*

Across the preceding examples, we observe that the concept of robustness is linked to the definition of a vicinity $V(\mathbf{x})$ associated with a given solution. This vicinity should normally correspond to an uncertainty domain relating to the design variables. However, this domain can be generalized to all or some of the parameters of the design problem, including the uncertainty over design variables, but also over other intermediary parameters, manufacturing constraints, and design criteria. A classification of the various sources of uncertainty is given in [BEY 07]. There are four main groups:

– uncertainty linked to environment, mission, and operating conditions;

– uncertainty associated with tolerances over the parameters and manufacturing imprecision;

– uncertainty relating to performance criteria resulting, among other things, from differences between the design models and reality (modeling error);

– uncertainty linked to design constraints also linked to modeling errors, establishing the link between parameters and constraints.

### 3.5.3. *Characterization of robustness*

#### 3.5.3.1. *Robustness indicators*

The characterization of robustness can notably be carried out from specific indicators. For example, we can use Taguchi's signal-to-noise ratio $SN_T$ (*nominal-is-best*) [TAG 05], based on a vicinity defined by $n$ points around the reference solution $\mathbf{x}_i$:

$$SN_T = 10\log\left(\frac{\mu_f}{\sigma_f}\right)^2 \qquad [3.8]$$

where $\mu_f = \frac{1}{n}\sum_{i=1}^{n} f(\mathbf{x}_i)$ and $\sigma_f = \sqrt{\frac{1}{n}\sum_{i=1}^{n}\left(f(\mathbf{x}_i) - \mu_f\right)^2}$

The higher the ratio, the lower the variability of the objective function in the considered vicinity and the better the robustness. Even more simply, the maximum degradation rate of criterion $\Delta f$ (%) [TRA 11; DIB 10] can be used as a robustness indicator. This is defined by:

$$\Delta f(\%) = \frac{f(\mathbf{x}) - \min_{i=1..n} f(\mathbf{x}_i)}{f(\mathbf{x})} \quad \text{for objective maximization} \qquad [3.9]$$

$$\Delta f(\%) = \frac{\max_{i=1..n} f(\mathbf{x}_i) - f(\mathbf{x})}{f(\mathbf{x})} \quad \text{for objective minimization} \qquad [3.10]$$

#### 3.5.3.2. *Use of robust effective functions*

Robustness can be directly integrated with optimization by using a *robust effective function* $\bar{f}$ in place of criterion $f$ to be optimized. Two distinct

formulations for this robust effective function are principally used, according to whether we are considering the most severe degradation of $f$ (the worst case) in the vicinity $V(\mathbf{x})$ of solution $\mathbf{x}$, or the average value of $f$ in this vicinity (the mean case). For example, if we are looking to minimize the objective, we could define $\bar{f}$ in accordance with equations [3.11] and [3.12]:

$$\tilde{f}(\mathbf{x}) = \max_{\mathbf{y} \in V(\mathbf{x})} f(\mathbf{y}) \quad \text{for the worst case} \qquad [3.11]$$

$$\tilde{f}(\mathbf{x}) = \frac{1}{|V(\mathbf{x})|} \int_{\mathbf{y} \in V(\mathbf{x})} f(\mathbf{y})\, d\mathbf{y} \quad \text{for a mean approach} \qquad [3.12]$$

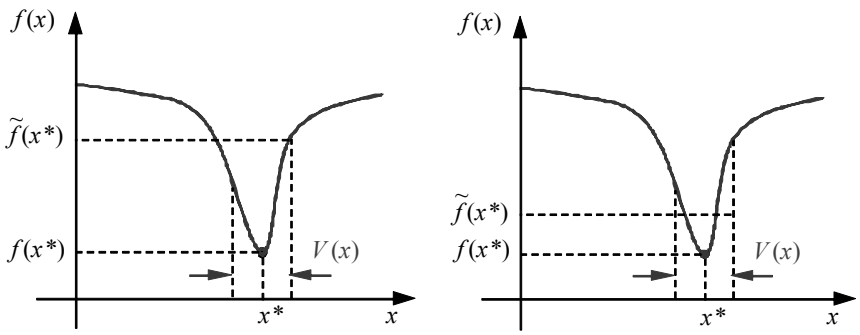


(*a*) *Worst case* (*b*) *Mean value*

**Figure 3.13.** *Illustration of robust effective functions for the minimization of a function f relating to variable x*

### 3.5.3.3. *Definition of the vicinity*

The vicinity of a solution is generally investigated using *screening* techniques, as for experiment designs [TAG 05]. Sampling can be deterministic or stochastic. The more significant the number of points in the vicinity, the better the characterization of robustness, but the higher the calculation cost for the optimization phase. There may then be a benefit in approaching the vicinity of a solution using response areas in order to locally characterize time-consuming CPU measurements.

## 3.6. Example applications

### 3.6.1. *Design of a passive wind turbine system*

#### 3.6.1.1. *Context*

In this first example, we deal with the design of a fully passive wind turbine system [SAR 09; TRA 10], where the static converter, which traditionally ensures the MPPT (maximum power point tracking) control, is suppressed, so as to reduce the cost of the system and increase its reliability (see Figure 3.14a). Such a structure *a priori* presents low energy efficiency, since it is no longer possible to control the wind turbine rotational speed in order to extract maximum power from it (see Figure 3.14b). In order to compensate for the absence of active impedance adaptation, the objective is to optimize the diode rectifier and synchronous generator association in regards to the turbine's characteristics and to the wind farm potential. This then enables a passive MPPT function to be obtained by natural impedance adaptation and thus guarantees performance comparable to that of "active" structures. This example is typical of optimization systems, as there is very little chance that a generator and wind turbine system chosen independently, but compatible regarding association (nominal torque/speed), will enable an acceptable level of efficiency to be guaranteed for the whole passive turbine system.

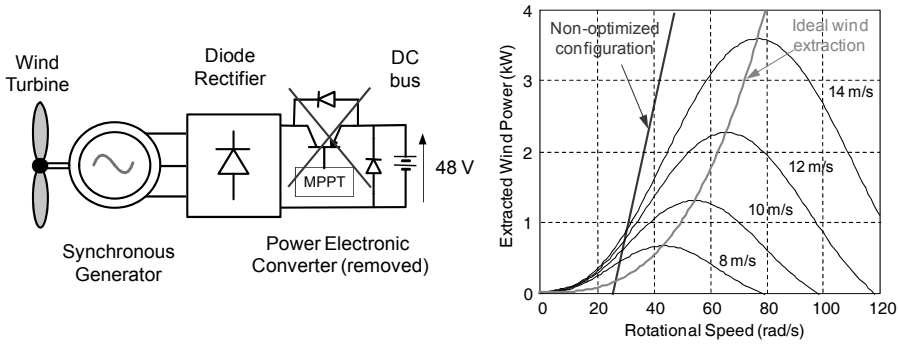


(*a*) *Structure* (*b*) *Typical wind power extraction*

**Figure 3.14.** *Characteristics of a passive wind turbine*

3.6.1.2. *Modeling of passive wind turbine systems*

3.6.1.2.1. Wind modeling

Wind speed is described deterministically by a sum of representative harmonics from a real profile [MIR 05]:

$$V_W(t) = 10 + 0.2\sin(0.105t) + 2\sin(0.267t) + \sin(1.293t) + 0.2\sin(3.665t) \quad [3.13]$$

NOTE.– This same approach can be adopted analogously with other types of wind modeling. Readers should also refer to Chapter 1, which deals with the compact synthesis of a wind speed profile.

3.6.1.2.2. Wind turbine model

The wind turbine considered here is a three-blade BERGEY XL.1 [WWB 11], with radius $R_W = 1.25$ m. It provides a wind power $P_{wind}$ defined by:

$$P_{wind} = \frac{1}{2}\rho C_p(\lambda)\pi R_W^2 V_W^3 \quad [3.14]$$

where $\rho$ denotes the air density, $V_W$ the wind speed and $C_p(\lambda)$ the power factor, which is expressed based on the reduced speed $\lambda = R_W\Omega_W/V_W$ relating to the rotation speed $\Omega_W$ of the turbine. For the wind turbine considered, the power factor can be approached using a polynomial interpolation of 7:

$$C_p(\lambda) = \sum_{k=0}^{7} a_k \lambda^k \quad [3.15]$$

where the interpolation coefficient values are: $a_7 = -3.9\times10^{-8}$, $a_6 = -4.2\times10^{-6}$, $a_5 = 2.1\times10^{-4}$, $a_4 = -3.1\times10^{-3}$, $a_3 = 1.6\times10^{-2}$, $a_2 = -1.8\times10^{-2}$, $a_1 = 1.7\times10^{-2}$, and $a_0 = -1.9\times10^{-3}$.

Finally, the dynamic wind turbine model is represented by a standard mechanical mode in accordance with [3.16]:

$$\Gamma_W - \Gamma_{em} = J_W \frac{d\Omega_W}{dt} + f_W\Omega_W \quad [3.16]$$

where $\Gamma_W$ and $\Gamma_{em}$ represent the wind and electromagnetic torques of the generator, respectively. The values of the wind inertia and associated viscous friction coefficient are $J_W = 1.5$ kg.m$^2$ and $f_W = 0.06$ N.m.s.

3.6.1.2.3. Synchronous generator sizing model

An analytical sizing model for synchronous generators has been developed in [SAR 09; TRA 10]. This has enabled a reduction in calculation times by factors of 10 to 100 for semi-analytical and finite element models, respectively, while guaranteeing acceptable results regarding the precision of the criteria requiring optimization.

There are far too many analytical modeling equations to detail here. We refer readers to previous references, as well as the analytical actuator model described in section 2.3. This model enables all of the geometric characteristics of the generator (bore radius $r_s$, generator length $l_r$, slot, and tooth sizes) to be extracted, as well as the associated circuit model parameters (stator resistance $R_s$, stator flux $\Phi_s$, stator inductance $L_s$) from the design variables that we will shortly detail. It also enables the electromagnetic measurements in the various parts of the generator (yoke, teeth, air gap) to be established.

3.6.1.2.4. Electromagnetic model of the generator/diode-rectifier association

An equivalent DC model for the generator/diode-rectifier association has been developed in [SAR 09] in order to reduce the simulation cost in CPU time, while preserving the pertinence of energy results (see Figure 3.15). This model is based on the correspondence relationships given in Table 3.2. It takes into consideration the armature reaction in the generator, as well as the commutation overlap in the diode rectifier represented by a "non-dissipative" resistance $R_{ov} = 3L_s\omega_s/p$.

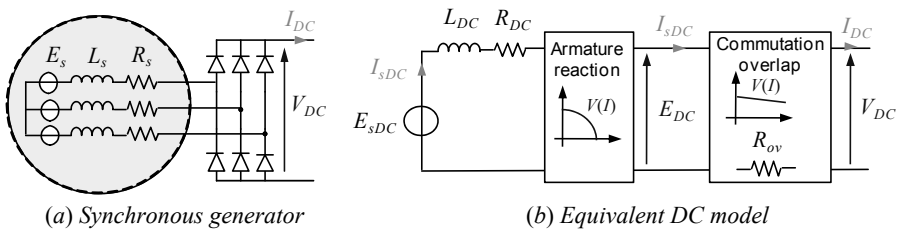


(*a*) *Synchronous generator* (*b*) *Equivalent DC model*

**Figure 3.15.** *Equivalent DC model of the generator/diode-rectifier association*

| Variable | Synchronous generator | Equivalent DC model |
|---|---|---|
| Voltage | $V_s$ | $V_{DC} = \frac{3\sqrt{6}}{\pi} V_s$ |
| Current | $I_s$ | $I_{DC} = \frac{\sqrt{6}}{\pi} I_s$ |
| Flux | $\Phi_s$ | $\Phi_{DC} = \frac{3\sqrt{6}}{\pi} \Phi_s$ |
| Inductance | $L_s$ | $L_{DC} = 3\left(\frac{\sqrt{6}}{\pi}\right)^2 L_s$ |
| Resistance | $R_s$ | $R_{DC} = 3\left(\frac{\sqrt{6}}{\pi}\right)^2 R_s$ |
| Electromotive force | $E_s$ | $E_{sDC} = \frac{3\sqrt{6}}{\pi} E_s$ |

**Table 3.2.** *Correspondence relationships for the equivalent DC model of the generator/diode-rectifier association*

### 3.6.1.2.5. Thermal generator/diode-rectifier association model

Thermal circuit models are used in order to determine temperatures in the various parts of the generator and the diode rectifier during system operation (see Figure 3.16). The thermal resistances and capacities of the various elements are calculated from the geometric structure characteristics and thermal material conductivities [REG 03]. The electrothermal coupling is expressed for the various losses, which constitute the inputs of thermal models. These losses are detailed in the following section.

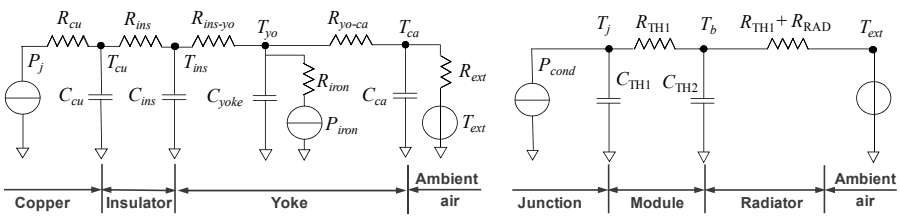


(*a*) *Thermal model of generator* (*b*) *Thermal model of rectifier*

**Figure 3.16.** *Thermal models associated with the generator/diode-rectifier set*

3.6.1.2.6. Modeling of losses in the wind turbine system

The transfer of power into the wind turbine system is illustrated in Figure 3.17. In this diagram we particularly distinguish the wind power $P_{wind}$, the maximum power recoverable by the wind turbine, from the effectively captured power $P_{WT}$.

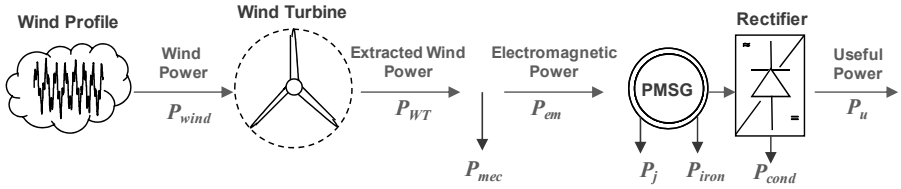


**Figure 3.17.** *Power balance in the wind turbine system*

Among the various losses in the energy conversion turbine, we have:

– Mechanical losses $P_{mec}$ in the wind turbine system, expressed by:

$$P_{mec} = f_W \Omega_W^2 \qquad [3.17]$$

Joule losses in the generator, defined by:

$$P_j = 3R_s^2 \qquad [3.18]$$

– Magnetic losses $P_{iron}$ in the generator, comprised of hysteresis $P_{Hyst}$ and eddy current $P_{ec}$ losses. These losses are determined in the stator yoke and in the teeth. Hysteresis losses per unit of volume are defined by:

$$P_{Hyst} = 2\frac{K_H}{\pi} B^2 \omega_s \qquad [3.19]$$

where $B$ denotes the maximum value for flux density in the considered region (yoke or gear) and $\omega_s$ represents the stator pulse. $K_H$ is a coefficient dependent on the material (typically, $K_H = 52$ W.s/m$^3$/T$^2$ for FeSi 3% strips).

Eddy current losses per unit of volume are expressed in the form:

$$P_{ec} \propto \alpha_p B^2 \omega_s^2 \qquad [3.20]$$

where the proportionality factor varies according to the region (yoke or teeth) [MI 03] and where $\alpha_p$ is a coefficient dependent on the material (typically $\alpha_p = 0.06$ W.s$^2$/m$^3$/T$^2$ for FeSi 3% strips).

– Conduction losses $P_{cond}$ in the diode rectifier, expressed by:

$$P_{cond} = 2\left(V_{DC0} I_{DC} + r_d I_{DC}^2\right) \quad [3.21]$$

where $V_{DC0}$ denotes the drop in direct voltage in the diodes and $r_d$ the dynamic diode resistance. Conduction losses are notably used to size the rectifier radiator using the thermal model previously discussed [SAR 09].

3.6.1.3. *Optimization of the passive wind turbine system*

3.6.1.3.1. Design objectives

The first objective aims to optimize the energy efficiency of the passive wind turbine system. For this, we look to maximize the useful power for the DC bus during the reference wind cycle defined by equation [3.13], over a two minute duration:

$$\max_{\mathbf{x}} \; P_u = \max_{\mathbf{x}} \; P_{WT} - P_{mec} - P_j - P_{iron} - P_{cond} \quad [3.22]$$

We note that maximization of this useful power enables the maximization of power extracted by the wind turbine (passive MPPT function optimization), which is to be combined with the minimization of losses for the whole conversion chain.

The second objective requiring optimization is the overall mass of the system, which, by the same token as the energy efficiency, is significant for this type of system, all the more so when the considered elements are suspended in the nacelle of the wind turbine system. Furthermore, minimizing the constituent masses leads to a minimization of the "material cost", even if the weighting coefficients for the cost/kilogram ratio were to modify the result, compared with a "truly technico-economic optimization". We look to minimize the mass of the electrical elements $M_\Sigma$ (synchronous generator/diode-rectifier set), the mass of the wind turbine being fixed at an estimated value of 34 kg.

$$\min_{\mathbf{x}} \; M_\Sigma = \min_{\mathbf{x}} \; M_{SG} + M_{RAD} \quad [3.23]$$

where $M_{SG}$ represents the mass of the synchronous generator and $M_{RAD}$ the mass of the associated radiator at the rectifier bridge. The mass of the generator is determined from the geometry of the machine and the densities of the various constituents (copper, iron, magnets) [SAR 09].

3.6.1.3.2. Design variables

Eight design variables are chosen in order to optimize the two criteria. These variables are listed in Table 3.3, where we additionally define their range of variation:

| Design variable | Type | Variation |
|---|---|---|
| Bore radius/active machine length | Continuous | $R_{rl} \in [0.1, 5]$ |
| Slot depth/bore radius | Continuous | $R_{dr} \in [0.03, 0.3]$ |
| Yoke flux density (T) | Continuous | $B_y \in [1.2, 1.8]$ |
| Number of pole pairs | Discrete | $p \in \{1,.., 30\}$ |
| Current density (A/mm$^2$) | Continuous | $J_c \in [0.5, 4]$ |
| Base power (W) | Continuous | $P_b \in [300, 3{,}000]$ |
| Number of slots per pole per phase | Discrete | $N_{spp} \in \{1,..,5\}$ |
| Base rotational speed (rad/s) | Continuous | $\Omega_b \in [25, 95]$ |

**Table 3.3.** *Design variables used in the optimization process*

3.6.1.3.3. Design constraints

In order to guarantee the feasibility of the wind turbine system when the design variables vary over their domain of definition, six constraints need to be introduced. These constraints, which are defined in Table 3.4, comprise three pre-simulation constraints ($g_1$, $g_2$ and $g_3$), which apply to the feasibility of the generator and three post-simulation constraints ($g_4$, $g_5$ and $g_6$), which enable deterioration of the system during operation to be avoided. Under constraint $g_1$, the number of conductors per slots $N_{cs}$ must be greater than 1. Conversely, constraint $g_2$ limits this in such a way that the cross-section of the conductor ($S_{slot}/N_{cs}$) remains greater than the minimum authorized cross-section (typically $S_{slot_\min} = 0.5$ mm$^2$). Constraint $g_3$ guarantees a limit to the slot width $w_s$ to a minimum value $w_{s\ \min} = 4$ mm. Constraint $g_4$ enables an

eventual demagnetization of the magnets to be avoided by imposing that the maximum flux density from the stator $B_s$ does not generate a flux density greater than $B_a - B_d$, where $B_a$ is the flux density generated by the magnets and $B_d$ is the demagnetization flux density of the magnets. Constraint $g_5$ ensures that the coil winding temperature $T_{cu}$ in the generator does not exceed the limit value tolerated by the insulator (typically $T_{ins\max}$ = 155°C). Finally, constraint $g_6$ similarly imposes a limit temperature $T_{j\max}$ at the diode junctions (typically $T_{j\max}$ = 150°C).

| Design constraints | Type |
|---|---|
| $g_1(\mathbf{x}) = 1 - N_{cs} \leq 0$ | Pre-simulation |
| $g_2(\mathbf{x}) = S_{slot_\min} - S_{slot} / N_{cs} \leq 0$ | Pre-simulation |
| $g_3(\mathbf{x}) = w_{s\,\min} - w_s \leq 0$ | Pre-simulation |
| $g_4(\mathbf{x}) = \hat{B}_y - (\hat{B}_a - B_d) \leq 0$ | Post-simulation |
| $g_5(\mathbf{x}) = T_{cu} - T_{ins\max} \leq 0$ | Post-simulation |
| $g_6(\mathbf{x}) = T_j - T_{j\max} \leq 0$ | Post-simulation |

**Table 3.4.** *Design constraints used in the optimization process*

Post-simulation constraints are calculated over all points of the wind cycle and combined over the whole cycle. The constraint graph is split into two levels, system simulation only being achieved if the three pre-simulation constraints are verified. When one first-level constraint is not verified, second-level (non-calculable) constraints are subjected to a *death penalty*, namely $g_i(\mathbf{x}) = +\infty$, $\forall i$ = 4, 5 and 6. When a constraint is verified ($g_i(\mathbf{x}) \leq 0$), it is automatically saturated at zero value so that design objectives are prioritized and not the scope of the constraints.

3.6.1.3.4. Optimization process

The optimization process used in order to improve the wind turbine system performance is illustrated in Figure 3.18. The design variables are investigated using evolutionary algorithm NSGA-II so as to concurrently optimize the two objectives, while fulfilling the design constraints. The population size is set at 100 and the number of generations at 600. Multiple

runs of the algorithm are performed with an initial population randomly chosen so as to take account of the stochastic nature of the algorithm and to ensure that the results obtained can be reproduced.

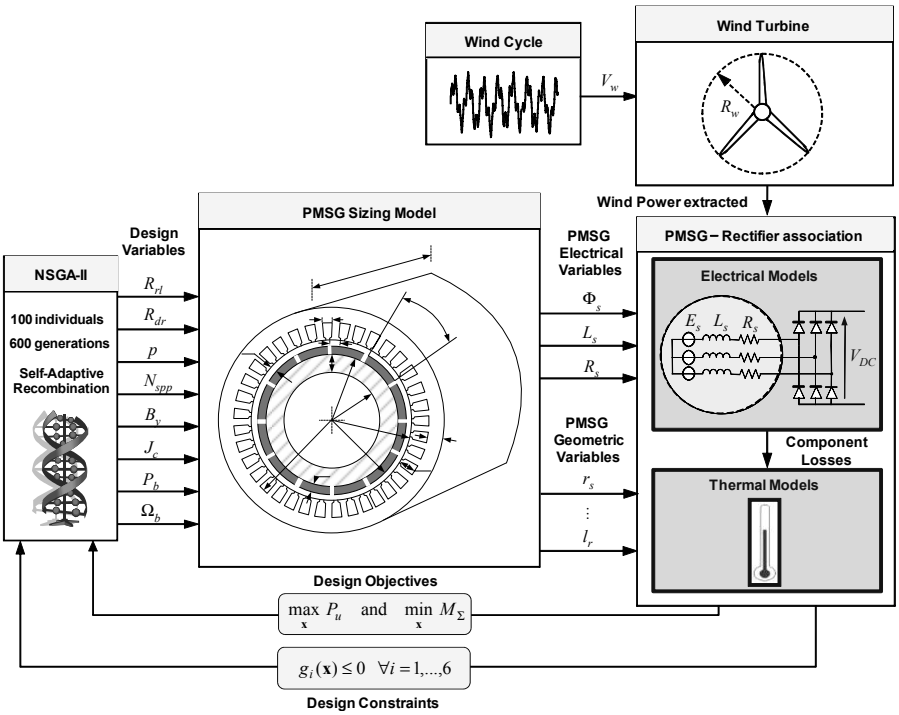


**Figure 3.18.** *Simultaneous design process with multi-objective evolutionary algorithm*

3.6.1.3.5. Results from the optimization of the passive turbine

Figure 3.19 illustrates the results obtained by the evolutionary algorithm following the optimization process previously discussed. Figure 3.19a shows the Pareto front obtained for the generator in the objective space (i.e. Mass/useful power). Note that only the generator mass is shown in this figure, the radiator mass being almost constant for the whole optimal front. We can compare the effectiveness of solutions optimized using any generator, which is efficient when used as part of an "active structure" with MPPT, but of "poor" efficiency when associated with a diode rectifier. As we have already mentioned, this is principally explained by the low wind power extraction capacity when the active electronics are suppressed (see

Figure 3.19b). A solution situated at the elbow of the Pareto front has been isolated in order to produce an experimental generator prototype. We can see that this solution presents a significantly improved wind extraction characteristic compared with an ordinary solution. This clearly approaches the cubic curve corresponding to ideal wind extraction joining all of the power optima for distinct wind speeds.

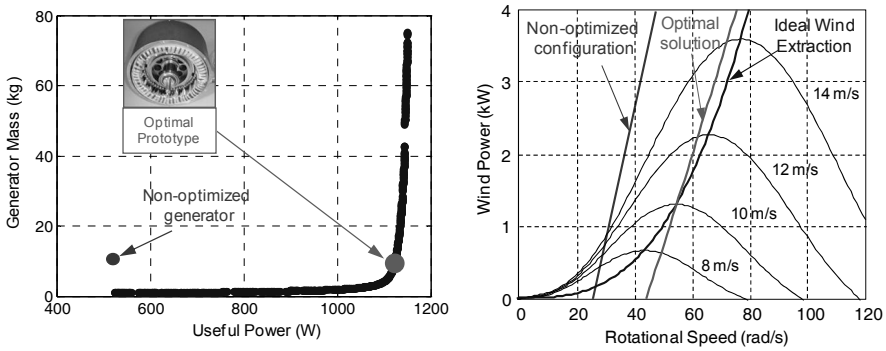


(*a*) *Pareto-optimal solutions* (*b*) *Wind extraction characteristic*

**Figure 3.19.** *Comparison of Pareto front with a non-optimized solution*

The generator prototype designed after optimization has been experimentally validated in [TRA 10]. For the wind profile considered within the optimization process, it enables an extraction efficiency $P_{WT}/P_{wind}$ of close to 90% and a general passive turbine efficiency $P_u/P_{wind}$ in the region of 70% to be obtained. Figure 3.20 illustrates this validation by showing the test bench used to evaluate performance for the passive turbine against the optimal generator prototype (Figure 3.20a). We also present a comparison of the wind powers extracted during the wind cycle, obtained experimentally and by simulation (Figure 3.20b). Quantitatively, the average wind power extracted by the prototype over the wind cycle considered is 1,310 W. The corresponding power value from simulation is 1,365 W. These values are close to the 1,411 W corresponding to optimal wind extraction (for an ideal MPPT with no losses). These results prove the efficiency of the optimized passive wind turbine, but also the good fit of the models developed and the pertinence of the design by means of optimization approach.

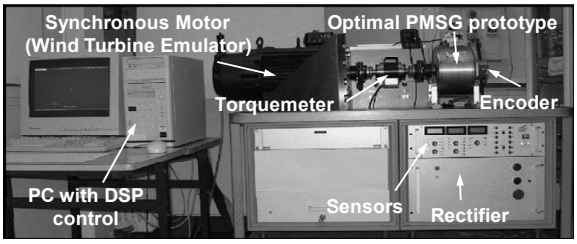


*(a) Test bench*

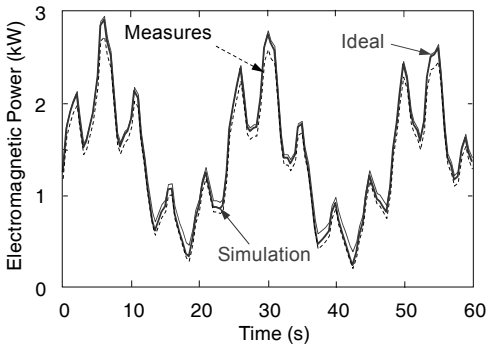


*(b) Wind power extracted during a cycle*

**Figure 3.20.** *Experimental validation of the prototype resulting from the optimization process*

### 3.6.1.4. Robust design of the passive wind turbine

The objective of this final section on the passive turbines is to illustrate the interest in robust design approaches, which were briefly described in section 3.5.3. Indeed, a sensitivity study of passive turbine parameters [TRA 11] has enabled us to show that the efficiency of wind extraction has been strongly influenced by the optimal stator flux value $\Phi_s$ and DC bus voltage $V_{DC}$. However, these values evidently vary during operation of the wind turbine (magnet ageing), based on external conditions (such as the state of battery charge, or changes in temperature). These parameter variations may result in a notable degradation in the energy efficiency of the system. A robust design approach has been investigated in order to reduce the sensitivity of the passive turbine with regards to variations in $\Phi_s$ and $V_{DC}$. For this, we have considered the robust effective functions $\widetilde{P}_u^{\min}$ and $\widetilde{P}_u^{\text{mean}}$, defined by [3.11] and [3.12], respectively, in the optimization process, instead of the useful power $P_u$. The vicinity used for the calculation of robust

effective functions is a two-dimensional vicinity comprising nine points (see Figure 3.21). The variation amplitudes around the reference point (point #1) are set at ±10%.

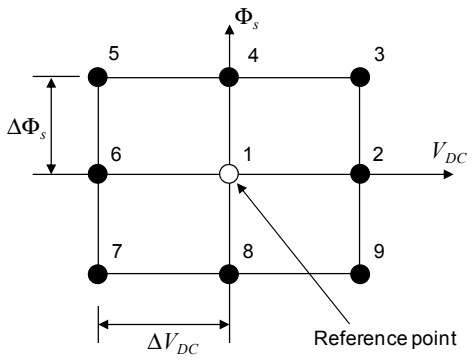


**Figure 3.21.** *Two-dimensional vicinity defining the uncertainty of variables $\Phi_s$ and $V_{DC}$*

The Pareto-optimal solutions obtained following optimizations of functions $P_u$, $\widetilde{P}_u^{\min}$, and $\widetilde{P}_u^{\text{mean}}$, by concurrently minimizing the mass of the system, are denoted by $\mathbf{x}^*$, $\mathbf{x}^*_{\min}$ and $\mathbf{x}^*_{\text{mean}}$, respectively. In Figure 3.22a we compare in the objective space, the robust optimal solutions ($\mathbf{x}^*_{\min}$ and $\mathbf{x}^*_{\text{mean}}$) located in the elbow of the Pareto front, with the $\mathbf{x}^*$ solutions traditionally optimized without robust formulation. We are able to remark that robust solutions are very close to the original solutions, suggesting that introducing robustness does not, in this instance, lead to any degradation in performance.

Additionally, by comparing the robust effective functions of these various solutions against each other, we see that the sensitivity of robust optimal solutions ($\mathbf{x}^*_{\min}$ and $\mathbf{x}^*_{\text{mean}}$) to variations in $\Phi_s$ and $V_{DC}$ is relatively reduced compared with the $\mathbf{x}^*$ solutions optimized without robust formulation (see Figure 3.22b). In this diagram we more specifically indicate three solutions $\mathbf{x}^*$, $\mathbf{x}^*_{\min}$ and $\mathbf{x}^*_{\text{mean}}$ of mass 9.8 kg (the solution $\mathbf{x}^*$ for this mass value corresponding to the prototype extracted from the initial front).

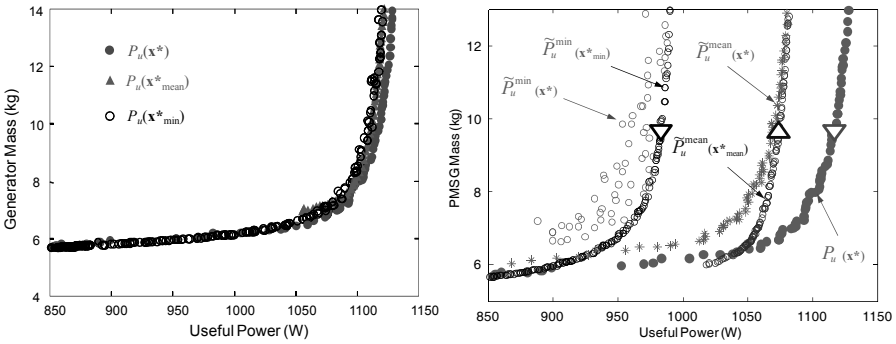


(*a*) *Characteristics of robust solutions* $\mathbf{x}^*_{min}$ *and* $\mathbf{x}^*_{mean}$ *in the objective space*

(*b*) *Comparisons of robust effective functions of solutions* $\mathbf{x}^*$, $\mathbf{x}^*_{min}$ *and* $\mathbf{x}^*_{mean}$

**Figure 3.22.** *Comparison of robust solutions* $\mathbf{x}^*_{min}$ *and* $\mathbf{x}^*_{mean}$ *with the original optimal solutions* $\mathbf{x}^*$ *(obtained without taking robustness into account)*

In Table 3.5 we list the values for the useful power, robust effective functions, and robustness indicators (see section 3.5.3.1) associated with these three particular solutions. From this table, we can see that the robustness indicators are improved for robust solutions, compared with the original prototype.

| | Optimum solution $\mathbf{x}^*$(9.8 kg) – prototype | Robust solution $\mathbf{x}^*_{moy}$(9.8 kg) | Robust solution $\mathbf{x}^*_{min}$(9.8 kg) |
|---|---|---|---|
| $P_u$ (W) | **1,115** | 1,107 | 1,105 |
| $\tilde{P}_u^{mean}$ (W) | 1,044 | **1,074** | 1,064 |
| $\tilde{P}_u^{min}$ (W) | 910 | 970 | **982** |
| $\Delta P_u$ (%) | 16.2 | 12.4 | **10.9** |
| $SN_T$ (dB) | 24.41 | 26.34 | **26.47** |

**Table 3.5.** *Characteristics of robust solutions of mass 9.8 kg (the optimal values for the objectives and robustness indicators are shown in bold text)*

### 3.6.2. *Simultaneous design of an autonomous hybrid locomotive*

#### 3.6.2.1. *Context*

The second application example has already been discussed in Chapter 1 of this book, on the processing of traffic missions, but here we return to it more specifically to illustrate the concurrent design by means of the optimization approach. It concerns the design of a power turbine for a BB 63 000 locomotive built to fulfill service and sorting missions on non-electrical lines. The replacement of the initial 600 kW diesel engine with a power turbine comprised of a reduced power diesel generator and hybridized using batteries and ultra-capacitors, was studied in the ANR PLATHEE project [THI 08]. The main characteristics of the conversion chain (architecture – sizing – energy management) were first established using a traditional sequential analysis approach (without optimization) [AKL 07] before moving on to a simultaneous design approach by means of optimization [AKL 09].

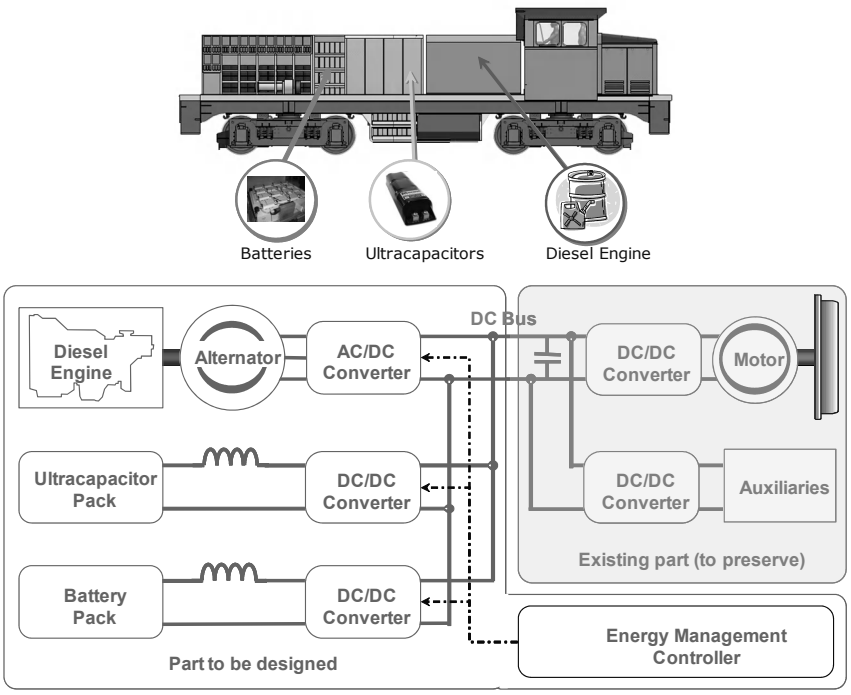


**Figure 3.23.** *Illustration of the PLATHEE project [THI 08]*

### 3.6.2.2. *Energy management strategy*

Figure 3.24 presents the reference mission used in order to evaluate the efficiency of the locomotive. This 8 hour mission was judged at the time to be the most constraining from an energy and power perspective, from among a mission set [AKL 08].

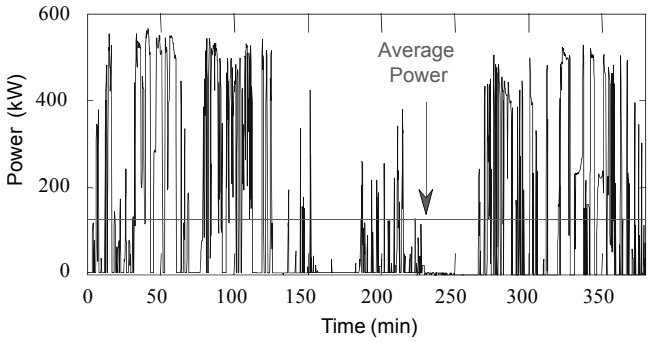


**Figure 3.24.** *Typical difficult mission profile for the BB 63 000 locomotive*

In order to satisfy this type of mission with the hybrid architecture previously presented, a frequency management strategy was implemented [AKL 07] (see Figure 3.25).

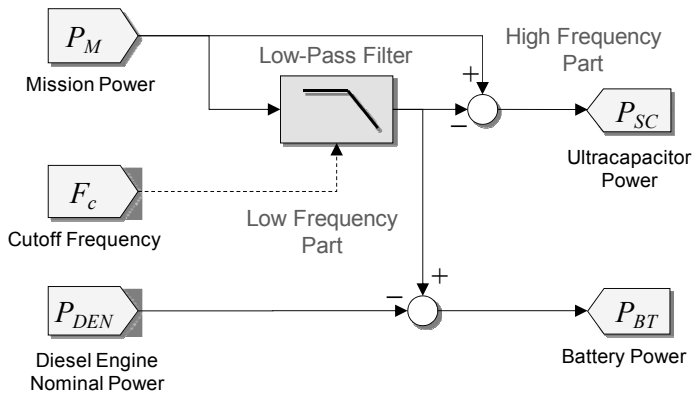


**Figure 3.25.** *Energy management based on a frequency approach*

This strategy takes into account the physical characteristics and natural dynamics relating to different sources of energy. Beyond a certain cut-off frequency ($F_c$), it distributes the high-frequency part of the mission power ($P_M$) to the ultra-capacitors. The rest of the power is assigned to the batteries and the diesel engine by assuming that the latter provides a null (a "stop and go" strategy) or constant power, which is close to its nominal sizing power ($P_{DEN}$) so as to maximize its energy efficiency and reduce diesel consumption.

3.6.2.3. *Hybrid locomotive modeling*

Various types of models associated with locomotives have been developed in [AKL 07; AKL 08; AKL 09] and briefly recapped in Chapter 1:

– *energy models* characterize the energy transfers in the locomotive. They are arranged into different levels according to the degree of precision accorded to the description of energy transfers:

- power flow models enable energy managers to deduce values for power and energy during a mission for the various sources on board locomotives (diesel, batteries and ultra-capacitors). They also provide the state of charge for storage elements, as well as the diesel consumption and the quantity of $CO_2$ emitted,

- electrical models enable the effort and flow variables (current and voltage) to be calculated from the energy variables (power and energy). These models are themselves divided into various sublevels according to whether or not control loops are considered and whether average value (over a breakdown period) or instantaneous value converters are modeled. The calculation cost in CPU time of the various models is illustrated in Figure 3.26. It varies significantly between models, according to the level of energy transfer representation for the whole system. Thus, power flow models and "static" electrical models (without taking control loops into account and with average value converters being modeled) will be well suited to simultaneous design. More precise models will, for their part, be used at the end of validation and in order to refine the system characteristics following sizing (such as controller synthesis and sizing of smoothing inductors);

– *geometric models* provide, for a given sizing, volumes for the diesel engine, battery packs, or ultra-capacitors and associated converters;

– *cost models* enable empirical estimation of the ownership costs of various energy sources. These costs include the raw purchase costs of these

elements as well as maintenance surcharges, evaluated from lifetime indicators.

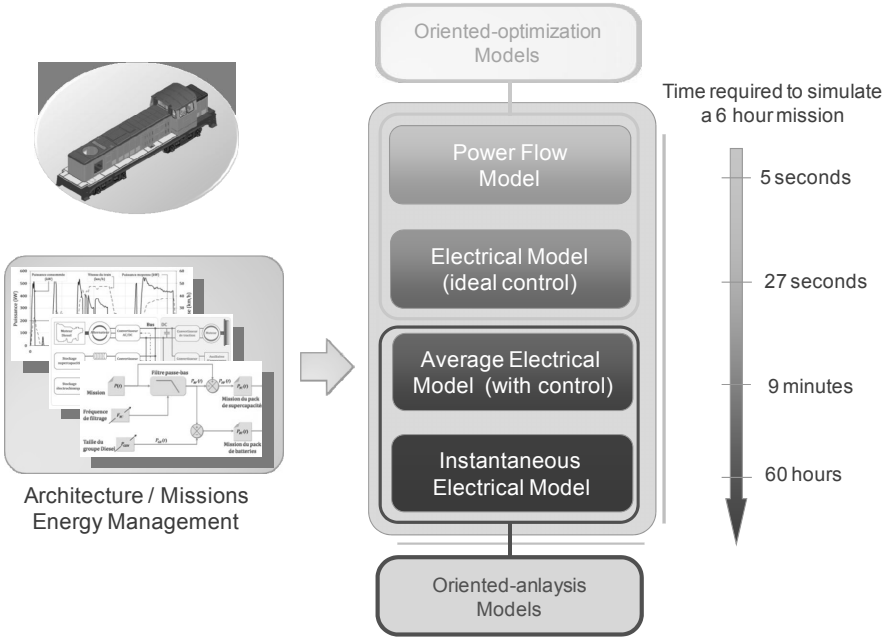


**Figure 3.26.** *Different levels of energy transfer representation and associated calculation costs*

### 3.6.2.4. *Hybrid locomotive optimization*

#### 3.6.2.4.1. Design objective

The first objective to be fulfilled is economic: to reduce the overall financial cost of ownership of system $C_\Sigma$, defined by the sum of the costs of the different energy sources:

$$\max_{\mathbf{x}} \; C_\Sigma = \min_{\mathbf{x}} \; C_{DE} + C_{BT} + C_{SC} + C_{fuel} \qquad [3.24]$$

where $C_{DE}$, $C_{BT}$ and $C_{SC}$ represent the ownership costs of the diesel engine, batteries, and ultra-capacitors, respectively (see section 1.6.1). We note that the fuel cost $C_{fuel}$, relating to the quantity of fuel, which is necessary for the operation of the locomotive during use, is also included in the overall financial cost.

The second objective is environmental, to minimize the climate cost $C_{CO2}$, defined by the quantity of $CO_2$ emitted during use of the locomotive:

$$\min_{\mathbf{x}} C_{CO2} = \min_{\mathbf{x}} Q_{CO2} \frac{\Delta\tau_{an}}{\Delta\tau_m} \qquad [3.25]$$

where $Q_{CO2}$ denotes the quantity of $CO_2$ emitted during the reference mission used in the optimization process, $\Delta\tau_m$ the duration of this mission and $\Delta\tau_{an}$ the total annual duration of use for the locomotive.

3.6.2.4.2. Design variables

Seven design variables are chosen to optimize the two criteria. These are listed in Table 3.6, where we also specify their range of variation.

| Design variable | Type | Variation |
|---|---|---|
| Number of battery cells in series | Discrete | $NS_{BT} \in \{0,.., 542\}$ |
| Number of battery packs in parallel | Discrete | $NP_{BT} \in \{0,.., 32\}$ |
| Number of ultra-capacitors in series | Discrete | $NS_{SC} \in \{0,.., 262\}$ |
| Number of ultra-capacitor packs in parallel | Discrete | $NP_{SC} \in \{0,.., 60\}$ |
| Converter switching frequency (kHz) | Continuous | $F_{sw} \in [1, 10]$ |
| DC bus voltage (V) | Continuous | $V_{bus} \in [50, 650]$ |
| Diesel engine nominal power (kW) | Continuous | $P_{DEN} \in [50, 600]$ |

**Table 3.6.** *Design variables used in the optimization process*

3.6.2.4.3. Design constraints

In order to guarantee the feasibility of the solutions, six constraints are integrated into the optimization process. The available volume for the energy sources on board the locomotive is limited to 32 $m^3$. Consequently, constraint $g_1$ ensures that the sum of the respective volumes of the diesel engine, batteries, and the ultra-capacitors ($\Omega_{DE}$, $\Omega_{BT}$ and $\Omega_{SC}$) does not exceed this limit (see section 1.6.1). Constraints $g_2$ and $g_3$ guarantee the limiting of the duty cycles of the associated battery pack and ultra-capacitor choppers to a value $\alpha_{max}$ = 0.93. Maintaining these three initial constraints

enables simulation of the system during its reference mission and refinement of converter sizing and smoothing inductors. Constraint $g_1$ can then be extended to constraint $g_4$, which considers the chopper volumes associated with the battery and ultra-capacitor packs ($\Omega_{CBT}$ and $\Omega_{CSC}$), as well as the volumes above. Constraint $g_5$ ensures that the charge time $\Delta\tau_{charge}$ for storage elements at the end of the mission does not exceed 40% of the mission time. Finally, constraint $g_6$ allows a low degradation of the mission, but then limits the missing energy $E_d$ to 1% of the total energy $E_m$ necessary to accomplish the mission.

| Design constraint | Type |
|---|---|
| $g_1(\mathbf{x}) = \Omega_{DE} + \Omega_{BT} + \Omega_{SC} - 32 \leq 0$ | Pre-simulation |
| $g_2(\mathbf{x}) = NS_{BT}V_{BT\max} - \alpha_{\max}V_{bus} \leq 0$ | Pre-simulation |
| $g_3(\mathbf{x}) = NS_{SC}V_{SC\max} - \alpha_{\max}V_{bus} \leq 0$ | Pre-simulation |
| $g_4(\mathbf{x}) = \Omega_{DE} + \Omega_{BT} + \Omega_{SC} + \Omega_{CBT} + \Omega_{CSC} - 32 \leq 0$ | Post-simulation |
| $g_5(\mathbf{x}) = \Delta\tau_{\text{charge}} / \Delta\tau_m - 0.4 \leq 0$ | Post-simulation |
| $g_6(\mathbf{x}) = E_d / E_m - 0.01 \leq 0$ | Post-simulation |

**Table 3.7.** *Design constraints used in the optimization process*

### 3.6.2.5. *Optimization process and results*

The optimization process implemented is similar to that previously presented for the passive wind turbine system. The NSGA-II is used to optimize the two objectives relating to the design variables. The Pareto-optimal solutions obtained after multiple independent runs of the algorithm are presented in Figure 3.27. We particularly compare three specific solutions ($S_1$, $S_2$, and $S_3$) extracted from the Pareto front with an initial configuration ($S_0$) sized using a traditional sequential analysis approach (without optimization) [AKL 07]. The design variables and objectives relating to these solutions are detailed in Table 3.8. We can observe, from these results, that the majority of Pareto-optimal solutions dominate the initial reference solution. The "very flat" shape of the Pareto front observed in Figure 3.27 is explained by the fact that there is no real compromise between the two objectives considered. Indeed, we can see in Table 3.8 that the overall usage cost of the various solutions is principally due to fuel costs (the cost of "heading for the gas station").

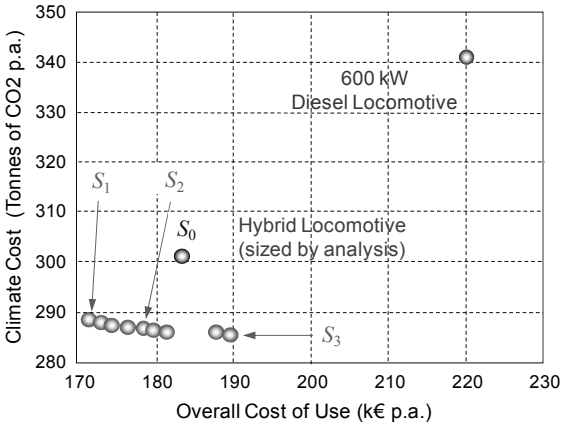


**Figure 3.27.** *Pareto-optimal solutions for the hybrid locomotive*

| Design variable/criterion | $S_0$ | $S_1^*$ | $S_2^*$ | $S_3^*$ |
|---|---|---|---|---|
| Number of cells in series | 300 | 249 | 230 | 143 |
| Number of battery blocks in parallel | 4 | 8 | 9 | 10 |
| Number of ultra-capacitors in series | 200 | 175 | 20 | 20 |
| Number of ultra-capacitor packs in parallel | 8 | 1 | 1 | 1 |
| Diesel engine nominal power (kW) | 215 | 174 | 162 | 151 |
| DC bus voltage (V) | 540 | 645 | 631 | 625 |
| Converter switching frequency (kHz) | 2 | 7 | 8 | 10 |
| Climate cost (tonnes of $CO_2$ p.a.) | 301 | 288 | 287 | 286 |
| Overall usage cost (k€ p.a.) | 183 | 172 | 178 | 189 |
| Fuel cost (k€ p.a.) | 153 | 146 | 145 | 145 |
| Diesel engine cost (k€ p.a.) | 22.4 | 19 | 18 | 17 |
| Battery and ultra-capacitor cost (k€ p.a.) | 7.6 | 7 | 18 | 27 |

**Table 3.8.** *Design variables and objectives relating to the three optimal solutions extracted from the Pareto front, compared with the initial sizing resulting from a classical analysis approach*

The second criterion is also directly correlated with this cost, since the quantity of carbon dioxide emitted into the atmosphere is directly proportional to the quantity of fuel consumed. It is interesting to note that optimizing the environmental cost addresses some economic concerns,

further justifying the interest in hybridization. The climate cost is minimal in $S_3$, a configuration keenly sized with the smallest diesel engine and the lowest number of storage components. This solution is not, however, optimal from a usage cost perspective, notably because of the increase in storage costs during use. Indeed, for this solution, batteries and ultra-capacitors are much more sought after and, therefore, present average lifetime indicators, impacting on the ownership cost of the storage.

## 3.7. Conclusions

This chapter has presented simultaneous design by means of the optimization approach, which enables the general integration of questions of system architecture, sizing, and energy management. Optimization approaches enable the complexity of this often combined process to be understood. We have thus shown the problems posed by such a process before tackling the question of so-called optimization algorithms. In the highly heterogeneous context of the systemic design process, we have highlighted the adequacy of multi-objective evolutionary algorithms, which notably enable the efficient resolution of mixed variable and constrained optimization problems. One section shows that the question of robustness, which is essential for design, may also be addressed during the optimization process. This view has been illustrated in the first application, dealing with a fully passive wind turbine system. Comparing the results of optimization with the behavior of a wind turbine generator prototype "extracted from the Pareto front" has demonstrated the pertinence of the approach, which relies strongly on the constancy of design models. Finally, the second illustration repeating the example of the hybrid locomotive discussed in Chapter 1 of this book, has enabled us to draw attention to the advantage of simultaneous design with regard to a traditional approach using sequential analysis. This chapter finally completes the previous one, which is specifically dedicated to the modeling approach. It is then finally completed by the next chapter, which deals with multi-level optimization methods. Indeed, to a certain extent of system complexity, it becomes illusory to want to "concurrently design everything" within one and the same optimization loop. It is then a case of being able to extract a system solution close to the overall optimum relating to the association of multiple separately optimized sub-systems.

## 3.8. Bibliography

[AKL 07] AKLI C.R., SARENI B., ROBOAM X., JEUNESSE A., "Energy management and sizing of a hybrid locomotive", *European Conference on Power Electronics (EPE'07)*, Aalborg, Denmark, 2007.

[AKL 08] AKLI C.R., Conception systémique d'une locomotive hybride autonome, PhD thesis, University of Toulouse, 2008.

[AKL 09] AKLI C.R., SARENI B., ROBOAM X., JEUNESSE A., "Integrated design of a hybrid locomotive with multiobjective genetic algorithms", *International Journal of Applied Electromagnetics and Mechanics*, vol. 30, pp. 151-162, 2009.

[BÄC 96] BÄCK T., *Evolutionary Algorithms in Theory and Practice: Evolution Strategies, Evolutionary Programming, Genetic Algorithms*, Oxford University Press, New York, 1996.

[BEY 07] BEYER H.G., SENDHOFF B., "Robust optimization – a comprehensive survey", *Computer Methods in Applied Mechanics and Engineering*, vol. 196, pp. 3190-3218, 2007

[COE 11] COELLO COELLO C.A., List of references on evolutionary multiobjective optimization, http://delta.cs.cinvestav.mx/~ccoello/EMOO/EMOObib.html, 2011.

[COL 02] COLLETTE Y., SIARRY P., *Optimisation Multiobjectif*, Paris, Eyrolles, 2002.

[COR 00] CORNE D.W., KNOWLES J.D., OATES M.J., "The Pareto envelope-based selection algorithm for multiobjective optimization", *Parallel Problem Solving from Nature VI Conference*, Paris, France, pp. 839-848, 2000

[DAR 59] DARWIN C., *The Origin of Species by Means of Natural Selection*, John Murray, London, 1859.

[DEB 00] DEB K., AGRAWAL S., PRATAB A., MEYARIVAN, "A fast-elitist non-dominated sorting genetic algorithm for multiobjective optimization: NSGA-II", *Parallel Problem Solving from Nature VI Conference*, Paris, France, pp. 849-858, 2000

[DIB 10] DI BARBA P., *Multiobjective Shape Design in Electricity and Magnetism*, Springer, Dordrecht, 2010.

[EIB 99] EIBEN A.E., HINTERDING R., MICHALEWICZ Z., "Parameter control in evolutionary algorithms", *IEEE Transactions on Evolutionary Computation*, vol. 3, pp. 124-141, 1999.

[FOG 66] FOGEL L.J., OWENS A.J., WALSH M.J., *Artificial Intelligence through Simulated Evolution*, Wiley, New York, 1966.

[FOG 91] FOGEL D.B., *System Identification Trough Simulated Evolution*, Ginn Press, Needham Heights, 1991.

[GOL 89] GOLDBERG D.E., *Genetic Algorithms in Search Optimization and Machine Learning*, Addison Wesley, Boston, 1989.

[HOL 75] HOLLAND J., *Adaptation in Natural and Artificial Systems*, University of Michigan Press, Ann Arbor, 1975.

[KEI 02] KEIJZER M., MERELO J.J., ROMERO G., SCHOENAUER M., "Evolving objects: a general purpose evolutionary computation library", *Evolution Artificielle*, Le Creusot, France, pp. 321-244, 2001.

[KNO 01] KNOWLES J.D., CORNE D.W., "Approximating the nondominated front using the Pareto archived evolution strategy", *Evolutionary Computation*, vol. 8, pp. 149-172, 2000.

[KOZ 92] KOZA L., *Genetic Programming: on the Programming of Computers by the Means of Natural Selection*, The MIT Press, Cambridge, Massachusetts, 1992.

[KRA 06] KRÄHENBÜHL L., "Algorithmes stochastiques d'optimisation: élargissons notre point de vue", *Techniques de sciences informatiques*, vol. 25, pp. 1209-1216, 2006.

[MAF 95] MAFOUD S., Niching methods for genetic algorithms, PhD thesis /Technical report No. 95001, University of Illinois at Urbana Champain, 1995.

[MEY 07] MEYER-NIEBER S., BEYER H.G., "Self-adaptation in evolutionary algorithms", *Parameter Setting in Evolutionary Algorithms*, Springer-Verlag, Berlin, pp. 47-75, 2007.

[MI 03] MI C., SLEMON G.R., BONERT R., "Modeling of iron losses of permanent-magnet synchronous motor", *IEEE Trans. On Industry Applications*, vol. 39, pp. 734-742, 2003.

[MIC 96] MICHALEWICZ Z., *Genetic Algorithms + Data Structures = Evolution Programs*, 3rd edition, Springer-Verlag, Berlin, 1996.

[MIR 05] MIRECKI A., Etude comparative de chaînes de conversion d'énergie dédiées à une éolienne de petite puissance, PhD thesis, National Polytechnic Institute of Toulouse, 2005.

[PAR 96] PARETO V., *Cours d'Economie Politique,* Rouge, Lausanne, 1896.

[RAN 03] RANDI S.A., Conception systémique de chaînes de traction synchrones pour véhicules électriques à large gamme de vitesse, PhD thesis, National Polytechnic Institute of Toulouse, 2003.

[RAO 09] RAO S.S., *Engineering Optimization: Theory And Practice*, 4th edition, John Wiley & Sons, Hoboken, New Jersey, 2009.

[REG 03] REGNIER J., Conception de systèmes hétérogènes en Génie Electrique par optimisation évolutionnaire multicritère, PhD thesis, National Polytechnic Institute of Toulouse, 2003.

[SAR 98] SARENI B., KRÄHENBÜHL L., "Fitness sharing and niching methods revisited", *IEEE Transactions on Evolutionary Computation*, vol. 2, pp. 97-106, 1998.

[SAR 09] SARENI B., ABDELLI A., ROBOAM X., TRAN D.H., "Model simplification and optimization of a passive wind turbine generator", *Renewable Energy*, vol. 34, pp. 2640-2650, 2010.

[SCH 92] SCHRAUDOLPH N.N., BELEW R.K., "Dynamic parameter encoding for genetic algorithms", *Machine Learning*, vol. 9, pp. 9-21, 1992.

[SCH 95] SCHWEFEL H.P., *Evolution and Optimum Seeking*, John Wiley & Sons, New York, 1995.

[STO 96] STORN R., PRICE K., "Minimizing the real functions of the ICEC'96 contest by differential evolution", *International Conference on Evolutionary Computation*, Nagoya, Japan, 1996.

[TAG 05] TAGUCHI G., CHOWDHURY S., WU Y., *Taguchi's Quality Engineering Handbook*, John Wiley & Sons, Hoboken, New Jersey, 2005.

[THI 08] THIOUNN M., "PLATHEE – a platform for energy efficiency and environmentally friendly hybrid trains", *8th World Congress on Railway Research*, *COEX*, Seoul, Korea, 2008.

[TRA 10] TRAN D.H., SARENI B., ROBOAM X., ESPANET C., "Integrated optimal design of a passive wind turbine system: an experimental validation", *IEEE Trans. on Sustainable Energy*, vol. 1, pp. 48-56, 2010.

[TRA 11] TRAN D.H., SARENI B., ROBOAM X., BRU E., DE ANDRADE A., "Sensitivity analysis and robust design of a passive wind turbine system", *Selected paper from OIPE'*08, *COMPEL*, 2011.

[VAN 99] VAN VELDUIZEN D.A., Multiobjective evolutionary computation: classifications, analyses, and new innovation, PhD thesis, Air Force Institute of Technology, 1999.

[WHI 91] WHITLEY D., MATHIAS K., FIZHORN P., "Delta-Coding: an iterative search strategy for genetic algorithms", *Fourth International Conference on Genetic Algorithms*, San Diego, CA, pp. 77-84, 1991.

[WWB 11] BERGEY website: http://www.bergey.com, 2011.

[ZIT 01] ZITZLER E., LAUMANNS M., THIELE L., "SPEA2: improving the strength Pareto evolutionary algorithm", *EUROGEN 2001*, *Evolutionary Methods for Design, Optimization and Control with Applications to Industrial Problems*, Athens, Greece, pp. 12-21, 2001.

Chapter 4

# Multi-Level Design Approaches for Electro-Mechanical Systems Optimization

## 4.1. Introduction

While the design of products and services is a fundamental part of business activity, its main purpose is to satisfy market needs and expectations. The expression of a product's list of specifications is therefore a crucial step influencing the success of the business and mobilizes numerous resources, such as market research. However, many technical difficulties remain in product definition. Two main difficulties are typical of equipment industries: the preponderance of the functionality achieved for the product itself and the correct integration of the product into where it will be used. The product thus becomes a component that needs to be integrated into a bigger system or sub-system and the component-to-system interaction then appears to be the critical design task for the component.

A systemic or holistic design approach, therefore, needs to be employed; sizing of the system and its constituent components are interdependent tasks. Thus, it has often been remarked that an assembly of components that would have been thought to be optimal, is, in fact, suboptimal and badly suited to its mission. This means that the traditional method of design using successive trials has been rendered inappropriate and so new tools and new

---

Chapter written by Stéphane BRISSET, Frédéric GILLON and Pascal BROCHET.

*Integrated Design by Optimization of Electrical Energy Systems* Edited by Xavier Roboam
© 2012 ISTE Ltd. Published 2012 by ISTE Ltd.

optimal design methods are required, which need to be tested and compared with current practice.

Designers currently have a large number of modeling tools at their disposal. These tools enable representation of the behavior of a device, but are often restricted to one area of physics or one discipline. Therefore, it is necessary to aggregate these models in order to obtain the desired representation of a component. It is also necessary, in defining the model, to introduce context and the interaction between elements around the component. In most cases, only the need is known and defined for the system, which indirectly influences the objectives and constraints applicable to the components to be deduced.

In order to design the best product, i.e. the product best suited to the function, it is no longer sufficient to rely on previously acquired experience. Tools and methods are needed that assist the designer in finding a feasible solution, but which also result in the most effective solution. To that end, numerical optimization tools appear to be well suited. However, numerical models and optimization tools do not enable this problem to be resolved; a method or design approach must be defined which ensures consistency of the optimizations performed, whether for the system or the components.

Therefore, we need to manage the complexity of a design approach, which is multi-physical and multi-disciplinary. This takes the requirement definition to an upper level, but also drives multiple optimization processes. Designers faced with this complexity are very often in search of a fair compromise between the system, i.e. an exhaustive description of the whole device, and the model; in other words the most detailed description possible for an element. The limit is generally linked to calculation capacity, but also to the sensitivity and knowledge of the designer. Thus, the aim of this chapter is to present two multi-level optimization approaches enabling traditional limits to be expanded, which are specific to the use of a unique model with a unique optimization process, and which deal with the complexity of a systemic design approach.

## 4.2. Multi-level approaches

Multi-level approaches are distinguished from traditional optimal design approaches by the use of multiple modeling levels with complementary characteristics. Indeed, traditional approaches are characterized by the

resolution of a unique optimization problem by means of an algorithm and of a unique model in order to determine objective functions and constraints. Traditionally, the optimal solution presented as a target is expressed by:

$$\text{find } x^* = \underset{\substack{x \in \Re^n \\ lb \le x \le ub}}{\arg\min} \left\| f(x) - y \right\| \text{ where } g(x^*) \le 0 \qquad [4.1]$$

where argmin provides the minimum argument, the symbol $\|.\|$ indicates the Euclidean norm $\|(x_1,...,x_n)\| = \sqrt{|x_1|^2 + ... + |x_n|^2}$, values for $x$ are optimization variables in real space and are limited by $lb$ and $ub$, $f$ represents the objectives and $y$ the target values for these objectives, which may be set at zero in the case of minimization. $g$ represents the constraints and $x^*$ represents the optimal values of $x$.

Conversely, for multi-level approaches, which are used in systemic optimal design, the approach enables management of multiple models, whose characteristics differ: *calculation time*, *precision*, and *complexity*. These result in multiple optimizations being linked together, whose formulations differ and which can be resolved using ultimately different algorithms. The multi-level approach enables various models of one component to be managed in order to accelerate the optimization process, or enables multiple optimizations of a decomposed and hierarchical model to be managed as part of a design process.

In Figure 4.1, the models used in the design are positioned along two axes: the scope of the model, ranging from system to component, or even to the material chosen, and the granularity of the model.

In the ideal case of a systemic design, it would be better to have a more detailed level of granularity and the widest scope, i.e. covering the whole system (point *I*). This defines an ideal solution but one that is generally unattainable due to the limited calculation capacities available to designers and the significant number of evaluations necessary for optimization. Thus, for a fixed calculation capacity (curve ①), a curve can be traced representing the whole compromise between the scope and granularity of the model. This representation is common in multi-objective optimization and is called the Pareto front. This frontier expresses the necessity for compromise between criteria. If calculation capacities increase, the Pareto frontier moves and

becomes curve ②. Thus, the models obtained dominate those of curve ①, since their granularity and scope are significantly better. Usually, designers focusing on the system use models whose characteristics are those of point $S_2$ in Figure 4.1, whereas designers of the components use models whose characteristics are those of point $C_2$.

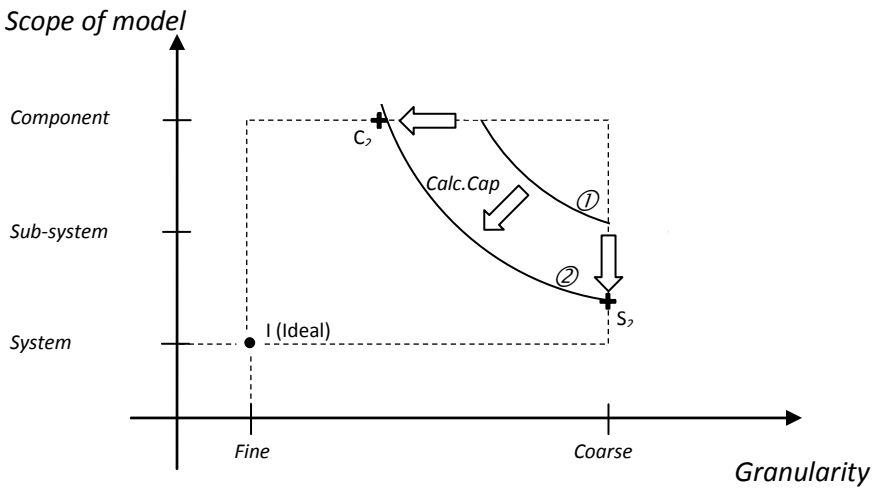


**Figure 4.1.** *Possible compromises between scope and granularity of the model*

So-called multi-level design approaches enable the granularity or scope of models used for systemic optimal design to be improved, without the need for increased calculation capacities. Approaches are distinguished according to the axis along which they are applied.

*Space mapping (SM)* approaches work along the horizontal axis and use two like-for-like models of the same device, but with different granularities. SM enables a coarse granularity model with low precision but a reduced calculation time to be managed alongside a model with fine granularity and high precision, but which requires a significant calculation time.

These models are described as being "simple" and "fine", respectively. Optimizations are performed with the simple model; the fine model is only occasionally evaluated, typically less than 10 times. The calculation time is thus significantly reduced, which enables designers to work with models with a finer level of granularity for the same calculation capacity. As a result

of this approach, the Pareto frontier is displaced from curve ① towards curve ③ in Figure 4.2. The SM approach enables the frontier to be displaced to the left and to thus use fine models in optimal design.

Hierarchical decomposition approaches, such as *target cascading (TC)*, work along the vertical axis and use a "system" level model, along with models of its constituent "components". All of the models have strong granularity, since they are directly used during optimization. The advantage of this approach is that it avoids the need for a large size model to be constructed in favor of multiple smaller models involving fewer design parameters.

Some optimizations are performed on each submodel and system consistency is addressed using the TC method. Optimizations are faster, as they are performed on smaller models, involving fewer design parameters, which enables more components to be modeled; therefore, the scope of the system is widened. As a result of this approach, the Pareto frontier becomes curve ④ in Figure 4.2. The target cascading approach enables the frontier to be displaced downwards and thus, integrates the needs and constraints of the optimally designed system.

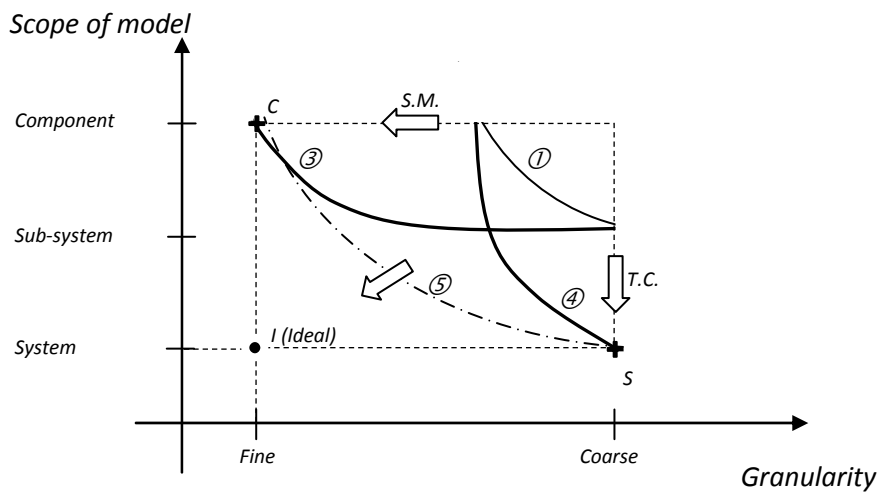


**Figure 4.2.** *The multi-level approach enables the limits to be pushed back*

Both of these approaches are detailed and applied to components and systems that are representative of electrical engineering design in the following sections.

### 4.3. Optimization using models with different granularities

The finite elements (FE) method is used to model electro-technical devices with a high level of precision. Two (2D) or three-dimensional (3D) FE models are often considered to be "virtual prototypes". However, multi-physical couplings and the high number of unknowns in 3D FE models demand a significant calculation time.

In electro-technical device design, some discrete design variables appear naturally in optimization problem formulation. For example, the numbers of notches and magnets are integers and the types of material and structure (for example, external rotor, internal rotor, or axial flow) are discrete. However, discrete optimization relies on different concepts to continuous optimization. The derivatives cannot be directly used for combinatory optimization problems, which prevent the use of high-speed algorithms. Thus, the number of model evaluations during discrete optimizations is much higher than that from optimizations of continuous variables.

The direct use of optimization models with 3D FE models results in excessive calculation times, ranging from several days to a few months. Other problems appear, such as numerical noise and a difficulty in obtaining derivatives precisely, i.e. there is no pertinent research direction available. Substituting the 3D FE model with a simplified model with a much shorter execution time and an easily calculated derivative is therefore an interesting way of reducing optimization time. However, the challenge is that the quality of the final solution should not be inferior to that found using the FE model alone.

Recent developments mean that global optimization with an FE model and its substitution model can be performed in two stages:

– the first stage consists of progressively constructing a response surface for the FE model. New points are added in areas where the substitution model is not precise enough;

– the global optimum is found in the second stage using any algorithm requiring a high number of evaluations, such as, for example, genetic algorithms.

Various methods are used to construct the substitution model: the diffuse element [COS 02], kriging [LEB 04], [KRE 08; BER 10], artificial neuron network [RAS 01; FAN 03; VIE 05], and radial basis functions [KOB 06] methods. The substitution model offers the benefit of high-speed execution, ease of derivation, continuity of operation and of its derivatives.

Other approaches use a low-precision substitution model, which is progressively improved in areas where temporary optima are found [PAH 00]. In the Efficient Global Optimization (EGO) method [JON 98], the substitution model is also refined by the addition of points pertaining to areas of low precision. Unfortunately, all of these methods require a high number of FE model evaluations in order to construct the substitution model. This strongly reduces the benefits of optimization using the substitution model, since the total identification and optimization time is similar to that of direct optimization using the FE model.

In order to significantly reduce the number of FE model loadings, the substitution model needs to initially contain some knowledge. This may take the form of analytical equations describing physical phenomena within a device or equivalent electrical circuit. The substitution model is then said to be the *simple model* and is locally improved by the FE model, which is called the *fine model*. The combined use of these two models is called multi-level optimization and SM techniques are highly effective for resolving them [CHO 09; BAN 04; ECH 06].

In many electro-technical devices, such as engines, transformers, electromagnets, etc., it is possible to make use of an FE model and an equivalent electrical circuit. Consequently, these components are well suited to multi-level optimization using these two types of models.

The component studied in this section is a safety transformer, for which the authors have constructed a 3D FE model, with meshing that is fine enough to obtain precise results for leakage inductance, in particular. The calculation times for fine and simple models are 2 hours and 50 ms, respectively. This problem of optimization and its associated models serves to quantify optimization algorithm performance and, more specifically, the calculation time, which can be expressed in terms of the number of 3D FE

model evaluations, for which the calculation time is not in line with that of the simple model.

In the following sections, the optimization problem and the *fine* and *simple* models are described. The results obtained using a traditional approach and three SM variants are presented in order to emphasize the interest in multi-level approaches for component optimization.

### 4.3.1. *Principle of SM*

The space projection method, proposed by [BAN 94] under the title of the technique for SM, is used in optimization with models that are very costly in terms of calculation time, typically FEs. It has been successfully applied to the area of hyper-frequency [BAN 04]. The method is based on the joint use of two models with differing levels of precision, where the evaluation rapidity of the "simple" model is combined with the precision of the "fine" model by aligning these models at each iteration so as to preserve this precision for the solution. [CHO 01], [ECH 05], and [ENC 07] applied a variant of this approach, known as aggressive SM (ASM), for the sizing of electromagnetic devices modeled using the FEs method (FEM) [BAN 95]. In [ECH 07], the manifold mapping (MM) approach is proposed, which enables certain disadvantages of the SM approach to be avoided and to facilitate the programming of the algorithm (which will be described later).

An optimization problem is formulated using a design variable vector $x_f \in \Re^n$ and targeted objectives $y \in \Re^m$. Modeling precision for electromagnetic devices is generally obtained at the cost of a very long calculation time. The response vector for the fine model is denoted by $f(x_f) \in \Re^m$, for objective functions, and $g_f(x_f) \in \Re^k$ for inequality constraints. The optimization problem is expressed by:

$$\text{find } x_f^* = \arg\min_{x_f} \left\| f(x_f) - y \right\| \text{ where } g_f(x_f^*) \leq 0 \qquad [4.2]$$

A second model, which is less precise, but faster in terms of calculation time, described as a simple model, analytical or even empirical, for example, has the same inputs and outputs. The response vector of the simple model is denoted by $c(x_c) \in \Re^m$ for objective functions, and $g_c(x_c) \in \Re^k$ for

inequality constraints. Thus, an auxiliary optimization problem may be formulated as:

$$\text{find } x_c^* = \arg\min_{x_c} \left\| c(x_c) - y \right\| \text{ where } g_c(x_c^*) \leq 0 \qquad [4.3]$$

The projection function, which is obtained using parameter extraction (PE), $p : \Re^n \mapsto \Re^n$ projects $x_f$ onto $p(x_f) = x_c$. It minimizes the gap between responses from the fine and simple models:

$$\text{Project } \mathrm{x_f} \rightarrow \mathrm{p(x_f)} = \mathrm{x_c} = \arg\min_{\mathrm{x_c}} \left\| \begin{matrix} \mathrm{c(x_c) - f(x_f)} \\ \mathrm{g_c(x_c) - g_f(x_f)} \end{matrix} \right\| \qquad [4.4]$$

The choice of this projection function is the cornerstone of the SM method. Some authors [LEA 01] recommend the use of projection for each of the $m + k$ objective functions and constraints. This function enables an approximation $c(p(x_f))$ of $f(x_f)$ for all $x_f$ to be obtained. The SM method consists of replacing problem [4.2] by problem [4.5], which is less expensive in terms of calculation time. Thus, the solution to the optimization problem is determined through the use of this approximation, as follows:

$$\text{find } x_f^* = \arg\min_{x_f} \left\| c(p(x_f)) - y \right\| \text{ where } g_c(p(x_f^*)) \leq 0 \qquad [4.5]$$

The extraction of parameters [4.4] is often obtained by using the least squares formulation. If, furthermore, $p$ is bijective then reverse transformation provides a fine solution $x_f^*$ from $x_c^*$:

$$x_f^* = p^{-1}(x_c^*) \qquad [4.6]$$

Figure 4.3 illustrates the concept of SM. Parameter extraction is the weak point of this conventional approach. In practice it is not advisable to use many points to construct $p$ because of the significant calculation time generated by this approach. The function $p$ is generally smaller and constitutes a local approximation, which is iteratively refined.

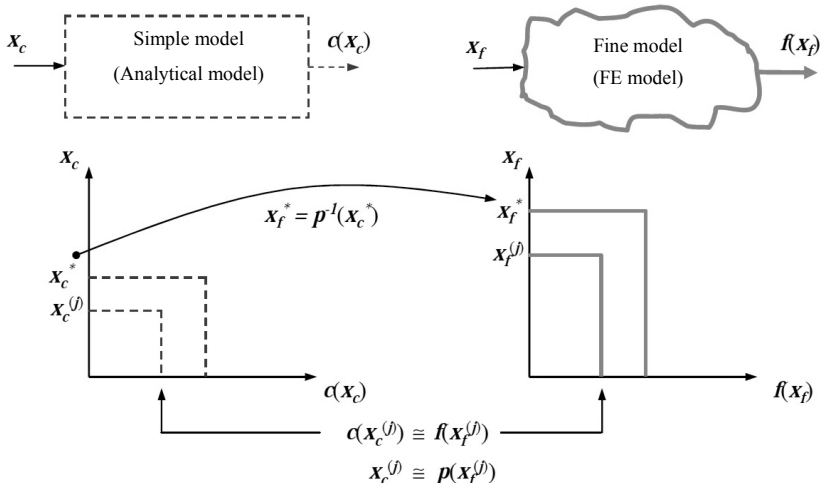


**Figure 4.3.** *General concept of the SM technique*

### 4.3.2. *Mathematical example*

In order to further clarify the SM technique, we illustrate the example of a third-order analytical function, for which the simple model is a parabolic function:

$$f(x_f) = x_f^3 - x_f^2 - x_f + 2 \qquad [4.7]$$

$$c(x_c) = x_c^2 - 4x_c + 2 \qquad [4.8]$$

To minimize the objective function, the targeted objective is equal to zero for a positive function, i.e. $y = 0$. The optimal solution within the range $[0;4]$ is:

$$x_f^* = 1 \quad \text{and} \quad f(x_f^*) = 1 \qquad [4.9]$$

The algorithm begins by solving problem [4.3], to find $x_c^* = 2$ and $c(x_c^*) = -2$ (left hand side of Figure 4.4). Around this temporary solution, some points are selected, for example [$x_{f1} = x_c^* - \Delta x$, $x_{f2} = x_c^*$, $x_{f3} = x_c^* + \Delta x$], where $\Delta x = 0.1$, and the fine model is evaluated in order to provide [$f(x_{f1})$, $f(x_{f2})$, $f(x_{f3})$].

Parameter extraction is performed at these points in order to provide $[\, x_{c1} = p(x_{f1}) \,,\, x_{c2} = p(x_{f2}) \,,\, x_{c3} = p(x_{f3}) \,]$ through the resolution of optimization problems [4.4]. There are as many problems to be solved as there are points, but they are quick to solve using the simple model. For these problems, the variable to find is $x_c$ and $f(x_f)$ is a constant.

It is then possible to obtain the projection function using interpolation (right-hand side of Figure 4.4, $c(p_1(x_f))$) and then to find the solution to [4.5], i.e. $\min c(p(x_f))$, which is the new temporary solution. Its convergence towards the optimal solution can be seen in on the right-hand side of Figure 4.5.

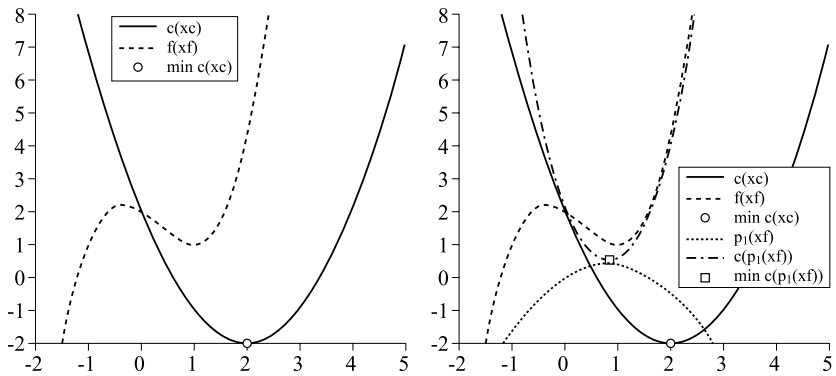


**Figure 4.4.** *Initialization and first iteration of the SM technique*

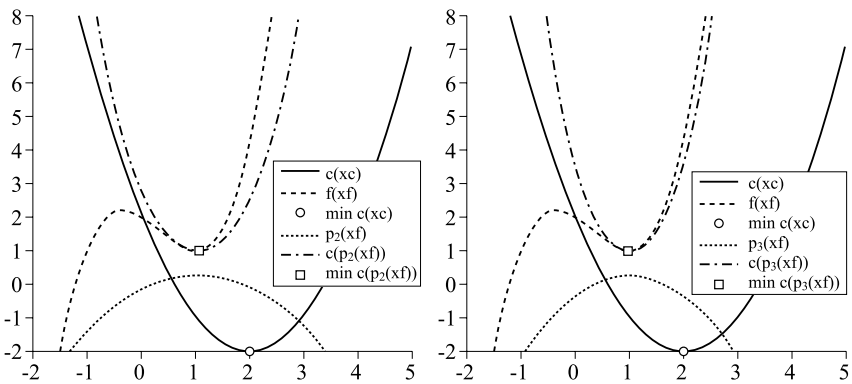


**Figure 4.5.** *Second and third iterations of the SM technique*

The number of points required for construction of function $p$ increases rapidly with the number of optimization variables; for example, $2n+1$ points are required at each iteration in order to obtain a second-order function. Furthermore, parameter extraction is time-consuming and has no unique solution, which may create convergence problems. Thus, improvements to the basic technique are proposed in other works, such as ASM [BAN 95], output SM [TRA 09], and MM [ECH 07].

### 4.3.3. *SM variants*

There are several variants of the SM technique. In this section, we classify them, according to the way in which the optimization problem [4.2] is transformed.

*ASM*

Typically, optimization problem [4.2] is replaced by [4.5], where function $p$ is a projection of inputs from the fine model input space onto the input space of the simple model. Within this class, we then rank the techniques according to the projection function $p$ and the method used to construct it.

Thus, ASM uses a first-order projection function constructed with the first derivative approximation obtained by using a rank-1 Broyden formula [BRO 65].

The desired projection function must project the optimal solution in the input space of the fine model $x_f^*$ onto the optimal solution in the input space of the simple model $x_c^*$, which involves determining a residual root, defined by:

$$r(x_f) = p(x_f) - x_c^* \qquad [4.10]$$

The residual first-order Taylor development is:

$$r(x_f) \approx r(x_f^i) + J_p(x_f^i) \cdot (x_f - x_f^i) \qquad [4.11]$$

where $J_p = \partial p / \partial x_f$ is the Jacobian matrix of the projection function and the residue, since their difference is constant and $x_f^i$ is the approximate solution

at the $i$ th iteration. We are looking for a solution $x_f^{i+1}$ such that the residue is null, i.e.:

$$r(x_f^{i+1}) = 0 \qquad [4.12]$$

$$r(x_f^i) + J_p(x_f^i) \cdot (x_f^{i+1} - x_f^i) \approx 0 \qquad [4.13]$$

The new approximate solution is:

$$x_f^{i+1} = x_f^i - J_p^{-1}(x_f^i) \cdot r(x_f^i) \qquad [4.14]$$

where $.^{-1}$ denotes the inverse matrix. Since it is difficult to know the precise value for matrix $J_p$, it is constructed progressively using the solutions above and by using the rank-1 Broyden formula [BRO 65]:

$$B^{i+1} = B^i + \frac{r(x_f^{i+1}) - r(x_f^i) - B^i \cdot (x_f^{i+1} - x_f^i)}{(x_f^{i+1} - x_f^i)^t \cdot (x_f^{i+1} - x_f^i)} \cdot (x_f^{i+1} - x_f^i)^t \qquad [4.15]$$

where $.^t$ denotes the transpose. If $B^i$ is an approximation for $J_p(x_f^i)$, then equation [4.14] enables [4.15] to be simplified by:

$$B^{i+1} = B^i + \frac{r(x_f^{i+1})}{(x_f^{i+1} - x_f^i)^t \cdot (x_f^{i+1} - x_f^i)} \cdot (x_f^{i+1} - x_f^i)^t \qquad [4.16]$$

where $B^0 = I$.

The weakness of this class of SM techniques is in the extraction of parameters. Indeed, the solution obtained from [4.4] is not necessarily unique and a condition is added to the derivative in order to increase the uniqueness probability of the solution.

In the SM technique, the projection function is such that $f(x_f) = c(p(x_f)) = (c \circ p)(x_f)$ and $g_f(x_f) = g_c(p(x_f)) = (g_c \circ p)(x_f)$, which enables the derivatives of the fine model to be expressed:

$$\frac{\partial f}{\partial x_f} = \frac{\partial c}{\partial p(x_f)} \frac{\partial p}{\partial x_f} = \frac{\partial c}{\partial x_c} \frac{\partial p}{\partial x_f} \qquad [4.17]$$

$$\frac{\partial g_f}{\partial x_f} = \frac{\partial g_c}{\partial p(x_f)} \frac{\partial p}{\partial x_f} = \frac{\partial g_c}{\partial x_c} \frac{\partial p}{\partial x_f} \qquad [4.18]$$

which in matrix form is written:

$$J_f = J_c \cdot J_p \approx J_c \cdot B \qquad [4.19]$$

$$J_{g_f} = J_{g_c} \cdot J_p \approx J_{g_c} \cdot B \qquad [4.20]$$

where $J_f$, $J_c$, $J_{g_f}$ and $J_{g_c}$ are Jacobian matrices of the objective functions and constraints of the fine and simple models. This enables an equality constraint to be added to the first-order derivatives and so parameter extraction [4.4] becomes:

$$p(x_f) = \arg\min_{x_c} \left\| \begin{matrix} c(x_c) - f(x_f) \\ g_c(x_c) - g_f(x_f) \end{matrix} \right\| + \left\| [\lambda \quad \beta] \cdot \begin{bmatrix} J_f(x_f) - J_c(x_c) \cdot B \\ J_{g_f}(x_f) - J_{g_c}(x_c) \cdot B \end{bmatrix} \right\| \qquad [4.21]$$

where $\lambda$ and $\beta$ are weighting factors.

Each iteration of the algorithm then requires the gradient of the fine and simple models to be calculated, which then becomes more costly in terms of calculation time, but this appreciably improves convergence. In practice, this ASM variant is rarely used due to its cost.

*Output SM*

For this second class of SM techniques, the principle is to correct the simple model using instant evaluations of the fine model [TRA 09]. The aim of projection functions is then to match the outputs from the simple model with those from the fine model. The inputs from the fine and simple models are identical, i.e. $x_f = x_c = x$.

Problem [4.2] is replaced by the equivalent problem:

$$\text{find } x^* = \arg\min_x \left\| p_c(c(x)) - y \right\| \text{ where } p_g(g_c(x)) \leq 0 \qquad [4.22]$$

where $p_c$ and $p_g$ are projection functions for the objectives and constraints and are defined by:

$$\begin{aligned} p_c &: \quad c(x) \rightarrow p_c(c(x)) = f(x) \\ p_g &: \quad g_c(x) \rightarrow p_g(g_c(x)) = g_f(x) \end{aligned} \qquad [4.23]$$

In practice, such functions are difficult to find and are replaced by simpler functions, which are valid locally. Thus, a proportional correction is proposed in [TRA 09] with functions:

$$\begin{aligned} p_c &: \quad c(x) \rightarrow p_c(c(x)) = diag(\theta) \cdot c(x) \\ p_g &: \quad g_c(x) \rightarrow p_g(g_c(x)) = diag(\theta_g) \cdot g_c(x) \end{aligned} \qquad [4.24]$$

where $diag(.)$ denotes diagonal matrix vector transformation and:

$$\begin{aligned} \theta_{i=1\cdots m} &= f_i(x) / c_i(x) \\ \theta_{g,i=1\cdots k} &= g_{f,i}(x) / g_{c,i}(x) \end{aligned} \qquad [4.25]$$

The algorithm is iterative and is completed when:

$$\left\| \begin{matrix} p_c(c(x)) - f(x) \\ p_g(g_c(x)) - g_f(x) \end{matrix} \right\| < \varepsilon \qquad [4.26]$$

where $\varepsilon$ denotes the desired precision level.

It is important to clarify that this method provides satisfactory results when the optimization problem is highly constrained. Corrections are not performed on the constrained functions, but on the outputs of the model, which avoids the issue of corrections having no effect if the constraint is active, i.e. $g_c(x) = 0$. Another solution would be to replace multiplication with addition in order to carry out the correction, or even to use a linear correction function.

*MM*

A third, more recent, class of SM techniques does not involve projection onto the input or output spaces of simple models, but uses defect correction functions that modify the target values, i.e. $y$ [ECH 07]. These correction functions $S$ and $S_g$ are applied to objectives and constraints, respectively, so that the outputs from simple corrected and fine models are equal at the optimal point:

$$S(c(x^*)) = f(x^*) \quad \text{and} \quad S_g(g_c(x^*)) = g_f(x^*) \qquad [4.27]$$

as for their first derivatives:

$$\begin{aligned} J_S(c(x^*)) \cdot J_c(x^*) &= J_f(x^*) \\ J_{S_g}(x^*) \cdot J_{g_c}(x^*) &= J_{g_f}(x^*) \end{aligned} \qquad [4.28]$$

where $J_S$ and $J_{S_g}$ denote the Jacobian matrices of projection functions $S$ and $S_g$, respectively.

Figure 4.6 illustrates the correction made using the MM technique.

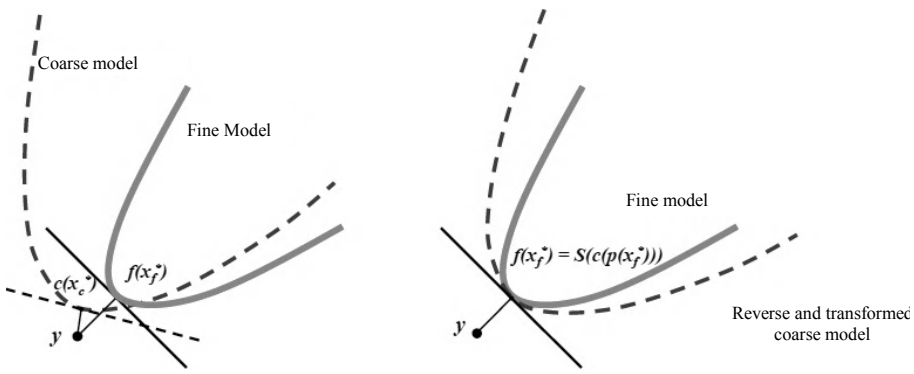


**Figure 4.6.** *Alignment of simple and fine models using MM [ECH 07]*

Problem [4.2] is replaced by the following problem:

$$\text{find } x^* = \arg\min_x \left\| S(c(x)) - y \right\| \text{ where } S_g(g_c(x)) \leq 0 \qquad [4.29]$$

This problem is equivalent to:

$$\text{find } x^* = \arg\min_x \left\| c(x) - S^{-1}(y) \right\| \text{ where } g_c(x) \leq S_g^{-1}(0) \qquad [4.30]$$

The correction functions are chosen affine. Thus, for values $v \in \Re^m$, $v_g \in \Re^k$, $z \in \Re^m$ and $z_g \in \Re^k$, we have the following:

$$\begin{aligned} v &= S(z) = S(c(x^*)) + J_S(z - c(x^*)) \\ v_g &= S_g(z_g) = S_g(g_c(x^*)) + J_{S_g}(z_g - g_c(x^*)) \end{aligned} \qquad [4.31]$$

Relationships [4.27] enable [4.30] to be simplified:

$$\begin{aligned} v &= S(z) = f(x^*) + J_S(z - c(x^*)) \\ v_g &= S_g(z_g) = g_f(x^*) + J_{S_g}(z_g - g_c(x^*)) \end{aligned} \qquad [4.32]$$

By multiplying the relationships above by the Jacobian pseudo inverse, denoted $.^+$, we obtain:

$$\begin{aligned} z &= c(x^*) + J_S^+ \cdot (v - f(x^*)) = S^{-1}(v) \\ z_g &= g_c(x^*) + J_{S_g}^+ \cdot (v_g - g_f(x^*)) = S_g^{-1}(v_g) \end{aligned} \qquad [4.33]$$

For specific values $v = y$ and $v_g = 0$, from [4.30], then:

$$\begin{aligned} S^{-1}(y) &= c(x^*) + J_S^+ \cdot (y - f(x^*)) \\ S_g^{-1}(0) &= g_c(x^*) - J_{S_g}^+ \cdot g_f(x^*) \end{aligned} \qquad [4.34]$$

In practice, $x^*$ is unknown and is replaced by a series $x_i$, which converges asymptotically towards $x^*$, where $x_0 = x_c^*$. Similarly, $J_S$ and

$J_{S_g}$ are initialized with $J_{S,0} = I^m$ and $J_{S_g,0} = I^k$, then replaced by $J_{S,i}$ and $J_{S_g,i}$, which are calculated by:

$$\begin{aligned}
&\Delta C_i = \left[ c(x_{i-1}) - c(x_i), \ldots, c(x_{i-\min(i,n)}) - c(x_i) \right] \\
&\Delta F_i = \left[ f(x_{i-1}) - f(x_0), \ldots, f(x_{i-\min(i,n)}) - f(x_i) \right] \\
&J_{S,i} = \Delta F_i \cdot \Delta C_i^+ \\
&\Delta G_{c,i} = \left[ g_c(x_{i-1}) - g_c(x_i), \ldots, g_c(x_{i-\min(i,n)}) - g_c(x_i) \right] \\
&\Delta G_{f,i} = \left[ g_f(x_{i-1}) - g_f(x_0), \ldots, g_f(x_{i-\min(i,n)}) - g_f(x_i) \right] \\
&J_{S_g,i} = \Delta G_{f,i} \cdot \Delta G_{c,i}^+
\end{aligned} \qquad [4.35]$$

We note that the MM technique is comparable to the output SM technique if it is left in the form of [4.29]. In these cases, the following expressions are used to represent projection functions:

$$\begin{aligned}
&S(c(x)) = S(c(x^*)) + J_S(c(x) - c(x^*)) \\
&S_g(g_c(x)) = S_g(g_c(x^*)) + J_{S_g}(g_c(x) - g_c(x^*))
\end{aligned} \qquad [4.36]$$

Relationships [4.27] enable [4.36] to be simplified:

$$\begin{aligned}
&S(c(x)) = f(x^*) + J_S(c(x) - c(x^*)) \\
&S_g(g_c(x)) = g_f(x^*) + J_{S_g}(g_c(x) - g_c(x^*))
\end{aligned} \qquad [4.37]$$

Formulation [4.29] is less popular, since it requires a simple model correction, while formulation [4.30] is concerned with target correction, which is easier to program.

### 4.3.4. *Safety transformer application*

Control and safety transformers are widely used in industry and the tertiary sector. Their function is to enable the galvanic isolation transformation of an alternating voltage of 230 V, linked to the primary circuit, into alternating voltage of 24 V at the secondary circuit.

The safety transformer is comprised of grain oriented E-I laminations. Primary and secondary coils are wound around the material surrounding the central core (see Figure 4.7).

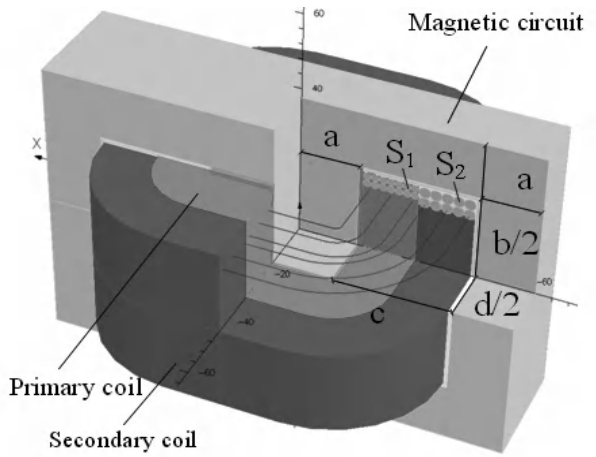


**Figure 4.7.** *Geometry of a safety transformer*

*Optimization problem*

The optimization problem comprises seven design variables, which can be seen in Figure 4.7. Three of these define the geometry of the lamination ($a$, $b$ and $c$), the other variables are the thickness of the laminated pack ($d$), the cross-sections of the primary ($S_1$) and secondary ($S_2$) conductors and the number of primary turns ($n_1$). Even if some of the variables are integers by nature, such as the number of turns, they are treated as continuous variables.

There are seven nonlinear constraints. The copper $T_{cu}$ and iron $T_{fe}$ temperatures should be below 120°C and 100°C, respectively. The efficiency $\eta$ should be greater than 80%. The magnetic current $I_\mu / I_1$ and the voltage drop $\Delta V_2 / V_2$ should be less than 10%. Finally, the filling factor for the two coils $f_1$ and $f_2$ are no more than 0.5 for the round wire.

The aim is to minimize the mass of the iron and copper. Thus the problem is expressed by:

$$\begin{array}{ll} \min & M_{tot} \\ \text{with} & \begin{array}{ll} 3\,\text{mm} \le a \le 30\,\text{mm} & 0.15\,\text{mm}^2 \le S_1 \le 19\,\text{mm}^2 \\ 14\,\text{mm} \le b \le 95\,\text{mm} & 0.15\,\text{mm}^2 \le S_2 \le 19\,\text{mm}^2 \\ 6\,\text{mm} \le c \le 40\,\text{mm} & 200 \le n_1 \le 1200 \\ 10\,\text{mm} \le d \le 80\,\text{mm} & \end{array} \\ \text{subject to} & \begin{array}{ll} T_{cu} \le 120°C & \\ T_{fe} \le 100°C & \eta \ge 0.8 \\ f_1 \le 0.5 & I_\mu / I_1 \le 0.1 \\ f_2 \le 0.5 & \Delta V_2 / V_2 \le 0.1 \end{array} \end{array} \qquad [4.38]$$

*Models*

Thermal, electrical, and magnetic phenomena are modeled using a 3D FE model with saturation of ⅛ of the transformer, due to symmetries. No-load and loaded simulations are used to calculate all of the characteristics.

For electromagnetic modeling, the hypotheses are:

– all quantities are sinusoidal;

– iron losses are estimated using Steinmetz's formula [TRA 09];

– inductances are calculated using magnetic co-energy.

For thermal modeling, it is assumed that:

– transfers between the central core and the coils are uniquely conductive;

– there is no transfer between the secondary (external) coil and the magnetic circuit;

– apart from the central core, there is no heat transfer between the primary coil and the magnetic circuit;

– contact between the two coils is perfect;

– all surfaces have the same convection coefficient.

The magneto-thermal weak-coupling shown in Figure 4.8 requires around 2 hours to be achieved. Iron and Joule losses are calculated using the electromagnetic model at full-load, then uniformly distributed to the nodes of the thermal model, which then provides an averaged temperature distribution and which is used to update the resistances from the electromagnetic model. This loop is interrupted as soon as the variation in the copper temperature is low, typically 0.1°C. The electromagnetic model is used to calculate the voltage drop and the magnetizing current.

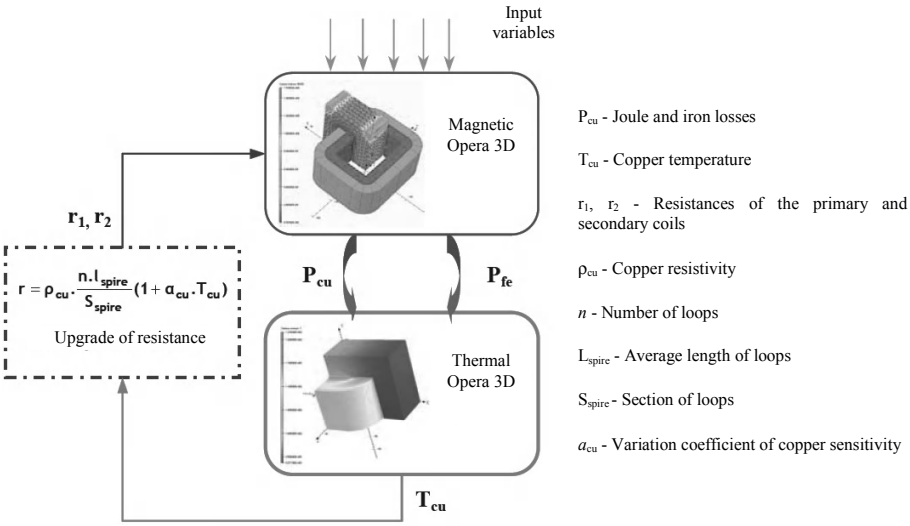


**Figure 4.8.** *Low 3D FE magneto-thermal coupling*

For simple models, the electromagnetic modeling hypotheses are:

– uniform magnetic flex density distribution in the iron;

– use of Boucherot's formula in order to calculate the maximum magnetic flux density;

– Kapp hypothesis, which results in the voltage drop created by the magnetizing current being ignored.

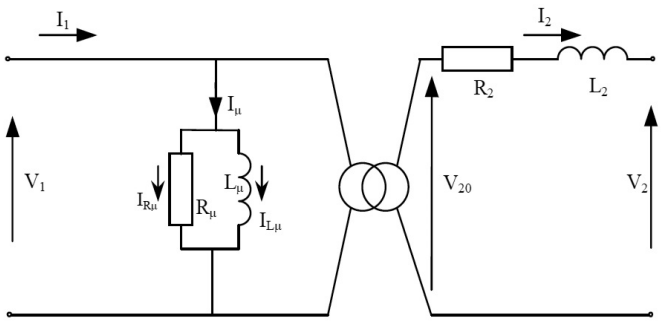


**Figure 4.9.** *Kapp transformer model*

The thermal hypotheses are the same as in 3D FE, with the exception of temperature, which is assumed to be uniform in the coils of the magnetic circuit.

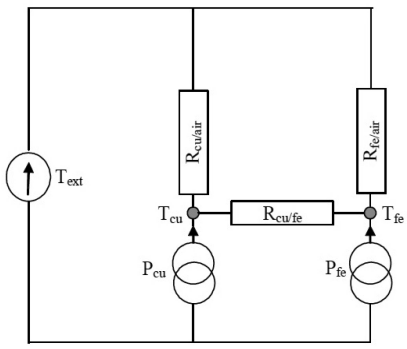


**Figure 4.10.** *Thermal transformer nodal model*

The electromagnetic and thermal models are aggregated and the system of equations, which thus creates a strong coupling, is thus solved in around 50 ms.

*Results*

The SM variants (ASM, output SM, and MM) are applied to the optimization of this transformer [TRA 09; TRA 07]. The results of optimization problem [4.38] are shown in Table 4.1.

| Parameters | Unit | SQP | | Single Level Opt. | Multi-level Optimization | | |
|---|---|---|---|---|---|---|---|
| | | Analyti. | 3D FE | SQP | ASM | MM | OSM |
| $a$ | (mm) | 12.92 | | 14.94 | 12.99 | 12.98 | 12.98 |
| $b$ | (mm) | 50.12 | | 48.43 | 51.32 | 50.35 | 50.37 |
| $c$ | (mm) | 16.61 | | 15.64 | 16.71 | 16.57 | 16.55 |
| $d$ | (mm) | 43.26 | | 38.27 | 44.26 | 42.81 | 42.71 |
| $S_1$ | ($mm^2$) | 0.325 | | 0.310 | 0.3302 | 0.3304 | 0.3080 |
| $S_2$ | ($mm^2$) | 2.912 | | 2.787 | 2.962 | 2.969 | 2.976 |
| $n_1$ | (-) | 640.77 | | 611.78 | 645.67 | 631.48 | 629.89 |
| $M_{tot}$ | (kg) | 2.311 | | 2.294 | 2.410 | 2.306 | 2.301 |
| 3D FE evaluations | (-) | 108 | 1 | 44 | 2 | 3 | 6 |
| $T_{cu}$ | °C | 108.82 | 121.72 | 120.65 | 118.17 | 119.26 | 119.05 |
| $T_{fe}$ | °C | 100.00 | 101.60 | 100.44 | 98.97 | 100.09 | 100.00 |
| $\eta$ | % | 89.55 | 89.15 | 89.24 | 89.30 | 89.42 | 89.45 |
| $I_\mu/I_1$ | % | 10.00 | 8.59 | 10.09 | 7.23 | 9.75 | 10.00 |
| $\Delta V_2/V_2$ | % | 6.91 | 7.94 | 7.60 | 7.79 | 7.58 | 7.52 |
| $f_1$ | % | 50.00 | 50.00 | 50.06 | 49.73 | 50.00 | 50.00 |
| $f_2$ | % | 50.00 | 50.00 | 50.09 | 49.77 | 50.00 | 50.00 |
| Maximum constraint | % | 100.00 | 101.62 | 100.90 | 99.54 | 100.09 | 100.00 |

**Table 4.1.** *Comparison of results from multi-level optimization*

In order to highlight the interest in SM, a first single-level optimization, which uses the simple model and the sequential quadratic programming (SQP) method, is performed and results in a solution after 108 evaluations of the simple model. The 3D FE model is then evaluated at the optimal point found. It appears that some constraints are not satisfied and this point should, strictly speaking, be eliminated.

A second single-level optimization is then performed using the FE model and the SQP method, with the same initial conditions. A solution is obtained after 44 evaluations, or 6 days of calculation time. This solution is better than the one above, but the convergence is not perfect and some constraints are slightly violated.

Three SM algorithms are then tested. ASM, MM and OSM reduce the maximum constraint to 99.54%, 100.09%, and 100.00%, respectively, after two, three, and six calls of the FE model. However, the total mass attained using ASM is not of interest, whereas OSM and MM perform well. The projection function used here for ASM does not impose derivative equality [4.21].

## 4.4. Hierarchical decomposition of an optimization problem

When a device is particularly complex, decomposition is traditionally used to address its design. Thus, by decomposing the problem and spreading the work, the global problem becomes approachable. For example, in the motor industry, businesses use this approach to design cars: specialists work on motorization, others on the chassis, others on the onboard network, and so on. Each sub-problem is easier to solve, but requires the demands of each component relative to the overall system to be defined. Thus, a custom list of specifications for each component must be written.

Multiple strategies can be used to decompose a device, whether based on product functionality, the constituent components, or even disciplines or tasks required for its design (such as electrical or mechanical). This decomposition impacts on the design method for the product.

Often, the very organization of the business is linked to the decomposition of the product to be designed. For businesses, this decomposition is performed specifically on factories, services, and teams, and drives the internal organizational personnel structure. Furthermore, in order to enable synchronization and transfers to take place, cross-department roles exist, for example that of project manager.

Decomposition forces interaction management between the elements that form the complex system. This is the main disadvantage of decomposition, knowing that each element is rarely completely independent of the others. The proposed approach consists of managing these interactions within an optimization strategy.

### 4.4.1. *Target cascading for optimal design*

Traditionally, the problem of complex system design has been decomposed into multiple sub-problems in order to elucidate and solve it.

These sub-problems are assigned to design teams who look to provide optimal solutions independent of others. Systems engineers need to coordinate these teams so that their combined efforts will enable a functional, and if possible, optimal solution to be reached for the system. This approach is currently used within industry. From this organization, and in the context of optimal systemic design, two approaches are possible.

The first approach consists of re-using models from each sub-problem and assembling them in order to solve the overall formulated problem using a single optimization method. However, this approach requires information and models to be concentrated and forces a single optimization process. A system engineer may be in charge of this task, but the multiplicity of sub-systems and their decomposition makes this work very complex, generating a combinatorial explosion of the test space.

The second approach consists of maintaining the hierarchical decomposition and constructing an optimization strategy to manage the decomposition. The general optimization problem is, itself, decomposed into multiple sub-problems which need to be synchronized. Each sub-system will be able to be effectively optimized using a suitable algorithm. Thus, the optimization problem leads to improvements in business structure and knowledge.

The first approach in which the optimization problem is unique requires reformulation of the design problem. Figure 4.11a presents a traditional optimization process with a single model and a single optimization algorithm. This approach requires long model construction and design formulation times.

The second approach in which the optimization problem is decomposed appears to be well suited to complex systems, since it enables reliance on experts for each sub-problem. Figure 4.11b presents a hierarchically decomposed optimization process. A model exists at each level, with an optimization process being linked to each model. The processes are shared in order to be synchronized by being assigned to the objectives and constraints, in order to guarantee overall consistency.

Multiple methods can be used to solve a decomposed optimization problem, but only the target cascading (TC) method will be presented in this chapter [ALL 04]. The TC approach is a multi-level formulation for optimization processes' coordination [KIM 03a]. This approach is used in

applications such as aeronautical [ALL 06] and automobile [KIM 03b] design. In order for the approach to be effective, the problem must be decomposed beforehand.

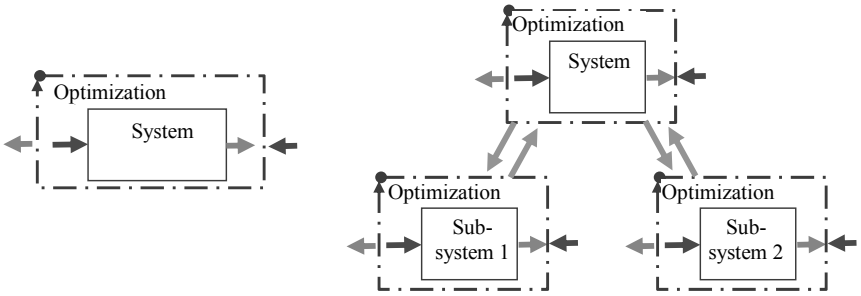


*a) Initial overall system* *b) System decomposed using TC*

**Figure 4.11.** *Hierarchical decomposition*

### 4.4.2. *Formulation of the TC method*

The overall problem is decomposed into a hierarchical sequence of optimization problems. The TC method solves the general optimization problem by setting objectives for the optimization sub-process and thus propagates the responses from the new system towards the sub-systems. The method integrates a downward phase for which the system sets the sub-system objectives and an ascending phase where the sub-systems impose constraints on the system. The optimization process seeks to fill the gap between the propagated objectives and their attained values. The optimization sub-problem tests the optimal values of local design variables and restricts the exchange variables to their target values, given by the lower level. When the general problem has converged, the sub-level targets have become identical.

Figure 4.12 presents an optimization problem decomposed into three levels: system, sub-system, and component. Each optimization sub-problem has its own local design variables and local constraints. An optimization sub-problem is linked to others through the objectives and constraints transmitted: $R_{ss}^{U}$, $R_{ss}^{L}$, $Y_{ss}^{U}$, and $Y_{ss}^{L}$. Any communication between sub-problems occurs through this intermediary. There is no direct link between two sub-problems from the same level. Sub-problems from the same level can communicate from link variables $Y_{ss}$ by passing through one

or more upper levels. Each sub-problem is independent but linked to the others by these exchanges. This formulation enables optimization sub-problems to be managed to attain general optimization of the studied system. Decomposition offers the possibility for parallel execution of optimization processes, which enables complex system optimization to be more achievable.

The TC process begins with the system, where a vector of target values is set. The problem of system optimization consists of finding local constrained variables. Once this optimization problem has been completed, the sub-level target values, calculated at the upper level, are then transferred ( $R_{ss}^{U}$ , $Y_{ss}^{U}$ ). The objective of sub-level optimization problems is to reduce the gap between the target values and those attained. The TC process transfers the objectives from level to level, down to the lowest level. Then, the optimization process for the lowest level transfers constraints ( $R_{ss}^{L}$ , $Y_{ss}^{L}$ ) to the next level up. The optimization processes restart and new constraints are set at the next upper level, and so on, up to the highest level, that of the system. An iteration of the TC process is thus achieved: one down and one up. This process continues for as long as a gap exists between ascent and descent variables ( $R_{ss}^{U}$ , $R_{ss}^{L}$ and $Y_{ss}^{U}$ , $Y_{ss}^{L}$ ).

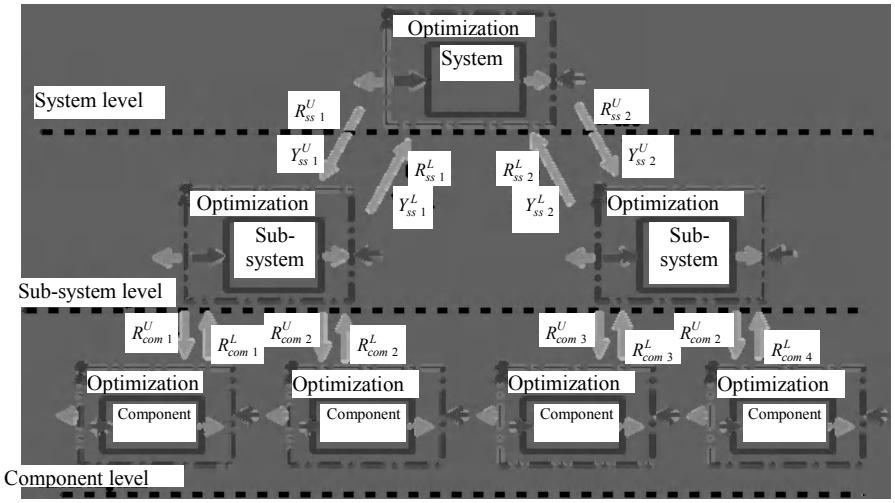


**Figure 4.12.** *Hierarchical decomposition linked to the TC method*

The decomposition of the optimization problem using the TC method can be written in mathematical form for the system [4.39], sub-system [4.40], and component [4.41]. The system and component levels are specific, as they are situated at opposite ends of the decomposition.

4.4.2.1. *System level*

At the system level, the optimization problem minimizes the error between a system-level response and a target value. Furthermore, another objective of the system is to minimize the gap between the desired system-level responses and those attained by sub-systems from the level just below.

$$
\mathrm{O_{sys}}: \quad
\begin{aligned}
&\min_{X_{sys},Y_{sys},R_{ss},\varepsilon_R,\varepsilon_Y} \left\| R_{sys} - T_{sys} \right\|^2 + \varepsilon_R + \varepsilon_Y \\
&\text{where} \quad R_{sys} = f\left(X_{sys}, R_{ss}\right) \\
&\left\| R_{ss} - R_{ss}^L \right\|^2 \le \varepsilon_R \\
&\left\| Y_{ss} - Y_{ss}^L \right\|^2 \le \varepsilon_Y \\
&G(X_{sys}, R_{ss}) \le 0 \\
&H(X_{sys}, R_{ss}) = 0 \\
&Lb_{sys} \le X_{sys} \le Ub_{sys} \\
&Lb_{Rss} \le R_{ss} \le Ub_{Rss}
\end{aligned}
\qquad [4.39]
$$

We see that $R_{sys}$ is based on system variables $X_{sys}$ and the expected sub-system responses $R_{ss}$ from the level just below. $R_{ss}^L$ and $Y_{ss}^L$ are the optimal values found by the lower level, passed to the next upper level. Some constraints are added in order to match the new system to the sub-system level responses $\left\| R_{ss} - R_{ss}^L \right\|^2 \le \varepsilon_R$ so that the general problem can be consistent.

Adding internal variables complicates the optimization problem and thus the bounds of $R_{ss}$ and $Y_{ss}$ have to be defined.

4.4.2.2. *Sub-system level*

Equation [4.40] represents the $j^{\text{th}}$ sub-system. All variables and responses are associated with this sub-system.

$$
\begin{aligned}
&\min_{X_{ss},Y_{ss},Y_{com},R_{com},\varepsilon_R,\varepsilon_Y} \left\|R_{ss}-R_{ss}^{U}\right\|^2+\left\|Y_{ss}-Y_{ss}^{U}\right\|^2+\varepsilon_R+\varepsilon_Y \\
&\text{where} \quad R_{ss}=f\left(X_{ss},Y_{ss},R_{com}\right) \\
&\qquad \left\|R_{com}-R_{com}^{L}\right\|^2 \le \varepsilon_R \\
O_{ss,j}: &\qquad \left\|Y_{com}-Y_{com}^{L}\right\|^2 \le \varepsilon_Y \\
&\qquad G(X_{ss},Y_{ss},R_{com}) \le 0 \\
&\qquad H(X_{ss},Y_{ss},R_{com},)=0 \\
&\qquad Lb_{ss} \le X_{ss} \le Ub_{ss} \\
&\qquad Lb_{com} \le R_{com} \le Ub_{com}
\end{aligned}
\qquad [4.40]
$$

The objective is to minimize the gap between the value given by the upper level $R_{ss}^{U}$, $Y_{ss}^{U}$ and the optimal value for the sub-system. The value for $R_{ss}^{U}$ comes from the system-level value for $R_{ss}$. Constraints are linked to the lower level and are dependent on the sub-system considered.

4.4.2.3. *Component level*

Equation [4.41] represents the optimization problem assigned to the $k^{th}$ component. As above, the upper level imposes its requirements by setting the value for $R_{com}^{U}$. No supplementary constraint is added, since the component level is considered here to be the lowest level.

$$
\begin{aligned}
&\min_{X_{com},Y_{com}} \left\|R_{com}-R_{com}^{U}\right\|^2+\left\|Y_{com}-Y_{com}^{U}\right\|^2 \\
&\text{where} \quad R_{com}=f\left(X_{coms},y_{com}\right) \\
O_{com,k}: &\qquad G(X_{com},R_{com}) \le 0 \\
&\qquad H(X_{com},R_{com})=0 \\
&\qquad Lb_{com} \le X_{com} \le Ub_{com}
\end{aligned}
\qquad [4.41]
$$

### 4.4.3. *Mathematical example*

To illustrate this we present a simple mathematical example. The non-decomposed general problem corresponds to a sum of independent, strictly

positive functions, which are cancelled out for $x_k = \frac{k}{3}$. A constraint is added so that the product of $x_3$ and $x_4$ is less than 1. The bounds for all of the variables are set between 0 and 2. The SQP method is used to resolve this problem and an initial value of 1 is chosen for each variable [VEN 02].

$$\text{O}_g: \quad \begin{aligned} & \min_{x_1,x_2,x_3,x_4,x_5,x_6} \left(R(X)-0\right)^2 \\ & R(X) = \sum_{k=1}^{6}\left(x_k - \frac{k}{3}\right)^2 \cdot \exp\left(x_k - \frac{k}{3}\right) \\ & g(x_3,x_4) = x_3 \cdot x_4 - 1 \le 0 \\ & 0 \le x_k \le 2 \quad k = 1,\ldots,6 \end{aligned} \qquad [4.42]$$

The optimal values for $x_1$, $x_2$, $x_5$, $x_6$, are trivial (1/3, 2/3, 5/3, 6/3). Due to the constraint, a compromise must be found for the values for $x_3$ and $x_4$ (0.816, 1.22).

General equation [4.42] is decomposed into a hierarchical series of optimization problems. The problem is split into three sub-problems. Two levels are created: one for the system and one for the component.

$$\text{O}_{sys}: \quad \begin{aligned} & \min_{x_1,x_2,R_{ss,1},R_{ss,2},\varepsilon_R} \left(R_{sys}-0\right)^2 + \varepsilon_R \\ \text{where} \quad & R_{sys} = f\left(x_1,x_2,R_{ss,1},R_{ss,2}\right) \\ & = \left(x_1 - \frac{1}{3}\right)^2 \cdot \exp\left(x_1 - \frac{1}{3}\right) + \left(x_2 - \frac{2}{3}\right)^2 \cdot \exp\left(x_2 - \frac{2}{3}\right) + R_{ss,1} + R_{ss,2} \\ & \left(R_{ss,1} - R_{ss,1}^L\right)^2 + \left(R_{ss,2} - R_{ss,2}^L\right)^2 \le \varepsilon_R \\ & 0 \le x_1 \le 2 \\ & 0 \le x_2 \le 2 \\ & 0 \le R_{ss,1} \le 2 \\ & 0 \le R_{ss,2} \le 2 \\ & 0 \le \varepsilon_R \le 2 \end{aligned}$$

[4.43]

The system objective is set at 0. The values for $R_{ss,1}$ and $R_{ss,2}$ are cascaded to the lower levels and fixed as target values ( $R_{ss,1} = R_{ss,1}^{U}$ ).

$$\min_{x_3,x_4}\left(R_{ss,1}-R_{ss,1}^{U}\right)^2$$

where $R_{ss,1}=f\left(x_3,x_4\right)$

$O_{ss,1}$: $$= \left(x_3-\frac{3}{3}\right)^2\cdot\exp\left(x_3-\frac{3}{3}\right)+\left(x_4-\frac{4}{3}\right)^2\cdot\exp\left(x_4-\frac{4}{3}\right)$$

$$g(x_3,x_4)=x_3\cdot x_4-1\le 0$$

$$0\le x_3\le 2$$

$$0\le x_4\le 2$$

[4.44]

$$\min_{x_5,x_6}\left(R_{ss,2}-R_{ss,2}^{U}\right)^2$$

where $R_{ss,2}=f\left(x_5,x_6\right)$

$O_{ss,2}$: $$= \left(x_5-\frac{5}{3}\right)^2\cdot\exp\left(x_5-\frac{5}{3}\right)+\left(x_6-\frac{6}{3}\right)^2\cdot\exp\left(x_6-\frac{6}{3}\right)$$

$$0\le x_5\le 2$$

$$0\le x_6\le 2$$

[4.45]

The method converges in four iterations. At each TC iteration, the optimization method is able to re-use variable values already found in order to accelerate the convergence. The variable values for the three optimization problems are:

$[x_1, x_2, R_{ss,1}, R_{ss,2}, \varepsilon_R]$ = [0.33333, 0.66667, 0.038127, 0.00063445, 4.5533e-007]

$[x_3, x_4]$ = [0.8168, 1.2243]

$[x_5, x_6]$ = [1.6328, 2]

The algorithm is stopped when the error between the cascaded variables ($R_{ss,1}^{U}$ $R_{ss,1}^{L}$ and $R_{ss,2}^{U}$ $R_{ss,2}^{L}$) is less than 0.5%. A cumulative weighting is added to the error variable $\varepsilon_R$ in order to facilitate convergence.

### 4.4.4. *Railway traction engine example*

This method has been used for the sizing of two components of a tramway traction engine. A simplified system is used, with the engine component and the converter radiator being chosen for their significant size within the traction system. A new system is added that takes the whole tramway into account. A two-level problem is thus addressed.

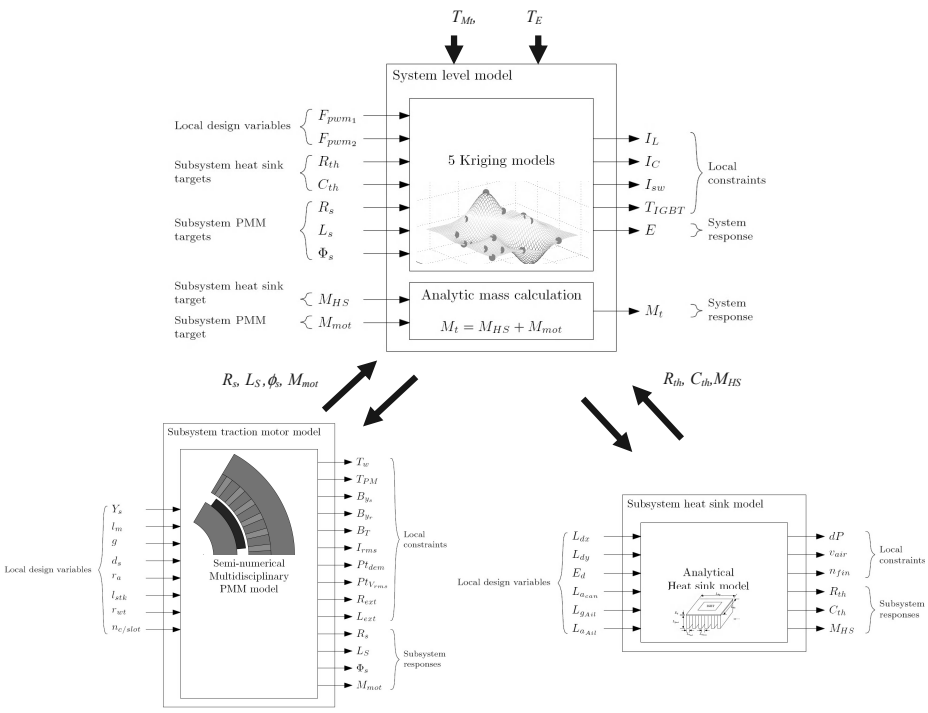


**Figure 4.13.** *Multi-level optimization for a railway traction system*

The component level enables the sizing of the two components from their own constraints and from system objectives. The system level manages the exchange variables that feed the system model. The radiator model

comprises six local dimensional variables, three local constraints, and exchanges three responses with the system level ($R_{th}$, $C_{th}$, $M_{HS}$). The motor model comprises eight local variables for sizing, 10 local constraints, and exchanges four responses with the system level ($R_s$, $L_S$, $\phi_s$, $M_{mot}$). The system model results from response surfaces constructed using business software. The tramway model comprises two dedicated variables resulting from the MLI motor and converter control, three local constraints, and two system responses ($M_t$, $E$). Thus, the total number of system-level variables is 10 (3+4+2+$\varepsilon_R$). Two objectives are set for the new system: total mass and energy ($M_t$, $E$). Figure 4.13 presents the problem in its entirety, an iterative loop enables convergence of this process from the moment that the values passed from the system to the component level become equal to those passed from the component to the system level.

This problem corresponds to the more complex case currently being addressed in our laboratory. More details are available in [KRE 09]. The strategy has also been improved to enable convergence when the objectives are unattainable [MOU 09]. However, a difficulty peculiar to this approach is access to, or availability of, system models and components. A significant part of the work is knowing how to re-use models and to develop missing parts relating to the specific requirements of the application.

The method offers many options for its use in electrical engineering, but especially modifies the vision and articulation between optimization algorithms and models.

## 4.5. Conclusion

The design of electro-mechanical systems is a complex task, which must be accomplished in order to handle new economic and social challenges.

Modeling tools have multiplied in order to help designers better understand device behavior. It is now essential to provide design tools to support designers in these tasks, with the objective of assisting in optimal systems design. Optimal design encompasses the management of the diversity of models and optimization tools, and also of the approach to problem resolution. The objective of optimal design is to aid the design of more effective products, in response to a multitude of imposed constraints that a single designer cannot simultaneously manage in overall terms.

Two multi-level approaches have been presented in this chapter. The first, SM, enables a component to be designed by iteration between fine and simple models of the same device, and aims to obtain an optimal solution with a reduced number of evaluations of the fine model. A large proportion of the evaluations is performed on the simple model. This approach enables optimal design using models that are precise, but costly in terms of calculation time (an example being the 3D FEM). The second approach, TC, enables components of a system to be designed from a hierarchical model decomposition and the creation of multiple optimization processes that exchange objectives and constraints between each other in order to obtain general problem consistency. This approach enables optimal design to be performed for complex systems and constraints.

Both multi-level approaches presented progress optimal design along two complementary directions, the first following the precision of models used and the second following the exhaustiveness of the system description. One point of view would be to combine the two approaches in order to simultaneously benefit from a system description using fine models. Curve ⑤ in Figure 4.2 thus shows a potential progression towards the ideal (point *I*).

These two approaches are, however, typical of a field of research that is suited to the problem of designing equipment or electrical sub-systems before being included in a wider context. Without doubt, we are only in the early stages and there are many ways forward, whether in terms of numbers of components, levels, or systemic optimization in a Pareto sense.

## 4.6. Bibliography

[ALL 04] ALLISON J.T., Complex system optimization: a review of analytical target cascading, collaborative optimization, and other formulations, MSc thesis, University of Michigan, 2004.

[ALL 06] ALLISON J.T., WALSH D., KOKKOLARAS M., PAPALAMBROS P.Y., CARTMELL M. "Analytical target cascading in aircraft design", *Proc of 44th AIAA Aerospace Sciences Meeting and Exhibit*, *AIAA-2006-1325*, Reno, Nevada, January 9-12 2006.

[BAN 94] BANDLER J.W., BIERNACKI R.M., CHEN S.H., GROBELNY P.A., HEMMERS R.H., "Space mapping technique for electromagnetic optimization", *IEEE Transactions on Microwave Theory and Techniques,* vol. 42, pp. 2536-2544, 1994.

[BAN 95] BANDLER J.W., BIERNACKI R.M., CHEN S.H., HEMMERS R.H., MADSEN K., "Electromagnetic optimization exploiting aggressive space mapping", *IEEE Transactions on Microwave Theory and Techniques*, vol. 43, pp. 2874-2882, 1995.

[BAN 04] BANDLER J.W., CHENG Q.S., DAKROURY S.A., MOHAMED A.S., BAKR M.H., MADSEN K., SONDERGAARD J., "Space mapping: the state of the art", *Transactions on Microwave Theory and Techniques*, vol. 52, pp. 337-361, 2004.

[BER 10] BERBECEA A.C., KREUAWAN S., GILLON F., BROCHET P., "A parallel multi-objective efficient global optimization: the finite element method in optimal design and model development", *IEEE Transactions on Magnetics*, vol. 46, pp. 2868-2871, 2010.

[BRO 65] BROYDEN, C.G., "A class of methods for solving nonlinear simultaneous equations", *Mathematics of Computation*, vol. 19, pp. 577-593, 1965.

[CHO 01] CHOI H., KIM D., PARK I., HAHN S., "A new design technique of magnetic systems using space mapping algorithm", *IEEE Transactions on Magnetics*, vol. 37, pp. 3627-3630, 2001.

[COS 02] COSTA C., COULOMB J.L., MARÉCHAL Y., DIETRICH A.B., NABETA S.I., "Diffuse-element method and quadtrees: two ingredients for an adaptive response surface", *IEEE Transactions on Magnetics*, vol. 38, pp. 1085-1088, 2002.

[ECH 05] ECHEVERRIA D., LAHAYE D., ENCIA L., LOMONOVA E. A., HEMKER P. W., "Optimization in electromagnetic with the space-mapping technique", *COMPEL*, vol. 24, pp. 952-966, 2005.

[ECH 06] ECHEVERRIA D., LAHAYE D., ENCICA L., LOMONOVA E.A., HEMKER P.W., VANDENPUT A.J.A., "Manifold-mapping optimization applied to linear actuator design", *IEEE Transactions on Magnetics*, vol. 42, pp. 1183-1186, 2006.

[ECH 07] ECHEVERRIA, D., Multi-level optimization, space mapping and manifold mapping, PhD thesis, University of Amsterdam, 2007.

[ENC 07] ENCICA L., ECHEVERRÍA D., LOMONOVA E., VANDENPUT A.J.A., HEMKER P.W., LAHAYE, D., "E-cient optimal design of electromagnetic actuators using space-mapping", *Structural and Multidisciplinary Optimization*, vol. 33, pp. 481-491, 2007.

[FAN 03] FANNI A., MONTISCI A., "Neural inverse problem approach for optimal design", *IEEE Transactions on Magnetics*, vol. 39, pp. 1305-1308, 2003.

[JON 98] JONES D.R., SCHONLAU M., WELCH W., "Efficient global optimization of expensive black-box functions", *Journal of Global Optimization*, vol. 13, pp. 455-492, 1998.

[KIM 03a] KIM H.M., MICHELENA N.F., PAPALAMBROS P.Y., JIANG T., "Target cascading in optimal system design", *Transactions of ASME: Journal of Mechanical Design*, vol. 125, pp. 481-489, 2003.

[KIM 03b] KIM H.M., RIDEOUT D. G., PAPALAMBROS P.Y., STEIN J.L., "Analytical target cascading in automotive vehicle design", *Transactions of ASME: Journal of Mechanical Design*, vol. 125, pp. 474-480, 2003.

[KOB 03] KOBETSKI A., COULOMB J.L., COSTA M.C., MARÉCHAL Y., JÖNSSON U., "Comparison of radial basis function approximation techniques", *COMPEL*, vol. 22, pp. 616-629, 2003.

[KRE 08] KREUAWAN S., GILLON F., BROCHET P., "Surrogate-assisted multiobjective optimization for optimal design using finite element analysis", *CEFC2008*, Athens, May 11-15, p. 487, 2008.

[KRE 09] KREUAWAN S., MOUSSOUNI F., GILLON F., BRISSET S., BROCHET P., NICOD L., "Optimal design of a traction system using target cascading", *International Journal of applied Electomagnetics and Mechanics*, vol. 30, no. 3-4, pp 163-178, 2009.

[LEA 01] LEARY S.J., BHASKAR A., KEANEA A.J., "Constraint mapping approach to the structural optimization of an expensive model using surrogates", *Optimization and Engineering*, no. 2(4), special issue, pp. 385–398, 2001.

[LEB 04] LEBENSZTAJN L., MARRETTO C.A.R., COSTA M.C., COULOMB J.L., "Kriging: a useful tool for electromagnetic device optimization", *IEEE Transactions on Magnetics*, vol. 40, pp. 1196-1199, 2004.

[MOU 09] MOUSSOUNI F., KREUAWAN S., GILLON F., BRISSET S., BROCHET P., NICOD L., "Multi-level design optimization using target cascading", *COMPLEL*, vol. 28, pp. 1163-1178, 2009.

[PAH 00] PAHNER U., HAMEYER K., "Adaptive coupling of differential evolution and multiquadratics approximation for the tuning of the optimization process", *IEEE Transactions on Magnetics*, vol. 36, pp. 1047-1051, 2000.

[RAS 01] RASHID K., RAMIREZ J.A., FREEMAN E.M., "Optimization of electromagnetic devices using sensitivity information from clustered neuro-fuzzy models", *IEEE Transactions on Magnetics*, vol. 37, pp. 3575-3578, 2001.

[TRA 07] TRAN T.V., BRISSET, S., BROCHET, P., "A benchmark for combinatorial, multi-level and multi-objective optimization of a safety isolating transformer", http://l2ep.univ-lille1.fr/come/benchmark-transformer.htm, 2007.

[TRA 09] TRAN T.V., Problèmes Combinatoires et Modèles Multi-Niveaux pour la Conception Optimale des Machines Électriques, PhD thesis, Ecole Centrale de Lille, 2009.

[VEN 02] VENKATARAMAN P., *Applied Optimization with MATLAB® Programming*, John Wiley & Sons, New York, 2002.

[VIE 05] VIEIRA D.G., VIEIRA D.A.G., CAMINHAS W.M., VASCONCELOS J.A., "A hybrid approach combining genetic algorithm and sensitivity information extracted from a parallel layer percepton", *IEEE Transactions on Magnetics*, vol. 41, pp. 1740-1743, 2005.

Chapter 5

# Multi-criteria Design and Optimization Tools

The objective of this chapter is to show that the system approach and optimization revolution must go hand in hand with a new approach using tools such as component-based software frameworks, which are interoperable and can be capitalized.

The underlying concepts and principles of the production of these frameworks are recalled by focusing on multi-criteria optimization for which we will show the contribution of a framework, such as CADES (Component Architecture for the Design of Engineering Systems) [DEL 07], in order to address constraint optimization problems and to produce dedicated optimization applications and environments.

We will see how various modeling formalisms can be taken into account in a general modeling system, based on automatic calculation code generation. We will also show how to automatically calculate the Jacobian of a model, which is then used to provide complementary information to enable sensitivity analysis and constraint optimization.

---

Chapter written by Benoit DELINCHANT, Laurence ESTRABAUD, Laurent GERBAUD and Frédéric WURTZ.

*Integrated Design by Optimization of Electrical Energy Systems* Edited by Xavier Roboam
© 2012 ISTE Ltd. Published 2012 by ISTE Ltd.

We will discuss how multi-criteria system optimization problems can be effectively addressed using tools that make up the frameworks to solve problems, such as the overall optimization of a structure, evaluation of the potential of a structure, comparison between two structures, and briefly, the sizing and optimization using a system vision.

Aside from tools and methods, we will also present the need to take into account capitalization dimensions and competency and knowledge management; this will lead us to consider possible collaborative web platforms for these tools.

## 5.1. The CADES framework: example of a new tools approach

Mechatronic systems, such as cars, aircraft, or even buildings, are systems created by assembling physical components. Thus, a car will be produced by assembling systems for navigation, injection, braking, and so on, with these systems themselves comprising a set of more basic components (such as power electronics, electro-mechanical actuators, and controls).

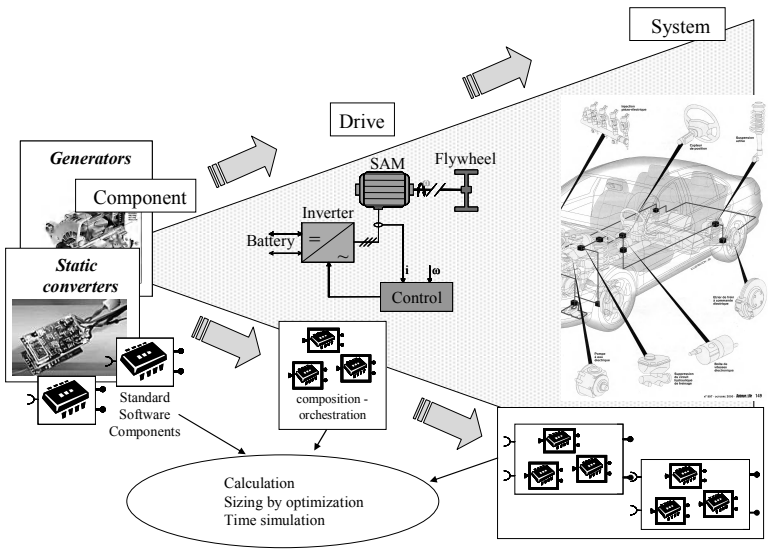


**Figure 5.1.** *Duality between physical and model components for a mechatronic system of a car*

A design framework should allow each physical component to have a model that is specified in terms of standard software components, which offer services necessary for simulation and optimal sizing.

The various participants of the process must be able to exchange or give access to the software component, which models the component or the physical system that they are designing or manufacturing. Thus, a car manufacturer will allow an electrical drive manufacturer access to a car model, who will, in turn, allow the car manufacturer access to its electrical drive model (Figure 5.1).

The software framework principles presented, as well as the resulting CADES implementation, should facilitate this new simulation approach to sizing and analysis of mechatronic systems.

## 5.2. The system approach: a break from standard tools

The systemic approach is founded on a breakdown principle within the context of a major epistemological revolution [WUR 08a], as we explained in the introduction to [ROB 12]. The principle of systemic modeling, "the whole is greater than the sum of its parts", responds to this *breakdown principle*:

*by substituting the reductionist approach:*

– in which the system "is only a simple assembly" of the parts:

- "therefore, if we understand the parts, we can deduce the operation of the system from them";

– this occurs in the context to which we are oriented:

- a single vision and objective for the device,

- an independent vision for the project and designers;

*to move towards the constructivist approach*:

– where the system is greater than the sum of its parts:

- therefore if we understand the parts, this does not imply understanding of the system,

- since there are emerging phenomena at a system level;

– this occurs in a context in which there is no single vision for the device, but points of view in constructing the system based on:

- the project,

- the context,

- the objectives (i.e. system models will not be the same for the control, pre-sizing and detailed analysis of phenomena),

- designers and their competencies.

This revolution should be accompanied by a revolution in software tools design to support:

– passing from the environment concept: i.e. a fixed and closed, non-interoperable tools structure, to the

– framework concept: i.e. an environment that is not fixed, but comprises a set of building blocks based on standards and enabling the building of custom-built interoperable software applications.

The framework will enable competencies to be created, expressed and coordinated, which will become completely operational in the context of collaborative web platforms, which will be developed around software frameworks.

### 5.2.1. *Some component definitions*

Before going any further, we are going to define various types of components:

– *physical component*: physical entity to be simulated, modeled and sized, such as an electrical motor, semi-conductor, etc.;

– *model component*: model of a physical component, such as a reluctance model of an electrical motor;

– *software component*: IT entity, which can be used in various contexts, which supports, for example, the program code for a model component;

– *component*: generic term, which is valid for the three types above if used without any qualification.

### 5.2.2. *From integrated environments to collaborative tool frameworks*

In this context, frameworks constitute a new paradigm for the computer-assisted design (CAD) calculation approach, notably compared with the environmental paradigm, which has, up to now, prevailed in this area. Tools that have now become the norm (such as Flux2D/3D[1] and Matlab/Simulink[2]) are indeed environmental, i.e. consistent software solutions.

A framework is not an environment. It should rather be seen like "Lego", enabling its own application to be formed. It is, therefore, open to receiving and accommodating applications and to make pre-existing environments interoperable. Its openness occurs through the use of standards and the occurrence of software component standards, as we will see later, offering standardized and recognized services.

The focus of frameworks is to make environments interoperable; thus other environments may generate or accommodate software components, provided that associated connection interfaces (ad hoc "plug in" and "plug out", see section 5.1.4) are developed. A framework may thus be distributed, or spread, whereas the focus of an environment is to be executed on a single computer.

Environments will remain incontrovertible, as in numerical simulation, enabling knowledge from approaches such as that of finite elements to be capitalized upon. However, use of single environments would slow down the resolution of multi-physical and multi-level modeling problems. With the "environment" paradigm, the single underlying perspective for the resolution of multi-physical problems was to move towards a single environment, a perspective that was both utopian and perhaps risky. It is a perspective that we now no longer believe, as a result of our work, because of the transverse view that we are using. We are faced with using environments such as CADENCE[3] for micro-electronics, AMESIM[4] in the area of mechatronic systems simulation, Matlab/Simulink in the area of real-time control, Flux2D/3D for electro-technical actuators and motors and Portunus/PSim/Saber/Simplorer for the simulation of power electronics applications, etc.

---

1 CEDRAT, Flux2D/3D: www.cedrat.com/en/software-solutions/flux.html.
2 MATHWORKS: Matlab/Simulink, www.mathworks.com.
3 CADENCE: www.cadence.com.
4 LMS IMAGINE: Amesim: www.lmsintl.com/imagine-amesim-suite.

CADES[5] [DEL 07], which is the framework that we have developed, is the acronym for "Component Architecture for the Design of Engineering Systems", since it effectively refers to a software component-based architecture for carrying out engineering systems design. CADES is not a software environment, but more a framework in which models may have to be created and then used with various heterogeneous tools or environments. In fact, the framework defines standardized processes and connections that enable consistent use of models and associated services, such as optimization.

### 5.2.3. *A centered model canvas: from generation to utilization*

Figure 5.2 gives the structure of this framework, centered around software components, which will be used to analyze or design physical components or systems.

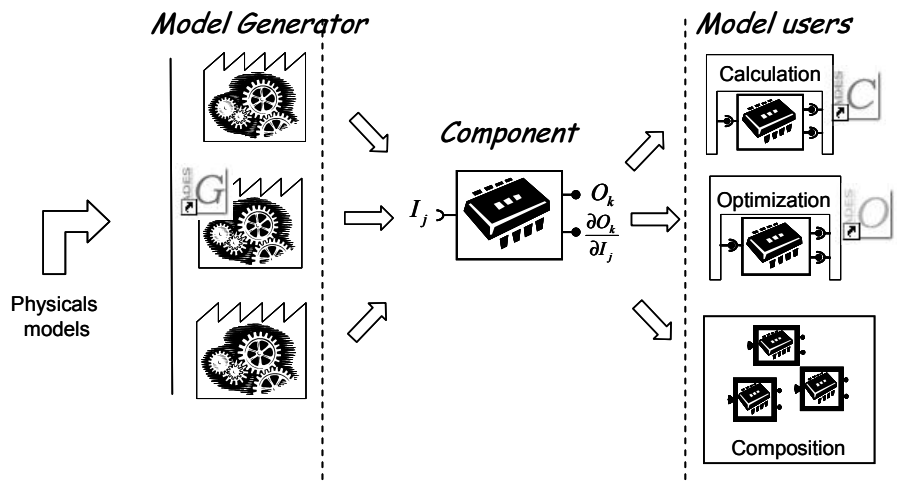


**Figure 5.2.** *CADES: an open framework for system design and analysis*

The aim of this framework is make consistent use of:

– software component *generators*: these enable the designer to describe the physical system models that he needs to design. These models are then automatically analyzed, in particular to calculate their parameter sensitivity

5 CADES: www.cades-solutions.com.

(∂Sj/∂Ei, where Sj denotes the outputs and Ei the inputs of the model) [DUP 06a; PTD 06; RAK 07b; ENC 09a; PHA 11b];

– software *components*, which contain calculable device models as well as complementary data (such as sensitivity) which is dependent on the generator used [DEL 03; FIS 04];

– *users*, who are going to utilize the component models in order to offer useful services in the pre-sizing and feasibility study phases, such as simulation, optimization and tolerance services [MAG 04; FIS 04].

A whole set of existing tools may be relevant to this framework, which is centered on the component (see Figure 5.3) via *plug-in* and *plug-out* concepts. A plug-in within the CADES framework is a programmed extension to the simulation of the concept:

– *plug-in*: program code that enables modeling/simulation functionality to be imported into an existing IT tool (such as a simulator), which specifies the way in which the plug-in works, via its communication interfaces;

– *plug-out*: by analogy, program code that enables modeling/simulation functionality to be exported to other tools (such as a simulator).

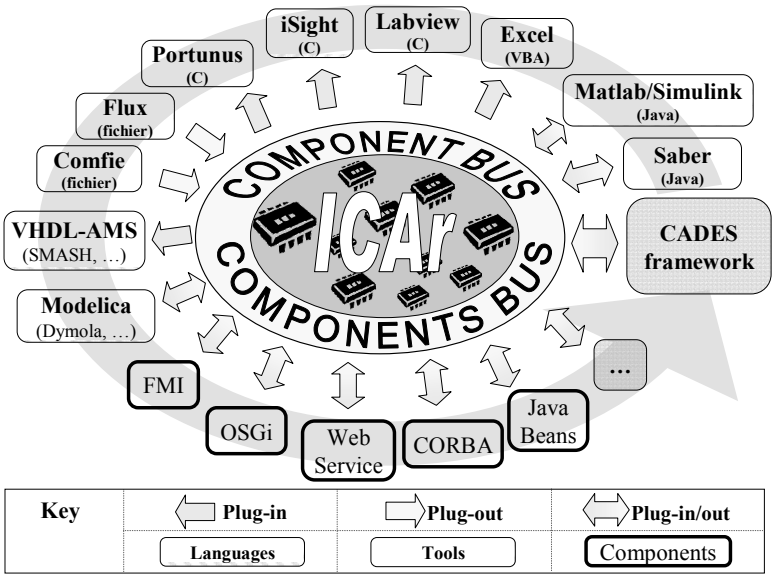


**Figure 5.3.** *ICAr software component bus, ensuring interoperability between model generators and model users*

Therefore, beyond internal CADES framework tools, the advantage of the framework approach is that it enables interoperability with pre-existing modeling and calculation environments.

Figure 5.3 illustrates some existing plug-ins and plug-outs, which enable importing and exporting between models and tools via software components.

#### 5.2.3.1. *Plug-out examples*

Two types of plug-outs may be produced depending on the possibilities offered by modeling software. The first enables the whole calculation capacity of the model to be exported to the component, making it completely autonomous as regards the generation tool. This encapsulation solution is preferred as it actually corresponds to the philosophy of the component approach, but it is not always possible, in which case an alternative is to drive the modeling/simulation tool via the component. A dependency between the component mode and the modeling tool is then preserved in this drive solution.

The following two tables provide a list of applications based on these two approaches.

| **Software** | **Application** |
|---|---|
| P-Spice | Circuit model [DUR 10] |
| Modelica | System simulation [GAA 11] |
| Comfie | Thermal building envelope [GAA 11] |

**Table 5.1.** *Examples of plug-outs using the encapsulation approach*

| **Software** | **Application** |
|---|---|
| Flux 2D | System simulation [REZ 11] |
| Flux 2D | Electromagnetic device optimization [DEL 02] |
| Saber | Power electronics simulation and optimization [NGU 10] |
| Matlab | Weak coupling [MOK 11] |

**Table 5.2.** *Examples of plug-outs using the drive approach*

5.2.3.2. *Plug-in examples*

The import of a model into an analysis tool is generally possible and largely facilitated using the component approach. Indeed, from the moment the software offers the possibility to import a model or "user function", the call to the component will certainly be achievable. The following table provides a list of plug-in applications.

| **Software** | **Application** |
|---|---|
| Smash | Circuit simulation [REZ 11] |
| Portunus | System simulation [REZ 11] |
| Matlab/Simulink | System simulation [DEL 04c; GAA 11] |
| Amesim | System simulation [DOT 10] |
| iSight | Optimization [DOT 10] |
| Excel | Calculation [DOT 10] |

**Table 5.3.** *Plug-in examples*

### 5.2.4. *Some "business" application frameworks*

Certain modeling approaches, which are easily done by hand for small problems, quickly become unattainable when these problems increase in size. Thus, it is easy to solve electrical circuit equations using a pencil and a sheet of paper if we are dealing with a simple resistor, inductor, capacitor (RLC) circuit. If we increase the number of components, then we must very quickly move to numerical methods, with automatic equations, such as in circuit simulation. In order to facilitate this implementation a schematic formalism, which we will call the "business" of the electronic or electrical technician, will be used in these tools.

Similarly, circuit formalism can be used to describe problems in other physical domains, such as in thermal physics or mechanics. However, in contrast with some unified formalisms, which are founded in energy analogies, such as the Bond Graphs [DAU 99; ROB 06] addressed in [ROB 12] Chapter 2, we refer, for example, to electrical and thermal

resistance, reluctance[6], friction, etc.; therefore, we use the term "business" to refer to the domain designer.

Rather than wanting to find a general formalism that groups all businesses together, a framework should propose various "*business views*" while relying on a general architecture.

In the case of design, it is important to propose business formalisms to the designer to enable their physicality to be described as easily and naturally as possible. Thus, in the CADES framework, we propose business formalisms so that users can focus better on the problem, without having to dive into programming code or numerical methods.

Therefore, designers formalize their problem using representations that are familiar to them and "striking" from the physical point of view, without being pre-occupied with the corresponding equations. Among these business approaches, we note:

– magnetic circuit formalism using reluctance schemes, such as that proposed in Reluctool [DUP 06a; DUP 06b], which enables the resulting magnetism to be formalized;

– magnetic system geometric formalization, which will be modeled using integral formulations, still masked from the user, as in MacMMems [RAK 07b]; in this case, radiated magnetism is modeled;

– frequency modeling of telecoms filters (ADSL) through the description of various passive circuits, taking account of different signal emission and reception configurations, in order to obtain the desired spectrums to be constrained, such as that proposed in electrical circuit modeling (ECM) [DUR 07];

– automatic equations for frequency models in power electronics (EMC). The main difficulty arising from the necessity to effect frequency simulations on temporally discontinuous applications (component control and commutation), while preserving acceptable calculation times for optimization [LAN 12; GER 12].

6 Note that there is no conformance with energy analogies here, a reluctance assimilated by circuit formalism to a resistance being a Bond Graph C-type storage element (equivalent to an electrical condenser).

## 5.3. Components ensuring interoperability around a framework

### 5.3.1. *Model types: white box, black box*

Models can be either oriented or non-oriented; they are also referred to as causal or non-causal, respectively [GER 00; ALL 03]. In this chapter, we propose to call an oriented model a "box" and a non-oriented model a "ball". This distinction is important, as it impacts strongly on the way in which models are assembled and the way their resolution is addressed once they have been put together (Figure 5.4).

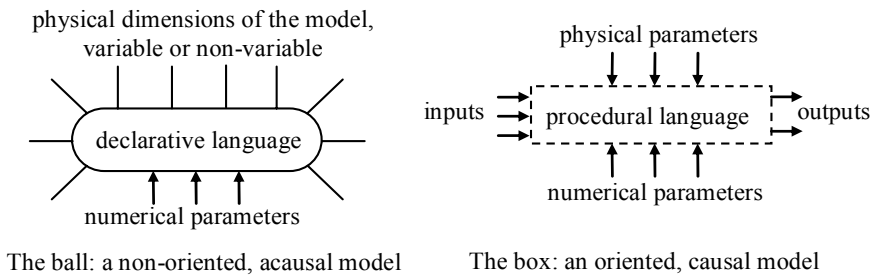


**Figure 5.4.** *A non-oriented (ball) or oriented (box) model*

Models may be formulated in different ways, explicitly and openly, through closed binary code or by a compromise between two approaches (Figure 5.5).

Models can be described within an *explicit formalism* in which equations, functions and algorithms are precisely defined; in this case we refer to "*white box*" or "*white ball*" models, such as those programmed in computing languages (e.g. Java, C, etc.), in numerical languages (e.g. Matlab or Scilab), or even normalized modeling languages (e.g. VHDL-AMS or Modelica).

Conversely, models may be accessible in binary form. In general, components modeled in this way appear in simulation model libraries (Matlab/Simulink, Portunus, Psim, Simplorer, Saber, Amesim, etc.). The user determines a graphical element that he inserts into the diagram and which he is going to connect to other elements over the course of the model's development. Help enables assumptions and the parameters for the model to be understood, but its equations are inaccessible. These components are "*black boxes*" or "*black balls*", since *the content is not*

*accessible* (from equations, functions, and algorithms, which represent the model). Recent developments in information technology (IT) and studies by the scientific community enable us to consider models formulated in this way to be portable between simulation environments. One example is the FMI project[7] for dynamic Matlab/Simulink system simulation.

Finally, in between these two levels of accessibility, we define models in which aspects of open ("white box") and closed ("black box") occur simultaneously. We refer to these as "gray box" models.

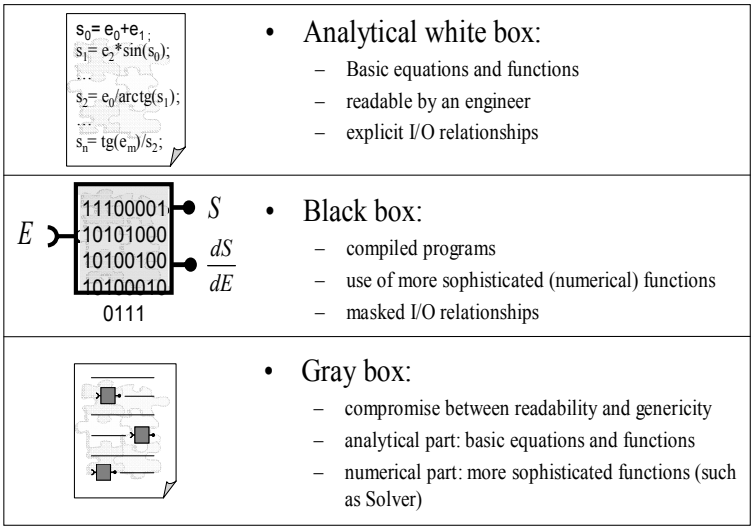


**Figure 5.5.** *White, black and gray boxes*

This model coloration (white, gray or black) is performed similarly for both boxes (oriented models) and balls (non-oriented models). For open ("white ball") models, equations will be automatically orientated in order to move them to the box (oriented) model. This is done for languages such as Modelica and VHDL-AMS. For closed ("black box") models a re-orientation of the model (moving through "black ball") is possible using an implicit resolution algorithm. Algorithms such as the Newton-Raphson use the Jacobian of the model. This is what is typically done when developing a component model in C, in software such as Simplorer or Portunus. These

7 Functional Mock-up Interface: http://www.functional-mockup-interface.org.

models then become "black balls", enabling acausality to be preserved thanks to the Jacobian, which is used in implicit resolution (Figure 5.6).

Nowadays, there are software packages that enable models to be passed from explicit, often normalized formalism to an explicit formalism, which is specific to given software. We illustrate this later in the context of the System Modeling Language (SML) design language, but this also exists in various simulation software packages written in Modelica and VHDL-AMS.

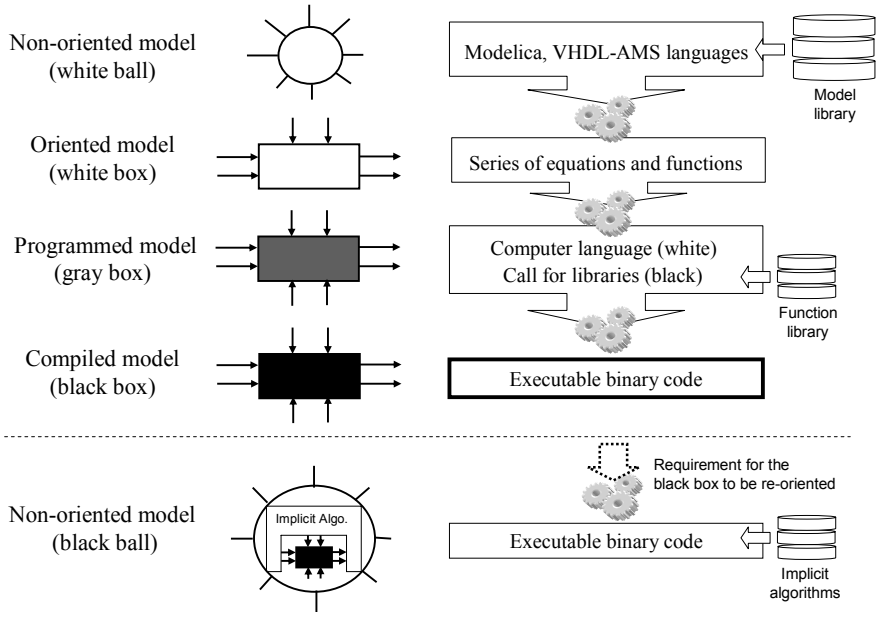


**Figure 5.6.** *Example of an orientation sequence from white ball to executable black box using different colored states. Possibility for re-orientation into a black box: the black ball*

### 5.3.2. *Black boxes: positive collaboration and re-use*

The black box concept enables the exchange and portability of models, without having to clarify their content. The aim is therefore to condition them to enable maximum portability between software contexts. The black box can therefore be used to:

– make models *collaborate* and make their calculations available, while guaranteeing their confidentiality;

– *re-use* models without fear of error from reprogramming and transcription.

This is a fundamental element in the move towards the creation of global models and global optimization by forcing collaboration between players who have, for example, confidentiality constraints (such as in the motor and aeronautical industries).

### 5.3.3. *Object, component, and service paradigms*

Various computing paradigms enable the implementation of code that defines models. As we see in Figure 5.7 [MAR 08], a hierarchical structure with three levels of granularity can be defined in terms of re-utilization [END 04]. *The concept of services, which aggregates that of components, which itself aggregates that of objects*. There are advantages and disadvantages to each layer, in terms of the coupling dynamic and strength.

Dynamic coupling is necessary to ensure rapid re-use of models. Models may be available "off the shelf" (DIMOCODE[8]) as components (models or software), or even available "online" as services.

Strong coupling is often antinomic with dynamic coupling. If calculation performance is required, strong coupling would be preferred and an object model could be implemented. However, according to component specifications, some superior performances may be obtained using "intelligent" weak coupling [MOK 10].

The object concept is very current in programming and is *de facto* imposed by object languages such as C++ or Java. The software component, on the other hand, has been in use since the 1990s within computer technology [SZY 98]. Re-utilization is the key word associated with the object, component, and service concepts. In computer programming, component-based re-utilization proposes a different vision to that associated with object programming [SZY 98]. The main difference comes from a greater clarity and certainty of definition of what the component requires to function. In other words, a component specifies couplings with which it can

8 DIMOCODE: *Diffusion Internet des Modèles pour la Conception Optimale des Dispositifs Energétiques* (Internet model diffusion for the optimal design of energy devices), www.dimocode.fr.

interact with other components. In contrast with a component, an object (in the object programming sense) can use external code without having to specify it, which may result in unsecured re-utilization (see Figure 5.8).

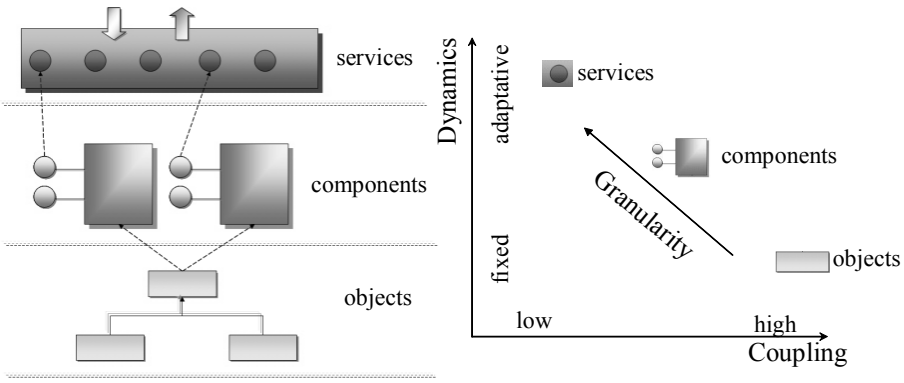


**Figure 5.7.** *Hierarchical architecture of objects, components and services and the dynamics/coupling compromise*

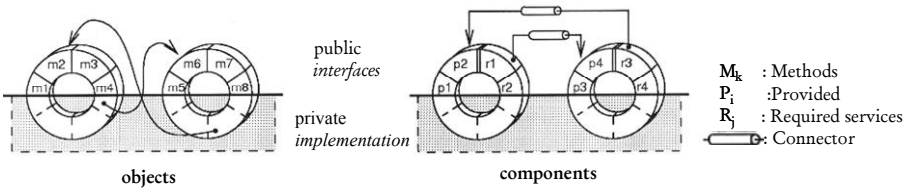


**Figure 5.8.** *In contrast with the "objects" approach, the "components" approach defines the services required*

A component will therefore be seen as follows (Figure 5.9), describing the services that it requires, the services it provides, and its parameters.

Various software component implementations are industrial (COM+[9], EJB[10], CCM[11]) and there are many other models (such as Fractal, SOFA, OpenCOM, ArchJava, FuseJ, and K-Component), each with various non-functional attributes (such as distribution, inter-operability, safety and

9 COM+: .NET framework Component Object Model (Microsoft).
10 EJB: Enterprise JavaBean (Sun Microsystems, Oracle Corporation since 2009).
11 CCM: Corba Component Model (OMG: Object Management Group).

persistence) as well as various lifecycle management modes for these components (static and dynamic).

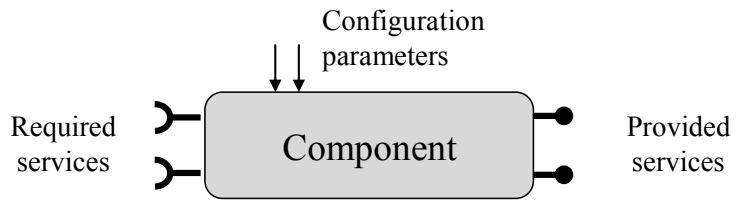


**Figure 5.9.** *Graphical representation of a component with its inputs/outputs and its configuration parameters*

The working vision of an IT component for simulation models may be revealed, in our field, from differential equation integration algorithms, sizing models, and optimization algorithms, for example.

In the context of an environment aimed at dynamic coupling, we have shown that using the CADES framework software components offer a formal context enabling automated methods to be developed, which guarantees composition dynamics and automatic code-generation techniques.

Therefore, the advantages of components comprise:

– capitalization/re-utilization:

- development of compact models as a result of re-utilization,

- robustness of calculation (already tested, guaranteeing results),

- portability and distribution;

– composition:

- systems construction through component assembly,

- improvement of modularity, functional approach, component replacement, etc.

### 5.3.4. *ICAr software components: model normalization for sizing*

A technical standard for software components has been specified: ICAr (Interface for Component Architecture). It has been engineered specifically for optimal design.

An ICAr may propose multiple views or "facets" for the device in question. It may refer to a calculation model (analytical or numerical, for instance), a sensitivity calculation, a document, a graphic visualization, etc. An ICAr will also be able to propose various physical models (such as thermal or electrical) or multiple versions of the model for different requirements (dynamic simulation, optimization or real-time drive, for example) as illustrated in Figure 5.10.

**Figure 5.10.** *Multi-faceted component approach*

Tools that use ICAr components are automatically matched using a dynamic discovery mechanism of services offered by the component. In Figure 5.11, we see that tabs proposing the "CADES-Calculator" tool are dependent on the component loaded.

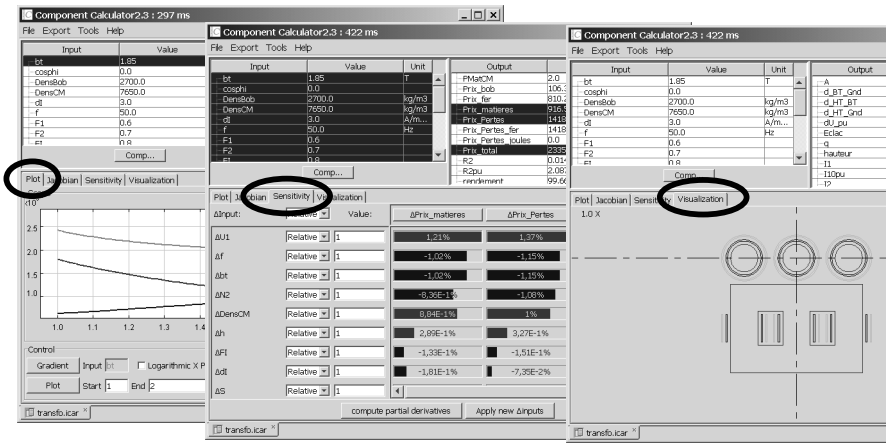


**Figure 5.11.** *Three views of the same component (plot, sensitivity and visualization)*

In the context of optimal design, the ICAr component proposes a facet corresponding to calculation of the model and an optional facet corresponding to the sensitivity calculation of the model from its Jacobian. It may thus be connected to optimization algorithms, which may or may not require gradient data.

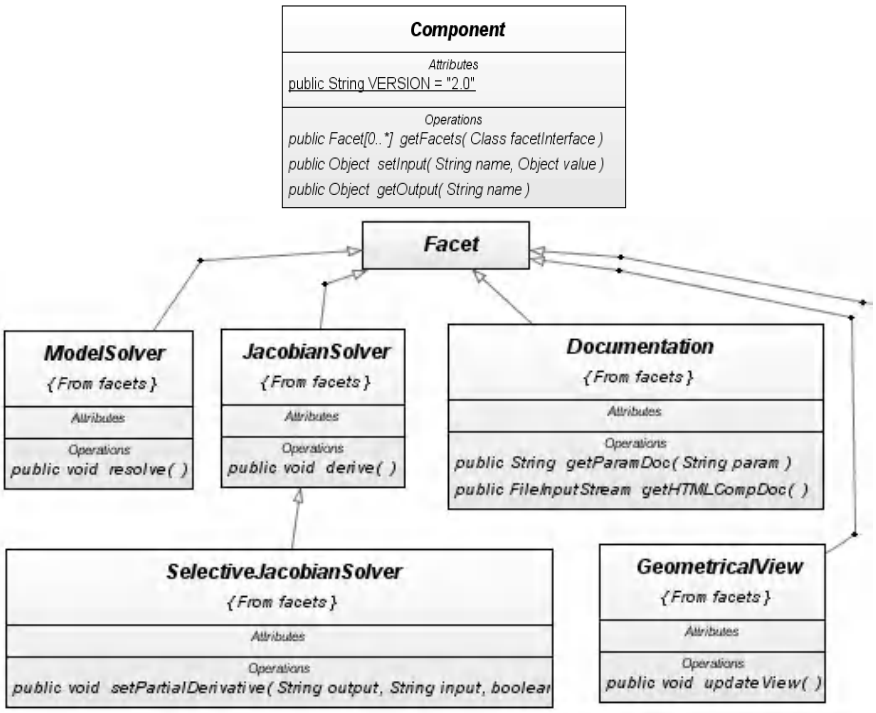


**Figure 5.12.** *Multi-facet ICAr component standard for optimal design*

## 5.4. Some calculation modeling formalisms for optimization

### 5.4.1. *Analytical formalisms: algebraic and algorithmic*

Within optimal design, we have defined SML as numerous specificities (external functions concept, specific key words) mean that there is no equivalent language and we wish to propose a very simple and natural analytical model description formalism to designers relying on analytical equations [ENC 10a]. For more complex models, calling on numerical methods or algorithms, we propose a more advanced formalism, which is

complementary to this basic language. Indeed, this language is meant to be very simple and very accessible to non-specialists in IT. Currently, it mainly enables us to describe an *analytical model* through:

– scalar or vectorial mathematical functions and equations (see Figure 5.13);

– use of external code, which may be complex, but which we propose for formulation assistance in certain business contexts;

– algorithms written in Java or C (see Figure 5.14).

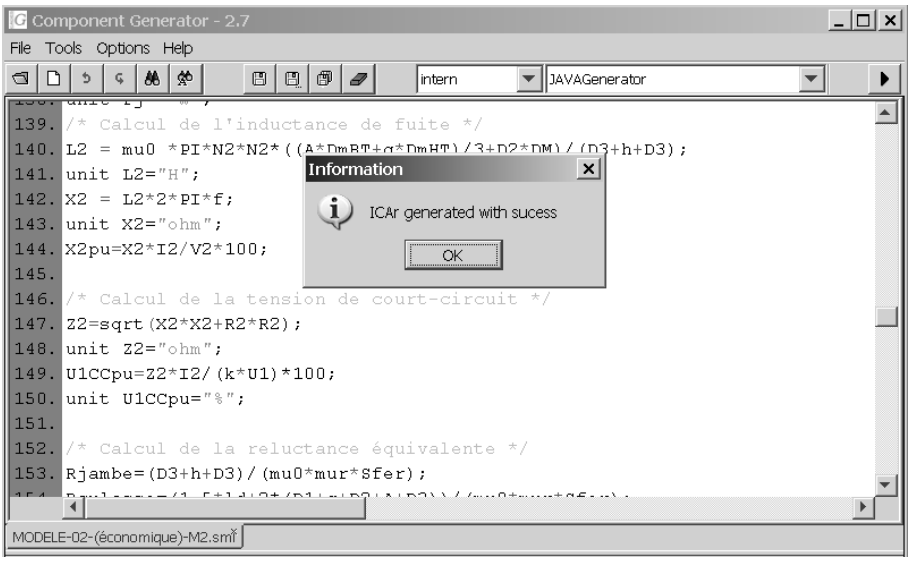


**Figure 5.13.** *Model generator described through the use of equations (SML language)*

In association with this language, which enables analytical and semi-analytical models to be described, we propose a generator that enables this description to be transformed into binary executable program code, encapsulated in a software component to enable its portability.

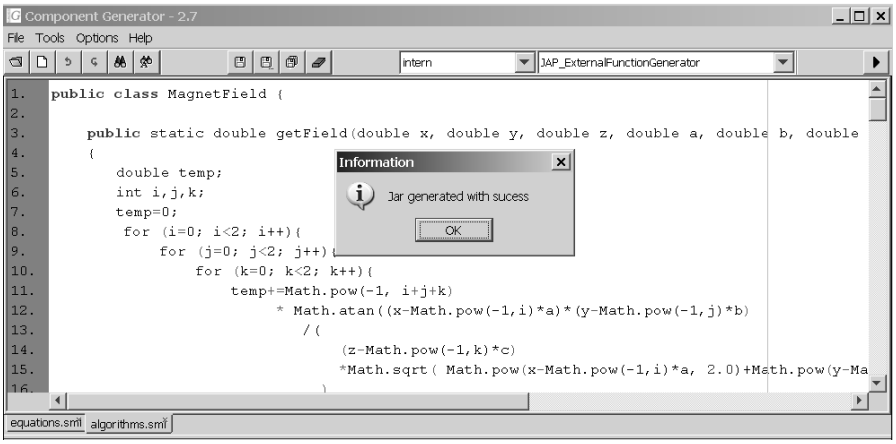


**Figure 5.14.** *Model generator described through the use of algorithms (Java or C)*

Therefore, we describe models using a declarative language, by giving access to analytical operators (+, –, * and /), traditional functions (sin, cos, pow, exp, log, etc.) and some semi-analytical operators (such as, for example, integrals and system inversions). In this regard, this generator offers:

– functionalities that enable us to analyze the model and reformulate it in a structured manner using a computer [DUR 06];

– sequencing functionalities, in order to explain calculation sequences being constructed in order to lead to calculation code corresponding to the model declared [ALL 03];

– projection functionalities for the model conditioned for calculation, using a programming language;

– model derivation functionalities in order to obtain the Jacobians required by certain optimization algorithms [ENC 09b] or to perform the sensitivity study [PHA 11b];

– creation functionalities for well-formed software components (in accordance with standards and norms), which enable the use of models in various software environments [DEL 07].

### 5.4.2. *Physical models within various formalisms*

In order to respond to the problem of availability of models using their formulations, we propose tools that would allow designers to create semi-numerical and semi-analytical models, which are suitable for providing useful data for the pre-sizing and feasibility study phases. Indeed, the definition of equations for certain models may become a complicated task if this is performed manually, all the more so if the problems being modeled are significant in size. However, such a task can be automated, from a "business" description, in the form of computer programs, which are referred to as model generators.

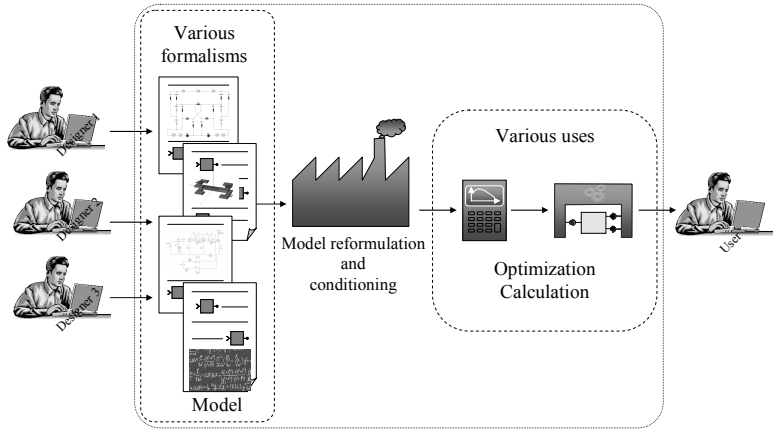


**Figure 5.15.** *One framework managing various modeling formalisms*

The unique nature of each of the approaches developed to create such models is not only the *automation of semi-analytical model generation*, but also in providing the calculation of their *formally exact gradients*. In fact, these are models providing maximum data for sizing using optimization techniques; we thus refer to sizing models.

This generative approach enables a designer to directly establish a high-level "business" formalism, such as an equivalent circuit or a geometric structure. Thus, electrical and magnetic circuits or three-dimensional (3D) geometries are possible. Of course, any branch of physics presenting an analogy with electricity could be modeled using such mechanisms; for

example, by making use of the thermics-electricity analogy, as we have done for the magnetism-electricity analogy.

In this context, Table 5.4 summarizes some of the approaches that we have implemented.

| | | | |
|---|---|---|---|
| Objective: | Sizing of passive circuits in the frequency domain | Sizing of electromagnetic devices | Sizing of electromagnetic devices |
| "Business" formalism: | Electrical circuit: 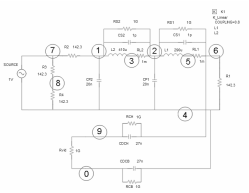 | Reluctance network: 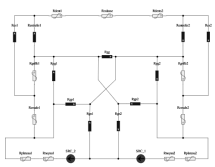 | 3D geometry: 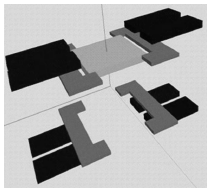 |
| Calculated measure-ments: | Impedances, gain | Magnetic flows, magnetic forces | Fields, forces/magnetic torques, deformations |
| Calculation method: | Equations from the Node potential method | Reluctance networks methods, calculation of mesh flows | Integral methods (Coulombian approach, magnetic moment method: MMM) |
| Gradient calculation methods: | Derivation of linear implicit functions | Derivation of nonlinear implicit functions | Symbolic derivation of numerical integration, adjoint method in MMM, Code derivation |
| Applications: | Passive filters in ADSL, EMC filters in PE. | Linear actuators, alternators, etc. | Micro-actuators and magnetic micro-sensors |
| References: | [DUR 07] | [DUP 06a; DUP 06b; DOT 10] | [RAK 07a; RAK 08; DEL 08; PHA 11c] |

**Table 5.4.** *Examples of model generation from business formalisms*

Thus, from these approaches, a designer can describe component and system models from electrical engineering using a formalism that is close to his culture. The generator then takes charge of the complicated, yet automated aspects, such as:

– programming these models;

– programming the sensitivity calculation of these models;

– processing of all this into a software component.

These generators therefore directly complement the generator based on CADES@Generator, presented initially and present within the CADES framework. In order to illustrate these generators we will briefly review three studies that have been developed in this area.

5.4.2.1. *Passive filter models*

The object of these studies is to develop a generator able to describe schemas consisting of passive electrical components, described as resistance components, condensers, and inductors (coupled or non-coupled) with voltage sources. This should enable software components to be generated, which then enable electrical circuits to be designed. Applications initially related to filtering in the telecoms industry (see Figure 5.16) [DUR 07; DUR 10], but may be used in order to study certain EMC filtering of power circuits [GER 12; LAN 12; NGU 10].

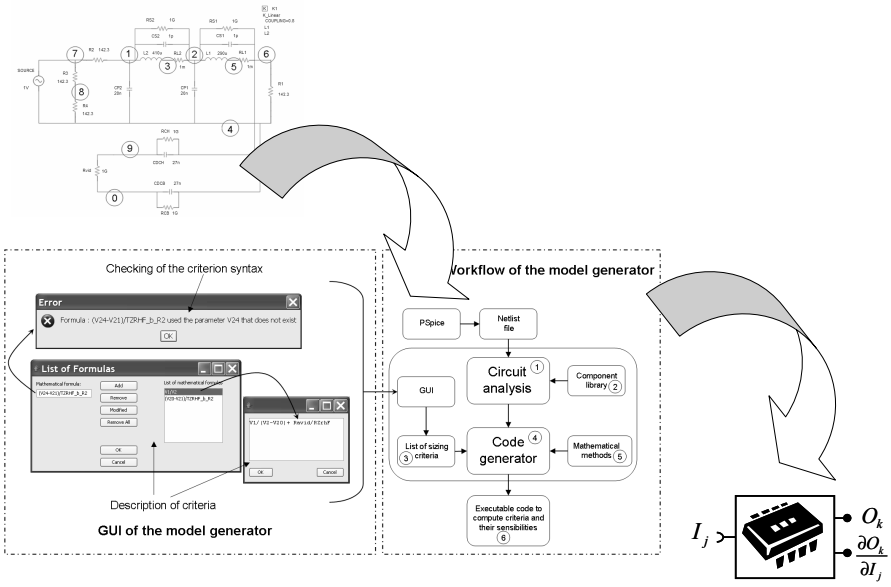


**Figure 5.16.** *Software component generator for the design of passive electrical circuits – application to the design of filters for telecoms use [DUR 07;DUR 10]*

5.4.2.2. *Reluctance models*

The objective of these studies is to develop a generator enabling models to be described using reluctance networks [ROT 41]. This formalism enables the operation of magnetic circuits to be described by performing an equivalence with the electrical circuits. For this approach, an automatic equation generation methodology is used, as notably described in [DEL 04a]. The Reluctool [ALB 04A; DUP 06b] software package associated with this methodology and this formalism has been developed in collaboration with Schneider Electric, with the aim of simulating and sizing the actuators and sensors used in circuit breakers.

Currently, Reluctool enables the processing of static sizing models, i.e. by describing reluctance circuits for given electro-mechanical component positions, whether for linear actuators [DUP 06a] or rotating machines [SES 11; LI 11]. Dynamic simulation of linear actuators and sensors is also available [DOT 10]. Our research studies into the dynamic study of electrical machines, as well as for the optimal sizing with dynamic models are ongoing.

5.4.2.3. *Non-channeled magnetic models*

The object of these studies is to develop a device generator that does not allow flux tubes to be defined. In this case, basic reluctance network approaches cannot be applied. This is, for example, the case with micro-systems, where the production of magnetic circuits is a technological challenge. To that end, we have developed the MacMMems generator, implementing an interactive approach between magnetic elements, based on an integral formulation [RAK 07b]. In short, components can be defined that are able to:

– react to an external magnetic field;

– create mechanical forces and torques;

– create a magnetic field.

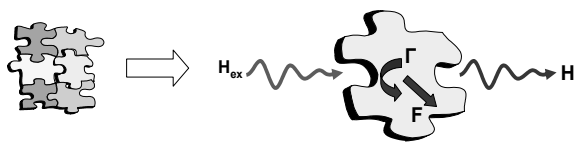


**Figure 5.17.** *Description of a magnetic component using MacMMems*

Three element classes have been defined, as shown in Table 5.5.

| *Element class* | *Description* |
|---|---|
| Magnetic field sources (magnets, conductors) | |
| Soft ferro-magnetic materials | 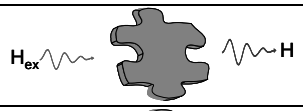  |
| Diamagnetic and paramagnetic materials (induced field ignored) | 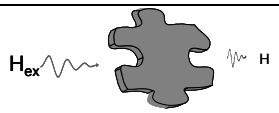  |

**Table 5.5.** *Element classes defined using MacMMems*

An elements library has been assembled from analytical field calculation models [RAK 07b; DEL 10]. The field calculation created by the conductors relies on the Biot-Savart law, which results in volume integral calculations. For the field created by the magnets, a Coulombian approach (equivalent load) is used and generally involves a surface, occasionally volume integral calculation.

This modeling principle has been successfully employed by researchers in various magnetic micro-system applications, such as [CHE 07], [PIG 09], [KAU 10] and [PHA 11a].

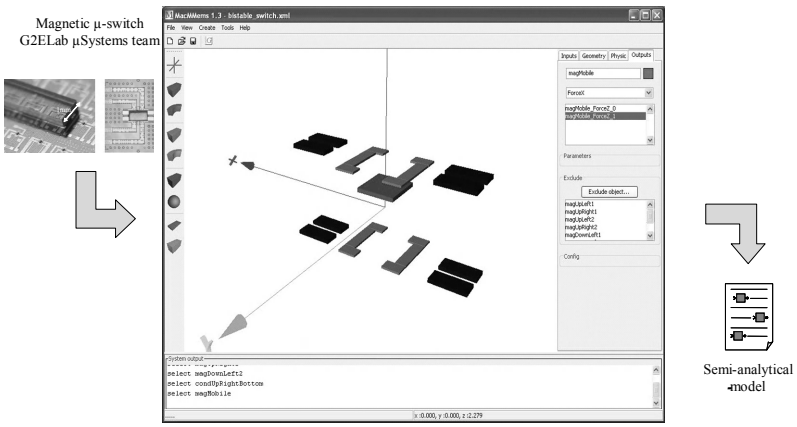


**Figure 5.18.** *Use of MacMMems to model a magnetic MEMS*

### 5.4.3. *The generation chain*

Business generators that make use of business modeling formalisms belong to the upper level of the standard CADES framework (see Figure 5.19). The principle behind the generation chain is the derivation of the expert formalism within the more generic formalism corresponding to SML. As white box formalism is not able to address all of the requirements of modeling, SML integrates the black box concept in order to obtain an overall semi-analytical or semi-numerical "gray box" model.

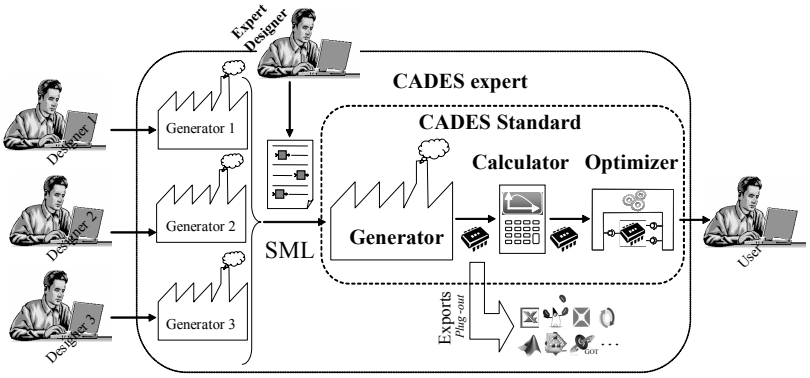


**Figure 5.19.** *The generation chain, from modeling formalisms to components*

Let us take the example of MacMMems, which generates a semi-analytical model from the geometric and physical description of the studied magnetic system. The resulting model, which may be modified or completed, if necessary, is then passed through the CADES generator in order to produce the ICAr component. This automatic generation phase may be totally hidden from the user for business applications. Ultimately, the user has an available component that can be used within the CADES framework, or otherwise by using plug-ins.

## 5.5. The principles of automatic Jacobian generation

### 5.5.1. *The Jacobian: complementary data for the model*

It is extremely difficult to symbolically derive models for optimization, to the extent that a common strategy is to ignore this in order to focus only on

algorithms that do not use information on the gradient (such as genetic algorithms, for instance). However, in our research work we have sought to explore another way aimed at *facilitating the acquisition of symbolically exact gradients*.

Obtaining the exact calculation of gradients is motivated by the fact that this calculation, when possible, results in a more effective optimization; since by finding the gradient, we have more information regarding the behavior of the model. Therefore, optimizations using gradients have a strong likelihood of being faster, which is important for feasibility study phases for which iterations need to be performed quickly and as reliably as possible.

Thus, for a strategy where the aim is to extend the exact calculation capacities of the gradients, we have performed the studies synthesized below. The points of view explored thus go beyond symbolic calculation to symbolic explicit analytical algebraic expressions (which was the approach initially conducted in our laboratory on PASCOSMA [WUR 96]).

### 5.5.2. *Derivation of mathematical expressions*

To begin, the simplest option is to derive mathematical expressions using traditional functions, such as cosine, exponential, etc., for which the derivatives are well-known. By applying derivative composition theorems, the derivatives of each function and equation, and thus, the Jacobian of a purely analytical model, are easily obtained.

For more complex formulations, it is advisable to use mathematical properties, which is what we propose, for example, for formulations requiring integral calculations [5.1] or the solving of implicit functions [5.3].

Let us, for example, consider the following integral expression:

$$I(d,c) = \int_{a(d)}^{b(d)} f(d,c,x).dx \qquad [5.1]$$

Its partial derivative relative to parameter $d$, which occurs in the integrand but also in the bounds, expands into two main terms which make use of other essential partial derivatives [GER 01].

$$\frac{\partial I(d,c)}{\partial d} = \begin{cases} \int_{a(d)}^{b(d)} \frac{\partial f(d,c,x)}{\partial d}.dx \\ + \frac{\partial b(d)}{\partial d} \cdot f(d,c,b(d)) - \frac{\partial a(d)}{\partial d} \cdot f(d,c,a(d)) \end{cases} \quad [5.2]$$

For a volume sizing for which one measurement is integrated (calculation of magnetic force, for example), only the partial derivative relative to the integration bounds will be necessary, which then results in a compact integration calculation for one dimension. We then occasionally obtain Jacobian calculations that are more rapid than the evaluation of the model itself.

Let us now consider the case of implicit functions defined as follows:

$$F_k(Pe_1, Pe_2, \cdots, Pe_n, X_1, \cdots, X_s) = 0, \quad k = 1, s \quad [5.3]$$

Functions $G_k$, which enable the measurements $X_k$ to be defined, are such that:

$$X_k = G_k(Pe_1, Pe_2, \cdots, Pe_n), \quad k = 1, s \quad [5.4]$$

Although the $G_k$ functions are calculated through a numerical resolution algorithm, we can symbolically calculate the exactly Jacobian of the implicit functions in order to obtain the following result by using the implicit functions derivation theorem [CIA 90]:

$$J = -Q^{-1} \cdot M \text{ , where} \quad [5.5]$$

$$J_{q,j} = \frac{\partial G_q}{\partial P_j}, Q_{q,k} = \frac{\partial F_q}{\partial X_k}, M_{q,j} = \frac{\partial F_q}{\partial P_j} \text{ and q=1,s, j=1,n and k=1,s}$$

Finally, more specifically, additional methods [GIT 89] may be developed on the basis of scientific calculation algorithms, such as those based on discretized partial differential equation resolution [RAK 08].

### 5.5.3. *Algorithm derivation*

We do not, however, always have access to mathematical properties that enable the derivatives of complex formulations. In this case we propose the formulation of models in program code form, using C or Java. By using code derivation, in many cases we are able to obtain the Jacobian of the model.

Automatic differentiation (AD) uses the same process as program code compilation. The derivatives of each elementary operation are combined according to the differential calculation chain rule, in order to obtain the derivative of a more complex instruction. This technique provides an effective way of calculating gradients, by significantly reducing the implementation effort. Our first automatic differentiation implementation (JavaDiff) was in 2004 [FIS 04; FIS 05] and was used in [DEZ 04] in order to optimize a linear actuator based on a reluctance network model. Currently, we use Adol-C [WAL 08] in order to derive algorithms written in C [ENC 09a; ENC 09b] and JAP in order to derive from Java code [PHA 11c].

Figure 5.20 illustrates the principle of direct propagation of automatic differentiation for a model with two inputs and two outputs.

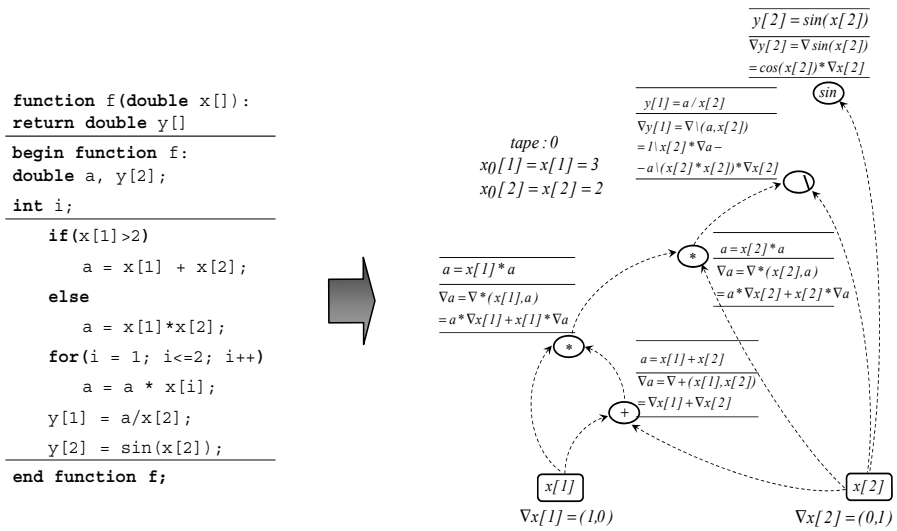


**Figure 5.20.** *Principle of AD for an example of direct propagation of derivatives*

However, AD does not resolve mathematical derivation limits, which are well known at certain non-derivable points of mathematical functions; for example, the discontinuity and non-derivability created by conditional statements, such as the following instruction where the derivative at point x0 is not defined:

*if (x<x0) then y=y0 else y=y1*

This type of difficulty is found in certain specific formulations, such as the search for an extreme measurement calculated using dynamic simulation that we seek to either constrain or optimize.

### 5.5.4. *Derivation of specific formulations*

In certain cases, the non-derivability of functions at certain points may disturb the optimization algorithm; therefore, it is necessary to manage these specific cases. This may sometimes refer to non-derivability introduced into the model and not presenting a physical characteristic, as for a function interpolated by affine parts (see the left-hand side of Figure 5.21) [SAU 00a]. This is also the case for the derivation of a minimum function research algorithm, which may "jump" from one local minimum to another depending on how the function evolves (see the right-hand side of Figure 5.21) [DEL 03] (optimization of a micro-actuator that is to impose a minimal force throughout its displacement).

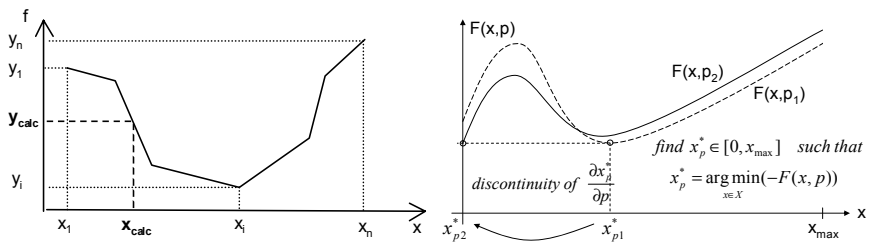


**Figure 5.21.** *Non-derivable functions example: to the left, a piecewise linear function; to the right, a minimization function*

## 5.6. Services using models and their Jacobian

### 5.6.1. *Sensitivity study*

The sensitivity study is a design phase that happens very quickly once the model is achieved. It enables the variation in calculated measurements, based on variations on the inputs and the parameters of the model, to be studied. Assuming low variations, a local sensitivity study may be carried out using the data provided by the Jacobian of the model. Thus, if these data are available in the software component of the model, then CADES-Calculator (Figure 5.22) enables a high speed sensitivity study around an operating point to be carried out.

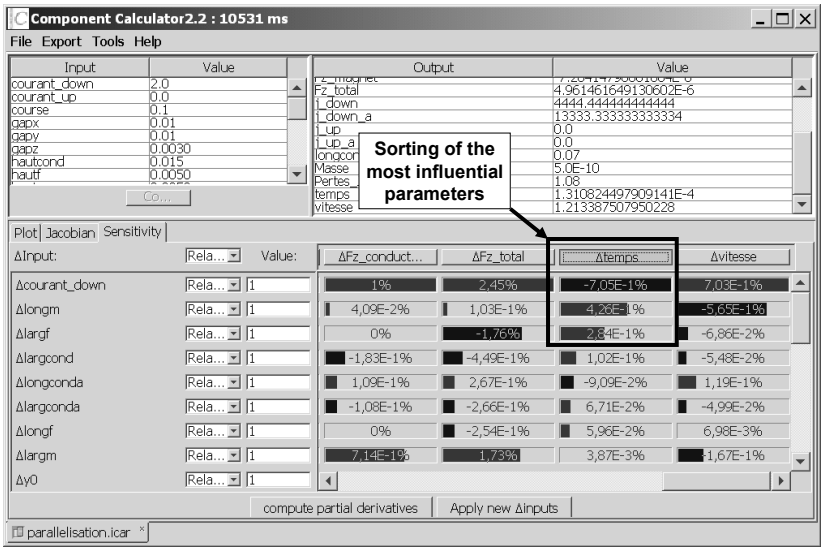


**Figure 5.22.** *Screen grab from CADES-Calculator enabling the sensitivity of the model to be analyzed*

With this analysis, we see that the most sensitive variables should be the focus of particular attention throughout the manufacture of the device, in order to guarantee a certain level of precision, and thus, to better fit with the simulation results. We also see how to change the parameters of the system in order to improve its performances, but these data will be better used by an optimization algorithm, as we will see in the next section.

### 5.6.2. *Composition of models*

A component can be defined as a unit of composition. Figure 5.23 presents the concept of recursive composition, which aims to define the hierarchical composition levels for our models. The resulting component is called a composite component. Thus, a system can be modeled through the assembly of components and can itself become a component of a larger system [DEL 04b].

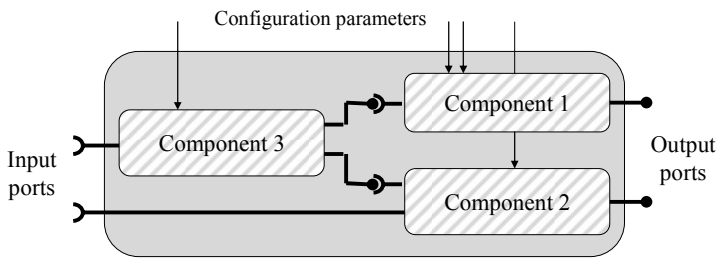


**Figure 5.23.** *Graphical representation of a recursive component which defines a composite component*

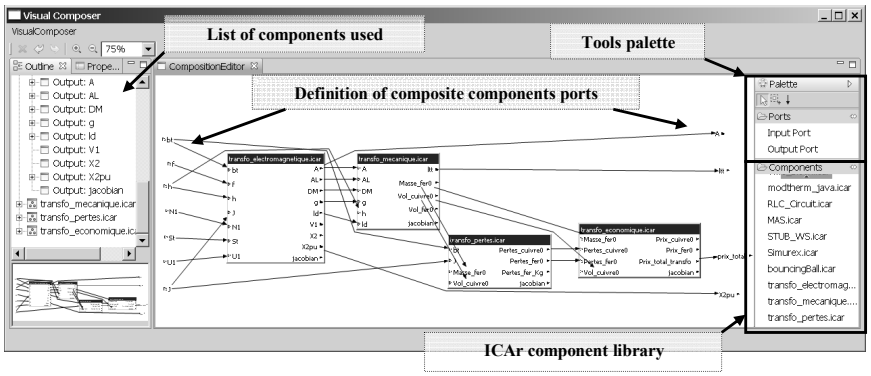


**Figure 5.24.** *Graphical recursive composition example of components comprising a distribution transformer model (electromagnetic, geometric, loss and economic models) [DEL 07]*

Various compositions are possible, depending on the nature of the component. Within the context of optimal design, it is particularly important to guarantee the composition of the sensitivity calculation. Two approaches can be considered in this regard: the first by studying the data from partial

derivatives and the second from data on directional or differential derivatives. With regards to composition, the differential approach makes composition much easier [DEL 04d].

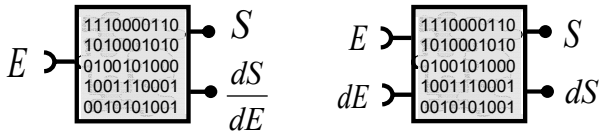


**Figure 5.25.** *Local sensitivity propagation mode: partial or differential derivative*

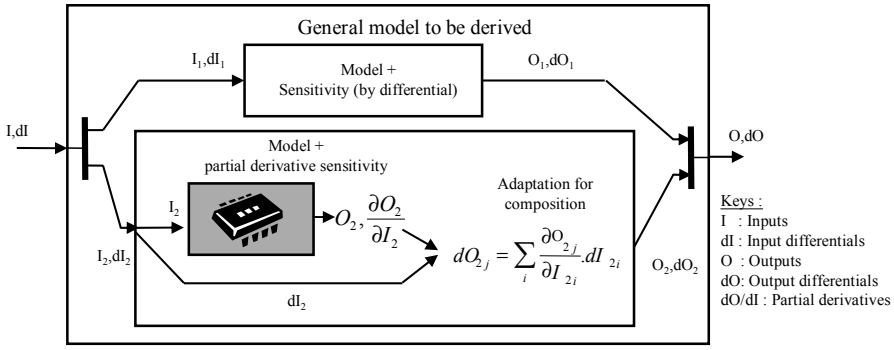


**Figure 5.26.** *Recursive composition example of calculation models offering two ways to propagate local sensitivity*

The CADES component generator offers two propagation modes, with the possibility of hybridizing them based on the models to be composed, as illustrated in Figure 5.26. A composition involving various derivative calculation methods is, therefore, possible, which is what was produced in [PHA 11c], where the following were coupled, for the optimization of a magnetic nano-switch:

– a magnetic model, the partial derivatives of which were symbolically generated;

– a mechanical deformation model, the differentials of which were obtained using code derivation (JAP, [PHA 11b]);

– an iterative coupling model, with symbolic partial derivatives obtained by the implicit function theorem;

– a supplementary equation model, with partial derivatives obtained using code derivation [ADOL-C].

### 5.6.3. *Optimal design*

The CADES optimizer (or ComponentOptimizer) is able to automatically connect the model, with its associated sensitivity calculation, to an optimization algorithm [MAG 04]. These optimization algorithms are themselves programmed within software components that specifically enable their composition [NGU 07]. The optimizer thus makes various optimization algorithms available:

– algorithms, which use the SQP (Sequential Quadratic Programming) gradient [WUR 96];

– genetic algorithms [NGU 08b];

– Pareto approach algorithms [NGU 08a];

– branch and bound approach algorithms;

– hybrid strategies from composition of these algorithms, in order to manage, for instance, the continuous and discrete variables and local and global minima.

Once the components containing the model and the optimization algorithm are loaded into the optimizer, it offers the following functionalities:

– the potential to define constraints on the input and output parameters for the model;

– the definition of one or more objective functions to be minimized or maximized;

– the potential to track the changes in the parameters over the course of the process.

Figure 5.27 gives an insight into the operation of this optimizer.

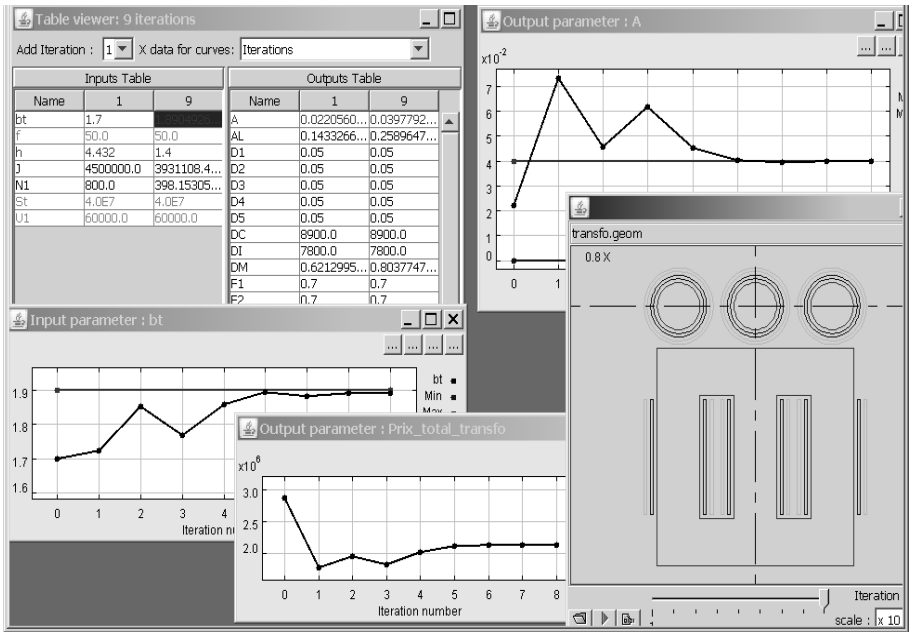


**Figure 5.27.** *The optimization service proposed using the CADES framework for the technico-economic optimization of a distribution transformer*

## 5.7. Applications of CADES in system optimization

### 5.7.1. *Overall optimization of a structure*

The first problem that can be addressed using our platforms is constrained design and automatic optimization, as illustrated in Figure 5.27 for a transformer. By combining the use of a generator (such as CADES-Generator) and then a composer, we are able to produce the software component that will be used in an optimizer (such as CADES-Optimizer). Thus, it is possible to use CADES-PostProcessor to study the changes in the geometry, as well as the change in cost over the course of the iterations intended to minimize it, as well as all the constraints to be satisfied (in Figure 5.27.: bt<1.9, A<4, and so on).

This approach enables sizings, pre-sizings, and feasibility studies using a vision system: a large number of parameters and constraints may indeed be considered, notably as a result of the symbolically exact gradient calculation

performed by the CADES generators. In addition, the model used is the one created by the recursive composition of electromagnetic, geometric, and economic sub-models (Figure 5.24), which enables a system approach to be used from the construction phase for the system model.

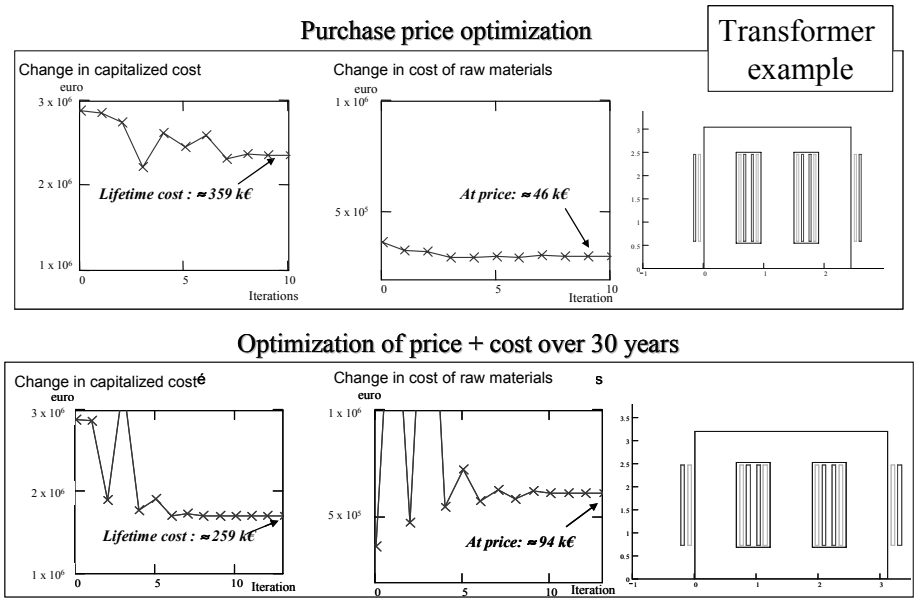


**Figure 5.28.** *Pre-sizing studies example – comparing two design alternatives for a transformer, one optimizing the purchase price and the other the lifetime price*

This enables studies, such as those in Figure 5.28, to be carried out very quickly; the upper section shows an optimization of purchase price of the structure, whereas the lower section shows an optimization of the capitalized cost of the system over its lifetime, i.e. 30 years, by integrating the cost of produced losses. The first structure is not as large, and is, therefore, less costly in terms of raw materials, than the second (46 k€ to 94 k€). Conversely, in terms of capitalized cost, the second is cheaper than the first (259 k€ to 359 k€). This method enables a vision system to be quantified and used for these questions, and shows that, in this case, the most significant initial investment is largely depreciated over the life of the product. Note that the typical execution time for such optimizations is around 1 second, which makes our approaches useful decision-making tools, enabling the designer to be extremely reactive and offering the possibility for yet more complex

strategies to be applied, such as an optimization that integrates robustness or reliability criteria.

References describing or making use of this example are [FAN 99], [SAU 00b] and [DEL 02]. In [WUR 08b], these approaches are applied to eco-design.

### 5.7.2. *Evaluation of the potential of a structure*

Our platform, and the methodologies contained therein, enable studies to be carried out that are more restricted in terms of design compromises. Let us take, for example, an alternator technology currently available in cars, and perform a study of the mass-efficiency compromise.

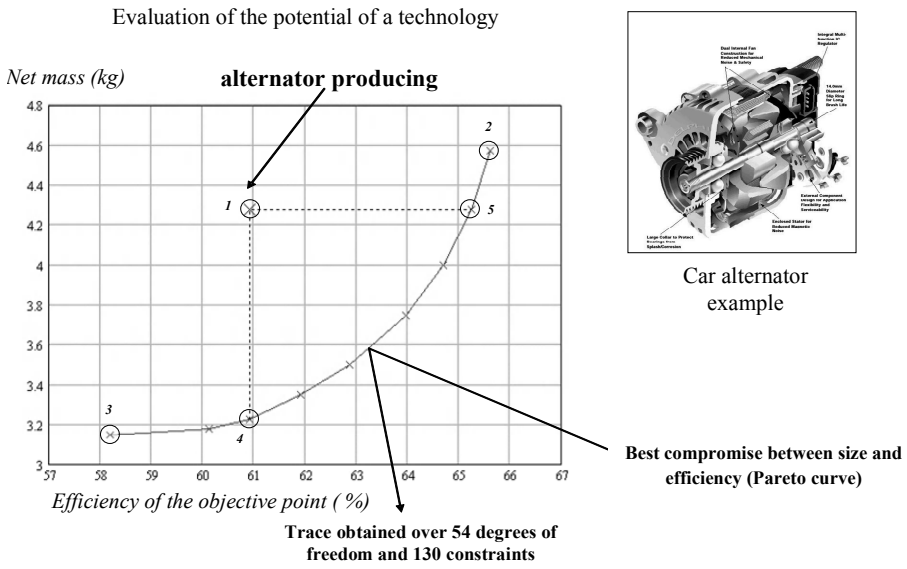


**Figure 5.29.** *Pre-sizing study example – evaluation of the potential of a car alternator in terms of its mass-efficiency compromises [ALB 05]*

Figure 5.29 [ALB 04a; ALB 05], shows how the series-manufactured alternator (point 1) is positioned relative to all of the best compromises to be obtained with the following procedure: reluctance network modeling using ReluctTool [DUP 06b], then optimization using CADES-Optimizer with the

"Pareto" algorithm [MAG 04]. We see that if we want the mass to remain constant, the efficiency can be improved by 4.2% (from 61% in (1) to 65.2% in (5)). We see that if we want the efficiency to remain constant, the mass of the active parts can be improved by 1.1 kg (4.3 kg in (1) to 3.2 kg in (4)). These results are significant [ALB 05], although they should finally be validated by fine numerical simulation or by the alternator manufacturer, particularly with regard to the modeling assumptions. However, what is interesting and cannot be contested is the fact that this curve has been obtained by running nearly 54 degrees of freedom and 130 constraints over just a few minutes.

Therefore, we have a vision system at our disposal and a high reactivity level to aid decision-making and feasibility studies, which presents an extremely interesting potential for industries such as the motor and aviation industries.

### 5.7.3. *Comparison between structures*

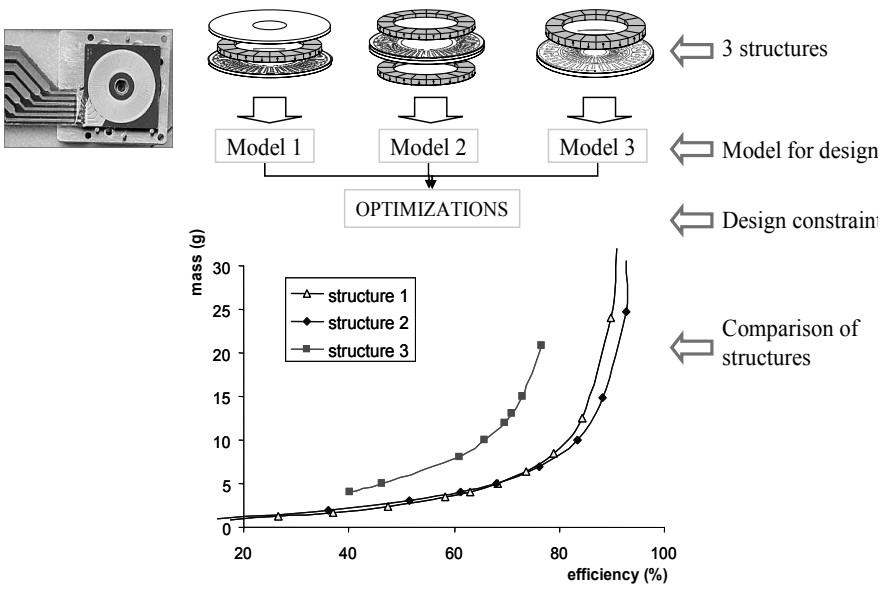


**Figure 5.30.** *Pre-sizing studies example – comparison of drone motor structures using a compromise between mass and efficiency [ACH 04]*

One of the main problems facing designers in the pre-sizing and feasibility study phases is the choice of structures. Multiple structures are often possible and, thanks to platforms such as CADES and their associated methodologies, a rigorous procedure to aim the decision-making process can be established. This consists of tracing Pareto curves of the different structures, having first generated models using our generators, and placing them on the same graph. We illustrate this in Figure 5.30 for a comparison of various possible micro-motor structures for an electrified drone [ACH 04]. Since this is an embedded system, we must determine the best compromise between mass and efficiency. On this graph, we see clearly that structure #3 is the least efficient: across the whole range of efficiency values, it systematically has a higher weight. Structures #1 and #2 are more comparable, with structure #2 having a higher weight at below 60% efficiency and structure #1 having the advantage at above 60% efficiency [DEL 04].

## 5.8. Perspectives

### 5.8.1. *Towards optimization using dynamic modeling*

#### 5.8.1.1. *Dynamic simulation components and services*

ICAr models can be defined using ordinary differential equations (ODE). N-order ODE models are derived from a system of N first-order equations. These models are explicit, linear or nonlinear and associated with an algebraic vectorial equation, which defines the outputs from the model based on the state vector:

$$\begin{cases} \dot{X}(t) = f(X(t), U(t), p, t) \\ Y(t) = g(X(t), U(t), p, t) \end{cases} \qquad [5.6]$$

where:

– X: state vector;

– U: source vector (or input vector);

– p: parameters;

– t: time variable;

– Y: output vector.

This differential system definition is traditionally adopted in simulation environments such as Simulink or by environments dealing with Modelica (such as Dymola, AMESim, and OpenModelica).

Associated with this type of model, we have defined some "solver" components, which include Euler, Trapezoidal and Runge-Kutta integration algorithms. The composition of a "dynamic" ICAr and a "solver" component recursively becomes a "static" component, which can be used within the CADES software framework.

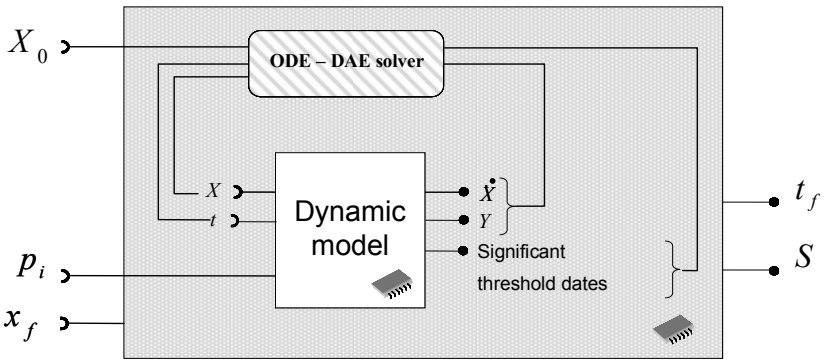


**Figure 5.31.** *Component for dynamic optimization*

Studies are being carried out which take into account differential algebraic equations (DAE). This formulation is particularly suited to "circuit" models, which lead to implicit modeling. DAE resolution algorithms therefore require the Jacobian of the model in order to solve this formulation. All of our developments that enable the Jacobian to be calculated are then automatically used to produce the composition of a dedicated DAE solver model.

5.8.1.2. *Model optimization using dynamic simulation*

Here we define optimization as the capacity to formulate sizing models over criteria resulting from the symbolic or numerical resolution of differential time equations. This may be the calculation of a response time, average or root mean square (rms) values, extreme values, or path tracking for controls. In this type of approach, the simplest solution consists of driving dynamic simulation codes or tools and calculating sizing criteria, either in parallel, or in post-processing of the results from simulation. This

type of approach poses no problems, with optimization algorithms requiring no model gradients, the main limitation being the often long calculation times associated with such an approach.

If the need is for more efficiency in terms of optimization time, while considering numerous sizing criteria, the criteria resulting from dynamic simulation need to be derived relative to the sizing parameters. This derivation is an area of research where certain solutions are beginning to emerge [ENC 10b], but it remains a significant task with regards to this problem.

### 5.8.2. *Towards robust design*

#### 5.8.2.1. *Sensitivity analysis components and services*

Sensitivity analysis relies on the uncertainty propagation methods that we traditionally find [SAL 00] and have implemented in various studies enabling sensitivity analysis to take place, which are listed below:

– the Min-Max approach, which enables a model output range to be calculated; two methods can be used:

- using an *optimization* algorithm [MAG 03], which is a costly, but robust technique,

- using *interval arithmetic* [DEL 06], which is a rapid technique, but overestimates the range; furthermore, it is intrusive and requires the availability of the "white box" model for the interval propagation;

– the statistical approach, which enables the average value and the dispersion to be calculated:

- using *sampling* on the actual model or on an approximate model (the traditional Monte Carlo (MC) method and the response surface method (RSM)): these methods are currently used but are expensive,

- using *Taylor approximation* (variance decomposition/perturbations method) [PHA 11b]. This technique is fast and reliable for low uncertainties. Nevertheless, it is intrusive and requires the use of the "white box" model to generate gradients.

It is possible to represent these couplings, whether using the Min-Max (optimization, intervals) or statistical (MC, Taylor approximation) methods.

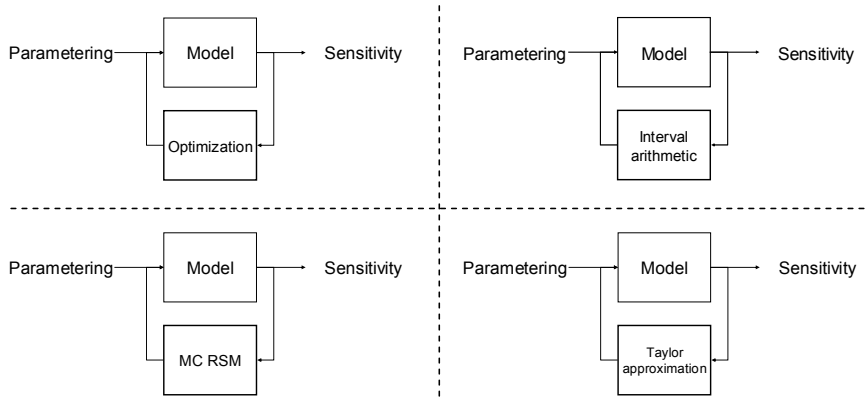


**Figure 5.32.** *Various couplings for uncertainty propagation*

### 5.8.3. *Robust optimization under reliability constraints*

By integrating this uncertainty propagation mechanism with the model, it becomes possible to create robustness and/or reliability (Figure 5.33). Robustness characterizes the capacity of a solution to be insensitive to variations in measurements subjected to uncertainty. Reliability guarantees that a system will not depart from its validity domain whatever the variations in measurements subject to uncertainty.

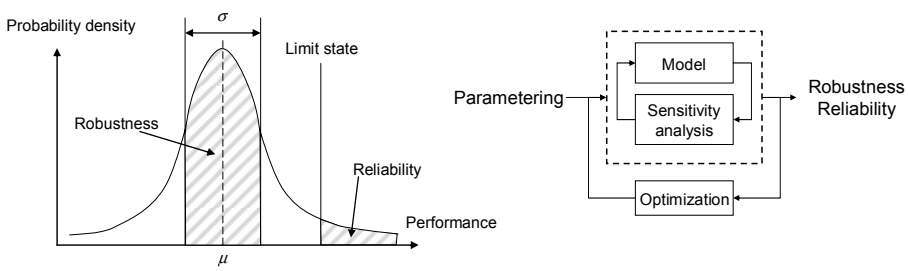


**Figure 5.33.** *Robustness and reliability concepts [TSO 07] and coupling of the optimization to the sensitivity analysis of the model*

A robust and reliable optimization must therefore continually take these concepts into account. In order to achieve this, the sensitivity analysis is

associated with the model to be used by the optimization (Figure 5.33). This oriented robustness approach is detailed in Chapter 4 of [ROM 12].

The MC sensitivity analysis technique (see Chapters 7 and 8 of [ROM 12]) is not used since it is too costly to be integrated into an optimization loop. Conversely, a Taylor development enables sensitivity data that can be used in optimization to be provided at low cost. If a first-order Taylor development (Jacobian) and a base gradient optimization are used, the model should then be able to provide its second-order development. However, in order to avoid heavy Hessien calculations, approximation using the perturbations method enables satisfactory results to be obtained [PHA 11b].

### 5.8.4. *Towards the Internet*

#### 5.8.4.1. *DIMOCODE: a collaborative capitalization platform*

The aim of the DIMOCODE (http://www.dimocode.fr) platform is the diffusion of explicit parts from models, not only in report and documentation form, but also in software component form (*typically ICAr components*): source code and data files that can be directly used within simulation (such as *Modelica*, *VHDL-AMS* and *Matlab*) and optimization (such as *CADES*) environments. This should enable a considerable amount of time to be saved in the move towards component and energy system optimization, by benefiting from access to models that are directly usable, as well as documentation enabling the assumptions and limitations of the model to be made.

However, this type of platform must also facilitate the direct link between model designers and users, for a more pertinent use of modeling, but also for a virtuous improvement in these models. Indeed, for each model made available, there are associated functionalities, such as wikis, forums, chats, even video-conferencing tools, which should:

– ensure linking from users of the model to the designer in order to benefit from his knowledge (by chat or video-conference);

– provide the designer of the model with virtual assistance in the formalization of equations, limits, and assumptions for the model, through direct feedback on model usage by users (through tools such as forums or wikis).

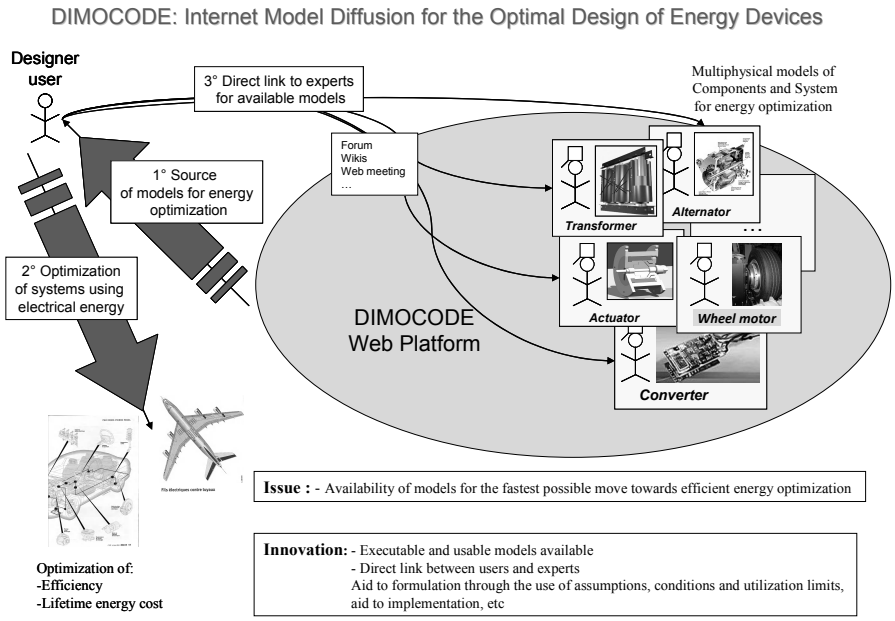


**Figure 5.34.** *DIMOCODE: proposal for a web platform for a new approach for the capitalization and diffusion of models*

### 5.8.4.2. *Web-services: decentralized calculation*

Beyond the component approach, the service approach [PAP 03] relies on the provider/consumer model, in which a set of service providers (e.g. a calculation service) is placed at the disposal of eventual consumers. The mechanism enabling this dynamic functionality to be attained is that of the "publication, discovery, invocation" trinity, as shown in Figure 5.35. Services are published when they are available; then, when a consumer needs a particular service, he finds it in a service registry via a service contract and then invokes it in order to use it. According to [PAP 03], services are entities that can be processed and auto-scripted using a computer and which are independent of the execution platform.

Service orchestration, or workflow, corresponds to the sequential, parallel, looped, conditional, synchronous, or synchronous linking of services. This occurs in the conceptual context of Service Oriented Architectures (SOA [BEL-10]), such as web services or numerous other implementations (such as JINI, OpenWings, Corba and UPnP).

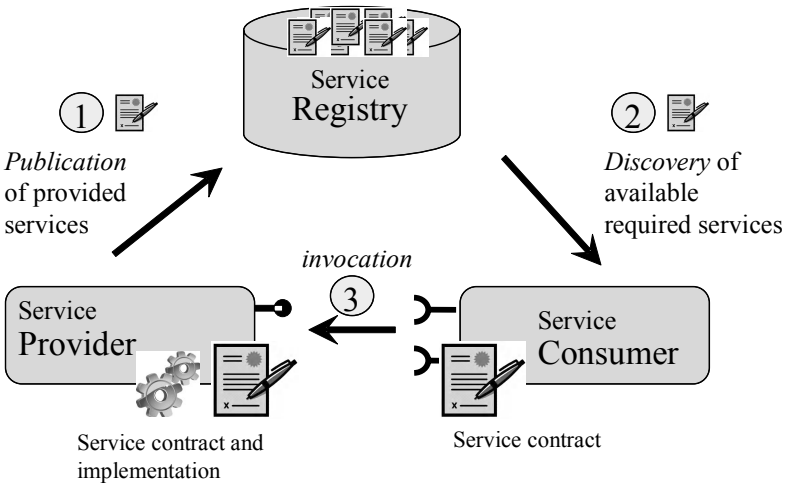


**Figure 5.35.** *The "publication, discovery and invocation" trinity*

A declination of the service-oriented approach has been introduced in order to effect the contribution of the component approach and to combine the dynamic aspect of service discovery with the recursive component composition approach. For example, we have the SCA (Service Component Architecture) model for web service composition and the iPOJO[12] model for the structural composition of OSGi[13] services.

The ICAr software component standard presented in this chapter is compatible with the OSGi and WebServices technologies. These components therefore offer a favorable landscape for the CAD platform of tomorrow, which will be web based. To illustrate this, the following example aims to optimize a temperature regulator associated with a dynamic thermal building model and a heating system (the ANR SIMINTHEC[14] project), without making local use of the model. To achieve this, the (local) optimizer interrogates (transparently) a distant web server at each iteration. The optimization of the distant model has been compared with a local optimization. The solutions found and the paths followed, are similar, and so show the robust behavior of the model.

12 iPOJO: injected POJO, http://cwiki.apache.org/confluence/display/FELIX/iPOJO.
13 OSGI: www.osgi.org.
14 SIMulation and INter-operability for THermal and EleCtric building energy management.

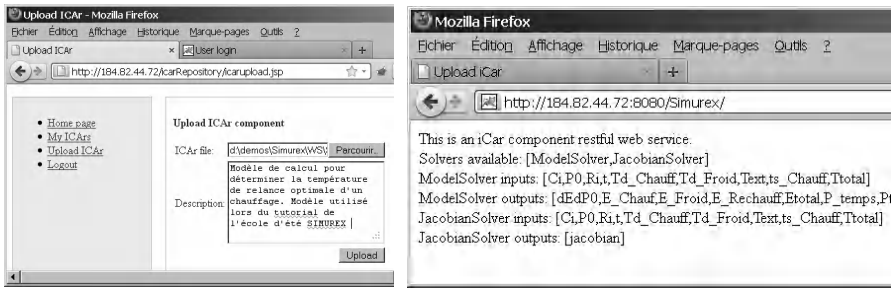


**Figure 5.36.** *Provision of a calculation component onto a web server (left). Request for a web service (right) (developed by P.Y. Gibello of Petals Link[15])*

This potential for easily publishing (web interface) and distantly interrogating a calculation model offers some interesting perspectives with regard, for example, to relationships between customers and providers during system design and optimization.

## 5.9. Conclusions

In this chapter, we have presented a vision of future tools for design and multi-criteria optimization by illustrating the solid example of the CADES framework. By relying on a component and cooperative module based architecture, these tools will be equipped to respond to model capitalization, reutilization, and interoperability problems in a vision system. They will be "model centered", thanks in particular to the transformation of high-level or "business" formalisms (such as electrical circuits and 3D representations) using automatic generation methods written in executable program code.

Model components will be able to be defined according to their degree of explicitness (black or white) and their orientation (ball or box). In this context, we have defined a "black box" software component standard called ICAr, which is dedicated to optimal sizing. The path from business formalism to component for optimization requires a generation chain being able to pass through various intermediary formalisms, which may or may not be standardized. For example, this is the case for our SML language, for semi-analytical modeling dedicated to optimization.

15 Petals Link, open source SOA solutions editor (www.petalslink.com).

In the context of sizing, the availability of the Jacobian of the model is a serious advantage. We have shown that it was possible to symbolically exactly and systematically produce this Jacobian, by symbolic derivation in the case of analytical formulae, by using mathematical theorems in the case of specific algorithms and by more generally using automatic code derivation for other algorithms.

Thanks to these software components, which offer a calculation service as well as complementary data via the Jacobian of the model, it is possible to undertake sensitivity and optimization studies. These components also aim to be composed to create a more global system. Thus, some example applications of the CADES framework have been given, such as the overall optimization of a structure, the evaluation of a structure's potential, or even comparisons between structures.

In terms of perspective, the optimization of systems increasingly integrating criteria and the taking into account of supplementary optimization measurements is becoming a necessity. We have, for instance, criteria resulting from a dynamic simulation, such as a response time or even from the notions of robustness, and reliability associated with an optimal solution. Finally, the perspectives relating to design and multi-criteria offered by the Internet must be considered for tools. For example, this is the case for the provision of modeling competencies and canvas optimization, as well as for the diffusion of models, which can be directly used in distributed ways in system optimization.

## 5.10. Bibliography

[ALB 04] ALBERT L., Modélisation et optimisation des alternateurs à griffes. Application au domaine automobile, PhD thesis, Grenoble Institute of Technology, 2004.

[ALB 05] ALBERT L., CHILLET C., JAROSZ A., ROUSSEAU J., WURTZ F., "Sizing of automotive claw-pole alternator based on analytical modeling", *Electromotion*, vol. 12, pp. 118-124, 2005.

[ALL 03] ALLAIN L., Capitalisation et traitement des modèles pour la conception en génie électrique, PhD thesis, Grenoble Institute of Technology, 2003.

[BEL 10] BELL M., *SOA Modeling Patterns for Service-Oriented Discovery and Analysis*, Wiley & Sons, New York, 2010.

[CIA 90] CIARLET P.G., *Introduction à l'analyse numérique matricielle et à l'optimisation*, Dunod, Paris, 1990.

[CHE 07] CHETOUANI H., HAGUET V., JEANDEY CH., PIGOT CH,. WALTHER A, DEMPSEY N.M., CHATELAIN F., DELINCHANT B., REYNE G., "Diamagnetic levitation of beads and cells above permanent magnets", *Transducers,* vol. 1, pp. 715-718, 2007.

[DAU 99] DAUPHIN-TANGUY G., "Les bond graphs et leur application en mécatronique", *Techniques de l'Ingénieur*, vol. S 7 222, pp. 1-24, 1999.

[DEL 04a] DELALE A., ALBERT L., GERBAUD L., WURTZ F., "Automatic generation of sizing models for the optimization of electromagnetic devices using reluctance networks", *IEEE Transactions on Magnetics,* vol. 40, pp. 830-833, 2004.

[DEL 02] DELINCHANT B., WURTZ F., FANDINO J., "Mixing of FEM and analytical modeling for the preliminary design of a transformer", *OIPE'02*, Lodz, Poland, 12-14 September, 2002.

[DEL 03] DELINCHANT B., Un Environnement à base de Composants, Intégrant le Concepteur et ses Outils, pour de Nouvelles Méthodes de CAO, PhD thesis, Grenoble Institute of Technology, 2003.

[DEL 04b] DELINCHANT B., WURTZ F., MAGOT D., GERBAUD L., "A component-based framework for the composition of simulation software modeling electrical systems", *Journal of Simulation, Society for Modeling and Simulation International, Special Issue: Component-Based Modeling and Simulation*, vol. 80, pp. 347-356, 2004.

[DEL 04c] DELINCHANT B., STEPANEK J., RAKOTOARISON L., DELAMARE J., CUGAT O., WURTZ F., "Capitalizing on computation tools to improve design and knowledge sharing of magnet based devices", *HPMA'04*, Annecy, France, 29 August - 2 September 2004.

[DEL 04d] DELINCHANT B., WURTZ F., ATIENZA E., "Reducing sensitivity analysis time cost of compound model", *IEEE Transactions on Magnetics*, vol. 40, pp. 1216-1219, 2004.

[DEL 04e] DELINCHANT B., ACHOTTE N., DU PELOUX B., WURTZ F., DELAMARE J., CUGAT O., "Design optimisation of integrated planar miniature magnetic motor", *DTIP 2004*, Montreux, Switzerland, pp. 329-334, 12-14 May, 2004.

[DEL 06] DELINCHANT B., "Interval arithmetic for the design of electrical engineering systems", *OIPE 2006*, Sorrento, Italy, 13-15 September, 2006.

[DEL 07] DELINCHANT B., DURET D., ESTRABAUT L., GERBAUD L., NGUYEN HUU H., DU PELOUX B., RAKOTOARISON H.L., VERDIERE F., BERGEON S., WURTZ F., "An optimizer using the software component paradigm for the optimization of engineering systems", *COMPEL*, vol. 26, pp. 368-379, 2007.

[DEL 08] DELINCHANT B., RAKOTOARISON H. L., ARDON V., CHADEBEC O., CUGAT O., "Gradient based optimization of semi-numerical models with symbolic sensitivity: application to a simple ferromagnetic MEMS switch device", *OIPE 2008*, Ilmenau, Germany, 14-17 September, 2008.

[DEL 09] DELINCHANT B., GRUOSSO G., WURTZ F., "Two levels modeling for the optimization of electromagnetic actuators", *IEEE Transactions on Magnetics*, vol. 45, pp. 1724-1727, 2009.

[DEL 10] DELINCHANT B., WURTZ F., YONNET J.-P., COULOMB J.-L., "Interaction between ring-shaped permanent magnets with symbolic gradients: application to magnetic bearing system optimization", *IEEE Transactions on Magnetics*, vol. 47, 2011.

[DOT 10] DO THAI P., Modélisation des actionneurs électromagnétiques par réseaux de reluctances. Création d'un outil métier dédie au prédimensionnement par optimisation, PhD thesis, Grenoble Institute of Technology, 2010.

[DUP 06a] DU PELOUX B., Simulation dynamique des actionneurs et capteurs électromagnétiques par réseaux de réluctances : modèles, méthodes et outils, PhD thesis, Grenoble Institute of Technology, 2006.

[DUP 06b] DU PELOUX B., GERBAUD L., WURTZ F., LECONTE V., and DORSCHNER F. "Automatic generation of sizing static models based on reluctance networks for the optimization of electromagnetic device", *IEEE Transactions on Magnetics*, vol. 42, pp. 715-718, 2006.

[DUR 07] DURET D., GERBAUD L., WURTZ F., KERADEC J.-P., COGITORE B., "Modeling of passive electronic circuits with sensitivity analysis dedicated to the sizing by optimization", *KES2007*, Vietri sul Mare, Italy, 12-14 September, 2007.

[DUR 10] DURET D., GERBAUD L., WURTZ F., REZGUI A., DELINCHANT B., COGITORE B., "Optimisation and simulation methodology for passive ADSL splitter design", *Symbolic and Numerical Methods, Modeling and Applications to Circuit Design*, *SM2ACD 2010*, Gammarth, Tunisia, 5-6 October, 2010.

[ENC 09a] ENCIU P., WURTZ F., GERBAUD L., DELINCHANT B., "Automatic differentiation for electromagnetic models used in optimization", *COMPEL*, vol. 28, pp. 1313-1326, 2009.

[ENC 09b] ENCIU P., Dérivation Automatique pour le calcul des sensibilités appliqué au dimensionnement en génie, PhD thesis, Grenoble Institute of Technology, 2009.

[ENC 10a] ENCIU P., WURTZ F., GERBAUD L., "Proposal of a language for describing differentiable sizing models for electromagnetic devices design", *CEFC 2010*, Chicago, 9-12 May, 2010.

[ENC 10b] ENCIU P., GERBAUD L., WURTZ F., "Automatic differentiation applied for optimization of dynamical systems", *IEEE Transactions on Magnetics*, vol. 46, pp. 2943-2946, 2010.

[END 04] ENDREI M. *et al.*, "Patterns: service-oriented architecture and web services", http://www.redbooks.ibm.com/redbooks/pdfs/sg246303.pdf, 2004.

[FAN 99] FANDINO J., WURTZ F., BIGEON J., "Nouvelle méthodologie de conception de dispositifs électrotechniques. PASCOSMA, un outil pour le dimensionnement avec des modèles analytiques", *Revue Internationale de Génie Electrique*, vol. 2, pp. 83–100, 1999.

[FIS 04] FISCHER V., Composants logiciels pour le dimensionnement en Génie Electrique – application à la résolution d'équations différentielles, PhD thesis, Grenoble Institute of Technology, 2004.

[GAA 11] GAALOUL S., VERDIÈRE F., DELINCHANT B., WURTZ F., "Interface component architecture for building simulation", *IBPSA 2011*, Sydney, November 2011.

[GER 01] GERBAUD L., BIGEON J., "Elaboration d'un modèle mixant des approches symboliques et numériques pour le dimensionnement des convertisseurs statiques: problème particulier des intégrales semi-numériques des formules efficaces et moyennes", *RIGE*, vol. 4, pp. 77-104, 2001.

[GER 93] GERBAUD L., Aide à la conception des ensembles machine – convertisseur – commande: apport d'une démarche système expert, PhD thesis, Grenoble Institute of Technology, 1993.

[GER 00] GERBAUD L., Gentiane: une Plate-Forme pour la Conception des Ensembles Machine-Convertisseur-Commande, Habilitation à diriger des recherches, Grenoble Institute of Technology, 2000.

[GER 12] GERBAUD L., TOURÉ B., SCHANEN J.-L., CARAYON J-P, "Modelling process and optimisation of EMC filters for power electronics applications", *COMPEL*, vol. 31, pp. 747-763, 2012.

[GIT 89] GITOSUSASTRO S., COULOMB J.L., SABONNADIÈRE J.C., "Performance derivative calculations and optimization process", *IEEE Transactions on Magnetics*, vol. 25, pp. 2834-2839, 1989.

[KAU 10] KAUFFMANN P., HAGUET V., REYNE G., DELINCHANT B., "Efficient multipoles modeling for linear magnetized beads manipulations", *CEFC 2010*, Chicago, IL, 9-12 May, 2010.

[LAN 12] LANGE J.-F., GERBAUD L., NGUYEN-HUU H., ROUDET J., "Using constrained optimisation algorithm for the modeling of static converter harmonics", *COMPEL*, vol. 31, pp. 764-779, 2012.

[LI 11] LI L., Etude et Mise au Point d'une Nouvelle Famille d'Alterno-démarreurs pour Véhicules Hybrides et Electriques, PhD thesis, Grenoble Institute of Technology, 2011.

[MAR 08] MARIN C., Une approche orientée domaine pour la composition de services, PhD thesis, Joseph Fourier University, 2008.

[MAG 03] MAGOT D., WURTZ F., COGITORE B., DELINCHANT B., KERADEC J-P., "Methodology and tools for worst-case tolerance design", *COMPUMAG 2003*, New York, 13-18 July, 2003.

[MOK 10] MOKHTARI L., DELINCHANT B., CHEVALIER T., COULOMB J.-L., "Comparing weak and strong PEEC-MoM coupling", *IEEE Transactions on Magnetics*, vol. 46, pp. 2775-2778, 2010.

[NGU 07] NGUYEN-HUU H., WURTZ F., RETIÈRE N., DELINCHANT B., "Composition of optimization algorithms by using software components for optimization of electromagnetic devices", *COMPUMAG 2007*, Aachen, Germany, 24-28 June, 2007.

[NGU 08a] NGUYEN-HUU H., RETIERE N., WURTZ F., "A new approach for building the global Pareto border of an electromagnetic system by using the Pareto borders of each sub-component of the system", *CEFC 2008*, 11-15 May, Seoul, Athens, p. 195, 2008.

[NGU 08b] NGUYEN-HUU H., SARENI B., WURTZ F., RETIÈRE N., ROBOAM X., "Comparison of self-adaptive evolutionary algorithms for multimodal optimization" *OIPE'2008*, Ilmenau, Germany, 15-17 September, 2008.

[NGU 10] NGUYEN-HUU H., GERBAUD L., RETIÈRE N., ROUDET J., WURTZ F., "Analytical modeling of static converters for optimal sizing of on-board electrical systems", *IEEE-VPPC'2010* (Vehicle power and propulsion conference), Lille, France, 1-3 September, 2010.

[PAP 03] PAPAZOGLOU M. P., "Service-oriented computing: concepts, characteristics and direction", *WISE'03*, *Fourth Int. Conf. on Web Information Systems Engineering*, Rome, Italy, December 10-12, 2003.

[PHA 11a] PHAM-QUANG P., DELINCHANT B., COULOMB J.L., DU PELOUX B., "Semi-analytical magneto-mechanic coupling with contact analysis for MEMS/NEMS", *IEEE Transactions on Magnetics*, vol. 47, pp. 922-925, 2011.

[PHA 11b] PHAM-QUANG P., Modélisation magnéto-mécanique d'un nano commutateur. Optimisation sous contraintes de fiabilité par dérivation automatique des programmes en Java, PhD thesis, University of Grenoble, 2011.

[PHA 11c] PHAM-QUANG P., DELINCHANT B., ILIE C., SLUSANSCHI E., COULOMB J.L., DU PELOUX B., "Mixing techniques to compute derivatives of semi-numerical models: application to magnetic nano switch optimization", *COMPUMAG'11*, Sydney, Australia, July 2011.

[PIG 09] PIGOT CH., DELINCHANT B., POULIN G., REYNE G., "Optimization of a 3D micro-accelerometer based on diamagnetic levitation", *International Journal of Applied Electromagnetics and Mechanics*, vol. 30, pp. 179-188, 2009.

[RAK 07a] RAKOTOARISON H.L., Méthode et outil de génération automatique de modèle pour l'optimisation fortement contrainte des microsystèmes magnétiques, PhD thesis, Joseph Fourier University, 2007.

[RAK 07b] RAKOTOARISON H.L., YONNET J.P., DELINCHANT B., "Using Coulombian approach for modeling scalar potential and magnetic field of a permanent magnet with radial polarization", *IEEE Transactions on Magnetics*, vol. 43, pp. 1261-1264, 2007.

[RAK 08] RAKOTOARISON H.L., ARDON V., CHADEBEC O., DELINCHANT B., GUÉRIN S., COULOMB J.-L., "Formal sensitivity computation of magnetic moment method", *IEEE Transactions on Magnetics*, vol. 44, pp. 1014-1017, 2008.

[ROB 06] ROBOAM X., ASTIER S., Graphes de liens causaux pour systèmes à énergie renouvelable, *Techniques de l'Ingénieur*, vol. D 3 970, pp. 1-18, 2006.

[ROB 12] ROBOAM X., *System Design Methodologies for Electrical Energy Systems*, ISTE, London, John Wiley & Sons, New York, 2012 (forthcoming)

[ROT 41] ROTERS H., *Electromagnetic Devices*, John Wiley and Sons, New York, USA, 1941.

[MAG 04] MAGOT D., Méthodes et outils logiciels d'aide au dimensionnement. application aux composants magnétiques et aux filtres passifs, PhD thesis, Grenoble Institute of Technology, 2004.

[MOK 11] MOKHTARI L., DELINCHANT B., COULOMB J-L., LE DUC T., CHADEBEC O., GUICHON J-M., MEUNIER G., "Software coupling and orchestration tool to the modeling of multi-physic problems", *COMPUMAG'11*, Sydney, Australia, July 2011.

[REZ 11] REZGUI A., GERBAUD L., DELINCHANT B., "VHDL-AMS to support DAE-PDE coupling and multilevel modeling" *COMPUMAG'11*, Sydney, Australia, July 2011.

[SAL 00] SALTELLI A., CHAN K., SCOTT M., *Sensitivity Analysis*, Wiley Series in Probability and Statistics, John Wiley and Sons, New York, 2000.

[SAU 00a] SAUVEY C., Environnement de conception pour machines à réluctance variable, PhD thesis, Grenoble Institute of Technology, 2000.

[SAU 00b] SAUVEY C., WURTZ F., BAR F., ROSNET P., FANDINO J., BIGEON J., "Intégration du calcul des racines d'un polynôme dans une méthodologie d'optimisation de type gradient", *NUMELEC'2000*, Poitiers, France, pp. 114-115, 20-22 March 2000.

[SES 11] SESSANGA B., Optimisation de Gammes: Application à la Conception des Machines Synchrones à Concentration de Flux, PhD thesis, University of Grenoble, 2011.

[SZY 98] SZYPERSKY C., *Component Software – Beyond Object-Oriented Programming*, Addison-Wesley, New York, 1998.

[TSO 07] TSOMPANAKIS Y., LAGAROS N.D., PAPADRAKAKIS M., *Structural Design Optimization Considering Uncertainties*, Structures and Infrastructures collection, Taylor & Francis, London, 2007.

[WAL 08] WALTHER A., GRIEWANK A., Adol-C: a package for the automatic differentiation of algorithms written in C/C++, Technical report, Institute of Scientic Computing, Technische Universität Dresden, Germany, Version 2.0.0, December 2008.

[WUR 96] WURTZ F., Une nouvelle approche pour la conception sous contraintes de machines électriques, PhD thesis, Grenoble Institute of Technology, 1996.

[WUR 08a] WURTZ F., Conceptions de la conception pour le génie électrique: de l'approche "Objets –Savoirs – Méthodes – Outils" à l'approche "Systèmes – Connaissances – Compétences – Organisations", thesis, Grenoble Institute of Technology, 2008.

[WUR 08b] WURTZ F., "Méthodes et outils d'optimisation pour une conception énergétique efficace des composants et systèmes électriques", *REE (Revue de l'Electricité et de l'Electronique)*, vol. 5, pp. 120-130, 2008.

Chapter 6

# Technico-economic Optimization of Energy Networks

## 6.1. Introduction

The first five chapters of this book have addressed problems linked to the sizing and optimization of energy systems. In this chapter, we tackle the problem of the optimal driving of an existing system. Short-term optimal management (from several hours to several days) of energy systems is indeed a major industrial and social issue [SAN 05a]. Indeed, from a purely technical perspective, the emergence of new technologies (high-efficiency installations such as, for example, co-generations and consumer-demand prediction methods), combined with advances in calculation power, has enabled the management of production installations to be improved. From an economical perspective, the expansion of energy markets [RIO 07] has led to a highly competitive field that is forcing producers to optimize the management of their production facilities. Finally, from an environmental perspective, the issue is the reduction of pollutants, which can be facilitated using optimal and reasoned production management.

Thus, the management of a production, distribution, or energy storage network has become as much an environmental issue as a technical one,

---

Chapter written by Guillaume SANDOU, Philippe DESSANTE, Marc PETIT and Henri BORSENBERGER.

*Integrated Design by Optimization of Electrical Energy Systems* Edited by Xavier Roboam
© 2012 ISTE Ltd. Published 2012 by ISTE Ltd.

before even considering environmental and legislative constraints. It appears, therefore, that management needs to be optimized so that the operational benefits of the network can be maximized, while observing the constraints imposed. This task is made more complex by virtue of the diversification of energy sources, which may coexist within the same network (such as electricity, gas, oil and steam). In addition, modeling this type of system should integrate uncertainties linked to parameter identification, or simplification of the model (with a view to its optimization), or uncertainties stemming from the provisional nature of the planning relating to system function (such as actual consumer demand and economic fluctuations). This being the case, it is imperative that this optimal management is robust, so that system performance can be guaranteed, in spite of the different sources of uncertainty. This robustness problem is similar to the problem of operational safety, which was addressed in Chapter 8 of [ROB 12].

Section 6.2 presents the modeling used for energy networks. This modeling is very similar to that used in "Unit commitment". We pay particular attention to the sources of uncertainty presented for the system being considered. Solving this problem in a deterministic case, i.e. with no uncertainty, is addressed in section 6.3. After recent development regarding possible methods that can be used to study this problem, we focus more specifically on solutions using dynamic programming and Lagrangian relaxation. This method can be extended to solving problems involving uncertainties.

We then address the optimization of an energy network subjected to uncertainties. Following a brief introduction into the consideration of uncertainties in section 6.4, section 6.5 presents the solution to the problem for the traditional case of uncertainties over consumer demand. Section 6.6 then shows the results obtained in the case of uncertainties over production costs. This type of uncertainty is specifically encountered for a co-generation installation for which the resale price of electricity would be uncertain as it is indexed over the electricity market. Finally, in section 6.7, we address a second approach enabling the system to be made more robust regarding errors in consumer-demand prediction. This approach uses the closed-loop philosophy and is based on the principles of predictive control.

## 6.2. Energy network modeling

### 6.2.1. *Context*

The objective is to optimize the operation of a network that transports energy from a set of producers to a set of consumers. The energy transported may be in the form of heat or electricity. The issue is thus to maximize the efficiency of the installation. Indeed, in general, network administrators, whether electrical or thermal, are in a virtual monopoly position. Consequently, optimization of cost-effectiveness involves minimizing operating costs. This criterion, therefore, provides a good indicator of the performance of an energy network.

These networks present physical impossibilities and constraints, the common one being the balance between production and consumption, at least for the electrical networks. Other notable constraints relate to production dynamics, stop-start cycles, and minimum shutdown or operation times. In addition, these same stop-start cycles lead to overspend due to wear and tear or due to the energy used to start production. Consequently, the decision to start a production center, or even keep it operating, has significant consequences.

As a result of these constraints and characteristics, the efficient direction of these networks must be made in advance by anticipating consumption for a particular temporal horizon and by readjusting production plans based on demand. Note that the different dynamics coming into play (such as propagation times in thermal networks and stop-start cycles) impose a significant anticipation horizon of around a day. This will have significant consequences on optimization by considerably increasing the number of variables to be taken into account, as well as introducing uncertainties linked to anticipation into the model, as we will see in the following sections.

### 6.2.2. *Notations*

We consider here a set of $K$ producers working together to satisfy consumer energy demand. The temporal horizon is split into $N$ temporal periods (typically a day split into 24 hour segments). A very traditional model is used. The following notations will be used throughout this chapter:

– $Q_n^k$ : power produced by installation $k$ during period $n$; this is a real variable;

– $u_n^k$ : operating state (on = 1, off = 0) of installation $k$ during period $n$; this is a binary variable;

– $Q_n^{dem}$ : consumer demand during period $n$.

### 6.2.3. *Objective function*

The objective function is written as follows, referring to the total costs linked to the operation of a production unit (fuel, usage, etc.). These costs are represented using the following function:

$$\sum_{n=1}^{N}\sum_{k=1}^{K} c_{prod}^k(Q_n^k, u_n^k) + c_{on/off}^k(u_{n-1}^k, u_n^k) \qquad [6.1]$$

The costs of production are expressed by:

$$c_{prod}^k(Q_n^k, u_n^k) = \alpha_1^k Q_n^k + \alpha_0^k u_n^k \qquad [6.2]$$

Here we have chosen a linear expression for the costs of production in order to simplify the illustration. It is quite clearly possible to use more complicated expressions, such as quadratics, in the production variable or even in table form from actual measurement points.

In equation [6.2], $\alpha_1^k$ represents the total costs based on production (typically fuels and fossil-based raw materials, for instance) and $\alpha_0^k$ represents the total fixed costs (linked to wear and tear, for example). Some of these costs may be affected by uncertainties. This is notably so for a cogeneration installation selling electricity at a variable price based on market conditions. This is also the case when there is a waste incinerator involved.

The calorific power from incinerated waste is indeed variable over time and the efficiency of the thermal energy production is therefore uncertain. In general, coefficients $\alpha_0^k$ and $\alpha_1^k$ are usually identified from measuring points and are therefore subject to estimation errors. How this uncertainty is handled will be studied in section 6.6.

The stop-start costs are expressed by:

$$c_{on/off}^k(u_{n-1}^k, u_n^k) = c_{start}^k u_n^k (1 - u_{n-1}^k) + c_{down}^k u_{n-1}^k (1 - u_n^k) \qquad [6.3]$$

$c_{start}^k$ represents the total costs linked to the startup of unit $k$ and $c_{down}^k$ the total costs linked to its shutdown. It is partly due to wear and tear, or to the energy used to start them up, that production units are affected by these operations. These costs are difficult to calculate and so the values used here are therefore estimates. These are again unknown parameters, which also make the cost function uncertain.

### 6.2.4. *Constraints*

#### 6.2.4.1. *Demand satisfaction constraint*

This is the main constraint of the problem. It is also called an equilibrium constraint, as the balance between production and consumption is a central problem for energy networks and, in particular, electrical networks. In the thematic for the unit commitment problem, it is also called a coupling constraint, as it links the production of various units between each other:

$$\sum_{k=1}^{K} Q_n^k \geq Q_n^{dem}, \quad \forall n \in \{1, \ldots, N\} \qquad [6.4]$$

In the case of electrical networks, this constraint is replaced by an equality. However, even in that case, an inequality can be used. Indeed, the optimal policy is to produce as little as possible. Consequently, the optimization algorithm will naturally find a solution that is very close to the equality. As a consequence of the various time constants implied in the operation of the network, production is planned in advance. The exact value

of $Q_n^{dem}$ is thus unknown and an estimate of consumption is used. This estimate is naturally affected by uncertainties, which will require an adjustment during production in order to retain the balance required for optimization.

6.2.4.2. *Capacity constraint*

This constraint restricts the production of units. This restriction may have a physical origin, or result from the network management policy. It is expressed as follows:

$$\underline{Q}^k u_n^k \le Q_n^k \le \overline{Q} u_n^k, \quad \forall n \in \{1,\ldots,N\}, \forall k \in \{1,\ldots,K\} \qquad [6.5]$$

$\underline{Q}^k$ (and $\overline{Q}^k$) represents the minimum (and maximum, respectively) production capacity for installation $k$. We note that the restrictions may be affected by uncertainties, for example for wind production or photovoltaic units.

6.2.4.3. *Minimum up- and downtime constraints*

These constraints reflect installation dynamics and the impossibility for a unit to alternate quickly between on and off states. They are expressed by the following logical implications:

$$\begin{aligned} &\left(u_{n-1}^k = 0, u_n^k = 1\right) \Rightarrow \left(u_{n+j}^k = 1, \forall j \in \left\{1,\ldots,T_{up}^k\right\}\right) \\ &\left(u_{n-1}^k = 1, u_n^k = 0\right) \Rightarrow \left(u_{n+j}^k = 0, \forall j \in \left\{1,\ldots,T_{down}^k\right\}\right) \\ &\qquad\qquad \forall n \in \{1,\ldots,N\}, \forall k \in \{1,\ldots,K\} \end{aligned} \qquad [6.6]$$

where $T_{up}^k$ and $T_{down}^k$ are the minimum on and off time intervals, respectively, specified for each unit.

### 6.2.5. *Expression of the problem and eventual linear reformulation*

The applied problem can finally be written as follows:

$$\min_{\left\{\substack{u_n^k, Q_n^k \\ n=1,\ldots,N \\ k=1,\ldots,K}\right\}} \sum_{n=1}^{N}\sum_{k=1}^{K}\begin{pmatrix} \alpha_1^k Q_n^k + \alpha_0^k u_n^k \\ +c_{start}^k u_n^k (1-u_{n-1}^k) + c_{down}^k u_{n-1}^k (1-u_n^k) \end{pmatrix}$$

$$\begin{aligned} s.t. \quad & \sum_{k=1}^{K} Q_n^k \geq Q_n^{dem}, \quad \forall n \in \{1,\ldots,N\} \\ & \underline{Q}^k u_n^k \leq Q_n^k \leq \overline{Q} u_n^k, \quad \forall n \in \{1,\ldots,N\}, \forall k \in \{1,\ldots,K\} \\ & \left(u_{n-1}^k = 0, u_n^k = 1\right) \Rightarrow \left(u_{n+j}^k = 1, \forall j \in \left\{1,\ldots,T_{up}^k\right\}\right) \\ & \qquad \forall n \in \{1,\ldots,N\}, \forall k \in \{1,\ldots,K\} \\ & \left(u_{n-1}^k = 1, u_n^k = 0\right) \Rightarrow \left(u_{n+j}^k = 0, \forall j \in \left\{1,\ldots,T_{down}^k\right\}\right) \\ & \qquad \forall n \in \{1,\ldots,N\}, \forall k \in \{1,\ldots,K\} \end{aligned} \qquad [6.7]$$

As such, the problem presents a quadratic cost function (from the start and stop costs, which involve products of optimization variables $u_n^k u_{n-1}^k$) and nonlinear constraints. If required (based on the resolution method used), it is possible to reformulate this problem linearly by introducing on and off variables $\delta_n^k$ and $\varepsilon_n^k$, respectively:

$$\begin{cases} \delta_n^k = u_n^k (1-u_{n-1}^k) \\ \varepsilon_n^k = u_{n-1}^k (1-u_n^k) \end{cases} \qquad [6.8]$$

Equivalently and linearly, these variables can be expressed by the following set of linear constraints:

$$\begin{cases} \delta_n^k \leq u_n^k \\ \delta_n^k \leq (1-u_{n-1}^k) \\ \delta_n^k \geq u_n^k - u_{n-1}^k \end{cases} \text{ and } \begin{cases} \varepsilon_n^k \leq u_{n-1}^k \\ \varepsilon_n^k \leq (1-u_n^k) \\ \varepsilon_n^k \geq u_{n-1}^k - u_n^k \end{cases} \qquad [6.9]$$

Hence, problem [6.7] can be re-written as:

$$\min_{\left\{\begin{matrix} u_n^k, Q_n^k, \delta_n^k, \varepsilon_n^k \\ n=1,\ldots,N \\ k=1,\ldots,K \end{matrix}\right\}} \sum_{n=1}^{N}\sum_{k=1}^{K}\left(\alpha_1^k Q_n^k + \alpha_0^k u_n^k + c_{start}^k \delta_n^k + c_{down}^k \varepsilon_n^k\right)$$

$$\begin{aligned} s.t. \quad & \sum_{k=1}^{K} Q_n^k \geq Q_n^{dem}, \quad \forall n \in \{1,\ldots,N\} \\ & \underline{Q}^k u_n^k \leq Q_n^k \leq \overline{Q} u_n^k, \quad \forall n \in \{1,\ldots,N\}, \forall k \in \{1,\ldots,K\} \\ & \sum_{j=1}^{T_{up}^k} u_{n+j}^k \geq T_{up}^k \delta_n^k, \quad \forall n \in \{1,\ldots,N\}, \forall k \in \{1,\ldots,K\} \\ & \sum_{j=1}^{T_{down}^k} (1-u_{n+j}^k) \geq T_{down}^k \varepsilon_n^k, \quad \forall n \in \{1,\ldots,N\}, \forall k \in \{1,\ldots,K\} \end{aligned} \qquad [6.10]$$

Therefore, the reformulated problem is totally linear. This may be some help for a completely mixed programming algorithm solution, such as "branch and bound" [LAN 60]. Indeed, this type of algorithm requires solutions to problems that ignore integer constraints. Since the corresponding problems are linear, they can be effectively solved using the simplex algorithm. In using this algorithm, it should be noted that an adapted "branch" (the "branch" phase of the algorithm) strategy means that, by introducing the on and off variables $\delta_n^k$ and $\varepsilon_n^k$, no supplementary combinatory complexity is added.

### 6.2.6. *Position of the problem processed relative to the problem of energy network management*

Attentive readers will have noticed that the modeling presented here corresponds more to production than to energy networks. However, in the vast majority of cases, the distribution aspect is virtually disconnected from the production aspect. A macro-model is available for the network itself so that production graphs can be established before being produced for each production site. To obtain complete satisfaction, this production graph must therefore be spread across these sites.

The model here is therefore applied to these production sites. Thus consumer demand can be interpreted on a case-by-case basis, as if for an actual consumer, or even as for the overall production curve applicable to the production site (the demand from the distribution network). Consideration of the distribution network may occur by introducing propagation delays by modifying, for instance, the equilibrium constraint [6.4] using the following constraint:

$$\sum_{k=1}^{K} Q_{n-n_k}^{k} \geq Q_n^{dem}, \quad \forall n \in \{1,\ldots,N\} \qquad [6.11]$$

where $n_k$ is the propagation delay between the producer and the consumer. This delay exists and cannot be ignored for district heating networks, where it corresponds to the fluid propagation delay. If there are multiple consumers, a constraint of this type must be introduced for each consumer and coupling constraints for the production of each site (the sum of energy delivered by a producer to all consumers must be equal to the energy generated by the producer). Of course there are more refined distribution network models (electrical or thermal), which take into account variable propagation times and line losses. In the case of heat networks, examples are [ARV 01], [SAN 05a] and [LAR 02].

The corresponding modeling can be achieved using partial differential equations. The handling of this type of problem goes beyond the context of this chapter. We are now going to address the resolution of the problem described in this section by starting with the deterministic case, i.e. with no uncertainty.

## 6.3. Resolution of the energy network optimization problem for a deterministic case

### 6.3.1. *State of the art*

A number of resolution methods have been used to solve this optimization problem. A very good bibliography on this subject can be found, for example, in [SEN 98]. Amongst the methods to be found in literature, the following can be distinguished:

– exact methods: amongst these methods, we essentially have the *branch and bound* [CHE 93] and dynamic programming [HOB 88; OUY 91] algorithms. As these algorithms solve the exact problem, their algorithmic complexity is exponential. This type of optimization method is therefore necessarily restricted to small-scale systems, i.e. those with a reduced number of producers;

– deterministic approximation methods: another class of method is made up of methods that are approximations but deterministic. Amongst these methods, we find, for example, priority list [SAN 05b; SEN 04], or expert system [LI 08] methods and relaxation-based methods such as Lagrangian relaxation [BAK 00; DOT 99; FER 93; ROO 94; TAK 00; ZHA 02];

– stochastic approximation methods: amongst these methods, we find simulated annealing [YIN 98; ZHU 98], genetic [KAS 96; MA 95; POO 08; SAN 08], and ant colony [SAN 04] based algorithms. This type of algorithm does not enable the exact solution to the optimization problem to be found, but allows solutions that are over-optimal but of good quality in a reasonable time. Except for the ant colony algorithm, which explicitly manages the problem constraints, quite specific attention must be paid to satisfying constraints due to the random characteristic of displacements within the search space;

– hybrid methods. The objective is the association of multiple resolution methods in order to combine the advantages from them. Thus, here we find methods that make use of genetic algorithms to optimize Lagrangian relaxation parameters [CHE 00; DUO 99; OHT 96; ORE 97; SHE 96], methods associating multiple stochastic methods (simulated annealing and genetic algorithms in [CHE 02; YIN 01], genetic and ant colony algorithms in [SAN 08b], and methods associating genetic algorithms with a tabu search in [MAN 99; RAJ 04]).

In the following section, we have chosen (section 6.3.2) to focus on resolution using dynamic programming algorithms, from the possibility of extension to robust optimization problems. We will finally resolve the problem using the genetic algorithm (section 6.3.3). Note that in the context of this section, we place ourselves within the deterministic context.

### 6.3.2. *Resolution by dynamic programming and Lagrangian relaxation*

#### 6.3.2.1. *Resolution by dynamic programming*

##### 6.3.2.1.1. Dynamic programming principle

Dynamic programming is an optimization technique that uses Bellman's optimality principle. Let us consider a system characterized at instant $n$ by state variables $x_n$ and driven by a decision quantity $u_n$. Under the impact of this decision, the system evolves into state $x_{n+1}$ according to its transition law:

$$x_{n+1} = \phi(x_n, u_n) \qquad [6.12]$$

In parallel, we seek to optimize system operation by searching for the optimal control policy in the form:

$$\begin{aligned} &\min_{\{u_n, n=1,\ldots,N\}} \sum_{n=1}^{N} c_{trans}(x_{n-1}, x_n) + c_{state}(x_n) \\ &s.t \quad x_{n+1} = \phi(x_n, u_n) \end{aligned} \qquad [6.13]$$

where:

- $c_{trans}(x_{n-1}, x_n)$ is the transition cost from $x_{n-1}$ to $x_n$;
- $c_{state}(x_n)$ is the cost of passing through state $x_n$.

In this case, the problem can be solved using the recurrence optimality equation, which is generally solved using countdown time:

$$\begin{aligned} F_n(x_n) &= \min_{u_n} c_{trans}(x_n, x_{n+1}) + F_{n+1}(x_{n+1}) \\ &= \min_{u_n} c_{trans}(x_n, \phi(x_n, u_n)) + F_{n+1}(\phi(x_n, u_n)) \end{aligned} \qquad [6.14]$$

##### 6.3.2.1.2. Elimination of real variables

In the context of unit commitment problem [6.10], it is possible to eliminate the real variables $Q_n^k$ and to calculate them from binary variables $u_n^k$. Let us thus assume that variables $u_n^k$ are given and correspond to production planning

that does not violate the constraints. The production variables $Q_n^k$ are then solutions to the following problem:

$$\begin{aligned}
&\arg \min_{\left\{\substack{Q_n^k \\ n=1,\ldots,N \\ k=1,\ldots,K}\right\}} \sum_{n=1}^{N}\left(\sum_{k=1}^{K}(c_{prod}^k(Q_n^k,u_n^k)+c_{on/off}^k(u_n^k,u_{n-1}^k))\right) \\
&= \arg \min_{\left\{\substack{Q_n^k \\ n=1,\ldots,N \\ k=1,\ldots,K}\right\}} \left(\sum_{n=1}^{N}\sum_{k=1}^{K}(c_{prod}^k(Q_n^k,u_n^k))\right) \\
&= \arg \min_{\left\{\substack{Q_n^k \\ n=1,\ldots,N \\ k=1,\ldots,K}\right\}} \left(\sum_{n=1}^{N}\sum_{k=1}^{K}\alpha_1^k Q_n^k u_n^k\right)
\end{aligned} \qquad [6.15]$$

Various simplifications introduced into the equation above result from the optimization of variables $Q_n^k$ at given values for $u_n^k$. Hence, any term that is not dependent on $Q_n^k$ can be suppressed from the cost function to be optimized. Planning is assumed to be feasible. Therefore there are no longer any constraints coupling multiple temporal periods and the problem can be divided into $N$ independent problems:

$$\begin{aligned}
&\min_{\left\{\substack{Q_n^k \\ k=1,\ldots,K}\right\}} \left(\sum_{k=1}^{K}\alpha_1^k Q_n^k u_n^k\right) \\
&\text{s.c} \begin{cases} \sum_{k=1}^{K} Q_n^k \geq Q_n^{dem} \\ \underline{Q}^k u_n^k \leq Q_n^k \leq \overline{Q}^k u_n^k \end{cases}
\end{aligned} \qquad [6.16]$$

Without loss of generality, let us consider that $\alpha_1^1 \leq \alpha_1^2 \leq \ldots \leq \alpha_1^K$, then the solution is to produce as much as possible with the most cost-effective installations. This comment results in the following recursively calculated values being chosen as production variables:

$$\begin{cases} Q_n^1 = \min\left(\max\left(Q_n^{dem} - \sum_{i=2}^{K} \underline{Q}^i u_n^i, \underline{Q}^1\right), \overline{Q}^1\right) u_n^1 \\ \vdots \\ Q_n^k = \min\left(\max\left(Q_n^{dem} - \sum_{i=1}^{k-1} Q_n^i - \sum_{i=k+1}^{K} \underline{Q}^i u_n^i, \underline{Q}^k\right), \overline{Q}^k\right) u_n^k \\ \vdots \\ Q_n^K = \min\left(\max\left(Q_n^{dem} - \sum_{i=1}^{K-1} Q_n^i, \underline{Q}^K\right), \underline{Q}^K\right) u_n^K \end{cases} \quad [6.17]$$

The optimization problem can therefore be reformulated into a completely binary variable problem, where the optimization variables are a sequence of on and off decisions from the production installations.

6.3.2.1.3. Resolution without consideration of minimum start and stop time constraints

In the case where minimum start and stop time constraints are not considered, the state of the production system is characterized by the states of each installation. Thus, in relation to the development of equation [6.14], we have:

$$\begin{cases} x_n = (u_n^1, u_n^2, \ldots, u_n^K) \\ u_n = (u_{n+1}^1, u_{n+1}^2, \ldots, u_{n+1}^K) \end{cases} \quad [6.18]$$

Hence, in this case, the recurrence optimality equation [6.14] becomes:

$$F_n(x_n) = \min_{u_n = (u_{n+1}^1, \ldots, u_{n+1}^K)} \left( \begin{array}{l} \sum_{k=1}^{K} \alpha_1^k Q_{n+1}^k + \alpha_0^k u_{n+1}^k \\ + c_{start}^k u_{n+1}^k (1 - u_n^k) + c_{down}^k u_n^k (1 - u_{n+1}^k) \\ + F_{n+1}(x_{n+1}) \end{array} \right) \quad [6.19]$$

6.3.2.1.4. Consideration of minimum start and stop times

In this case, the start state of each installation is no longer an indicator of the system's past. It is necessary to know length of the start or stop states in consecutive hours in order to understand future development. Thus, in this case, we introduce a quantity $x_n^k$, which characterizes the number of consecutive start ($x_n^k$ is thus positive) or stop ($x_n^k$ is thus negative) hours:

$$\begin{cases} \left(x_n^k > 0 \;\&\; u_{n+1}^k = 1\right) \Rightarrow x_{n+1}^k = x_n^k + 1 \\ \left(x_n^k > 0 \;\&\; u_{n+1}^k = 0\right) \Rightarrow x_{n+1}^k = -1 \\ \left(x_n^k < 0 \;\&\; u_{n+1}^k = 1\right) \Rightarrow x_{n+1}^k = 1 \\ \left(x_n^k < 0 \;\&\; u_{n+1}^k = 0\right) \Rightarrow x_{n+1}^k = x_n^k - 1 \end{cases} \qquad [6.20]$$

This equation thus characterizes the transition relation $\varphi$. In this case, the following are therefore used:

$$\begin{cases} x_n = (x_n^1, x_n^2, \ldots, x_n^K) \\ u_n = (u_{n+1}^1, u_{n+1}^2, \ldots, u_{n+1}^K) \end{cases} \qquad [6.21]$$

6.3.2.1.5. Limitations on the use of dynamic programming

The use of dynamic programming enables the problem to be solved exactly. However, this type of algorithm is impacted by combinatorial explosion when the number of units increases. Indeed, when the minimum start and stop time constraints are not considered, the number of possible states for the system at a given instant $n$ is $2^K$. Complexity is aggravated when temporal constraints are taken into account. In order to reduce this combinatorial explosion, Lagrangian relaxation is often used to decompose the problem into multiple reasonably sized sub-problems.

6.3.2.2. *Use of Lagrangian relaxation*

6.3.2.2.1. Problem formulation

In order to reduce the combinatorial complexity of the problem, we relax the constraints coupling multiple units, i.e. the demand satisfaction constraints.

Thus we introduce $N$ Lagrange multipliers $\lambda_n, n \in \{1,\ldots,N\}$ and the corresponding Lagrangian:

$$L = \sum_{n=1}^{N}\sum_{k=1}^{K}\begin{pmatrix} \alpha_1^k Q_n^k + \alpha_0^k u_n^k \\ +c_{start}^k u_n^k (1-u_{n-1}^k) + c_{down}^k u_{n-1}^k (1-u_n^k) \end{pmatrix} + \sum_{n=1}^{N}\lambda_n \left( Q_n^{dem} - \sum_{k=1}^{K} Q_n^k \right) \quad [6.22]$$

By changing the order of the terms and inverting the sums, the Lagrangian can be re-written:

$$L = \sum_{k=1}^{K}\left(\sum_{n=1}^{N}\begin{pmatrix} \left(\alpha_1^k - \lambda_n\right) Q_n^k + \alpha_0^k u_n^k \\ + c_{start}^k u_n^k (1-u_{n-1}^k) + c_{down}^k u_{n-1}^k (1-u_n^k) \end{pmatrix}\right) + \sum_{n=1}^{N}\lambda_n Q_n^{dem} \quad [6.23]$$

Using Lagrangian duality, we now need to resolve the following dual problem:

$$\max_{\left\{\lambda_n \atop n=1,\ldots,N\right\}} \min_{\left\{\begin{matrix} Q_n^k, u_n^k \\ n=1,\ldots,N \\ k=1,\ldots,K \end{matrix}\right\}} L$$

$$= \max_{\left\{\lambda_n \atop n=1,\ldots,N\right\}} \min_{\left\{\begin{matrix} Q_n^k, u_n^k \\ n=1,\ldots,N \\ k=1,\ldots,K \end{matrix}\right\}} \left( \begin{matrix} \sum_{k=1}^{K}\left(\sum_{n=1}^{N}\begin{pmatrix} (\alpha_1^k - \lambda_n) Q_n^k + \alpha_0^k u_n^k \\ + c_{start}^k u_n^k (1-u_{n-1}^k) \\ + c_{down}^k u_{n-1}^k (1-u_n^k) \end{pmatrix}\right) \\ + \sum_{n=1}^{N}\lambda_n Q_n^{dem} \end{matrix} \right) \quad [6.24]$$

6.3.2.2.2 Problem resolution method

For given Lagrange multipliers, problem [6.24] is a unit commitment problem with $K$ units, but which can be decomposed into $K$ problems with a single unit each. Each of these sub-problems can, therefore, be easily resolved using dynamic programming without being affected by combinatorial complexity.

The Lagrange multipliers $\lambda_n, n \in \{1,\ldots,N\}$ should then be optimized. One of the advantages arising from use of Lagrangian relaxation is the fact that the problem obtained is one of maximization of a concave function, for which any local optimum is, therefore, a global one.

Once dual equation [6.24] has been resolved, there is no guarantee that the solution found will be one that satisfies all of the constraints of the problem. Indeed, the initial resolved problem is a non-convex optimization problem and a duality "gap" may exist. Therefore, it is necessary to set up a post-processing stage, which enables the solution obtained to be "fixed". One possible method is to slightly increase the solution multipliers of the dual problem until a solution is obtained that satisfies all of the constraints.

### 6.3.3. *Resolution by genetic algorithm*

Here we present resolution of the problem using a method of approximation, the genetic algorithm. The advantage of this type of algorithm is in the ability to handle large-scale cases, and to be easily extended to multi-objective problems. These algorithms were introduced in Chapter 2 of this book, more specifically for optimal simultaneous design problems.

6.3.3.1. *Consideration of constraints*

As we have seen, the unit commitment problem is a highly constrained one. The genetic algorithm is a non-constrained optimization algorithm requiring some care so that constraints can be taken into account. In our case, we choose to have recourse to a penalty function. The objective of equation [6.7] is therefore transformed into:

$$\min_{\left\{\begin{matrix} u_n^k, Q_n^k \\ n=1,\ldots,N \\ k=1,\ldots,K \end{matrix}\right\}} \sum_{n=1}^{N}\sum_{k=1}^{K} \left( \begin{matrix} \alpha_1^k Q_n^k + \alpha_0^k u_n^k \\ +c_{start}^k u_n^k (1-u_{n-1}^k) + c_{down}^k u_{n-1}^k (1-u_n^k) \\ \left((1+\varepsilon)\, c^f + h\left(\left\{u_n^k, Q_n^k\right\}\right)\right).B\left(\left\{u_n^k, Q_n^k\right\}\right) \end{matrix} \right) \qquad [6.25]$$

which is an equation in which:

– $\varepsilon$ is a small positive real number;

– $c^f$ is the cost of a known feasible solution;

– $h\left(\left\{u_n^k, Q_n^k\right\}\right)$ is a penalty function (for example, the number of violated constraints, or the quadratic deviation of the constraint violations);

– $B\left(\left\{u_n^k, Q_n^k\right\}\right)$ is a Boolean equal to 1 if the solution violates the constraints and equal to 0 if it satisfies them.

The proposed objective enables assurance that there is a higher cost associated with any solution violating the constraints than with the known feasible solution. We note that it is not very difficult to find such a solution, a solution where all units are active over the temporal periods being generally feasible.

6.3.3.2. *Introduction of suitable genetic operators for the problem*

Traditional genetic algorithm operators only have a low probability of creating feasible individual solutions. Indeed, if we take the mutation operator example, complementing a variable will most likely lead to violation of the minimum start/stop time constraints. In order to improve the quality of results, it is useful to introduce supplementary genetic operators, which increases the probability of obtaining feasible individuals, by using *a priori* system knowledge.

Therefore, we have introduced the following operators: the exchange operator, the selective mutation operator, and operators that are “all on” and “all off”.

6.3.3.2.1. Planning exchange operator

The planning exchange operator is represented in Figure 6.1 and refers to internal crossing for an individual by exchanging the planning of two production units. Creation of this operator is motivated by the fact that some production installations are more cost-effective than others.

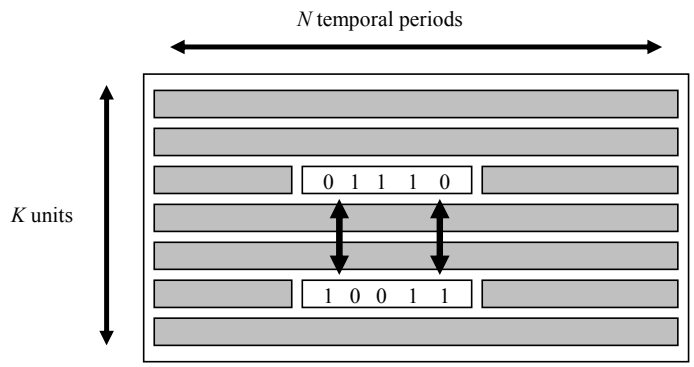


**Figure 6.1.** *Planning exchange operator*

6.3.3.2.2. Selective mutation operator

The genes that are more likely to mutate and thus to result in a feasible solution are those that we can switch on or off. Therefore, we need to detect these genes for the individual concerned and then carry out a random sampling for these genes. This operator is represented in Figure 6.2.

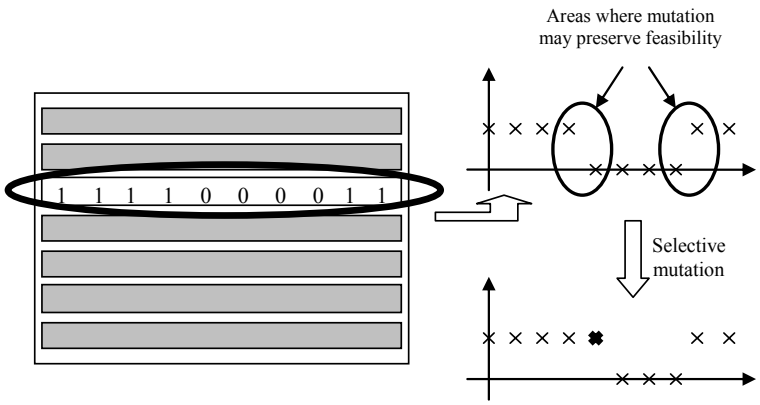


**Figure 6.2.** *Selective mutation operator*

6.3.3.2.3. “All on” and “all off” operator

Let us consider the situation in Figure 6.3: a constraint, in this case a minimum stop time constraint, may prevent a solution being reached where the production unit in question is on over the whole temporal horizon, which would result in interesting start/stop costs. With the operators above, one of the only possibilities would be two successive mutations (traditional or selective); the probability is low. We have therefore add an “all on” operator (and a complementary “all off” operator), which fires up (or puts out) a boiler between two randomly chosen instants.

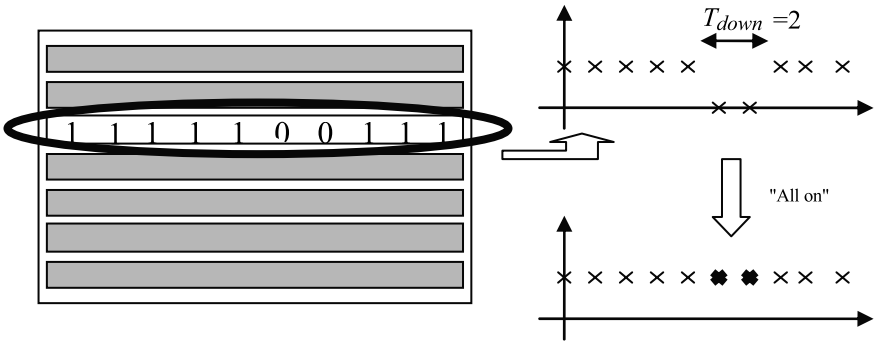


**Figure 6.3.** *“All on” operator*

6.3.3.2.4. Conclusion regarding these new operators

The operators presented here remain stochastic. Based on the *a priori* knowledge of the problem, they increase the probability of staying in feasibility space. We touch on a capital element here: a method is never frozen and we must make use of the *a priori* knowledge of the system to direct the solution.

6.3.3.3. *Numerical results*

Table 6.1 presents the results obtained for large-scale examples, over a temporal horizon of 24 hours. These tests have been carried out for given techniques and a given consumption, which enables advance knowledge of the optimal solution. Therefore, it is possible to work out the percentage cost deviation compared with the optimal solution. Generally, this is not possible. The results obtained are highly satisfactory, even for cases with 100 units or 2,400 binary variables.

Since the genetic algorithm is stochastic by nature, it is necessary to statistically validate it. Thus, each test is carried out 100 times and the best result obtained is shown, as well as the mean results and their standard deviation $\sigma$. Furthermore, we indicate the number of iterations for the algorithm used, as well as the corresponding computation times. In each case, the population size is fixed at 50 individuals.

| No. of units | No. of iterations | Best | Mean | $\sigma$ | Time |
|---|---|---|---|---|---|
| 10 | 500 | 29,815 € (+0.07%) | 30,016 € (+0.74%) | 185 € | 188 s |
| 20 | 500 | $1.50\times10^5$ € (+ 0.1%) | $1.51\times10^5$ € (+ 0.9%) | 710 € | 466 s |
| 40 | 1,000 | $5.56\times10^5$ € (+ 0.07%) | $5.59\times10^5$ € (+ 0.7%) | $1.76\times10^3$ € | 3,100 s |
| 60 | 1,500 | $1.21\times10^6$ € (+ 0.21%) | $1.22\times10^6$ € (+ 0.37%) | $3.45\times10^3$ € | 12,000 s |
| 80 | 2,000 | $2.14\times10^6$ € (+ 0.32%) | $2.15\times10^6$ € (+ 0.61%) | $6.83\times10^3$ € | 21,000 s |
| 100 | 2,000 | $3.34\times10^6$ € (+ 0.85%) | $3.36\times10^6$ € (+ 1.51%) | $1.50\times10^4$ € | 34,000 s |

**Table 6.1.** *Optimization results using the genetic algorithm*

## 6.4. Introduction to uncertainty consideration

### 6.4.1. *Consideration of uncertainties*

In section 6.3 we saw the problem of technico-economic optimization of an energy network being solved in a deterministic context. This deterministic approach to optimization problems for uncertain systems gives imperfect results. The optima obtained are affected by two defects:

– results presenting risks. Optimization algorithms generally force the system to its operating limits. Since the system parameters cause the operating point of the system and/or its constraints to vary, it is possible that the solution, initially thought to be feasible, could be found to be unworkable. This defect can generally be corrected by imposing an arbitrary

margin on the system, which comes at the cost of the performance of the solution;

– suboptimal results. When parameters vary, the location of the optimum also generally varies. Consequently, the optimum location obtained by the *a priori* resolution of the deterministic problem is not that of the real optimum, which can only be obtained *a posteriori* following observation of the parameters.

The optimization of uncertain systems is commonly called stochastic or robust optimization. The first developments in the field of stochastic optimization date back to the 1960s. The algorithms and theory have seen a boom over the past 20 years, particularly for chemical and economic problems [ACE 98; BEN 02; SAH 04]. The main challenge is to define a stochastic optimum in planning problems. In general, a stochastic optimum is one that minimizes the criterion expectancy or its standard deviation. Particularly in planning problems for energy networks, the general interest is in production cost expectancy. However, it is not easy to calculate this expectancy. The systems are not linear and the calculation time for evaluation of the criterion function is a barrier to the expectancy calculation over the uncertainty domain.

In addition, since the objective is to optimize a series of staggered decisions over time, these decisions may need to be modified in line with prediction readjustments. These readjustments use the new data acquired over time, such as new weather forecasting data, or variances in consumption compared with predictions. The integration of the readjustment into robust optimization problems draws on the notion of recourse, which is a central theme in stochastic optimization. Studies in this field draw on stochastic dynamic programming and multi-stage stochastic programming methods [PHI 00; NOW 00; DEN 98; GRO 05; CAR 98].

### 6.4.2. *Recourse notion*

The objective of robust optimization is to obtain an optimum that minimizes the expectancy of a criterion based on optimization variables. However, the system is not necessarily passive as far as uncertainty is concerned. It may include some adjustment mechanisms in order to adapt to risk. This adjustment is optional when it is a question of improving costs; on the other hand, it is indispensable in being able to satisfy constraints

impacted by an uncertain parameter. This is particularly so for energy and specifically electrical networks where the equilibrium constraint is fundamental to the stability of the network.

Regarding optimization, the stochastic system model may involve two types of optimization variable:

– traditional optimization variables (also known as "main stage" or "first stage" variables), for which all uncertain parameters are unknown;

– recourse variables (also known as "second stage" variables), for which some or all of the uncertain parameters are revealed.

More precisely, let us consider the simple two-stage recourse problem:

$$\min_x E_\alpha \left( \min_y f(x, y, \alpha) \right) \qquad [6.26]$$

where $\alpha$ is a random variable, $E_\alpha$ is the expectancy in relation to this variable, $x$ is the optimization variable and $y$ is the recourse variable. There is no limit to the number of stages that may make up an optimization problem with recourse. Indeed, if the recourse variables are decisions to come, they may also be disturbed by uncertainties and be the subject of adjustments. This is called multistage optimization.

Physically, the decision variables $x$ are variables that may be considered slow. They are important decisions, for which the consequences are spread over a relatively long period of time. They do not enable rapid reaction compared with a production risk or consumption prediction error, for example. In energy networks, most decisions to start up production units fall into this category. Very generally, they are actions that cannot be delayed.

Recourse variables, denoted here by $y$, are variables associated with higher-speed production methods, to "wait and see" decisions. This may be a heat production adjustment in furnaces for thermal networks, or even the start up of thermal units within electrical networks. More generally, these are decisions taken "later" relative to the first decision category, at an instant where the value of uncertain parameters will be known.

## 6.5. Consideration of uncertainties on consumer demand

In this section we focus on the consideration of uncertainty on the consumer demand curve. For electrical networks, the production-consumption balance is a strong constraint. In this study we do not need to know the prediction method for the load curve. Some methodology examples may be found in [DOT 02; NIE 00]. Consumer demand will simply be random data possessing a certain probability density.

### 6.5.1. *Safety margin*

A very simple way of taking the uncertainties on a load curve into account is to provide a safety margin. Thus, the following constraints are added to the optimization problem:

$$\sum_{k=1}^{K} \bar{Q}^k u_n^k \geq Q_n^{dem} + R_n, \quad \forall n \in \{1, \ldots, N\} \qquad [6.27]$$

where $R_n$ is the desired reserve or safety margin. Thus, the maximum producible power is greater than the predicted demand plus the reserve, which compensates for prediction errors. The implied hypothesis is that production variables can be adjusted in real time, whereas the on and off decisions are taken in advance. This is a recourse optimization hypothesis (see section 6.4.2).

### 6.5.2. *Scenario tree uncertainty modeling*

Consumer demand is considered to be a random series of $N$ values. This series is modeled using a scripted decomposition method known as a scenario tree. An example tree is given in Figure 6.4.

A scenario consists of a temporal series, where a value is taken for each period of the temporal horizon considered. In the tree, a scenario is represented by a set of $N$ nodes linked to each other from the root up to a leaf. There are as many scenarios as there are leaves. Therefore, the scenarios have common parts (the root and possibly other nodes), which are then differentiated, thus modeling successive risks. The number of scenarios corresponds directly to the level of detail to which the risk has been

modeled. On the other hand, the complexity of optimization problems is also directly linked to the number of nodes in the tree; therefore, it is necessary to establish a compromise between modeling finesse and problem complexity. Furthermore, a scenario tree enables the following elements to be taken into account:

– estimation error persistence: an error committed at a given instant has repercussions on later instances;

– the growth of uncertainty while the prediction is temporarily far away.

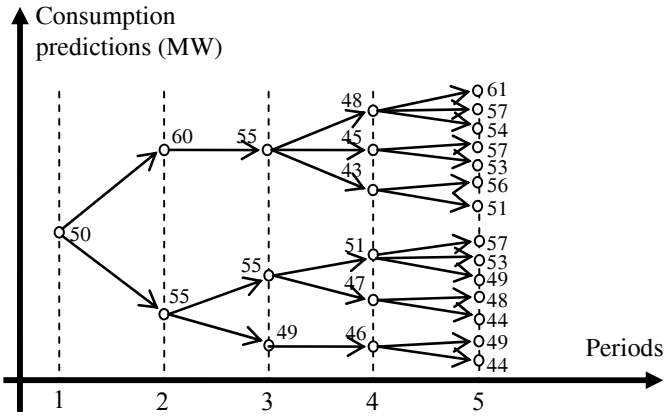


**Figure 6.4.** *Scenario tree example*

### 6.5.3. *Resolution by dynamic programming and Lagrangian relaxation*

We now use scenario tree uncertainty modeling in order to resolve the optimization problem. In order to do this, we extend the results developed in section 6.3, obtained using dynamic programming and Lagrangian relaxation. We refer to this as stochastic dynamic programming, an accepted solution for this type of problem solving [GRO 02; GRO 05].

At period $n$, the number of possible scenarios (i.e. the node number) is denoted by $\Xi_n$. Predicted demand is associated with each scenario and is denoted by $Q^{dem}_{n,\xi_n}, \xi_n = \{1,\ldots,\Xi_n\}$. A conditional probability is associated with each transition on the scenario tree. In order to simplify the notations, let us pose the following:

$$p_{\xi_n \to \xi_{n+1}} = p\left(Q_{n+1}^{dem} = Q_{n+1,\xi_{n+1}}^{dem} \,/\, Q_n^{dem} = Q_{n,\xi_n}^{dem}\right) \qquad [6.28]$$

This quantity is the probability that scenario $\xi_{n+1}$ is realized over a period $n+1$ if scenario $\xi_n$ is realized at period $n$.

The optimal controls must then be determined for each installation, for each period and scenario denoted by $u_{n,\xi_n}^k$. The quantities of corresponding energy produced, $Q_{n,\xi_n}^k$ may be deduced from these binary variables by re-using the recursive algorithm [6.17]. The demand satisfaction constraint is thus written:

$$\sum_{k=1}^{K} Q_{n,\xi_n}^k \geq Q_{n,\xi_n}^{dem}, \forall n \in \{1,\ldots,N\}, \forall \xi_n \in \{1,\ldots,\Xi_n\} \qquad [6.29]$$

By analogy with [6.17], if minimum start and stop times are not considered, then we can define that state control variables for scenario $\xi_n$:

$$\begin{cases} x_{n,\xi_n} = (u_{n,\xi_n}^1, u_{n,\xi_n}^2, \ldots, u_{n,\xi_n}^K) \\ u_{n,\xi_n} = (u_{n+1,\xi_n}^1, u_{n+1,\xi_n}^2, \ldots, u_{n+1,\xi_n}^K) \\ u_n = (u_{n,1}, u_{n,2}, \ldots u_{n,\Xi_n}) \end{cases} \qquad [6.30]$$

Henceforth, recurrent optimality equation [6.19] becomes:

$$F_{n,\xi_n}(x_{n,\xi_n}) = \min_{u_n} \left( \begin{array}{l} \displaystyle\sum_{\xi_{n+1}=1}^{\Xi_{n+1}} \left( p_{\xi_n \to \xi_{n+1}} \cdot \sum_{k=1}^{K} \left( \begin{array}{l} \alpha_1^k Q_{n+1,\xi_{n+1}}^k + \alpha_0^k u_{n+1,\xi_{n+1}}^k \\ + c_{start}^k u_{n+1,\xi_{n+1}}^k (1 - u_{n,\xi_n}^k) \\ + c_{down}^k u_{n,\xi_n}^k (1 - u_{n+1,\xi_{n+1}}^k) \end{array} \right) \right) \\ + \displaystyle\sum_{\xi_{n+1}=1}^{\Xi_{n+1}} \left( p_{\xi_n \to \xi_{n+1}} F_{n+1,\xi_{n+1}}(x_{n+1,\xi_{n+1}}) \cdot \right) \end{array} \right)$$

[6.31]

In order to solve this equation practically, it is advisable to use Lagrangian relaxation. By relaxing consumer satisfaction and [6.28], Lagrange multipliers, denoted $\lambda_{n,\xi_n}$, must be introduced. Similarly, it is advisable to improve the state in the same way as in [6.20] and [6.21] in order to take into account the minimum start and stop times. Finally, reparation mechanisms for the solution must be added, in the case of resolution, using Lagrangian relaxation, with the initial problem not being convex.

### 6.5.4. *Conclusion*

In this section we have seen a stochastic optimization resolution method that enables uncertainties around consumer demand for an energy network to be taken into account. This optimization method is based on stochastic dynamic programming and Lagrangian relaxation. Indeed, uncertainty is initially part of the constraints of the problem (the consumption/production balance). The use of Lagrangian relaxation enables constraint uncertainty to "pass towards cost". The dual problem is then resolved by stochastic dynamic programming using a scenario tree.

The complexity of this resolution method is intrinsically linked to the scenario tree. The problem's complexity in terms of the number of optimization, size and state space variables for dynamic programming is indeed dependent on the number of nodes making up the scenario tree. This is where we find the compromise between calculation time and model detail. In fact, the higher the number of scenarios, the greater the likelihood will be of a detailed uncertainty model. From this, the major advantage of this method is the fact that the resolution scheme is identical to the one used in the deterministic case. Nevertheless, the major disadvantage of this type of method is the increase in complexity of the problem. Indeed, where initially for the deterministic case we had an on/off optimization variable by producer and by period, we now have a variable by producer, period, and scenario.

Finally, we note the fact that the "recourse" variables notion is, by implication, very influential in this method. Indeed, complete variables that are characteristic of the on /off states of installations correspond to important decisions. Decisions are, therefore, taken at the start of production planning for all periods, all units, and all scenarios. Conversely, the use of algorithm [6.16] in order to calculate the production variables from these states

demonstrates that we believe that they can be chosen at the last minute when the real demand is known.

## 6.6. Consideration of uncertainties over production costs

### 6.6.1. *Introduction*

In this section we focus on the consideration of uncertainties over production costs. This type of uncertainty is common in energy networks. This is the situation, for example, when a production factory is a waste incinerator for a thermal energy network, or when there are co-generation plants (where the sale price is uncertain if it is indexed over the electricity market) in an electrical network.

We recall the mathematical description of the unit commitment problem:

$$\begin{aligned}
&\min_{\left\{\substack{u_n^k, Q_n^k \\ n=1,\ldots,N \\ k=1,\ldots,K}\right\}} \sum_{n=1}^{N}\sum_{k=1}^{K}\begin{pmatrix} \alpha_1^k Q_n^k + \alpha_0^k u_n^k \\ +c_{start}^k u_n^k (1-u_{n-1}^k) + c_{down}^k u_{n-1}^k (1-u_n^k) \end{pmatrix} \\
&s.c. \quad \sum_{k=1}^{K} Q_n^k \geq Q_n^{dem}, \quad \forall n \in \{1,\ldots,N\} \\
&\qquad \underline{Q}^k u_n^k \leq Q_n^k \leq \overline{Q} u_n^k, \quad \forall n \in \{1,\ldots,N\}, \forall k \in \{1,\ldots,K\} \\
&\qquad \left(u_{n-1}^k = 0, u_n^k = 1\right) \Rightarrow \left(u_{n+j}^k = 1, \forall j \in \left\{1,\ldots,T_{up}^k\right\}\right) \\
&\qquad\qquad \forall n \in \{1,\ldots,N\}, \forall k \in \{1,\ldots,K\} \\
&\qquad \left(u_{n-1}^k = 1, u_n^k = 0\right) \Rightarrow \left(u_{n+j}^k = 0, \forall j \in \left\{1,\ldots,T_{down}^k\right\}\right) \\
&\qquad\qquad \forall n \in \{1,\ldots,N\}, \forall k \in \{1,\ldots,K\}
\end{aligned} \qquad [6.32]$$

In this section we consider that uncertainties apply to one or more coefficients $\alpha_1^k$. In order to shorten this expression, we now ignore the capacity and minimum start and stop time constraints, even though they are always taken into account. One way of considering this uncertainty is to consider the expectancy of criterion [6.32] as a criterion to be optimized:

$$\min_{\left\{\substack{u_n^k, Q_n^k \\ n=1,\ldots,N \\ k=1,\ldots,K}\right\}} E_{\alpha_1^k}\left(\sum_{n=1}^{N}\sum_{k=1}^{K}\left(\begin{array}{l}\alpha_1^k Q_n^k + \alpha_0^k u_n^k \\ +c_{start}^k u_n^k (1-u_{n-1}^k) + c_{down}^k u_{n-1}^k (1-u_n^k)\end{array}\right)\right)$$

$$s.t. \quad \sum_{k=1}^{K} Q_n^k \geq Q_n^{dem}, \quad \forall n \in \{1,\ldots,N\} \qquad [6.33]$$

We will now use the recourse optimization notion in order to formulate most closely the problem of the physics of the system.

### 6.6.2. *Mathematical formulation*

We once more consider that binary variables correspond to important decisions, which must be anticipated, whereas the production variables can be adjusted in almost real time. This leads to problem [6.32] being reformulated as follows:

$$\min_{\left\{\substack{u_n^k \\ n=1,\ldots,N \\ k=1,\ldots,K}\right\}} E_{\alpha_1^k}\left(\min_{\left\{\substack{Q_n^k \\ n=1,\ldots,N \\ k=1,\ldots,K}\right\}}\left(\sum_{n=1}^{N}\sum_{k=1}^{K}\left(\begin{array}{l}\alpha_1^k Q_n^k + \alpha_0^k u_n^k \\ +c_{start}^k u_n^k (1-u_{n-1}^k) \\ +c_{down}^k u_{n-1}^k (1-u_n^k)\end{array}\right)\right)\right) \qquad [6.34]$$

$$s.t. \quad \sum_{k=1}^{K} Q_n^k \geq Q_n^{dem}, \quad \forall n \in \{1,\ldots,N\}$$

Let us now introduce Lagrange multipliers in order to relax the demand satisfaction constraints. The dual optimization problem is written:

$$\max_{\left\{\substack{\lambda_n \\ n=1,\ldots,N}\right\}}\left(\min_{\left\{\substack{u_n^k \\ n=1,\ldots,N \\ k=1,\ldots,K}\right\}} E_{\alpha_1^k}\left(\min_{\left\{\substack{Q_n^k \\ n=1,\ldots,N \\ k=1,\ldots,K}\right\}}\left(\begin{array}{l}\sum_{n=1}^{N}\sum_{k=1}^{K}\left(\begin{array}{l}\alpha_1^k Q_n^k + \alpha_0^k u_n^k \\ +c_{start}^k u_n^k (1-u_{n-1}^k) \\ +c_{down}^k u_{n-1}^k (1-u_n^k)\end{array}\right) \\ +\sum_{n=1}^{N}\lambda_n\left(Q_n^{dem} - \sum_{k=1}^{K} Q_n^k\right)\end{array}\right)\right)\right)$$

[6.35]

By reordering the summation operators and by removing the terms that are not dependent on $\alpha_1^k$ from the expectancy, we obtain:

$$\max_{\left\{\lambda_n \atop n=1,\ldots,N\right\}} \left( \sum_{k=1}^{K} \left( \min_{\left\{u_n^k \atop n=1,\ldots,N\right\}} \left( \sum_{n=1}^{N} \left( \begin{array}{l} \alpha_0^k u_n^k + c_{start}^k u_n^k (1-u_{n-1}^k) \\ +c_{down}^k u_{n-1}^k (1-u_n^k) \\ +E_{\alpha_1^k}\left( \min_{Q_n^k} \left(\alpha_1^k - \lambda_n\right) Q_n^k \right) \end{array} \right) \right) \right. \right. \\ \left. \left. +\sum_{n=1}^{N} \lambda_n Q_n^{dem} \right) \right) \qquad [6.36]$$

### 6.6.3. *Resolution*

Let us now see the solution to the problem by reiterating the various embedded sub-problems.

6.6.3.1. *Minimization resolution over the production variables*

The first sub-problem to resolve is:

$$\min_{Q_n^k} \left(\alpha_1^k - \lambda_n\right) Q_n^k \qquad [6.37]$$

which is easily resolved:

$$\widetilde{Q}_n^k = \arg\min_{Q_n^k} \left(\alpha_1^k - \lambda_n\right) Q_n^k = \begin{cases} \overline{Q}^k & if\ \lambda_n > \alpha_1^k \\ \underline{Q}^k & if\ \lambda_n < \alpha_1^k \end{cases} \qquad [6.38]$$

6.6.3.2. *Expectancy calculation*

We will now resolve:

$$E_{\alpha_1^k} \left( \min_{Q_n^k} \left(\alpha_1^k - \lambda_n\right) Q_n^k \right) \qquad [6.39]$$

We assume that the probability density of $\alpha_1^k$ is denoted $p_{\alpha_1^k}$ and bound at interval $\left[\underline{\alpha}_1, \overline{\alpha}_1\right]$. We additionally assume that $\lambda_n$ pertains to this interval. Hence, [6.38] can be calculated as follows:

$$\begin{aligned} E_{\alpha_1^k}\left(\min_{Q_n^k}\left(\alpha_1^k - \lambda_n\right) Q_n^k\right) &= \int_{\underline{\alpha}_1}^{\overline{\alpha}_1}\left(\min_{Q_n^k}\left(\alpha_1^k - \lambda_n\right) Q_n^k\right) p_{\alpha_1^k}(\alpha_1^k) d\alpha_1^k \\ &= \int_{\underline{\alpha}_1}^{\lambda_n}\left(\alpha_1^k - \lambda_n\right)\overline{Q}^k \; p_{\alpha_1^k}(\alpha_1^k) d\alpha_1^k + \int_{\lambda_n}^{\overline{\alpha}_1}\left(\alpha_1^k - \lambda_n\right)\underline{Q}^k \; p_{\alpha_1^k}(\alpha_1^k) d\alpha_1^k \end{aligned} \quad [6.40]$$

This expression is based on $\lambda_n$. If the expression for $p_{\alpha_1^k}$ is simple, then the calculation can be performed analytically. Otherwise, it is possible to calculate the value for this expression for a number of values for $\lambda_n$ and to use an interpolation. In all cases, this calculation can be performed offline. In the interests of brevity, we use $E(\lambda_n)$ to denote the value for the expression given by equation [6.38].

6.6.3.3. *Unit commitment calculation*

Using the developments above, problem [6.35] can finally be rewritten as follows:

$$\max_{\left\{\lambda_n \atop n=1,\ldots,N\right\}}\left(\sum_{k=1}^{K}\left(\min_{\left\{u_n^k \atop n=1,\ldots,N\right\}}\left(\sum_{n=1}^{N}\begin{pmatrix} \alpha_0^k u_n^k + c_{start}^k u_n^k (1-u_{n-1}^k) \\ +c_{down}^k u_{n-1}^k (1-u_n^k) \\ +E\left(\lambda_n\right) + \lambda_n Q_n^{dem} \end{pmatrix}\right)\right)\right) \quad [6.41]$$

We have a problem structure that is fairly comparable to that used during the resolution of the deterministic problem. We thus have, for given multipliers $\lambda_n$, $K$ sub-problems to one unit, which can easily be resolved using dynamic programming. The optimization of the multipliers can then be effected in the same way as in the deterministic case.

6.6.3.4. *Resolution of the stochastic problem: report*

Finally, we see that taking uncertainties over the production costs does not add to the problem's complexity. Indeed the same decomposition and the same methods can be used for the deterministic example. The only

supplementary element is in the preprocessing stage, which enables expectancies [6.39] to be calculated.

### 6.6.4. *Example*

Here we consider a relatively simple example of four production units over a 24 hour horizon. Table 6.2 presents the characteristics of installations (measurements without units). The production costs $\alpha_1^k$ are considered to be Gaussians with mean $E(\alpha_1^k)$ and standard deviation $\sigma^k$.

| Unit | $\alpha_0^k$ | $E(\alpha_1^k)$ | $\sigma^k$ | $c_{start}^k$ | $c_{down}^k$ | $\underline{Q}^k$ | $\overline{Q}^k$ | $T_{up}^k$ | $T_{down}^k$ |
|---|---|---|---|---|---|---|---|---|---|
| 1 | 10 | 3 | 0.2 | 10 | 2 | 10 | 40 | 2 | 4 |
| 2 | 10 | 4.3 | 0.2 | 10 | 2 | 10 | 40 | 2 | 4 |
| 3 | 10 | 4.6 | 0.2 | 10 | 2 | 10 | 40 | 3 | 3 |
| 4 | 10 | 5 | 0.2 | 10 | 2 | 10 | 40 | 3 | 3 |

**Table 6.2.** *Characteristics of production units*

These four units must satisfy the demand given in Figure 6.5. Table 6.3 presents the optimization results obtained in the deterministic case ($\alpha_1^k = E(\alpha_1^k)$), and [6.34] presents those obtained for the stochastic problem resolution [6.33].

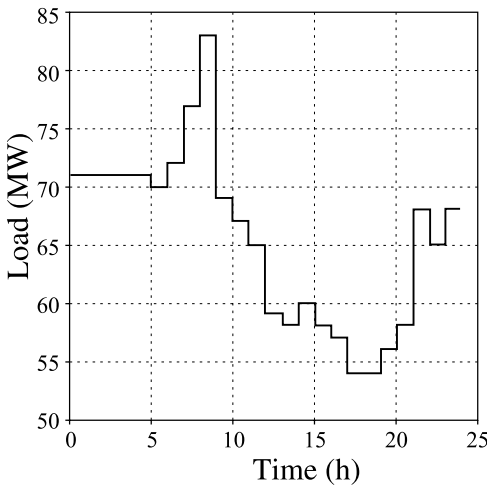


**Figure 6.5.** *Consumer demand*

| $u_n^k$ | Temporal period | | | | | | | | | | | |
|---|---|---|---|---|---|---|---|---|---|---|---|---|
| **Unit** | 1 | 2 | 3 | 4 | 5 | 6 | 7 | 8 | 9 | 10 | 11 | 12 |
| **1** | 1 | 1 | 1 | 1 | 1 | 1 | 1 | 1 | 1 | 1 | 1 | 1 |
| **2** | 1 | 1 | 1 | 1 | 1 | 1 | 1 | 1 | 1 | 1 | 1 | 1 |
| **3** | 0 | 0 | 0 | 0 | 0 | 0 | 0 | 1 | 1 | 1 | 0 | 0 |
| **4** | 0 | 0 | 0 | 0 | 0 | 0 | 0 | 0 | 0 | 0 | 0 | 0 |
| $u_n^k$ | Temporal period | | | | | | | | | | | |
| **Unit** | 13 | 14 | 15 | 16 | 17 | 18 | 19 | 20 | 21 | 22 | 23 | 24 |
| **1** | 1 | 1 | 1 | 1 | 1 | 1 | 1 | 1 | 1 | 1 | 1 | 1 |
| **2** | 1 | 1 | 1 | 1 | 1 | 1 | 1 | 1 | 1 | 1 | 1 | 1 |
| **3** | 0 | 0 | 0 | 0 | 0 | 0 | 0 | 0 | 0 | 0 | 0 | 0 |
| **4** | 0 | 0 | 0 | 0 | 0 | 0 | 0 | 0 | 0 | 0 | 0 | 0 |

**Table 6.3.** *Results for the deterministic case*

| $u_n^k$ | Temporal period | | | | | | | | | | | |
|---|---|---|---|---|---|---|---|---|---|---|---|---|
| **Unit** | 1 | 2 | 3 | 4 | 5 | 6 | 7 | 8 | 9 | 10 | 11 | 12 |
| **1** | 1 | 1 | 1 | 1 | 1 | 1 | 1 | 1 | 1 | 1 | 1 | 1 |
| **2** | 1 | 1 | 1 | 1 | 1 | 1 | 1 | 1 | 1 | 1 | 1 | 1 |
| **3** | 1 | 1 | 1 | 1 | 1 | 1 | 1 | 1 | 1 | 1 | 0 | 0 |
| **4** | 0 | 0 | 0 | 0 | 0 | 0 | 0 | 0 | 0 | 0 | 0 | 0 |
| $u_n^k$ | Temporal period | | | | | | | | | | | |
| **Unit** | 13 | 14 | 15 | 16 | 17 | 18 | 19 | 20 | 21 | 22 | 23 | 24 |
| **1** | 1 | 1 | 1 | 1 | 1 | 1 | 1 | 1 | 1 | 1 | 1 | 1 |
| **2** | 1 | 1 | 1 | 1 | 1 | 1 | 1 | 1 | 1 | 1 | 1 | 1 |
| **3** | 0 | 0 | 0 | 0 | 0 | 0 | 0 | 0 | 0 | 0 | 0 | 0 |
| **4** | 0 | 0 | 0 | 0 | 0 | 0 | 0 | 0 | 0 | 0 | 0 | 0 |

**Table 6.4.** *Results for the stochastic case*

Considering the stochastic element led to the "on" state of the third unit from the start of the temporal horizon, which was not necessary to satisfy demand. The cost obtained for the stochastic example is 2.5% less than the cost obtained for the deterministic problem. This is the average gain. Of course, if the creation of the risk corresponds to the nominal case, the cost obtained will be more significant since more installations would be "on". However, the solution found is more robust.

## 6.7. From optimization to control

### 6.7.1. *The predictive approach principle*

In the previous sections we have tried to take into account the uncertainties influencing the system by making use of the concepts and methods relating to robust optimization. The results obtained enable this approach to be validated. Another way to produce robust behavior in a system subjected to uncertainties is the closed loop drive. Indeed the optimization results obtained may be considered as an open loop control for the system.

An accepted method to extend optimization results within a closed loop drive context is to use the principle of the horizon receding from the predictive control. Here we make use of this principle to strengthen the system against errors relating to consumer demand. This principle is as follows:

– the solution to the optimization problem is firstly calculated over interval $[m, m+N-1]$ from consumer demand prediction $\hat{Q}_n^{dem}$; the deterministic algorithm is used at this stage;

– the first installation controls $u_m^k$ at instant $m$ are applied to the production system;

– the system model is updated based on the production of $Q_m^{dem}$ (actual consumer demand);

– the process is repeated for the next period over interval $[m+1, m+N]$.

### 6.7.2. *Example*

The algorithm above is tested for a four-unit problem. We place ourselves within the most unfavorable situation, i.e. where predictions are always under-valued, in this case by 5%. Figure 6.6 presents simulation results obtained over 4 days. Without closed loop control, production would be equal to the predicted demand. The use of the closed loop enables the gap between production and consumption to be reduced or even eradicated.

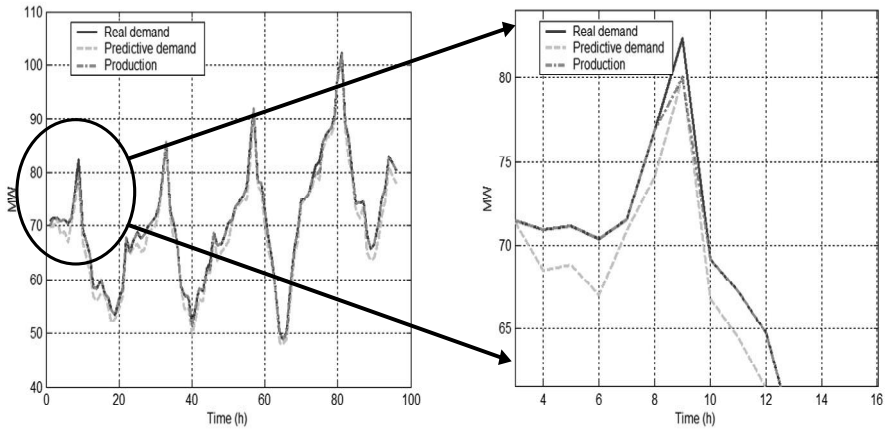


**Figure 6.6.** *Results of predictive control*

## 6.8. Conclusions

In this chapter we have seen multiple methodologies for technico-economic optimization of energy networks. The problem is formulated in the form of a cost minimization problem under a set of technical constraints. The corresponding problems are unit commitment problems.

Firstly, we have explored several methods enabling the problem to be resolved in a deterministic context. We thus firstly presented an exact resolution from dynamic programming. The joint use of dynamic programming and a Lagrange formulation has enabled the effect of combinatory complexity in decomposing the problem unit by unit to be restricted. We then presented a stochastic method based on the use of genetic algorithm utilization. In this case, it is apparent that available *a priori* knowledge of the system could enable new genetic operators, leading to a sensible reduction in the number of iterations necessary to obtain good quality solutions, to be defined.

Secondly, we worked towards the solution to the problem by taking into account uncertainties having a bearing on the system using robust optimization methods. We thus successively considered uncertainties regarding consumer demand (which include the constraints of the problem) and production costs. In both cases, the use of dynamic programming and

recourse optimization has enabled the results obtained for the deterministic case to be re-used.

Finally, an approach was presented that enabled the consideration of uncertainties and increased the robustness of the system's operation, namely the use of closed loop utilization. The principle of the horizon receding from the predictive control has thus enabled optimization results to be extended in a closed loop context.

## 6.9. Bibliography

[ACE 98] ACEVEDO J., PISTIKOPOULOS E.N., "Stochastic optimization based algorithms for process synthesis under uncertainty", *Computers and Chemical Engineering*, vol. 22, pp. 647-671, 1998.

[ARV 01] ARVASTSON L., Stochastic modelling and operational optimization in district heating system, PhD Thesis, Lund Institute of Technology, 2001.

[BAK 00] BAKIRTZIS A., ZOUMAS C., "Lambda of Lagrangian relaxation solution to unit commitment problem", *Generation, Transmission and Distribution, IEE Proceedings*, vol. 147, pp. 131-136, 2000.

[BEN 02] BEN-TAL A., NEMIROVSKI N., "Robust optimization – methodology and applications", *Mathematical Programming*, vol. 92, pp. 453-480, 2002.

[CAR 98] CAROE C. C., SCHULTZ R., *A Two-Stage Stochastic Program for Unit Commitment Under Uncertainty in a Hydro-Thermal Power System*, Preprint 98-13, Konrad-Zuse-Zentrum für Informationstechnik, Berlin, Germany, 1998.

[CHE 93] CHEN C.-L., WANG S.-C., "Branch and bound scheduling for thermal generating units", *IEEE Transactions on Energy Conversion*, vol. 8, pp. 184-189, 1993.

[CHE 00] CHENG C.-P., LIU C.-W., LIU C.-C., "Unit commitment by Lagrangian relaxation and genetic algorithms", *IEEE Transactions on Power Systems*, vol. 15, pp. 707-714, 2000.

[CHE 02] CHENG C.-P., LIU C.-W., LIU C.-C., "Unit commitment by annealing-genetic algorithm", *Electrical Power and Energy Systems*, vol. 24, pp. 149-158, 2002.

[CLA 87] CLARKE, D.W., MOHTADI, C., TUFFS P.S., "Generalized Predictive Control – Part I. The Basic Algorithm", *Automatica*, vol. 23, pp. 137-148, 1987.

[DEN 98] DENTCHEVA D., ROMISCH W., "Optimal power generation under uncertainty via stochastic programming", *Lecture Notes in Economics and Mathematical Systems*, vol. 458, pp. 22-56, 1998.

[DOT 99] DOTZAUER E., HOLMSTRÖM K., RAVN H. F., "Optimal unit commitment and economic dispatch of cogeneration systems with a storage", *13th Power Systems Computation Conference 1999*, Trondheim, Norway, pp. 738-744, 1999.

[DOT 02] DOTZAUER E., "Simple model for prediction of loads in district-heating systems", *Applied Energy*, vol. 73, pp. 277-284, 2002.

[DUO 99] DUO H., SASAKI H., NAGATA T., FUJITA H., "A solution for unit commitment using Lagrangian relaxation combined with evolutionary programming", *Electric Power Systems Research*, vol. 51, pp. 71-77, 1999.

[FER 93] FERREIRA L., "On the duality gap for thermal unit commitment problems", *IEEE International Symposium on Circuits and Systems*, *ISCAS93*, pp. 2204-2207, 1993.

[GRÖ 02] GRÖWE-KUSKA N., KIWIEL K. C., NOWAK M. P., RÖMISCH W., WEGNER I., "Power management in a hydro-thermal system under uncertainty by Lagrangian relaxation", in GREENGARD C., RUSZCZYNSKI A., *Decision Making under Uncertainty, Energy and Power*, IMA vol. Math. Appl. 128, Springer, New York, pp. 39-70, 2002.

[GRÖ 05] GRÖWE-KUSKA N., RÖMISCH W., "Stochastic unit commitment in hydro-thermal power production planning", in WALLACE S.W., ZIEMBA W.T., *Applications of Stochastic Programming*, MPS-SIAM Series in Optimization, Cambridge University Press, Cambridge, 2005.

[HOB 88] HOBBS W.J., HERMON G., WARNER S., SHEBLÉ G.B., "An enhanced dynamic programming approach for unit commitment", *IEEE Transactions on Power Systems*, vol. 3, pp. 1201-1205, 1988.

[KAS 96] KASARLIS S. A., BAKIRTZIS A. G., PETRIDIS V., "A genetic algorithm solution to the unit commitment problem", *IEEE Transactions on Power Systems*, vol. 11, pp. 83-92, 1996.

[LAN 60] LAND A. H., DOIG A. G., "An automatic method of solving discrete programming problems", *Econometrica*, vol. 28, pp. 497-520, 1960.

[LAR 02] LARSEN H. V., PALSSON H., BOHM B., RAVN H. F., "Aggregated dynamic simulation model of district heating networks", *Energy Conversion Management*, vol. 43, pp. 995-1019, 2002.

[LI 08] LI Y., HUANG G., NIE X., NIE S., "A two-stage fuzzy robust integer programming approach for capacity planning of environmental management systems", *European Journal of Operational Research*, vol. 189, pp. 399-420, 2008.

[MA 95] MA X., EL-KEIB A.A., SMITH R.E., MA H., "A genetic algorithm based approach to thermal unit commitment of electric power systems", *Electric Power Systems Research*, vol. 34, pp. 29-36, 1995.

[MAC 02] MACIEJOWSKI J.M., *Predictive Control with Constraints*, Prentice-Hall, Pearson Education Limited, Harlow, UK, 2002.

[MAN 99] MANTAWY A.H., ABDEL-MAGID Y.L., SELIM S.Z., "A new genetic-based tabu search algorithm for unit commitment problem", *Electric Power Systems Research*, vol. 49, pp. 71-78, 1999.

[NIE 00] NIELSEN H.A., MADSEN H., Predicting the heat consumption in district heating system using meteorological forecast, PhD thesis, Technical University of Denmark, 2000.

[NOW 00] NOWAK M.P., RÖMISCH W., "Stochastic Lagrangian relaxation applied to power scheduling in a hydro-thermal system under uncertainty", *Annals of Operations Research*, vol. 100, pp. 251-272, 2000.

[OHT 96] OHTA T., MATSUI T., TAKATA T., KATO M., AOYAGI M., KUNUGI M., SHIMADA K., NAGATA J., "Practical approach to unit commitment problem using genetic algorithm and Lagrangian relaxation method", *Intelligent Systems Applications to Power Systems, Proceedings*, 28th January-2nd February, Orlando, Florida, pp. 434-440, 1996.

[ORE 97] ORERO S.O., IRVING M.R., "A combination of the genetic algorithm and Lagrangian relaxation decomposition techniques for the generating unit commitment problem", *Electric Power Systems Research*, vol. 43, pp. 149-156, 1997.

[OUY 91] OUYANG Z., SHAHIDEHPOUR S.M., "An intelligent dynamic programming for unit commitment application", *IEEE Transactions on Power Systems*, vol. 6, pp. 1203-1209, 1991.

[PHI 00] PHILPOTT A.B., CRADDOCK M., WATERER H., "Hydro-electric unit commitment subject to uncertain demand", *European Journal of Operational Research*, vol. 125, pp. 410-424, 2000.

[POO 08] POOJARI C.A., VARGHESE B., "Genetic algorithm based technique for solving chance constrained problems", *European Journal of Operational Research*, vol. 185, pp. 1128-1154, 2008.

[RAJ 04] RAJAN C.C.A., MOHAN M.R., "An evolutionary programming-based tabu search method for solving the unit commitment problem", *IEEE Transactions on Power Systems*, vol. 19, pp. 577-585, 2004.

[RIO 07] RIOUS V., Le développement du réseau de transport dans un système électrique libéralisé, un problem de coordination avec la production, PhD thesis, Paris-Sud University, 2007.

[ROB 12] ROBOAM X., *Systemic Design Methodologies for Electrical Energy Systems*, ISTE Ltd and John Wiley, London and New York, 2012 (forthcoming).

[ROO 94] ROOIJERS F. J., VAN AMERONGEN R. A. M., "Static economic dispatch for cogeneration systems", *IEEE Transactions on Power Systems*, vol. 9, pp. 1392-1398, 1994.

[SAH 04] SAHINIDIS N.V., "Optimization under uncertainty: state-of-the-art and opportunities", *Computers and Chemical Engineering*, vol. 28, pp. 971-983, 2004.

[SAN 04] SANDOU G., FONT S., TEBBANI S., HIRET A., MONDON C., "Optimisation par colonies de fourmis d'un site de génération d'énergie", *Journal Européen des Systèmes Automatisés*, Numéro spécial Métaheuristiques pour l'optimisation difficile, vol. 38, pp. 1097-1119, 2004.

[SAN 05a] SANDOU G., Modélisation, optimisation et commande de parcs de production multi-énergies complexes, PhD thesis, Paris Sud University, 2005.

[SAN 05b] SANDOU G., FONT S., TEBBANI S., HIRET A., MONDON C., "Short term optimization of cogeneration systems considering heat and electricity demands", *15th Power Systems Computation Conference*, Liège, Belgium, August, 2005.

[SAN 08a] SANDOU G., FONT S., TEBBANI S., HIRET A., MONDON C., "Enhanced genetic algorithm with guarantees of feasibility for the Unit Commitment problem", *Lecture Notes in Computer Science*, vol. 4926, pp. 291-302, 2008.

[SAN 08b] SANDOU G., FONT S., TEBBANI S., HIRET A., MONDON C., "Feeding a genetic algorithm with an ant colony for constrained optimization – an application to the unit commitment problem", *5th International Conference on Informatics in Control, Automation and Robotics*, Funchal, Madeira, Portugal, 11-15 May, 2008.

[SEN 98] SEN S., KOTHARI D. P., "Optimal thermal generating unit commitment: a review", *Electrical Power and Energy Systems*, vol. 20, pp. 443-451, 1998.

[SEN 04] SENJYU T., SHIMABUKURO, K., UEZATO K., FUNABASHI T., "A fast technique for unit commitment problem by extended priority list", *IEEE Transactions on Power Systems*, vol. 19, pp. 2119-2120, 2004.

[SHE 96] SHEBLÉ G.B., MAIFELD T.T., BRITTIG K., FAHD G., FUKUROZAKI-COPPINGER S., "Unit commitment by genetic algorithm with penalty methods and a comparison of Lagrangian search and genetic algorithm – economic dispatch example", *International Journal of Electrical Power and Energy Systems*, vol. 18, pp. 339-346, 1996.

[TAK 00] TAKRITI S., BIRGE J., "Using integer programming to refine Lagrangian-based unit commitment solutions", *IEEE Transactions on Power Systems*, vol. 15, pp. 151-156, 2000.

[YIN 98] YIN W., WONG S., "An enhanced simulated annealing approach to unit commitment", *Electrical Power and Energy Systems*, vol. 20, pp. 359-368, 1998.

[YIN 01] YIN W., WONG S., "Hybrid simulated annealing/genetic algorithm approach to short-term hydro-thermal scheduling with multiple thermal plants", *Electrical Power and Energy Systems*, vol. 23, pp. 565-575, 2001.

[ZHA 02] ZHAI Q., GUAN X., "Unit commitment with identical units: successive subproblems solving method based on Lagrangian relaxation", *IEEE Transactions on Power Systems*, vol. 17, pp. 1250-1257, 2002.

[ZHU 98] ZHUANG F., GALIANA F. D., "An enhanced simulated annealing approach to unit commitment", *Electrical Power and Energy Systems*, vol. 20, pp. 359-368, 1998.

# List of Authors

Henri BORSENBERGER
Supélec
Control Department and Power and Energy Systems Department
Gif-sur-Yvette
France

Stéphane BRISSET
L2EP Laboratory
Ecole Centrale Lille
France

Pascal BROCHET
UTBM
University of Technology of Belfort-Montbéliard
France

Benoit DELINCHANT
G2Elab
University of Grenoble
France

Daniel DEPERNET
FEMTO ST Institute
University of Technology of Belfort-Montbéliard
France

Philippe DESSANTE
Supélec
Power and Energy Systems Department
Gif-sur-Yvette
France

*Integrated Design by Optimization of Electrical Energy Systems* Edited by Xavier Roboam
© 2012 ISTE Ltd. Published 2012 by ISTE Ltd.

Christophe ESPANET
FEMTO ST Institute
University Franche-Comte
France

Laurence ESTRABAUD
G2Elab
University of Grenoble
France

Laurent GERBAUD
G2Elab
University of Grenoble
France

Frédéric GILLON
L2EP Laboratory
Ecole Centrale Lille
France

Amine JAAFAR
LAPLACE
University of Toulouse
France

Marc PETIT
Supélec
Power and Energy Systems Department
Gif-sur-Yvette
France

Xavier ROBOAM
LAPLACE
University of Toulouse
France

Guillaume SANDOU
Supélec
Control Department
Gif-sur-Yvette
France

Bruno SARENI
LAPLACE
University of Toulouse
France

Anne-Claire SAUTTER
FEMTO ST Institute
University Franche-Comte
France

Zhenwai WU
FEMTO ST Institute
University Franche-Comte
France

Frédéric WURTZ
G2Elab
University of Grenoble
France

# Index


**A, C, D**

analytical model, 48, 61, 73, 82, 91, 132, 210
characterization indicator, 7-12, 22
classification, 6, 16, 32, 117
compacting, 7, 24, 33, 40
constraint, 99, 109, 120, 123, 136, 159, 168
converter, 74
cost of ownership, 25, 32, 108
criteria, 97, 107
design through optimization, 139
dynamic programming, 257

**E, F, G**

electrical machine, 61
energy management, 8, 108, 144
energy network, 249, 255
environmental variable, 1, 3, 117
environment-system coupling, 13
epicyclic gear set, 83
evolutionary algorithm, 113
fine, 162
fine model, 158, 167, 188
framework, 194, 197-198, 201-203
general optimization, 101, 161, 181
genetic algorithm, 262
granularity, 111, 158-160, 206

**H, I, J**

hierarchical decomposition, 178
hybrid locomotive, 25, 143
hybrid vehicle, 58, 64, 83
integrating the finality (mission), 15
integration of the finality, 112
interaction, 56, 178
interactive, 216
interoperability, 199, 203
Jacobian, 218, 223

**L, M, N**

Lagrangian relaxation, 257
link variable, 92, 180
mission, 2-3, 52, 95, 109
mission profile, 7, 21, 96-97, 144
multi-criteria, 193
multi-level, 156, 177
multi-objective, 110, 120-121, 125
niching, 118


*Integrated Design by Optimization of Electrical Energy Systems* Edited by Xavier Roboam
© 2012 ISTE Ltd. Published 2012 by ISTE Ltd.

## O, P, R, S

objective, 92, 119, 157, 250
operating cycles, 94, 112
optimization problem with recourse, 268
Pareto, 99, 119, 139, 149, 157, 226
predictive control, 279
profile synthesis, 21-22
robust, 126, 142, 234, 267
robust optimization, 234, 267
robustness, 119
scope of the model, 158-159
sensitivity, 54, 140, 209, 223, 233
simple model, 158, 162, 168, 188
simultaneous design, 37, 107, 143
software component, 198, 209, 235
space mapping (SM), 162, 166

## T, U, W

target cascading, 178-180
technico-economic, 227
tools, 187, 193-195, 209
uncertainties over demand, 269
uncertainties over production costs, 273
uncertainty, 266
wind energy resource, 6, 130